بسم الله الرحمن الرحيم

Sudan University of Science and Technology

College of Graduate Studies

QSAR, Molecular modeling, Molecular docking and Preparation of Some N-substituted Acridinedione and Polyhydroquinoline Derivatives

العلاقة الكمية بين البنية والفعالية والنمذجة الجزيئية والإلتحام الجزيئي و تحضيربعض مشتقات مستبدلات الاكريدين- داي- ون والبولي هيدروكينولين

A Thesis Submitted for the Fulfillment of the Requirements of the Degree of Doctor of Philosophy in Chemistry

By:

Ahmed Abaker Ahmed Ali

M. Sc. (Chemistry), (2008)

Supervisor: Prof. Dr. Ahmed Elsadig Mohammed Saeed

April 2022

إستـهلال

قال الله تبارك وتعالى :-

إقرأ بإسم ربك الذي خلق(١) خلق الانسان من علق(٢) إقرأ وربك الأكرم (٣) الذي علم بالقلم (٤) علم الإنسان مالم يعلم (٥).

صدق الله العظيم.

سورة العلق الآيات (١-٥).

Dedication

I dedicate this work

To my late parents,

Sister, wife, daughters, and to all my Friends.

Acknowledgements

First of all I would like to grease almighty Allah for giving me abundant grace and energy to complete and write this work.

I would like to take this opportunity to thank my supervisor Prof. Dr. Ahmed Elsadig M. Saeed, for suggesting the idea of this work.

My gratitude goes to Mr. Ahmed Abdel Alazeem, the lab technician at Sudan University of Science and Technology for his help.

I would like profoundly thank the following persons for their contribution which made the completion of this work successfully, Mr. Abdelhamid Farog in the lab of instruments at Sudan University of Science and Technology for his help.

Ustaz Jihad Mohammed at the International center for Industrial consults for his help in the Infra-Red spectroscopic analysis, and Dr. Elsadig Rodwan at Amipharma laboratories, Sudan, for his help.

My gratitude extends to Dr. Abu baker Mohammed Osman, at King Khalid University- Abha/Saudi Arabia- for his help in 1H-NMR, and Mass Spectrometric analysis.

In addition to I would like to thanks my teachers, friends and family who put me in a position to be a part of this programme and to whom I will always be indebted to.

List of Abbreviations

- Å = Angstrom
- ACD = Advance Chemistry Development
- [$AlPO_4$] = Aluminum phosphate
- a-aac = Number of hydrogen bond acceptor atoms
- a-don = Number of hydrogen bond doner atoms
- Asym = Asymmetry
- Asn = Spargine
- Asp = Spartic acid
- ATP-ABC= Adenosine triphosphate binding cassette
- [bmim] HSO_4 = 1- Butyl-3-methylimidazolin hydrogen sulfate
- 1, 4-DHPs = 1, 4-Dihydropyridines
- 3D = Three-dimensional
- 3D-QSAR= Three-dimensional
- 3MCR = Three components reaction
- Concentration
- CAN = Ceric Ammonium nitrate
- CD = Compact disk
- CdO = Cadmium oxide
- CFTR= Cystic fibrosis trans-membrane conductance regulator
- COMFA = Comparative molecular field analysis
- $Cs_{2.5}H_{0.5}PW_{12}O_{40}$ = Ahydrogen cesium salt of dodecatungstophosphoric acid
- CTAB = Cetyltrimethylammoniumbromide

- CV= Cross-validation
- 1D = One- dimensional
- 2D = Two- dimensional
- 3D = Three- dimensional
- DHPs = Dihydropyridines
- DNA= Deoxyribonucleic acid
- E = Energy
- Ele = Electronic Energy
- FT- IR = Fourier transform- infrared
- GC - MS = Gas Chromatography- Mass Spectrometer
- Glu = Glutamic acid
- Gln = Glutamine
- Gly = Glycine
- HB = Hydrogen bond
- HF = Heat of formation
- His = Hitidine
- HOMO = High occupied molecular orbital
- hr = Hour
- IC_{50} = Inhibitory concentration, 50%
- IP = Ionization potential
- IR = Infra-red.
- IUPAC = International union of pure and applied Chemistry
- J = Geminal coupling
- K_1, K_2, K_3 = constants derived from regression analysis
- KBr = Potassium bromide
- Lab = Laboratory
- Leu = Leucine

- Lip-acc = Lipinski acceptor count
- Lip- don = Lipinski donor count
- Log P (o/w) = Logarithm of the molecule's partition coefficient between 1-octanol/water
- LOO = Leave one out
- LMO = Leave more out
- m = multiblet
- Met = Methionine
- MCF-7 = human breast cancer cell lines
- MCRs = Multi-component reactions
- MDR = Multi-drug resistance
- MLR = Multi-linear regression
- MOE = Molecular operation environment
- m.p = Melting point
- Mr = Molar refractivity
- MS = Mass spectroscopy
- Mol.wt = Molecular weight
- NADH = Nicotineamide adenine dinucleotide coenzymes
- NH_4OAc = Ammonium acetate
- NMR = Nuclear magnetic resonance
- nm = nanometer
- PDB = Protein data bank
- Phe = Phenylalanine
- PHQs = Polyhydroquinolines
- PIC_{50} = Anti- cancer potential
- PLS = Partial least squares

- Pro = Proline
- PTSA = Para toluene sulfonic acid. (As catalyst)
- PTSA = Polar topological surface area. (As descriptor)
- q = quartet
- QSARs = Quantitative structure-activity relationships
- QSPRs = Quantitative structure-property relationships
- R = correlation coefficient
- R_f = Retardation factor
- rmsd = Root mean square deviation
- RMSE = Root mean square error
- RNA = Ribonucleic acid
- RSA = Retro-synthetic analysis
- R^2 = Square of correlation coefficient
- s = standard error of estimate
- s = singlet
- S = Score of energy by kcal/mol
- SBA-15 or (SBA-pr-SO_3H) = Sulfonic acid functionalized silica (catalyst)
- Ser = Serine
- SLC = Solute carrier
- SPSS = Statistical package for social sciences
- Str- vib = Stretching- vibration
- Symm = Symmetry
-TLC = Thin layer chromatography
- Trp = Triptophan
- TUD = Thiourea dioxide
- Tyr = Tyrocine
- UV = Ultra violet

- $Yb(OTF)_3$ = Ytterbium (III) triflouromethanesulfonate
- λmax – Maximum wavelength
- Zn = Zinc metal

Abstract

Quantitative Structure-activity relationship (QSAR) study was carried out using ACD/lab and MOE software's, for developing a correlation between the structural properties of acridinedione and polyhydroquinoline derivatives (in which the 1,4- dihydropyridine is the basic molecule in their structure), and their anti-cancer activities. From this correlation, new chemical were designed, and their biological activities were predicted from their physicochemical descriptors by using multiple linear regression method. The QSAR models were considered to be good according to the acceptable statistical values obtained. (R= 0.993). Statistical parameters were also calculated for the two groups respectively.

R=0.966 R^2 =0.933 RMSE=0.03817

Q=0.9085 Q^2 = 0.990 s= 0.013 F= 283.74 p= 0.004

R=0.9011 R^2 = 0.812 RMSE=0.05156

Q= 0.7917 Q^2 = 0.6267 s= 0.021 F= 34.511 p= 0.0001

1, 4-Dihydropyridines as analogues of Nicotineamide adenine Dinucleotide (NADH) coenzymes exhibit a wide range of biological activities, such as Calcium blocking, and today used in pharmacology.

Acridines which possess the 1,4-dihydropyridine parent nucleus have interesting pharmaceutical properties such as a positive ion tropic effects promoting the eatery of Calcium to the intracellular space, and acridine-1,8-

(2H,5H)- diones are known as laser dyes. Members of these class characterizes by having several common chemical and biological activities.

Acridinediones were synthesized by the one-pot Hantzsch condensation of aromatic aldehydes, 5, 5-dimethyl-1, 3-cyclohexanedione (Dimedone) and aniline in refluxing. This method has then been extended to the four-component reaction of aromatic aldehydes, 5, 5-dimethyl-1, 3-cyclohexanedione (Dimedone) ethyl acetoacetate and ammonium acetate for the synthesis of polyhydroquinoline derivatives.

Chapter one of this work covers a concise review of methods of synthesis of these class with their biological activities a alongside other topics.

In chapter two from this study ten compounds derived from both acridinedione and polyhydroquinoline were prepared. The synthetic designing of these compounds was worked out through the suitable retro-synthetic analysis and the use of the disconnection approach.

Cyclization was achieved through Hantzsch condensation followed by Michael type addition reaction mechanisms which sometimes catalyzed by CTAB in refluxing water was discussed in chapter three.

The reaction course were monitored by TLC technique, recrystalization and TLC were used for purification purposes.

The structures of the prepared compounds were elucidated by IR, UV, 1H-NMR and Mass Spectrometer.

Molecular docking was also carried out so as to find out the binding affinity of target compounds with suitable protein that was obtained from the Protein Data Bank (PDB).

The obtained spectroscopic data showed that the prepared compounds gave closed results.

المستخلص

تمت دراسة كمية للعلاقة بين البنية والنشاط بإستخدم برنامج (أم أو إي) لايجادعلاقة بين الخصائص البنيوية لمشتقات الأكريدين – ١,٨- أون وهيدروكينولين كجزيئات أساسية ، ونشاطها المضاد للسرطان ومن ثم تم هذا الإجراء بإستخدام طريقة الإنحدار الخطي المتعددة . كانت هذه الدراسة جيدة على حسب القيم والدلالات الإحصائية الناتجة للمجموعتين الأولى والثانية.

$R=0.966$ $R^2=0.933$ $RMSE=0.03817$

$Q=0.9085$ $Q^2=0.990$ $s=0.013$ $F=283.74$ $p=0.004$

$R=0.9011$ $R^2=0.812$ $RMSE=0.05156$

$Q=0.7917$ $Q^2=0.6267$ $s=0.021$ $F=34.511$ $p=0.0001$

مركبات ١،٤- ثنائي الهيدروبيريدينات هي عبارة عن مركبات شبيهة بالنيوكوتين أميد ثنائي النيوكليوتيد مساعدات الانزيمات والتي تظهر مدى واسع من الانشطة الحيوية.

الاكريدينات التي تمتلك تركيب ، ١،٤- ثنائي هيدروالبيريدين هي التي تتمتع بخواص صيدلانية مثل التأثير الاينوتروبي الايجابي ، والذي يعزز دخول الكالسيوم داخل المسافات البين خلوية.مركبات ١،٨- أكريدين –داي-أونات تعرف أيضاً بأصباغ الليزر.

أعضاء هذه المجموعة تتميز بأنها تمتلك عدة نشاطات كيميائية وحيوية. حيث يتم تحضير مشتقات الاكريدين- داي-أون بواسطة تكثيف هانتش عن طريق تفاعل الالدهيدات العطرية مع ، ٥،٥- ثنائي ميثيل ، ٣،١- هكسان – داي- أون الحلقي(الديميدون) والانيلين بواسطة التكثيف الترجيعي – هذه الطريقة تمتد لتحضير (تفاعل ذو الاربع مكونات) مشتقات متعدد هيدروكينولين وذلك عن طريق تفاعل الالدهيدات العطرية ، مع إيثيل أسيتوأسيتات،الامين، والديميدون.

يغطي الفصل الاول من هذه الدراسة ، طرق تحضير هذه الطائفة من هذه المشتقات مع التركيز على خواصها ونشاطاتها الحيوية، إلى جانب مواضيع أخرى.

في الفصل الثاني من هذه الدراسة تم تحضيرعدد عشرة من هذه المشتقات والتي تشمل كل من الاكريدين- داي- أون، والبولي هيدروكينولين.

تم تصميم خطة لتخليق هذه المشتقات عن طريق تخليق التحليل التضديدي المناسب، إلى جانب إستخدام طرق التكسير.

تمت إنجاز عملية التحولق عبر تكثيف هانتش، متبوعة بميكانيكية إضافة مايكل والتي تحفز أحياناً بإستخدام بروميد ستايل ثلاثي ميثيل الامونيم عن طريق التكثيف الترجيعي ، والتي تمت مناقشتها إجمالاً في الفصل الثالث من هذه الدراسة.

كذلك تمت مراقبة سير ومتابعة هذه التفاعلات عن طريق إستخدام تقنية كروماتغرافيا الطبقة الرقيقة ، وإعادة البلورة حيث إستخدمت لأغراض التنقية.

إستخدمت وسائل طيفية مختلفة ، وذلك للتعرف على المركبات المحضرة، مثل طيف الاشعة تحت الحمراء، طيف الأشعة فوق البنفسجية، بروتون الرنين النووي المغناطيسي و طيف الكتلة.

تم إجراء دراسة أخرى للإلتحام الجزيئي التي تم تحضيرها لتكون مركبات مستهدفة وتطابقها مع البروتين الذي تم الحصول عليه من بنك بيانات البروتين، بإستخدام الدوكسوريوبسين كعقار مرجعي.

البيانات الطيفية التي تم الحصول عليها للمركبات التي تم تحضيرها، أعطت نتائج متقاربة.

Table of Contents

List of Figures

List of Schemes

List of Tables

1 .Introduction

1.1. Multi-component reactions

Multi-component reactions (MCRs) are convergent reactions, in which three or more starting materials react to form a product, where basically all or most of the atoms contribute to the newly formed product. In an MCR, a product is assembled according to cascade of elementary chemical reactions. Thus, there is a network of reaction equilibria, which all finally flow into an irreversible step yielding the product. The challenge is to conduct an MCR in such a way that the network of pre-equilibrated reactions channel into the main product and do not yield side products. The result is clearly dependent on the reaction conditions: solvent, temperature, catalyst, concentration, the kind of starting materials and functional groups. Such considerations are of particular importance with the design and discovery of novel MCRs (Domoling, 2004). Multi-component reactions (MCRs) play an important role in combinatorial chemistry because of its ability to synthesized small drug-like molecules with several degrees of structural diversity. A MCR is defined as three or more different starting materials that react to form a product, where most, if not all of the atoms are incorporated in the final product. This reaction tool allows compounds to be synthesized in a few steps and usually in a one-pot operation. Another typical benefit from these reactions is simplified purification, because all of the reagents are incorporated into the final product (Zhu and Bienaymé, 2006). That makes MCRs an extremely ideal and eco-friendly reaction system. One-pot (MCR) offers significant advantages over usual bimolecular reactions due to their economy, operation simplicity, convergence, structural diversity and shortness of the synthetic process (Ugi *et al*., 2001).

MCR research has become the most desirable synthetic approach favored by chemists in the industrial and academic realms(Gröger, 2003).

1.1.1. Strecker reaction

This reaction extremely famous for the synthesis of α-amino acids. This reaction is an MCR which comprises three components, aldehydes, hydrogen cyanide, and ammonia as substrares, and recognized as the world's first MCR (Gröger, 2003).

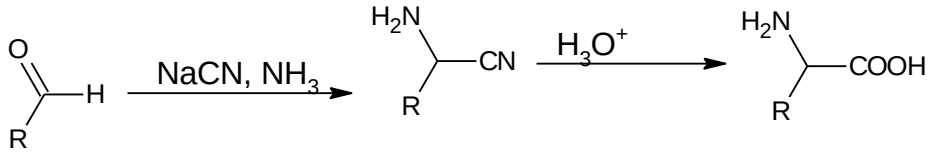

Figure (1.1): Strecker reaction.

1.1.2. Hantzsch dihydropyridine synthesis

This reaction was reported by A. R. Hantzsch, and is the best-known three-component MCR, which affords 1,4-dihydropyridine derivatives using β-keto esters, aldehydes, and ammonia (Hantzsch, 1881). For an example, a calcium channel blocker, Nifedipine is also synthesized by this reaction (Alajarín *et al*., 1992).

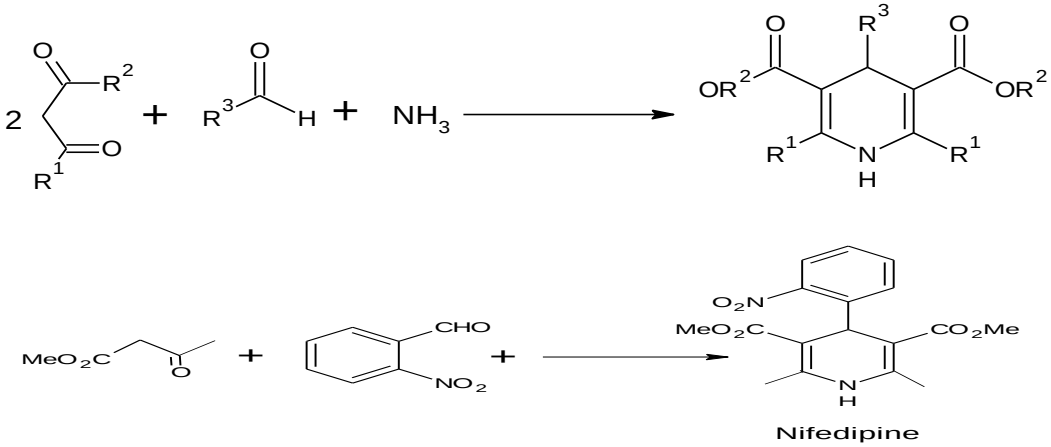

Figure (1.2): Hantzsch reaction.

1.1.3. Hantzsch pyrrole synthesis

This is a three multi-component condensation between cholroacetone, β-ketoester and a primary amine:

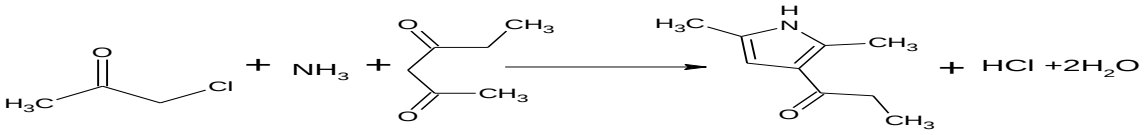

(Finar, 1967).

Figure (1.3): Hantzsch pyrrole synthesis.

1.1.4. Biginelli reaction

A three-component MCR uses β-keto esters such as ethyl acetoacetate, aromatic aldehydes such as benzaldehyde, and ureas (or thioureas) in the presence of acid catalyst (Bronsted or Lewis acids), known as Biginelli reaction affording dihydropyrimidinone derivatives (Panda *et al.,* 2012).

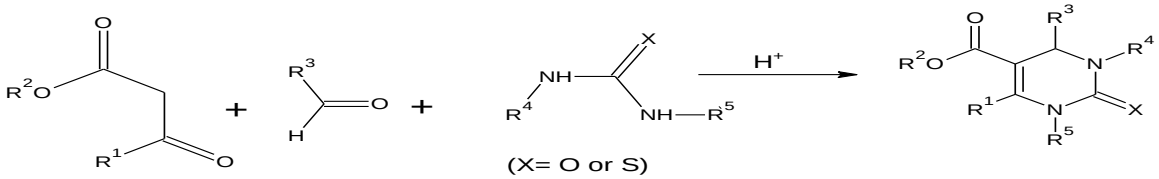

Figure (1.4): Biginelli reaction.

1.1.5. Passerini reaction

A three-component reaction Using carboxylic acids, aldehydes, and isonitriles, affording α- acyloxy amides (Domling *et al.*, 2012).

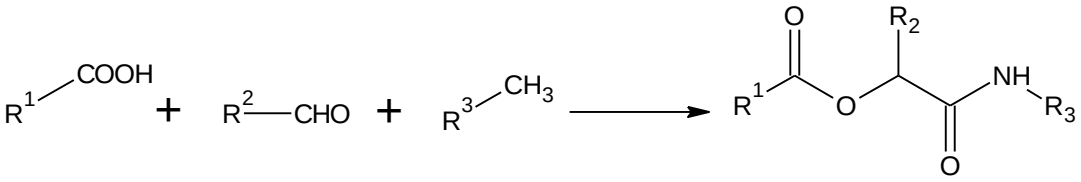

Figure (1.5) Passerini reaction.

1.1.6. Grobcke-Blackburn-Bienayme reaction

This reaction is a three- component MCR using aldehydes, isonitriles, and α-amino-azines such as 2-aminoimidazole or 2-aminopyridine in the presence of acid catalyst (Wang *et al*., 2010).

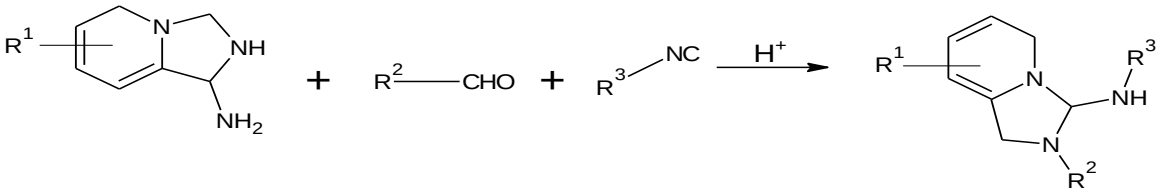

Figure (1.6): Grobcke-Blackburn- Bienayme reaction.

1.1.7. Kabachinik-fields reaction

A three-component MCR using aldehydes, amines, and dialkylphosphites in the presence of acid catalyst, affording αaminophosphonates ((Kursanov *et al*., 1952).

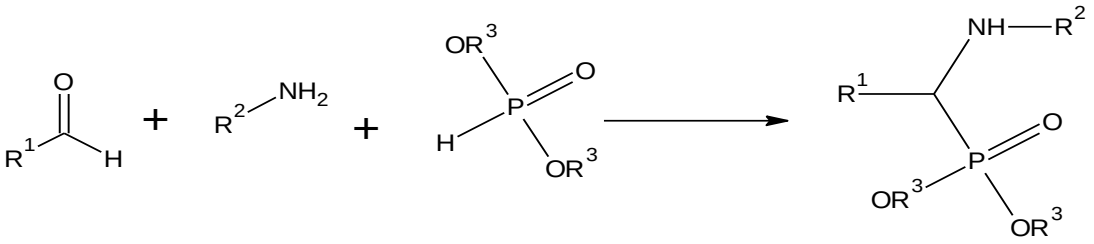

Figure (1.7): Kabachinik-fields reaction.

1.1.8. Ugi reaction

Ugi reaction is a one-pot condensation of four components (aldehydes, amines, isonitriles, and carboxylic acids), thus it can be said that the Ugi reaction is the most versatile among MCRs (Waki and Meienhofer, 1977).

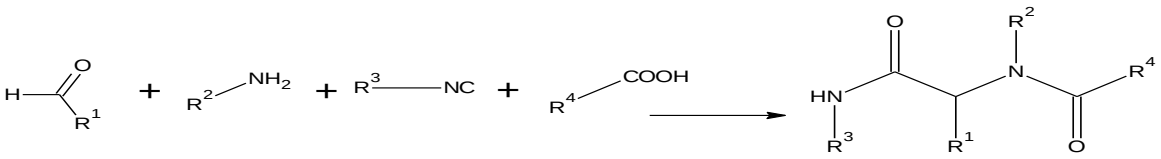

Figure (1.8): Ugi reaction.

1.1.9. The Hantzsch synthesis of 1, 4-dihydropyridine

Hantzsch reported first synthesis of symmetrically substituted 1, 4-dihydropyridine by the one-pot, four-component condensation for two molecules of ethyl acetoacetate, aromatic aldehyde and ammonia (Ghorbani *et al.*, 2008). The standard Hantzsch procedure does not need the intervention of any additive or reagent and the reaction was originally conducted either in acetic acid or at reflux in alcohol for further long periods, resulting in low or modest yields of condensation products (Leov and Association,1965). Replacement of ammonia by ammonium acetate allowed the efficient synthesis of Hantzsch compounds in aqueous medium as well as under solvent conditions (Wang *et al*., 2006). The product from the classical Hantzsch synthesis is necessarily a symmetrically substituted 1, 4-dihydropyridine, since two mole equivalents of one dicarbonyl component are utilized, the aldehyde carbonyl carbon becoming the pyridine C-4. The precise sequence of intermediate steps is not known for certain, and may indeed vary from case to case.

The 1, 4-dihydropyridines produced in this approach, carrying conjugating substituents at each β-position, are stable, and can be easily isolated before dehydrogenation.

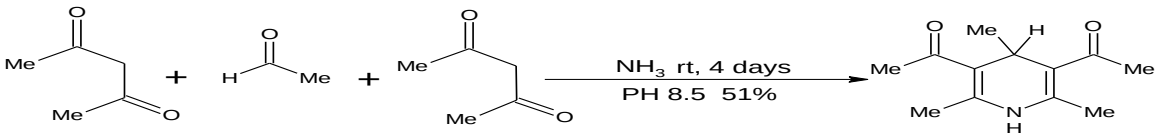

Figure (1.9a): 1, 4 –Dihydropyridine synthesis.

More often, unsymmetrical 1,4-dihydropyridines are produced by conducting the Hantzsch synthesis in two stages, i.e. by making the (presumed) aldol condensation product separately, then reacting with

ammonia and a different 1,3-dicarbonyl component, or enamino-ketone, in a second step(Joule and Mills, 2013).

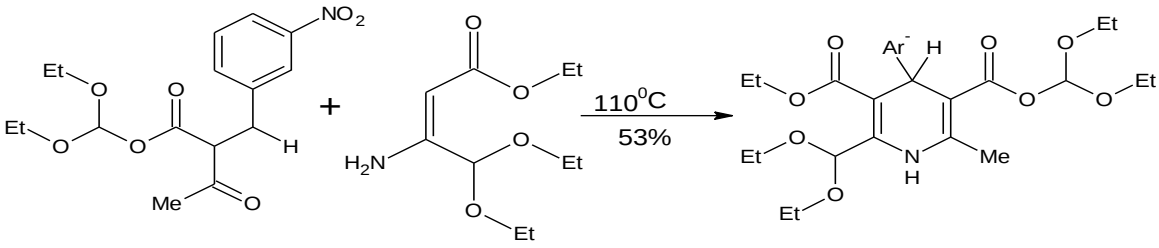

Figure (1.9b): 1, 4 –Dihydropyridine synthesis.

1.2. Acridinediones

Heterocyclic ring system, such as Acridinedione is generally considered to be among the most prevalent ring systems in medicinal chemistry (Kruithof *et al.,* 2011).

1.2.1. Synthesis of acridinediones

A rapid, improved, and environmentally benign synthesis of 4-acridinediones is reported via one pot-multicomponent reaction of aromatic aldehydes, dimedone, and ammonium acetate in water without any catalyst under micro wave irradiation. Excellent yields shortness reaction time and easy work-up are attractive features of this green protocol (Singh and Singh, 2011). The greener, clean and efficient protocol for the synthesis of Acridinedione derivatives has been achieved by reacting aromatic aldehyde, dimedone, and amines using methyltrioctylammoniumchloride as a catalyst under ultrasonic irradiations (Kaur and Kumar, 2013).

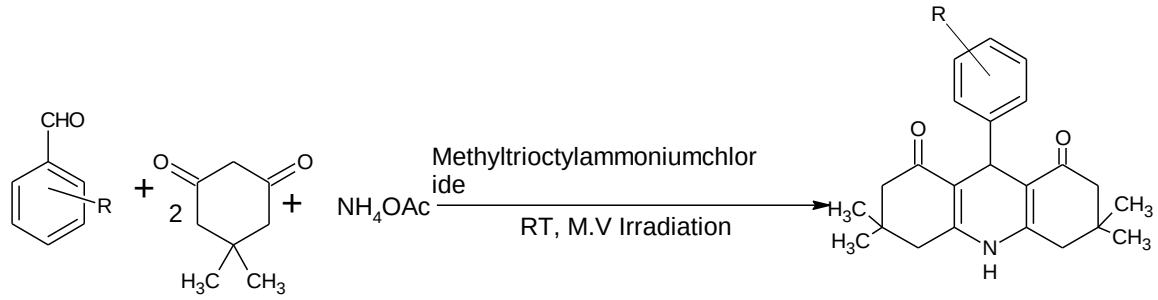

Figure (1.10): Synthesis of acridinediones under microwave irradiation.

Microwave irradiation of three component reactions of dimedone, appropriate aromatic aldehydes and amino alcohols in astoichiometrical ratio 2:1:1 for few minutes afforded acridinedione derivatives synthesized(Abdelhamid *et al*., 2014). Acridinediones containing thiourea and piperazine moieties, and vanillin derived acridinediones were synthesized (Joseph *et al*., 2005); An attempt to prepare reduced 5-quinolines from cyclo hexane-1, 3-diones (or their tautomers) and 3-amino-2-methylacrolein gave 1, 8-acridindiones with the loss of one carbon atom. The acridinediones were also synthesized from the cyclohexanedione, propanal and ammonium acetate (Ellis, 2009).

The solvent-free and aqueous conditions used to give good yields that cannot be achieved in organic solvents. The process provides a simple and green method to obtain a variety of novel unsymmetrical acridinediones, which may have potential biological activities (Guan *et al*., 2006).

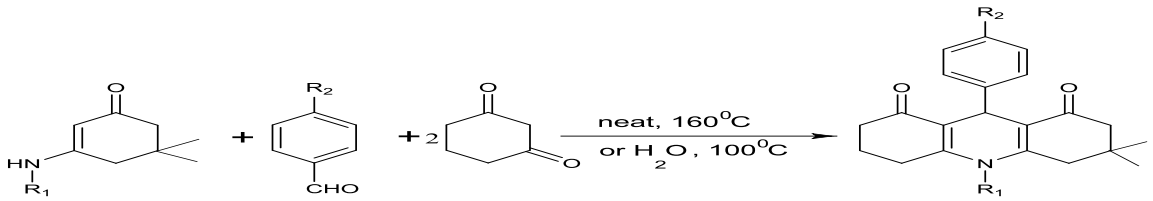

Figure (1.11): Synthesis of acridinediones under solvent-free and aqueous conditions.

CdO nanoparticle-catalyzed efficient synthesis of acridinediones by multicomponent reaction of aromatic aldehyde, cyclic diketone, and ammonium acetate has been investigated. The method has several advantages, for example high product yields, short reaction time, and simple work up procedure, and are environmentally benign. The catalyst used is inexpensive, stable, and can be recycled several times with consistent activity (Borhade *et al*., 2015) . Synthesis of 10-(halo phenyl)-9-(4-methoxyphenyl)-3, 4, 6, 7, 9, 10-hexahtdroacridine-1, 8-(2H, 5H)-Dione derivatives have been prepared and their absorption, emission properties have been evaluated.

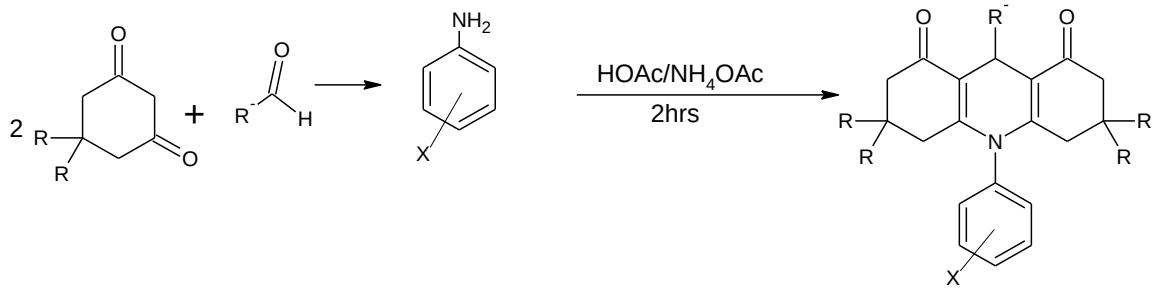

Figure (1.12): Synthesis of acridinedione by using CdO nanoparticle catalyst.

An efficient, one-pot multicomponent synthesis of novel naphthalimide-based acridine- 1,8-dione derivatives was achieved by condensation of dimedone, aromatic aldehydes, hydrazine hydrate, and 1,8-naphthanoic anhydride in the presence of a 1- Butyl-3-methylimidazolin hydrogen sulfate, [bmim] HSO_4 ionic liquid, which acts as a green solvent medium. Mild conditions with excellent conversions and simple isolation procedure are noteworthy advantages of this method. The recovery and recyclability of the ionic liquid make this protocol environmentally desirable (Kumar *et al.*, 2015).

Synthesis of an assemely of structurally important N-H and N-substituted acridine-1,8-diones by (Ceric ammonium nitrate) (CAN) catalyzed one-pot four-component reaction of electron-deficient and electron-rich aromatic aldehydes and aromatic amines or ammonium acetate and dimedone or cyclohexyl-1,3-diones at 26^0C under sonic condition is reported. The method is clean and energy efficient as it uses a green method and an eco-friendly catalyst (Sudha and Pasha, 2013). Synthesis of 1, 8-aridinediones has been developed via one-pot multicomponent conditions of 1, 3-cyclohexanedione/dimedone, aromatic aldehydes, and ammonium acetate utilizing poly (4-vinylpyridinium) hydrogen sulfate as catalyst in aqueous medium. Excellent yields in shorter reaction time, simple work-up procedure, easy recovery, and reusability for the catalyst are attractive features for this green protocol (Banothu *et al*., 2013).

1.2.2. Biological activities of acridinediones

Acridinediones containing thiourea and piperazine moieties, and vanillin derived acridinediones were synthesized. Antimicrobial activities of eight acridinediones were studied against four vibro isolates (Joseph *et al*., 2005). Deoxyfloxacine derivatives are selected from a series of synthesized 3-aryl-7-chloro-3,4-dihydro-1,9-(2H,10H) acridinediones were evaluated for blood schizontotial activities in mice infected with a sexual stages of various drug-resistant lines of P.berghei and new world monkeys infected with blood Schizonts of different chloroquine resistant strains of *P.falciparum* (Raether *et al.,* 1989).

A scaffold of N-(9-(ortho/meta/para-(benzyloxy) phenyl) -3,3,6,6-teramethyl-1,8-dioxo-1,2,3,4,5,6,7,8-octahydro-acridine-10(9H)-yl) isonicotinamide (HI-3) was reported as a SISRT1 activity. Individual 3D-QSAR analysis using Schrödinger showed distribution of hydrophobic and

non-polar positive co-efficient at ortho position essential for bioactivity (Alvala *et al.*, 2012).

Acridines the earliest known antibiotics are toxic towards bacteria and particularly towards malarial parasites due to their ability to inhibit DNA and RNA synthesis (Acheson, 1956 ; Wilson, 1992).

Acridine derivatives have a wide spectrum of biological activities as antibacterial, anti-malarial, anticancer and mutagenic properties, acridine systems have attracted considerable attention due to their potential pharmacological activity, and there are many industrial applications for acridine derivatives. (Srividya *et al.*, 1996).

Acridinium cations substituted at the endocyclic N atom find numerous applications in immunological assays as well as in chemical, biochemical and environmental analyses (Wróblewska *et al*., 2004). acridine systems have antileshmanial activities (Julien *et al*., 2005). DNA-binding and DNA photo-damaging ability (Hardman, 2006).

1.3. Polyhydroquinoline derivatives

1.3.1. Synthesis of polyhydroquinoline derivatives

Polyhydroquinoline have been synthesized in good to excellent yields (80-90%) and short times (15- 30 min) in the presence of aluminum phosphate [$AlPO_4$]which can be easily separated from the product and reused (Purandhar *et al.*, 2012). The synthesis of polyhydroquinoline derivatives via a four-component unsymmetrical Hantzsch reaction induced by solar thermal energy is reported.

The process proved to be simple, environmentally friendly, and economic and high yielding (Mekheimer *et al*., 2008).

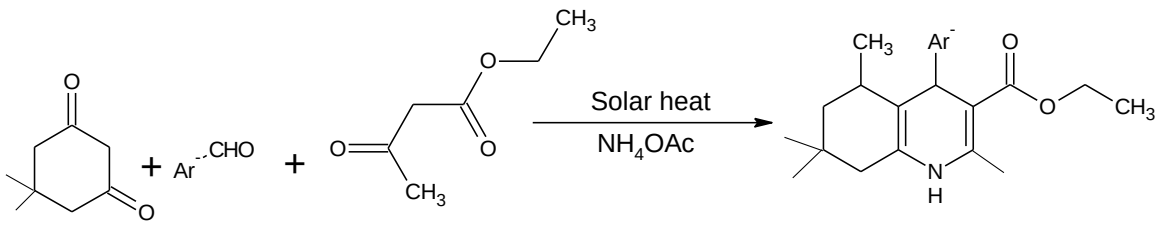

Figure (1.13): Synthesis of polyhydroquinoline derivatives by solar thermal energy.

An efficient and newer Hantzsch reaction of the synthesis of polyhydroquinoline derivatives have been reported via four-component condensation of aldehydes, cyclic 1,3-diketones, β-keto esters, NH_4OAc and catalytic amount of ionic liquid 1-vinyl-3-Ethyl imidazolium iodide. This methodology is operationally simple, economical, rapid and high yielding (Nirmal *et al.*, 2010). Thiourea dioxide (TUD) in water was found to be an efficient and reusable organo catalyst system for the one-pot synthesis of polyhydroquinoline derivatives via the Hantzsch-type coupling of aldehyde, dimedone, acetoacetate, and ammonium acetate under mild reaction conditions. The use of an economically affordable catalyst, environmentally benign conditions, high product yields, and reusability of the catalyst system were the advantageous features of the developed method (Kumar *et al.*, 2012).

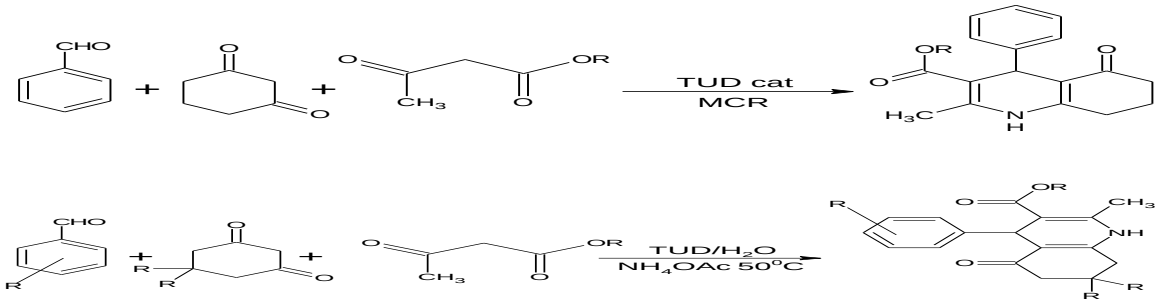

Figure (1.14): Synthesis of polyhydroquinoline derivatives by using thiourea dioxide in water.

Ytterbium(III) triflouromethanesulfonate $Yb(OTF)_3$ catalyzed an efficient, operationally simple and environmentally benign Hantzsch reaction via a four-component coupling reaction of aldehydes, dimedone, ethyl acetoacetate and ammonium acetate at ambient temperature to yield polyhydroquinoline derivatives in an excellent yield (Wang *et al*., 2005).

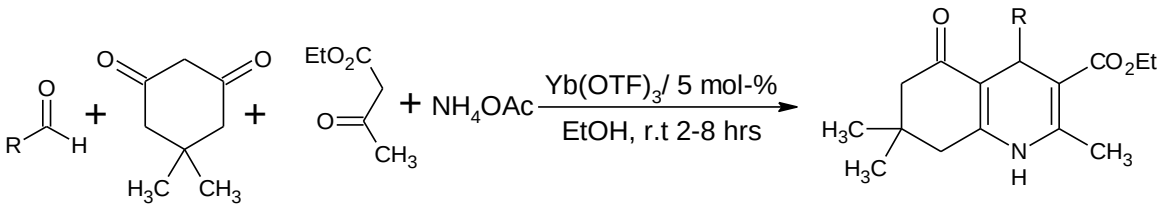

Figure (1.15): Synthesis of polyhydroquinoline derivatives by using Yb $(OTf)_3$ as catalyst.

Hantzsch 1, 4-dihydropyridine and polyhydroquinoline derivatives were synthesized in excellent yields in aqueous micelles. The reaction is catalyzed By (Para toluene sulfonic acid) PTSA and strongly accelerated by ultrasonic irradiation (Kumar and Maurya, 2008).

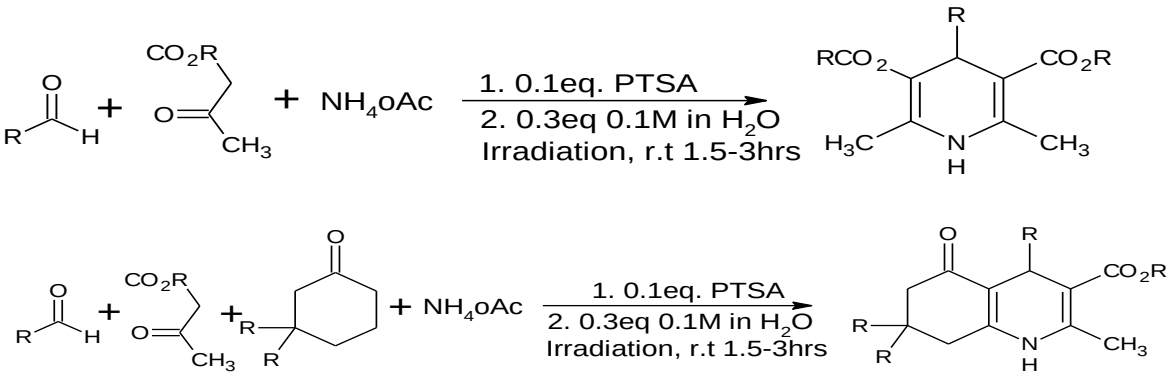

Figure (1.16): Synthesis of polyhydroquinoline derivatives in aqueous micelles.

A simple and convenient protocol is described for the preparation of polyhydroquinoline via one-pot, multicomponent reaction of an aromatic aldehyde, ethyl acetoacetate, ammonium acetate, and dimedone using iron

loaded mesoporous materials as an efficient catalyst in good yields (Heravi *et al.*, 2010). Sulfonic acid functionalized SBA-15(SBA-pr-SO_3H) as a new nanoporous acid catalyst was used in the one-pot synthesis of polyhydroquinoline derivatives via the Hantzsch four component condensation reaction of aldehyde, β-ketoesters, dimedone and ammonium acetate under solvent free conditions with short reaction time in excellent yields. SBA-Pr-SO_3H was proved to be an efficient heterogeneous nanoporous solid acid catalyst which could be easily handled and removed from the reaction mixture by simple filtration, and also recovered and reused without loss of reactivity (Mohammadi *et al.*, 2010).

Polyhydroquinoline derivatives have been prepared efficiently in a one-pot synthesis via Hantzsch condensation using nano sized Nickel (Ni) as a catalyst. The method does not involve any hazardous organic solvents or catalyst. The smaller size of Ni having a higher surface to volume ratio has promising features for the reaction response such as the shortest reaction time, excellent product yields, simple work-up procedure, and purification by non-chromatographic methods (Sapkal *et al.*, 2009).

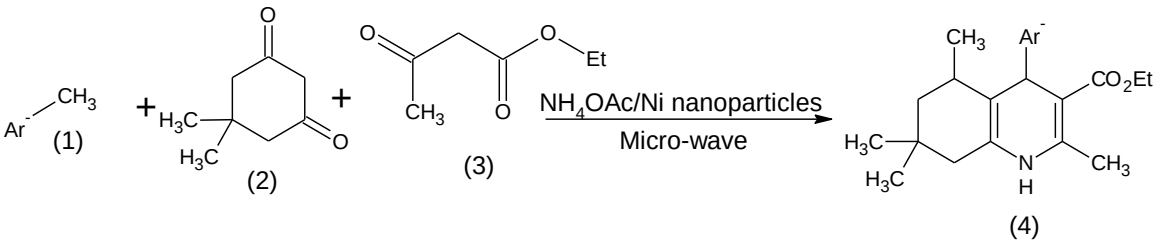

Figure (1.17): Synthesis of polyhydroquinoline derivatives using nano sized Nickel.

L-proline has been found as an efficient catalyst for the one-pot synthesis of polyhydroquinoline derivatives via four component Hantzsch reaction. This method provides several advantages such as being environmentally benign,

possessing high yields with increased variations of the substituents in the product and preparative simplicity (Karade *et al.,* 2007).

Polyhydroquinoline derivatives have been prepared efficiently in one-pot synthesis via Hantzsch condensation using a hydrogen Cesium salt of dodecatungstophosphoric acid $Cs_{2.5}H_{0.5}PW_{12}O_{40}$ as a heterogeneous and reusable catalyst. Methodology offers several advantages such as simple procedure, excellent yields, and a short reaction time (Khabazzadeh *et al.*, 2012). A facile and efficient one-pot, four component synthesis of polyhydroquinoline derivatives via the Hantzsch condensation reaction using sulphamic acid as heterogeneous catalyst by green approach are described. Methodology offers several advantages such as excellent yields, economy of cost and time, absence of side products and operational simplicity, eco-friendly, recyclability and reusability of the catalyst are some of the salient features of this reaction (Lambat *et al.,* 2014) .

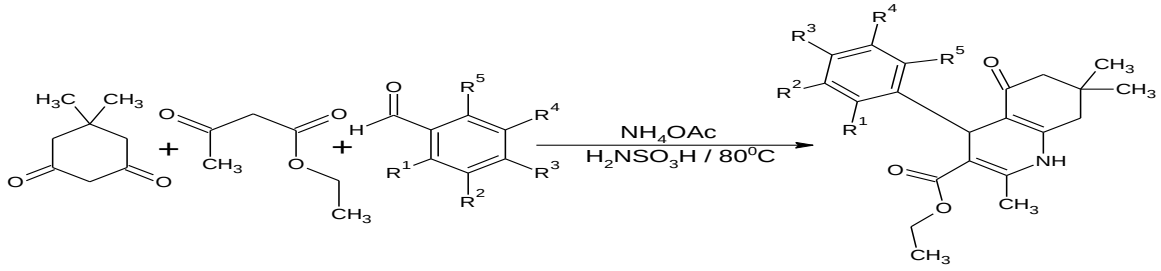

Figure (1.18): Synthesis of polyhydroquinoline derivatives using sulphamic acid as catalyst.

A simple and convenient protocol is described for the preparation of polyhydroquinoline via one-pot multicomponent reaction of an aromatic aldehyde, ethyl acetoacetate, ammonium acetate and dimedone using iron loaded mesoporous materials as an efficient catalyst in good yields (Ashraf *et al.,* 2020). Copper perchlorate hexahydrate as an efficient catalyst was used for the synthesis of Polyhydroquinolines by four-component

condensation reaction of aldehyde, ethyl acetoacetate, dimedone, and ammonium acetate in excellent yields and short reaction time at room temperature under ultrasound irradiation. This novel synthetic method is especially favoured because it provides synergy between copper perchlorate hexahydrate and ultrasound irradiation which offers the advantages of high yields, short reaction times, simplicity, and easy work-up compared to the conventional methods reported in literature (Puri *et al.*, 2011).

1.3.2. Biological activities of polyhydroquinolines

Polyhydroquinolines (PHQs) derivatives are of considerable interest due to their widespread biological properties which expands their applications as vasodilator, antitumor, bronchodilator, anti-atherosclerotic, gyro-protective and heptoprotective agent (Nikpassand *et al*., 2009). Furthermore, these compounds exhibit diverse medicinal utility such as neuroprotectant, platelet antiaggregatory activity and chemsensitzer acting in tumor therapy (Safari *et al.*, 2011).

Among the nitrogen heterocycles, polyhydroquinoline derivatives are a significant class of well-known calcium Ca^{+2} channel blockers and establish the skeletons of drug molecules utilized in the treatment of hypertension and cardiovascular diseases (Nishiya *et al*., 2002).

These heterocycles possess a wide range of biological activities such as antitumor, bronchodilator, vasodilator and antiatherosccclerotic and antidiabetic properties (Van der Lee *et al.*, 2000); (Sirisha *et al.*, 2010); (Bazargan *et al*., 2008). These derivatives are also utilized as antiishemics and in the treatment of Alzheimer‘s disease(Guven *et al.*, 2005). These facts expose the noteworthy pharmacological use of polyhydroquinolines as drug moieties in organic synthesis. As a result, the synthesis of

polyhydroquinolines has become an area of remarkable attention (Jadhvar *et al.*, 2017).

1.4. Quantitative structure activity relationship (QSAR)

Quantitative structure activity relationships, often simply known as QSARs, are an analytical application that can be used to interpret the quantitative relationship between the biological activities of a particular molecules and its structure. It is considered a major method of chemical researching all over world today and is frequently used in agricultural, biological, environmental, medicinal, and physical organic studies (Perkins *et al.*, 2003).

Many types of model are possible, with mathematical and statistical models being particularly common. Such models are often referred to as Quantitative Structure-Activity Relationships (QSARs) or Quantitative structure-property relationships (QSPRs) (Tropsha *et al*. 2003). Hansch was the first one to use QSARs to explain the biological activity of series of structurally related molecules (Fujita *et al.*, 1964); (Hansch *et al.*, 1968). Hansch pioneered the use of descriptors related to a molecule's electronic characteristics and to its hydrophobicity. This led him to propose that biological activity could be related to the molecular structure via equations of the following form: $\text{Log } (1/C) = K_1\text{LogP}+K_2\sigma+K_3$

C= the concentration of compound required to produce a standard response a given time.

Log P= the logarithm of the molecule's partition coefficient between 1-octanol and water.

σ = the appropriate Hammett substitution parameter.

K_1, K_2, K_3 = constants derived from regression analysis

This formalism expresses both sides of the equation in terms of free energy.

Hansch rationale for suggesting the parabolic dependence on log p was that the drug's hydrophobicity should not be so low that the drug did not partion into the cell membrane or so high that once in the membrane it simply remained there.

An early example of such a non-linear relationship between a biological response and the partition coefficient is the following equation derived for the narcotic effect of thirteen barbiturates on mice (Hansch *et al*., 1968).

Log $(1/C)$ = -0.44$(\log P)$ + 1.93

The electronic characteristics of a molecule are also important in determining its activity against the target: the Hammett parameters provided a concise and convenient way to quantify these. Hammett and others had shown that for related compounds reaction rate (e.g. for the ionization constants of substituted benzoic acid) could be quantified using equations of the following form (Leach and Gillet, 2007). Log $(k/k^o) = \rho\sigma$, Log $(K/K^O) = \rho\sigma$

k= these equations express the rate or equilibrium

K= constant for a particular substituent relative to that for a reference compound (indicated using the subscript and typically that for which the substituent is hydrogen).

The substituent parameter σ is determined by the nature of the substituent and whether it is *meta para* to the carboxylic acid or ester on the aromatic ring.

The so-called 3D-QSAR models, however, are more representative of these new QSAR methods, and the *Comparative Molecular Field Analysis* (COMFA) method is probably one of the most of these.

In the (COMFA) method, the molecular descriptors are taken as steric and electric fields calculated at a large number of points surrounding each molecule (Cronin, 2010).

The main problem with 3D-QSAR methods such as (COMFA) is the alignment of the molecules in the test set (Sullivan *et al*., 2000). Biological activity can be expressed quantitatively as a function of structure described by electronic attributes, hydrophobicity, and steric properties to give a certain biological response (Hansch,1979). Additionally, when physiochemical properties or structures are expressed by numbers, it can form a mathematical relationship, or quantitative activity- relationship, between the two. The mathematical expression can then be used to predict biological response of other chemical structures. Recently, computational techniques have ensured to delineate and refine the many variables and approaches that define the QSAR paradigm.

It is more than a century ago that the QSAR paradigm first found its way into the practice of pharmaceutical chemistry and toxicology. Grum-Brown and Fraser expressed the idea that physiochemical action of a substrate or ligand could expressed as a function of its chemical composition and constitution (Selassie and Verma, 2003). In 1893 Richert showed that the cytotoxicity of adverse set of single organic molecules was inversely related to their corresponding water solubility. In the 20 century, Meyer and overtone independently suggested that the narcotic (depressant) action of a group of organic compounds is correlated with their olive oil water partition coefficient in a parallel manner (Selassie and Verma, 2003).

In 1939, Ferguson introduced a thermodynamic generalization to the correlation of dependent action with relative saturation of volatile

compounds. Bell and Robin, on the other hand established the importance of ionization of bases and weak acids in bacteriostatic activity (Ishikawa *et al.*, 2012).

The modern QSAR paradigm with the molecular mechanistic basis was implemented by Hansch and Fujita, using octanol/water system, a whole series of partion coefficient were measure, and thus new hydrophobic scale was introduced (Selassie and Verma, 2003). In the QSAR paradigm, the basic assumption for all molecule-based hypotheses is that similar molecules have similar activities. The underlying problem is therefore, how to define small difference on a molecular level, since each kind of activity, e.g. reaction ability biotransformation ability, solubility, target activity, and so on, might depend on another difference.

1.4.1. Importance of validation of QSAR models

The QSAR models are useful for various purposes including the prediction of activities of untested chemicals. The success of drug discovery efforts depends heavily on the use of structure-activity relationship techniques (Kolossov and Stanforth, 2007). Over the years of development, many methods, algorithms and techniques have been applied in QSAR studies (Jalali *et al*., 2008). Main challenge in QSAR is to select the group of descriptors which describe the most critical structural and physiochemical features associated with activity. Quality of biological data and the effective descriptor or variable selection is an initial essential part of the QSAR modeling process.

The application of QSAR model is depend on statistical significance and predictive ability of these models. The regulatory decisions, justification of usage and use of a particular QSAR is depending on the model ability to predict unknown chemicals with some more degree of certainty. QSAR

model can lead to false prediction of biological activity if the developed QSAR model is not validated. So validation of QSAR models, after model development, is most important part in QSAR studies (Veerasamy *et al.*, 2011).

1.4.2. Validation methods for QSAR models

Validation methods are needed to establish the predictiveness of a model on unseen data and to help determine the complexity of an equation that the amount of data justifies. Using the data that created the model (an external method) can help validate the QSAR model. The methods of least squares fit (R^2), cross validation (Q^2**)**, adjusted R^2 (R^2 Adjusted), chi-squared test (x^2), root-mean-squared error (RMSE), bootstrapping and scrambling (Y-Randomization) are internal methods of validating a model. The best method of validating a model is an external method, such as evaluating the QSAR model on a test set of compounds. These are statistical methodologies used to ensure the models created are sound and unbiased (good model). A poor model can do more harm than good, thus confirming the model is a good model is of utmost importance (Veerasamy *et al.*, 2011).

1.4.3. Internal validation

The most common internal method of validating the model is least squares fitting. This method of validation is similar to linear regression and is the R^2 (squared correlation coefficient) for the comparison between the predicted and the experimental activities. The difference between the R^2 and R^2 adjusted value is less than 0.3 indicates that the number of descriptors involved in the QSAR model is acceptable. The number of descriptors is not acceptable if the difference is more than 0.3. Fit of the QSAR models can be determined by the methods of chi-squared (x^2) and root-mean squared error

(RMSE). These methods are used to decide if the model possesses the predictive quality reflected in the R^2. The chi squared value exhibits the difference between the experimental and predicted bioactivities.

Large chi-square or RMSE values (>0.5 and1.0, respectively) reflect the model is poor ability to accurately predict the bioactivities even the model is having large R^2 value (>0.7). For good predictive model the chi and RMSE values should be low (< 0.5 and >0.3, respectively). However, excellent values of R^2, X^2 and RMSE are not sufficient indicators of model validity. Thus, alternative parameters must be provided to indicate the predictive ability of models. In principle, two reasonable approaches of validation can be envisaged one based on prediction and the other based on the fit of the predictor variables to rearranged response variables(Veerasamy *et al.*, 2011)

1.4.4. Cross validation

A common method for internally validating a QSAR model is cross validation (CV) Q^2, q2 or jack-knifing). The jack-knife is an alternative resampling scheme used for bias correction and variance estimation that predates the bootstrap. Jack-knife analysis showed that hypactivations in right inferior frontal gyrus and caudate nucleus were found in all combinations of studies, including a high replicability. It is a rough and ready that can improvise a solution for a variety of problems even through specific problems may be more efficiently solved with a purpose designed tool (Cameron *et al*., 2005). (CV) process repeats the regression many times on subset of data. Usually each molecule is left out once (only), in turn and the R is computed using the predicted values of the missing molecule. Sometimes more than one molecule leave more out (LMO) is left out at a time. CV is often used to determine how large a model can be used for a given data set. A cross validated R^2 is usually smaller than the overall R^2 for

a QSAR equation. It is used as a diagnostic tool to evaluate the predictive power of an equation.

CV used to measure a model predictive ability and draw attention to the possibility a model has been over fitting refers to the phenomenon in which a predictive model may well describe the relationship between predictors and response, but many subsequently fail to provide valid predictions for new compounds. Over fitting of the model is usually suspected when the R^2 value from the original model is significantly larger (25%) than the Q^2 value (the difference between R^2 and Q^2 should not be more than 0.3). CV values are considered more characteristic of the predictive ability of the model. Thus, CV is considered a measure of goodness of prediction and not fit in the case of R^2. The process of CV begins with the removal of or a group of compounds, which becomes a temporary test set, from the training set. A CV model is created from the remaining data points using the descriptors from the original model, and tested on the removed molecules for its ability to correctly predict the bioactivities (Veerasamy *et al*., 2011).

1.4.5. External validation

The only way to estimate the true predictive power of a QSAR model is to compare the predicted and observed activities of an (sufficiently large) external test set of compounds that were not used in the model development. The problem in external validation is how to select the training set and test set?

To estimate the predictive power of a QSAR model, Golbraikh and Tropsha recommended use of the following statistical characteristics of the test set, correlation coefficient R between the predicted and observed activities; coefficient of determination (R^2) , and slopes k and k` of the regression lines

through the origin. A developed QSAR model can be accepted generally by multi-linear regression and partial least squares (MLR and PLS) in QSAR studies when it can satisfy the following criterion (The following values are the minimum recommended values for significant model:

-If correlation coefficient $R \geq 0.8$ (for in vivo data)

-If coefficient of determination $(R^2) \geq 0.6$.

-If the standard deviation s is not much larger than standard deviation of the biological data.

-If its F value indicate that overall significance level is better than 95%.

-If its confidence interval of all individual regression coefficients provides that they are justified at the 95% significance level.

-If cross validated R^2 $(Q^2) > 0.6$.

-If R^2 for external test set $R^2_{pre} > 0.6$.

-Randomized R^2 value should be as low as to R^2

-Randomized (Q^2) value should be as low as to Q^2.

-In addition, the biological data should cover at least one, two or even more logarithmic units: they should be well distributed over whole distance. Also, physiochemical parameter should be spread over a certain range and should be more or less evenly distributed. (Veerasamy *et al.,* 2011).

1.4.6. The needs of QSAR model

All chemical substances need to be tested in terms of their toxicological and environmental properties before their use. There are several reasons to use QSAR models as they very fast, often free, reduce the number of animals used in experiments (Gadaleta *et al.,* 2016).

1.4.7. Purpose of QSAR

1- To predict biological activity and physiochemical properties by rational means.

2- To comprehend and rationalize the mechanism of action within a series of chemicals.

3- Saving in the cost of product development.

4- Prediction could reduce the requirement for length and expensive animal tests.

5- Reduction of animal tests, thus, reducing animal use and obviously pain and discomfort to animals.

6- Other areas of promoting green and greener chemistry to increase efficiency and eliminate waste (Puzyn *et al.*, 2010).

1.4.8. Requirements for QSAR

1- Set of molecules.

2- Set of molecular descriptors.

3- Measured biological activity or property.

4- Statistical methods

(Tropsha, 2010).

1.4.9. The number of compounds required to develop a QSAR

To provide some guide, it is widely accepted that between five and ten compounds are required for every descriptor in a QSAR (Aptula and Ropers, 2006). The QSAR model should meet the requirements of the Organisation of economic co- operation and development (OECD) principles:

1-A defined endpoint

2-An unambiguous logarithm

3-Adefined domain of applicability

4-Appropriate measures and predictively

5-A mechanistic interpretation if possible (Tropsha, 2010).

1.4.10. SAR model common errors

1-Uninformative descriptors

2-Poor descriptor selection and chance correlations

3-Modeling complex, nonlinear structure property relationships with linear models

4-Incorrectly validating QSAR models

5-Not understanding the domain of applicability of models (Greenland, 1989).

1.4.11. Methods of QSAR modeling

QSAR Modeling process consists of five main steps:

1-Begins with the selection of molecules to be used.

2-Selection of descriptors; numerical represents of molecular features, e.g. number of carbon atoms.

3-Original descriptor pool must be reduced in size.

4-Model building

5-The reliability of the model should be tested (Khan, 2016).

1.4.12. The main steps of QSAR

1-Molecular structure

2-Molecular Descriptors

3-Predictive Model

4-Model Validation

5-Applicabily Domain of QSAR.

1.4.13. Applications of QSAR

There are a large number of applications of these models within industry, academia and governmental (regulatory) agencies:

1-The estimation of physio-chemical properties, biological activities and understanding the physio-chemical features behind a biological response in drug designing.

2-The rational design of numerous other products such as surface active agents, perfumes, dyes, and fine chemicals.

3-The prediction of fate of molecules.

4-The identification of hazardous compounds at every stages of product development, the prediction of toxicity to human and environment (Abdel-llah *et al.*, 2017).

1.5. Molecular modeling and computational chemistry

1.5.1. The definition of molecular modeling

Molecular modeling is anything that requires the use of a computer to point, describe or evaluate any aspect of the properties of the structure of a molecule (Boyd, 1990). Methods used in the molecular modeling arena regard automatic structure generation, analysis of three-dimensional (3D) databases, and construction of protein models by techniques based on sequence homology, diversity analysis, docking of ligands or continuum methods. Thus, today molecular modeling is regarded as a field concerned with the use of all sort of different strategies to model and to deduce information of a system at the atomic level. On the other hand, this discipline includes all methodologies used in computational chemistry, like computation of the energy of a molecular system, energy minimization, Monte Carlo methods or molecular dynamics. In other words, it is possible to conclude that computational chemistry is the nucleus of molecular modeling. Identification of bimolecular moieties involved in the interaction with a specific receptor permits to understand the molecular mechanism

responsible of its specific biological activity. In turn, this knowledge is aimed at designing new active molecules that can be successfully used as drugs. Due to the fact that simulation accuracy is limited to the precision of the constructed models, when it is possible, computational simulations have to be compared with experimental results to confirm model accuracy and to modify them if necessary, in order to obtain better representations of the system (Patny *et al.,* 2006).

To use these tools for effectively, need to understand the method of implementation of this technique and the nature of the database used in the Parameterization of the method. With this knowledge, can redesign the tools for specific investigations and define the limits of confidence in results (Veerasamy *et al.,* 2011).

1.5.2. Molecular modeling and drug design

Molecular modeling is a tool for doing chemistry. Models are central for understanding of chemistry. Molecular modeling allows doing and teaching better by providing better tools for investigating, interpreting, explaining and discovering new phenomena. Molecular modeling is easy to perform with currently available software, but the difficulty lies in getting the right model and proper interpretation. Molecular modeling is the general term used to describe the use of computers to construct molecules and perform a variety of calculations on those molecules in order to predict their chemical characteristics and behavior. The term molecular modeling is often used synonymously with the term computational chemistry. Computational chemistry is a broader term, referring to any use of computers to study chemical systems.

Molecular modeling encompasses all theoretical methods and computational techniques use to model or mimic the behavior of molecules. The techniques

are used in the field of computational chemistry, computational biology and materials science for studying molecular systems to large biological molecules and material assemblies (Mukesh and Rakesh, 2011).

Drug design is a process which is driven by technological breakthrough implying advance experimental and computational methods. Nowadays, the techniques or the drug design methods are of paramount importance for prediction of biological profile, identification of hits, generation of leads, and moreover to accelerate the optimization of leads into drug candidates (Patel *et al.*, 2014).

Drug discovery has often evolved from serendipitous and fortuitous findings, for example, the discovery of penicillin by Alexander Fleming in 1928 triggered the Antibiotic Revolution which contributed tremendously to humankind`s quest of longevity. If not by chance, such discoveries may be achieved through random systematic experimentation or chemical intuition where combinatorial libraries are synthesized and screened for potent activities. Such approach is extremely time consuming, labor intensive, and impractical in term of costs. A more lucrative solution to this problem is too rationally design drugs using computer-aided tools via molecular modeling, simulation, and virtual screening for the purpose of identifying promising candidates prior to synthesis (Nantasenamat *et al.*, 2009).

1.6. Docking study

Molecular docking of the drug molecule with the receptor (target) gives important information about drug receptor interactions and its commonly used to fine out the binding orientation of drug candidates to their protein targets in order to predict the affinity and activity ((Bano *et al*. 2015)).

Molecular docking software's are mainly used in drug development. The most important application of docking software is virtual screening. In virtual screening molecules are selected from existing database for further research (Mukesh and Rakesh 2011) .

Some of acridinedione derivatives were subjected to docking study to investigate their binding mechanism with 5MO7 protein which down loaded from protein data bank (PDB). Doxorubicin was used as a reference drug, molecular docking of the ligand was carried out and corresponding docking score which was obtained. See table (2.14).

1.6.1. Main steps in molecular docking

1- Step one: building the receptor.

Downloaded PDB structure of the receptor.

Removal of the water molecules from the protein cavity, and stabilizing charges, filling in the missing residues, and generation the side chains.

2- Step two: Identification of the active site.

After the receptor is build, the active site within the receptor should be identified.

The receptor may have active sites but the one of the interest should be selected.

3- Step three: Ligands preparation.

Ligands can be obtained from various databases like Zinc, pubChem or can be sketched using tools like ChemSketch.

While selecting the ligand, the Lipinski rule of five should be applied.

4- Step four: Docking:

This is the final step, where the ligand is docked onto the receptor and the interactions were checked. The scoring function generates scores depending on which the ligand with the best fit is selected (Torres *et al*., 2019).

1.7. Aims and objectives

The main aim and objectives of this study can be summarized shortly as:

- ✓ Quantitative structure activity relationship (QSAR).
- ✓ Molecular modeling and structure drug design.
- ✓ Docking studies of designed compounds.
- ✓ Synthesis of certain designed N-substituted acridinedione derivatives through one-pot Hantzsch condensation approach.
- ✓ Synthetic designing of the target molecules and their preparation based upon retro- synthetic analysis and disconnection approach.
- ✓ Analysis of the synthesized compounds using spectroscopic instruments such as IR, ^{1}HNMR, and Mass spectroscopy (MS).
- ✓ Testing some of the synthesized compounds for possible biological activities if possible.

2. Materials and methods

2.1. Materials, soft wares and instruments

2. 1.1. Materials

2. 1.1.1. Common reagents

Hydrochloric acid, iodine, silica gel G and concentrated sulphuric acid, are obtained from Ridle DeHean, AG, West Germany.

2.1.1.2. Chemicals

Dimedone, 99.5% AR (Methon) UN No. : NA LOBA Chemie CAS: 126818. (India). Aromatic aldehydes include: N, N-dimethyl benzaldehyde, benzaldehyde, vanillin, cinnamaldehtde, and salicylaldehyde. Obtained from Alpha Chemika India, Ethyl acetoacetate Assay >98% Alpha Chemika India, Sulfanilamide Assay 99% Lab Cheime pvt. Ltd. India, and Aniline Assay 99% Alpha Chemika, India.

2. 1.1.3. Solvents

Acetone Assay (GC) 99% LOBA Chemie India, Methanol Assay 97% , Chloroform Assay 99.5% Alpha Chemika India, Diethyl ether, Ethanol Assay 99.8% Mombai-400005. India. Petroleum ether and Hexane was obtained from Central Drug House (P) Ltd. Bombay, New Delhi.

2. 1.1.4. Thin Layer Chromatography (TLC)

Thin Layer Chromatography was carried out using Per-coated plates (Aluminum), or in plastic or by using Silica Gel 60 GF_{254} coated in glass plate's slides (Merk, Germany), with different mobile phases (solvent system).

2.1.2. Database

In this QSAR studies, a total of 6 substituted acridinedione aerivatives were gathered from (Jamalian *et al*., 2011). The *vitro cytotoxicity* of these

derivatives was reported against various human cancer cell lines (Hela, MCF-7, LS-180, and Raji cells). The target human cell line in this study is human breast cancer cells (MCF-7 adenocarcinoma cells). Its biological activities were expressed as IC_{50} (the concentration of drug at which 50% of the target is inhibited), and were compared with Doxorubicin as a reference drug, for group (I).

Also, in this QSAR studies, a total of 15 substituted hexahydroquinoline derivatives were gathered from (Gündüz *et al.*, 2009). The in vitro of these derivatives was reported as Calcium Channel Modulators, in rat ileum and rat thorasic aorta, the group (II).

2.1.3. Soft wares

2.1.3.1. ACD/Labs software

ACD/ChemSketch is a modeling program used to create and modify images of chemical structures. Also there is software that allows molecules and molecular models displayed in two and three dimensions, to understand the structure of chemical bonds and the nature of the functional groups.

Using ACD/ChemSketch is primarily for educational use. With this program it is possible to write and perform chemical equations, diagrams laboratories and chemical structures of various entities.

ACD/Lab free ware 2015 downloaded from www. ACD/labs.com. There were two modes to ACD/Chem. sketch, namely structure and draw, structure mode was used to draw chemical molecules, while draw mode used to create and edit graphical objects. Upon startup, the draw normal mode and carbon automatically selected by clicking and dragging the cursor in the windows, C-C bonds were created. Clicking on carbon atom produced a brace

structure. The change was made by selecting heteroatom from the element list in the left lobar and clicking .On an atom in the structure to repeat it.

Radicals were made by selecting it from table which including carbon ring, carbon-based side chain and functional groups. A reaction requires were drawing by using the reaction arrow and reaction plus icons. Bond lengths and bond angle standardized by clicking on clean structure. The calculated properties were inserted into the chemo sketch window as text field; on the tools menu, point to calculate and choose the desired property. By selecting structure and clicking on generating name for structure, the IUPAC name was generated as text field underneath the structure

2.1.3.2. Molecular operating environment (MOE) software

MOE is a molecular modeling program, which is specifically designed to handle large biological molecules. MOE is a drug discovery software platform that integrates visualization, modeling and simulations, as well as methodology development, in one package. It‘s scientific applications are used by biologist, medicinal chemist and computational chemists in pharmaceutical, biotechnology and academic research.

2.1.3.3. Statistical package for social sciences (SPSS) software

SPSS is a package of programs for manipulating, analyzing, andpresenting data; the package is widely used in the social and behavioral sciences.

2.2. Spectroscopic methods

2. 2.1. Infra-red spectroscopy (IR)

Infra-Red (IR) was recorded on FT-IR-8400s instrument (SIMADZU, Japan) using KBr disc.

2.2.2. Ultra violet spectrophotometer (UV)

Ultra violet spectral data were obtained using UV- 310IPC- Shimadzu-Japan.

2.2.3. Proton-nuclear magnetic resonance (^{1}HNMR)

(^{1}HNMR) was recorded on ultrashield-500 plus instrument (BRUKER), Germany using DMSO as solvent and operating at 500.13 MHz for protons. Employing a 5mm high resolution broad-band tetra methyl silane (TMS).

2. 2.4.Gas chromatography- Mass spectrometer (GC- MS)

The mass spectra were recorded on Gas chromatography-Mass spectrometer GC- MS instrument Shimadzu Model QP-2010 EX plus spectrometer.

2.3. General instruments

Electronic sensitive balance, Japan. Magnetic stirrer with hot plate BTL, England. Melting point apparatus, Gallenkamp, Cat. No. MFO 600,010 and another one made in UK by Bibby Sterilin Ltd, Stone, and Staffordshire.

2.3. Methods

2.3.1. QSAR modeling

The activity in terms of IC_{50} for training set and IC_{50} for test set compounds was expressed in microgram per milliliter were converted to the negative logarithmic concentration in moles (anti-cancer potential PIC_{50}), in order to obtain higher mathematical values when the structures are biologically very efficient (Mahama *et al*., 2020) .

The anti-cancer activity which is expressed by the anti-cancer potential.

ChemSketch/ADC/lab software was used for drawing sets of studied compounds see table (2.1) and (2.2). Then the data sets of the Imidazolyl derivatives of 1, 8- acridinediones were divided into two sets, training set (9 compounds) and test set (2), random selection.

Table (2.1): Structures, IC_{50}, and PIC_{50} of the derivatives of imidazolyl derivatives of 1, 8-acridinediones, the training sets, and test set (Jamalian *et al.*, 2011):-

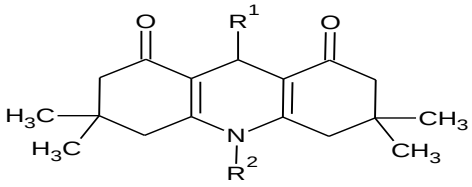

Comp. No	R_1	R_2	IC_{50}	PIC_{50} (exp)	PIC_{50} (pred)	Res
1/T	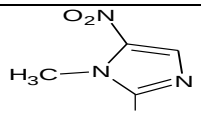	H	31.7	4.5000	4.4944	0.0056
2	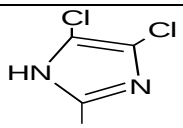	H	54	4.2700	4.2935	-0.0235
3	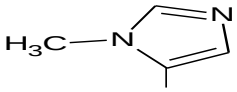	H	100	4.0000	3.9991	0.0009
4	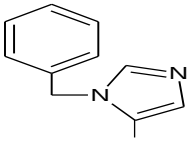	H	54.8	4.2600	4.2429	0.0171
5/T*	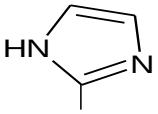	H	10	5.0000	5.00	0.00
6	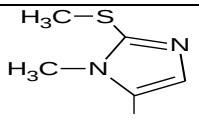	H	25	4.6000	4.60	0.00

T= Training set T*= Test set

Table (2.2): Structures, IC_{50}, and PIC_{50} of the 7-substituted hexahydroquinoline derivatives, the training set, and test set (Gündüz *et al*., 2009).

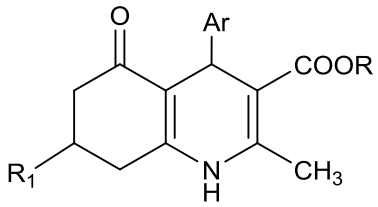

compound	R	R_1	Ar	IC_{50}	PIC_{50}(exp)	PIC_{50} (Pred)	Res
I/T	C_2H_5	CH_3	2,3-dichlorophenyl	57.83	4.24	4.2850	-0.0450
II	C_2H_5	CH_3	2,4-dichlorophenyl	40.00	4.40	4.3323	0.0677
III	CH_3	CH_3	2,5-dichlorophenyl	84.17	4.07	4.1152	-0.0452
IV	C_2H_5	CH_3	2,5-dichlorophenyl	73.50	4.13	4.1475	-0.0175
V	CH_3	CH_3	2,6-dichlorophenyl	83.80	4.08	4.0430	0.0370
VI	CH_3	C_6H_5	2,3-dichlorophenyl	60.00	4.22	4.2418	-0.0218
VII	CH_3	C_6H_5	2,5-dichlorophenyl	47.25	4.33	4.3087	0.0213
VIII	C_2H_5	C_6H_5	2,5-dichlorophenyl	52.13	4.28	4.3502	-0.0702
IX	CH_3	C_6H_5	2,6-dichlorophenyl	46.00	4.34	4.2687	0.0713
X	C_2H_5	C_6H_5	2,6-dichlorophenyl	53.50	4.27	4.2677	0.0023
XI /LO	C_2H_5	CH_3	2,6-dichlorophenyl	28.00	4.55	4.4807	0.0693
XII/LO	C_2H_5	C_6H_5	2,3-dichlorophenyl	32.60	4.49	4.5736	-0.0836
XIII/T*	CH_3	CH_3	2,4-dichlorophenyl	24.00	4.62	4.6510	-0.0310
XIVI /T*	CH_3	C_6H_5	2,4-dichlorophenyl	21.25	4.67	4.7422	-0.0722
XV/T*	C_2H_5	C_6H_5	2,4-dichlorophenyl	13.53	4.87	4.7525	0.1175

T= Training set T*= Test set LOO = Leave One Out.

2.5. Molecular modeling parameters

Molecular descriptors tabulated in table (2.3) were calculated directly for each compound in the training sets by using MOE and ACD/lab. 2D and 3D descriptors such as (Mr, In-R) was calculated by ACD/lab programme, the other 2D, 3D descriptors and logP (o/w) were calculated by MOE programme.

Table (2.3) Illustrated values of descriptors that calculated by MOE and ACD/lab programmes for training set compounds, acridinediones group (I)

com. No	E	logP(o/w)	MNDO_IP	Mr	PM3_IP	M.wt	AM1-IP	a-acc	a-_don	Lip-acc	Lip-don	MNDO-Eele	MNDO-HF	MNDO-HOMO	TPSA
1/T	47.14	2.50	9.178	10.59	8.94	398.46	8.910	3.00	1.00	8.00	1.00	-995168.18	-1.6203	-9.1778	109.8100
2	35.87	3.77	9.072	10.58	8.44	408.33	8.534	4.00	3.00	5.00	2.00	-886186.56	-36.6303	-9.0724	74.8500
3	40.44	2.17	8.747	10.05	8.53	353.47	8.426	3.00	1.00	5.00	1.00	-837239.12	-20.2847	-8.7472	63.9900
4	63.79	4.26	8.576	13.47	8.62	457.62	8.255	3.00	1.00	5.00	1.00	-1180912.2	-4.0609	-8.5760	63.9000
5/T*	35.16	1.78	8.724	9.59	8.70	339.44	8.482	4.00	3.00	5.00	2.00	-780437.25	-22.5276	-8.7243	74.8500
6	52.52	3.16	8.838	11.24	8.77	399.56	8.405	3.00	1.00	5.00	1.00	-945555.68	-21.8426	-88379	63.9900

Table (2.4) Illustrated values of descriptors that calculated by MOE programme for training set, and test set compounds for group (II).

com.No	AMI-IP	dipole	LogP(o/w)	PM3-IP	TPSA	weight	density	E	mr	PM3-E	PM3-HF
I	8.7418	1.6235	4.4440	8.7964	55.4000	394.298	0.8006	42.1155	10.3979	-100785.67	-88.8090
II	8.7638	1.8271	4.4830	8.8232	55.4000	394.298	0.8006	35.3298	10.3941	-97336.796	-103.492
III	8.7099	0.9911	4.1420	8.7855	55.4000	380.271	0.8124	38.9999	9.9270	-100782.87	-97.6824
IV	8.6181	0.9416	4.4830	8.6816	55.4000	394.298	0.8006	37.5863	10.3941	-97332.632	-100.6851
V	8.5100	0.6685	4.1030	8.6688	55.4000	380.271	0.8124	39.2247	9.9308	-97335.968	-93.5184
VI	8.6816	1.6207	4.1030	8.8050	55.4000	380.271	0.8124	44.2478	9.9308	-111686.91	-96.7402
VII	8.6377	1.3593	5.0750	8.7424	55.4000	442.342	0.7919	68.5937	11.9727	-115135.33	-61.3053
VIII	8.6028	1.3537	5.4160	8.7475	55.4000	456.369	0.7827	58.0488	12.4400	-115135.33\\	-66.4069
IX	8.5176	1.1912	5.0360	8.6706	55.4000	442.342	0.7919	68.4003	11.9764	-111684.50	-58.6474
X	8.7986	0.9820	5.3770	8.9540	55.4000	456.369	0.7827	111.975	12.4437	-115105.28	-36.3635
XI/LO	8.4678	1.2315	4.4440	8.6431	55.4000	394.298	0.8006	37.4546	10.444	-100781.13	-98.6812
XII/LO	8.5763	0.8004	5.3770	8.7215	55.4000	456.369	0.7827	62.7706	5.3770	-115134.04	-65.1184
XIII/T*	8.7916	1.8308	4.1420	8.8357	55.4000	380.271	0.8124	37.4999	9.9270	-97337.046	-97.9303
XIV/T*	8.7186	1.3957	5.0750	8.8294	55.4000	442.342	0.7919	57.6669	11.972	-111689.25	-63.4036
XV/T*	8.5826	1.1838	4.4160	8.7418	55.4000	456.369	0.7827	56.2910	12.440	-115136.17	-67.2419

T= Training set T*= Test set LO= Leave One Out.

Table (2.5) A list of molecular descriptors with their details used in QSAR modeling, for group (I) and (II).

No	Descriptor	The definitions
1	logP(octanol/water) (LogP (o/w).	Is a measure of the chemical compound hydrophilicity ((Jacek *et al*., 2012)).
2	Number of H-bond donor atoms (a-don).	In hydrogen bond, the electronegative atom not covalently attached to the hydrogen is named proton donor.
3	Number of H-bond donor atoms (a-acc).	In hydrogen bond, the electronegative atom covalently attached to the hydrogen is named proton acceptor.
4	Topological Polar Surface Area (TPSA).	Is defined as the surface sum over all polar atoms, primarily oxygen and nitrogen, also including their attached hydrogen atoms.
5	Molar refractivity (Mr).	Is the measure of the total Polarizabilities of a mole of a substance and its dependent on the temperature, index of refraction and temperature
6	Potential energy (E)	Is the energy of an object or a system due to the position of the body or the arrangement of the particles of the system
7	Ionization Potential (IP)	The ionization potential of an element is the minimum potential (measured in volts) required to remove electron from a gaseous neutral atom.
8	Electronic Energy	The energy of diatomic molecule in a given electronic state.
9	HOMO	Highest Occupied Molecular Orbital.
10	Heat of Formation(HF)	The increase in enthalpy resulting from the formation of one mole of a substance from its elements at constant pressure.

2.6. Selection of subset descriptors

The ratio of number of compounds to the physiochemical descriptors used for the correlation is usually 5: 1(Vaidya *et al*., 2012). To select the best subset of physiochemical properties in training and in test set, highly correlated molecular descriptors were excluded through co-variable analysis using correlation matrix, figures, (2.1) and (2.2).

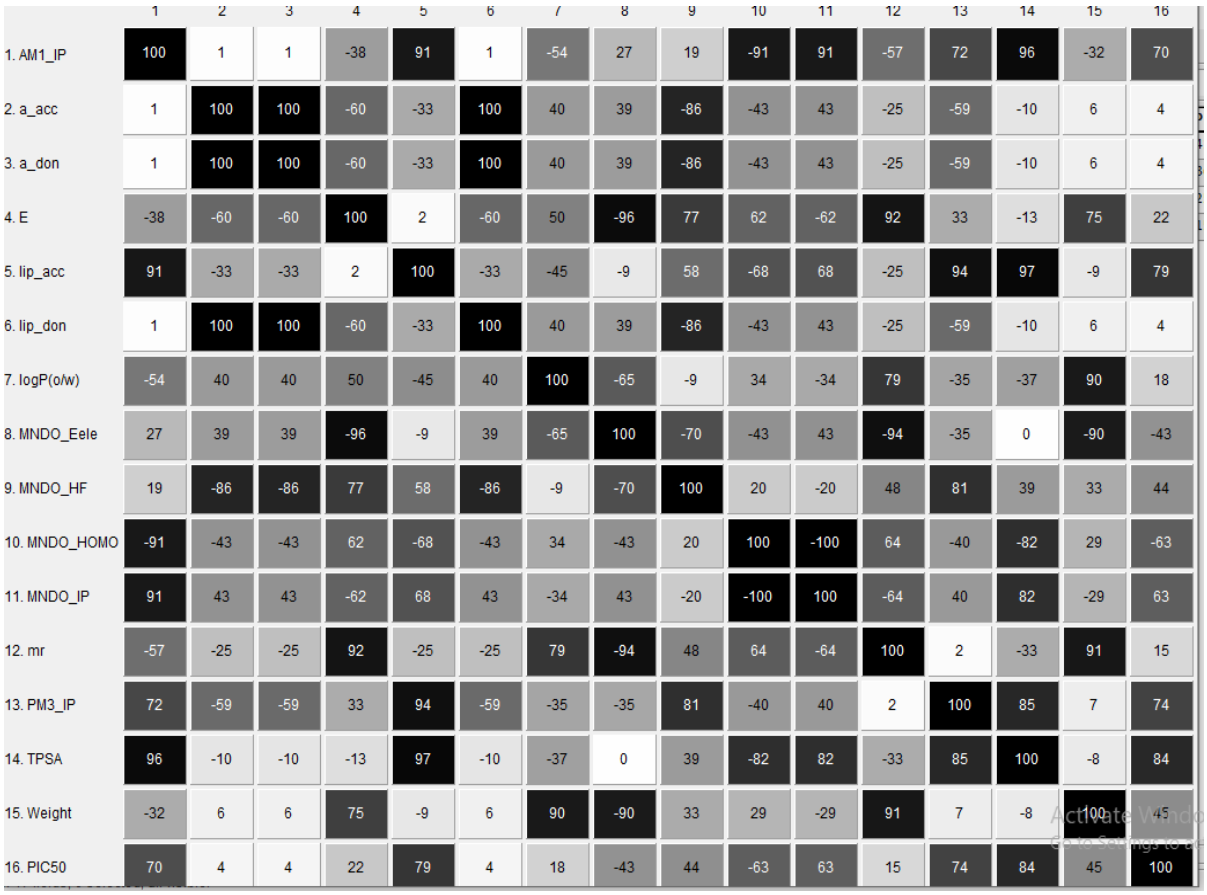

	1	2	3	4	5	6	7	8	9	10	11	12	13	14	15	16
1. AM1_IP	100	1	1	-38	91	1	-54	27	19	-91	91	-57	72	96	-32	70
2. a_acc	1	100	100	-60	-33	100	40	39	-86	-43	43	-25	-59	-10	6	4
3. a_don	1	100	100	-60	-33	100	40	39	-86	-43	43	-25	-59	-10	6	4
4. E	-38	-60	-60	100	2	-60	50	-96	77	62	-62	92	33	-13	75	22
5. lip_acc	91	-33	-33	2	100	-33	-45	-9	58	-68	68	-25	94	97	-9	79
6. lip_don	1	100	100	-60	-33	100	40	39	-86	-43	43	-25	-59	-10	6	4
7. logP(o/w)	-54	40	40	50	-45	40	100	-65	-9	34	-34	79	-35	-37	90	18
8. MNDO_Eele	27	39	39	-96	-9	39	-65	100	-70	-43	43	-94	-35	0	-90	-43
9. MNDO_HF	19	-86	-86	77	58	-86	-9	-70	100	20	-20	48	81	39	33	44
10. MNDO_HOMO	-91	-43	-43	62	-68	-43	34	-43	20	100	-100	64	-40	-82	29	-63
11. MNDO_IP	91	43	43	-62	68	43	-34	43	-20	-100	100	-64	40	82	-29	63
12. mr	-57	-25	-25	92	-25	-25	79	-94	48	64	-64	100	2	-33	91	15
13. PM3_IP	72	-59	-59	33	94	-59	-35	-35	81	-40	40	2	100	85	7	74
14. TPSA	96	-10	-10	-13	97	-10	-37	0	39	-82	82	-33	85	100	-8	84
15. Weight	-32	6	6	75	-9	6	90	-90	33	29	-29	91	7	-8	100	45
16. PIC50	70	4	4	22	79	4	18	-43	44	-63	63	15	74	84	45	100

Figure (2.1) Details of correlation matrix for molecular descriptors in training set compounds for group (I).

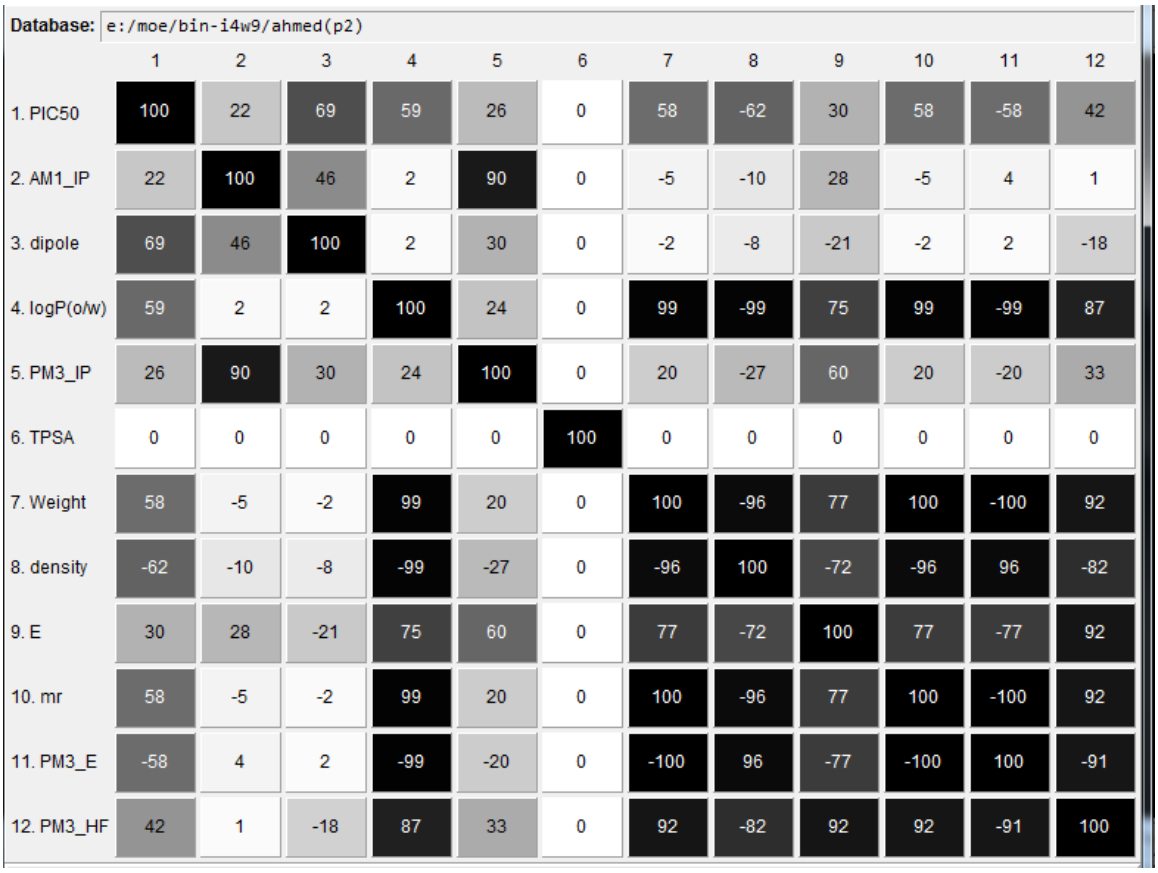

Database: e:/moe/bin-i4w9/ahmed(p2)

	1	2	3	4	5	6	7	8	9	10	11	12
1. PIC50	100	22	69	59	26	0	58	-62	30	58	-58	42
2. AM1_IP	22	100	46	2	90	0	-5	-10	28	-5	4	1
3. dipole	69	46	100	2	30	0	-2	-8	-21	-2	2	-18
4. logP(o/w)	59	2	2	100	24	0	99	-99	75	99	-99	87
5. PM3_IP	26	90	30	24	100	0	20	-27	60	20	-20	33
6. TPSA	0	0	0	0	0	100	0	0	0	0	0	0
7. Weight	58	-5	-2	99	20	0	100	-96	77	100	-100	92
8. density	-62	-10	-8	-99	-27	0	-96	100	-72	-96	96	-82
9. E	30	28	-21	75	60	0	77	-72	100	77	-77	92
10. mr	58	-5	-2	99	20	0	100	-96	77	100	-100	92
11. PM3_E	-58	4	2	-99	-20	0	-100	96	-77	-100	100	-91
12. PM3_HF	42	1	-18	87	33	0	92	-82	92	92	-91	100

Figure (2.2) Details of correlation matrix for molecular descriptors in training set compounds for group (II).

QSAR model equation with High Square of correlation coefficient (R^2) was selected.

Table (2.6) The QSAR model between descriptors and biological activity of imidazolyl derivatives of 1, 8- acridinediones for MCF-7 cancer cell lines (training set compounds): (group-I).

No	Removed Descriptors	QSAR equations	RMSE*	R^{2*}
1	E, log(o/w)	PIC_{50} = 4.06440+0.00288 * E+0.01840*logP(o/w)	0.1722	0.0531
2	E, MNDO-IP	PIC_{50} = -1.93890+0.00950 * E+0.67417 * AM1-IP	0.0215	0.9851
3	E, Mr	PIC_{50} = 4.30681+0.00811 * E-0.03840 * mr	0.1716	0.0600
4	E ,PM3-IP	PIC_{50} =-1.71705-0.00048 * E+0.69490 * PM3-IP	0.1189	0.5485
5	E, Weight	PIC_{50} =3.18549-0.00485 * E+0.00321 * Weight	0.1542	0.2411
6	E,AM1-IP	PIC_{50} = -1.93890+0.00950 * E+0.67417 * AM1-IP	0.0865	0.7609
7	E, a-acc	PIC_{50} = 3.61395+0.00626 *0.10792 *a_acc	0.1686	0.0919
8	E, a-don	PIC_{50} = 3.88374+0.00626 *E+0.05396 *a_don	0.1686	0.0919
9	E, lip-acc	PIC_{50} = 3.48215+0.00339 *E+0.10728 * lip_acc	0.1021	0.6669
10	E, lip-don	PIC_{50} = 3.82978+0.00626 * E+0.10792 * lip-don	0.1686	0.09189
11	E, MNDO-Eele	PIC_{50} = 3.70104+0.00000 * E-0.00000 * MNDO-Eele	0.16014	0.18120
12	E, MNDO-HF	PIC_{50} = 4.62410-0.00502 * E+0.00842 *MNDO-HF	0.1555	0.2280
13	E, MNDO-HOMO	PIC_{50} = - 4.48678+0.01627 * E-0.89757*MNDO-HOMO	0.02157	0.9851
14	E, TPSA	PIC_{50} = 3.34403+0.00556 * E+0.00836 *TPSA	0.07454	0.8226
15	logP(o/w),MNDO-IP	PIC_{50} = -3.20129+0.15696 *logP(o/w) +0.81590 * AM1-IP	0.1167	0.5650
16	logP(o/w), Mr	PIC_{50}= 4.10187+0.02877 * logP(o/w) +0.00576 * mr	0.1742	0.03145
17	logP(o/w),PM3-IP	PIC_{50} = -3.40145+0.10204 * logP(o/w) +0.84998 * PM3-IP	0.08562	0.7659
18	logP(o/w), Weight	PIC_{50} = 2.02256-0.25366 * logP(o/w) +0.00752 * Weight	0.1259	0.4938
19	logP(o/w),AMP-IP	PIC_{50} = - 3.20129+0.15696 * logP(o/w) +0.81590 * AM1-IP	0.05415	0.9064
20	logP(o/w),a-acc	PIC_{50} = 4.17999+0.03855 * logP(o/w) -0.01380 * a-acc	0.1741	0.0317
21	logP(o/w), a-don	PIC_{50} = 4.14549+0.03855 * logP(o/w) -0.00690 * a-don	0.1741	0.0317
22	logP(o/w),lip-acc	PIC_{50} = 2.97797+0.13501 * logP(o/w) +0.14800 * lip-acc	0.0278	0.9753
23	logP(o/w),lip-don	PIC_{50} = 4.15239+0.03855 * logP(o/w) -0.01380 * lip-don	0.1741	0.0317

24	LogP(o/w),MNDO-Eele	PIC_{50} = 3.70104+0.00000 * logP(o/w) -0.00000 * MNDO_Eele	0.1601	0.1812
25	LogP(o/w), MNDOHF	PIC_{50} = 4.20609+0.04459 * logP(o/w) +0.00576 *MNDO-HF	0.1544	0.2388
26	LogP(o/w),MNDO-HF	PIC_{50} = -1.06410+0.08905 * logP(o/w) -0.56659 * MNDO-HOMO	0.1167	0.5650
27	LogP(o/w),TPSA	PIC_{50} = 3.11067+0.11632 * logP(o/w) +0.00995 * TPSA	0.0148	0.9930
28	MNDO-IP, Mr	PIC_{50} = -5.16348+0.90278 * MNDO-IP+0.12462 * mr	0.0484	0.9252
29	MNDO-IP, PM3-IP	PIC_{50} = -2.98053+0.29062 * MNDO-IP+0.53924 * PM3-IP	0.0999	0.6810
30	MNDO-IP, Weight	PIC_{50} = -2.48571+0.60718 * MNDO-IP+0.00332 * Weight	0.07123	0.8380
31	MNDO-IP, AM1-IP	PIC_{50} = - 0.11072+0.52097 * AM1-IP-0.00858 *MNDO-IP	0.1269	0.4854
32	MNDO-IP, a-acc	PIC_{50} = - 0.23258+0.54646 * MNDO-IP-0.11378 * a-acc	0.1301	0.4599
33	MNDO-IP, a- don	PIC_{50} = - 0.51704+0.54646 * MNDO-IP -0.05689 * a-don	0.1301	0.4599
34	MNDO-IP, lip-acc	PIC_{50} = 2.60479+0.12649 * MNDO-IP+0.09179 * lip-acc	0.1058	0.6421
35	MNDO-IP, lip-don	PIC_{50} = - 0.46015+0.54646 * MNDO-IP - 0.11378 * lip-don	0.1301	0.4599
36	MNDO-IP, MNDO-Eele	PIC_{50} = 3.70104+0.00000 * MNDO-IP - 0.00000 * MNDO-Eele	0.1601	0.1812
37	MNDO-IP, MNDO-HF	PIC_{50} = - 0.49135 + 0.54702 * MNDO-IP + 0.00741 * MNDO-HF	0.0919	0.7298
38	MNDO-IP, MNDO-HOMO	PIC_{50} = 0.16860 +0.22988 * MNDO-IP - 0.22988 * MNDO-HOMO	0.1375	0.3965
39	MNDO-IP, TPSA	PIC_{50} = 4.80330 - 0.14473 * MNDO-IP + 0.00949 * TPSA	0.0925	0.7268
40	Mr,PM3-IP	PIC_{50} = -1.85452 + 0.01872 * mr + 0.68402 * PM3-IP	0.11632	0.5680
41	Mr, Weight	PIC_{50} = 2.96094-0.19298 * mr + 0.00854 *Weight	0.11456	0.5809
42	Mr, AM1-IP	PIC_{50} = - 4.25041 +0.10759 * mr + 0.85638 * AM1-IP	0.0446	0.9366
43	Mr, a-acc	PIC_{50} = 3.88483+0.02321 * mr + 0.03488 * a-acc	0.1742	0.0308
44	Mr, a- don	PIC_{50} = 3.97202 +0.02321 * mr + 0.01744 * a - don	0.1742	0.0308
45	Mr, lip-a-acc	PIC_{50} = 3.01129 +0.04949 * mr + 0.12058 * lip- acc	0.0870	0.7585
46	Mr, lip-don	PIC_{50} = 3.95459 +0.02321 * mr +0.03488 * lip- don	0.1742	0.0308
47	Mr, MNDO-Eele	PIC_{50} = 3.70104 +0.00000 * mr - 0.00000 * MNDO-Eele	0.1601	0.1812

48	Mr, MNDO-HF	PIC_{50} = 4.45159 -0.00909 * mr + 0.00592 * MNDO -HF	0.1587	0.1953
49	Mr, MNDO-HOMO	PIC_{50} = - 5.16348 +0.12462 * mr - 0.90278 * MNDO -HOMO	0.0.0484	0.9252
50	Mr, TPSA	PIC_{50} = 2.81029+0.06351 * mr + 0.00944 * TPSA	0.04942	0.9220
51	PM3-IP, Weight	PIC_{50} = - 2.22259 +0.66045 * PM3 -IP + 0.00193 * Weight	0.09533	0.7098
52	M3-IP, AM1-IP	PIC_{50} = -1.83455 + 0.45929 *PM3-IP + 0.24950 * AM1-IP	0.1116	0.6026
53	PM3-IP, a-ac	PIC_{50} = -5.99987 + 1.07763 * PM3-IP + 0.29468 * a-acc	0.0588	0.8895
54	PM3-IP, a-don	PIC_{50} = -5.26316 + 1.07763 * PM3-IP + 0.14734 * a-don	0.0588	0.8895
55	PM3-IP, lip-acc	PIC_{50} = 4.03560 - 0.05079 * PM3-IP + 0.11481 * lip-acc	0.1082	0.6262
56	PM3-IP, lip-don	PIC_{50} = -5.41050 +1.07763 * PM3-IP + 0.29468 * lip-don	0.0588	0.8895
57	PM3-IP, MNDO-Eele	PIC_{50} = 3.70104 + 0.00000 * PM3-IP - 0.00000 * MNDO-Eele	0.1601	0.1812
58	PM3-IP, MNDO-HF	PIC_{50} = - 4.95753 +1.05665 * PM3-IP - 0.00616 * MNDO-HF	0.0.107	0.6287
59	PM3-IP, MNDO-HOMO	PIC_{50} = - 2.98053 + 0.53924 * PM3-IP -0.29062 * MNDO-HOMO	0.0995	0.6810
60	PM3-IP, TPSA	PIC_{50} = 3.03173 + 0.07594 * PM3-IP + 0.00730 * TPSA	0.9433	0.7158
61	Weight, AM1-IP	PIC_{50} = -3.13167 + 0.00363 * Weight + 0.69421 * AM1-IP	0.0019	0.9998
62	Weight, a-acc	PIC_{50} = 3.36538 + 0.00216 * Weight + 0.00554 *a-acc	0.1578	0.2051
63	Weight, a-don	PIC_{50} = 3.37924 + 0.00216 * Weight + 0.00277 * a-don	0.1578	0.2051
64	Weight, lip-acc	PIC_{50} = 2.57065 + 0.00254 * Weight + 0.11456 * lip-acc	0.0543	0.9059
65	Weight, lip-don	PIC_{50} = 3.37647 + 0.00216 * Weight + 0.00554 * lip-don	0.1578	0.2051
66	Weight, MNDO-Eele	PIC_{50} = 3.70104 + 0.00000 * Weight - 0.00000 * MNDO-Eele	0.1601	0.1812
67	Weight, MNDO-HF	PIC_{50} = 3.65192 + 0.00165 * Weight + 0.00407 * MNDO-HF	0.1483	0.2983
68	Weight, MNDO-HOMO	PIC_{50} = - 2.48571+0.00332 * Weight -0.60718 * MNDO-HOMO	0.0713	0.8380
69	Weight, TPSA	PIC_{50} =2.58357+0.00252 * Weight+0.00837 * TPSA	0.0177	0.9899
70	AM1-IP, a-acc	PIC_{50} = - 0.16690+0.51296 * AM1-IP+0.01486 * a-acc	0.1268	0.4867
71	AM1-IP, a-don	PIC_{50} = - 0.12976+0.51296 * AM1-IP+0.00743 * a-don	0.1268	0.4867

72	AM1-IP, lip-acc	PIC_{50} = 4.41481- 0.10275 * AM1-IP+0.12508 * lip-acc	0.1078	0.6292
73	AM1-IP, lip-don	PIC_{50} = - 0.13719+0.51296 * AM1-IP+0.01486 * lip-don	0.1268	0.4867
74	AM1-IP, MNDO-Eele	PIC_{50} = 3.70104+0.00000 *AM1-IP-0.00000 * MNDO-Eele	0.1601	0.1812
75	AM1-IP, MNDO-HF	PIC_{50} = 0.31916+0.46896 * AM1-IP+0.00399 * MNDO-HF	0.1143	0.5825
76	AM1-IP, MNDO-HOMO	PIC_{50} = - 0.11072+0.52097 * AM1-IP+0.00858 * MNDO-HOMO	0.1267	0.4854
77	AM1-IP, TPSA	PIC_{50} = 12.47517-1.16769 * AM-IP+0.02231 * TPSA	0.0563	0.8989
78	a-acc, a-don	PIC_{50} = 4.23667+0.00333 * a-acc+0.00667 * a-don	0.1768	0.0002
79	a-acc, lip-acc	PIC_{50} = 3.09333+0.14000 * a-acc+0.12333 * lip-acc	0.0919	0.7302
80	a-acc, lip-don	PIC_{50} = 4.22000+0.00833 * a-acc+0.00833 * lip-don	0.1768	0.0017
81	a-acc, MNDO-Eele	PIC_{50} = 3.70104+0.00000 * a-acc-0.00000 * MNDO-Eele	0.1601	0.1812
82	a-acc, MNDO-HF	PIC_{50} = 2.48030+0.65706 *a-acc+0.02289 * MNDO-HF	0.0658	0.8627
83	a-acc, MNDO-HOMO	PIC_{50} = - 0.23258-0.11378 * a-acc-0.54646 * MNDO-HOMO	0.1301	0.4599
84	a-acc, TPSA	PIC_{50} = 3.45636+0.05230 * a-acc+0.00808 * TPSA	0.0919	0.7302
85	a-don, lip-acc	PIC_{50} = 3.44333 +0.07000 * a-don+0.12333 * lip-acc	0.0919	0.7302
86	a-don, lip-don	PIC_{50} = 4.24333+0.00667 * a-don+0.00333 * lip-don	0.1768	0.0017
87	a-don, MNDO-Eele	PIC_{50} = 3.70104+0.00000 * a-don-0.00000 * MNDO-Eele	0.1601	0.1812
88	a-don, MNDO-HF	PIC_{50} = 4.12294+0.32853 * a-don+0.02289 * MNDO-HF	0.0658	0.8627
89	a-don, MNDO-HOMO	PIC_{50} = - 0.51704-0.05689 * a-don-0.54646 * MNDO-HOMO	0.1301	0.4599
90	a-don, TPSA	PIC_{50} = 3.58712+0.02615 * a-don+0.00808 * TPSA	0.0919	0.7302
91	Lip-acc, lip-don	PIC_{50} = 3.37333+0.12333 * lip-acc+0.14000 * lip-don	0.0919	0.7302
92	Lip-acc, MNDO-Eele	PIC_{50} = 3.70104+0.00000 * lip-acc-0.00000 * MNDO-Eele	0.1601	0.1812
93	Lip-acc, MNDO-HF	PIC_{50} = 3.62092+0.10982 * lip-acc-0.00033 * MNDO-HF	0.1082	0.6263
94	Lip-acc, MNDO-HOMO	PIC_{50} = 2.60479+0.09179 * lip-acc-0.12649 * MNDO-HOMO	0.1059	0.6421

95	Lip-acc, TPSA	PIC_{50} = 3.67289-0.07356 * lip-acc+0.01289 * TPSA	0.0919	0.7302
96	Lip-don, MNDO-Eele	PIC_{50} = 3.70104+0.00000 * lip-don-0.00000 * MNDO-Eele	0.1601	0.1812
97	Lip-don,MNDO-HF	PIC_{50} = 3.79441+0.65706 * lip-don+0.02289 * MNDO-HF	0.0658	0.8627
98	Lip-don, MNDO-HOMO	PIC_{50} = - 0.46015-0.11378 * lip-don-0.54646 * MNDO-HOMO	0.1301	0.4599
99	Lip-don, TPSA	PIC_{50} = 3.56097+0.05230 * lip-don+0.00808 * TPSA	0.0919	0.7302
100	MNDO-Eele, MNDO-HF	PIC_{50} = 3.70104-0.00000 * MNDO-Eele+0.00000 * MNDO-HF	0.1601	0.1812
101	MNDO-Eele,MNDO-HOMO	PIC_{50} = 3.70104-0.00000 * MNDO-Eele-0.00000 * MNDO-HOMO	0.1601	0.1812
102	MNDO-Eele, TPSA	PIC_{50} = 3.70104-0.00000 * MNDO-Eele+0.00000 * TPSA	0.1601	0.1812
103	MNDO-HF,MNDO-HOMO	PIC_{50} = - 0.49135+0.00741 * MNDO-HF-0.54702 * MNDO-HOMO	0.0919	0.7298
104	MNDO-HF,TPSA	PIC_{50} = 3.69701+0.00158 * MNDO-HF+0.00749 * TPSA	0.0924	0.7274
105	MNDO-HOMO,TPSA	PIC_{50} = 4.80330+0.00949 * TPSA+0.14473 * MNDO-HOMO	0.0925	0.7268

RMSE* = Root main square error **R^{2}*** = Square of the correlation coefficient.

From the table, the best QSAR model equation with High Square of the correlation coefficient (R^2 = (0. 0.9930) and low Root Mean Square Error (RMSE = 0.01480) was QSAR equation No (27).

PIC_{50} = -1.93890+0.00950 * E+0.67417 * AM1-IP…….. ……..….... (2)

PIC_{50} = - 4.48678+0.01627 * E-0.89757 * MNDO-HOMO. ……..….. (13)

PIC_{50} = 3.11067+0.11632 * logP(o/w) +0.00995 * TPSA ……. . (27)

PIC_{50} = -3.13167 + 0.00363 * Weight + 0.69421 * AM1-IP . …… (61)

PIC_{50} =2.58357+0.00252 * Weight+0.00837 * TPSA …….....…. (69)

Quantitative structure- activity relationship (QSAR) models, described the effect of these derivatives on the activity of calcium antagonist activity. To

obtain the effects of the structural parameters of the investigated acridinedione derivatives on their calcium antagonist activity, QSAR analysis with different types of molecular descriptors was operated. The octanol-water partition coefficient (logp(o/w), and(topological polar surface area) TPSA have been considered as descriptors for their biological effects.

The best QSAR model equation was equation (27) with high square of the correlation coefficient (R^2 = (0.9930) and low Root Mean Square Error (RMSE=(0.0148)

Table (2.7): The QSAR model between descriptors of 7- substituted hexahydroquinoline derivatives and their Calcium channel modulator effects (10 training set compounds): (group-II).

No	Removed Descriptors	QSAR Equation	RMSE*	R^2*
1	AMI-IP, dipole	PIC_{50} = 5.15050- 0.1388* AMI-IP+ 0.22919* dipole	0.07574	0.49258
2	AMI-IP, LogP(o/w)	PIC_{50} = 1.62285+ 0.23347*AMI-IP+ 0.12680* LogP(o/w)	0.08311	0.38890
3	AMI-IP, PM3-IP	PIC_{50} = 1.20717- 0.11373* AMI-IP+ 0.45777*PM3-IP	0.10242	0.07197
4	AMI-IP, TPSA	PIC_{50} = 2.08214+ 0.24877*AMI-IP+0.0000* TPSA	0.10373	0.04814
5	AMI-IP, weight	PIC_{50} = 0.97504+ 0.2813*AMI-IP+ 0.00200*weight	0.08286	0.39265
6	AMI-IP, density	PIC_{50} = 7.35061+0.18343*AMI-IP-5.88712*density	0.08192	0.40634
7	AMI-IP, E	PIC_{50} = 2.7974+0.01650*AMI-IP+0.00128*E	0.10023	0.11124
8	AMI-IP,mr	PIC_{50} = 1.13957+0.28063*AMI-IP+0.06071*mr	0.08286	0.39262
9	AMI-IP, PM3-E	PIC_{50} = 3.34637+0.0000*AMI-IP-0.00001*PM3-E	0.08679	0.33367
10	AMI-IP, PM3-HF	PIC_{50} = 2.30570+0.24181*AMI-IP+0.00203*PM3-HF	0.09386	0.22074
11	dipole, LogP(o/w)	PIC_{50} = 3.39051+0.20874*dipole+0.12501*LogP(o/w)	0.04610	0.81198
12	dipole, PM3-IP	PIC_{50} = 3.30180+0.20655*dipole+0.07697*PM3-IP	0.07638	0.48394
13	dipole, TPSA	PIC_{50} = 3.96963+0.21210*dipole+0.0000*TPSA	0.07662	0.48070
14	dipole, weight	PIC_{50} = 3.13653+0.21581*dipole+0.00201*weight	0.04400	0.82870
15	dipole, density	PIC_{50} = 8.41367+0.19855*dipole-5.5494*density	0.04765	0.79911
16	dipole, E	PIC_{50} = 3.81014+0.24250*dipole+0.00230*E	0.05900	0.69207
17	dipole, mr	PIC_{50} = 3.29567+0.21574*dipole+0.06096*mr	0.04401	0.82864
18	dipole, PM3-E	PIC_{50} = 3.34637+0.0000*dipole-0.00001*PM3-E	0.08679	0.33367
19	dipole, PM3-HF	PIC_{50} = 4.15167+0.24335*dipole+0.00275*PM3-HF	0.04904	0.78725
20	LogP(o/w), PM3-IP	PIC_{50} = 2.17185+0.12101*LogP(o/w)+0.17103*PM3-IP	0.08485	0.36313
21	LogP(o/w), TPSA	PIC_{50} = 3.6950+0.12784*LogP(o/w)+0.0000*TPSA	0.08595	0.34652
22	LogP(o/w), weight	PIC_{50} = 3.77953+0.20288*LogP(o/w)-0.00119*weight	0.08578	0.34901
23	logP(o/w), density	PIC_{50} = 15.18293-0.15239*LogP(o/w)-12.81365*density	0.08270	0.39408

24	LogP(o/w), E	PIC_{50} = 3.47972+0.17965*LogP(o/w)-0.00155*E	0.08299	0.39068
25	LogP(o/w), mr	PIC_{50} = 3.68548+0.20305*LogP(o/w)-0.03615*mr	0.08579	0.34897
26	LogP(o/w), PM3-E	PIC_{50} = 3.34637+0.0000*LogP(o/w)-0.00001*PM3-E	0.08679	0.33367
27	LogP(o/w), PM3-HF	PIC_{50} = 3.11444+0.20579*LogP(o/w)-0.00201*PM3-HF	0.08331	0.38605
28	PM3-IP, TPSA	PIC_{50} = 1.243557+0.34131*PM3-IP+0.0000*TPSA	0.10153	0.07007
29	PM3-IP, weight	PIC_{50} = 1.69498+0.20263*PM3-IP+0.00186*weight	0.08539	0.35496
30	PM3-IP, density	PIC_{50} = 7.64107+0.13635*PM3-IP-5.75911*density	0.08299	0.39077
31	PM3-IP, E	PIC_{50} = 2.71479+0.16688*PM3-Ip+0.00110*E	0.10073	0.10244
32	PM3-IP,mr	PIC_{50} = 1.84889+0.20178*PM3-IP+0.05628*mr	0.08539	0.35502
33	PM3-IP, PM3-E	PIC_{50} = 3.34637+0.0000*PM3-IP-0.00001*PM3-E	0.08679	0.33367
34	PM3-IP, PM3-HF	PIC_{50} = 2.78037+0.18269*PM3-IP+0.00182*PM3-HF	0.09550	0.19315
35	TPSA, weight	PIC_{50} = 3.42793+0.0000*TPSA+0.00196*weight	0.08695	0.33123
36	TPSA, density	PIC_{50} = 4.15788+0.0000*TPSA+0.00148*E	0.10133	0.09174
37	TPSA, E	PIC_{50} = 4.15788+0.0000*TPSA+0.00148*E	0.10133	0.09174
38	TPSA, mr	PIC_{50} = 3.58274+0.0000*TPSA+0.05949*mr	0.08693	0.33150
39	TPSA, PM3-E	PIC_{50} = 3.34637+0.0000*TPSA-0.00001*PM3-E	0.08679	0.33367
40	TPSA, PM3-HF	PIC_{50} = 4.40055+0.0000*TPSA+0.0205*PM3-HF	0.09655	0.17527
41	weight, density	PIC_{50} = 3.42793+0.00196*weight-0.0000*density	0.08695	0.33123
42	weight, E	PIC_{50} = 3.14521+0.00286*weight-0.00168*E	0.08376	0.37936
43	weight, mr	PIC_{50} = 3.42810+0.00196*weight+0.00006*mr	0.08695	0.33123
44	weight, PM3-E	PIC_{50} = 3.34637+0.0000*weight-0.00001*PM3-E	0.08679	0.33367
45	weight, PM3-HF	PIC_{50} = 2.2967+0.00406*weight-0.00329*PM3-HF	0.08206	0.40430
46	density, E	PIC_{50} = 4.1570-0.0000*density+0.00148*E	0.10133	0.09174
47	density, mr	PIC_{50} = 10.50116-7.6054*density-0.01728*mr	0.083553	0.38278
48	density, PM3-E	PIC_{50} = 3.34637-0.0000*density-0.00001*PM3-E	0.08679	0.33367
49	density, PM3-HF	PIC_{50} = 4.40055-0.0000*density+0.00205*PM3-HF	0.09655	0.17527
50	E, mr	PIC_{50} = 3.36961-0.00169*E+0.08703*mr	0.08371	0.38016
51	E, PM3-E	PIC_{50} = 3.02544-0.00169*E-0.00001*PM3-E	0.083771	0.38016
52	E, PM3-HF	PIC_{50} = 4.72537-0.00256*E+0.00441*PM3-HF	0.09401	0.21817
53	mr, PM3-E	PIC_{50} = 3.3437+0.0000*mr-0.00001*PM3-E	0.09401	0.21817

54	mr, PM3-HF	PIC_{50}= 2.6296+0.12358*mr-0.00331*PM3-HF	0.08200	0.40517
55	PM3-HF,PM3-E	PIC_{50}= 2.16284-0.00322*PM3-HF-0.00002*PM3-E	0.08199	040533

RMSE* = Root main square error **R^2*** = Square of the correlation coefficient

From the table, the best QSAR model equation with High Square of the Correlation coefficient (R^2= (0.81198) and low Root Mean Square Error (RMSE = 0.04610) was QSAR equation No (11).

PIC_{50}= 3.39051+0.20874*dipole+0.12501*LogP (o/w)……...…….. (11)

PIC_{50}= 3.13653+0.21581*dipole+0.00201*weight……..…….… (14)

PIC_{50}= 8.41367+0.19855*dipole-5.5494*density....……..……... (15)

PIC_{50}= 3.29567+0.21574*dipole+0.06096*mr……..…...… (17)

PIC_{50}= 4.15167+0.24335*dipole+0.00275*PM3-HF……..…….… (19)

Previous nonlinear quantitative structure- activity relationship (QSAR) models, described the effect of these derivatives on the activity of calcium entry blockers. To obtain the effects of the structural parameters of the investigated hexadroquinoline derivatives on their calcium channel blocker activity, QSAR analysis with different types of molecular descriptors was operated. The octanol-water partition coefficient (logp(o/w), and dipole moment have been considered as descriptors for the bioavailability or hydrophilic effect.

The best QSAR model equation was equation (11) with high square of the correlation coefficient (R^2 = (0.81198) and low Root Mean Square Error (RMSE = (0.04610).

2.7. Calculation of statistical parameters

The statistical quality of the model was justified by statistical parameters such as the root mean square error (RMSE), correlation coefficient (R), square correlation coefficient (R^2), standard error of estimate(S), and (F- test

value) or (the ratio between the variances of observed and calculated activities).

Calculation of statistical parameter was carried out by using statistical programme SPSS version IBM-22

Model No: (27), R= 0.996, R^2= 0.993, Adjusted (R^2) = 0.990, the standard error of estimate = 0.124, s = 0.209, F value = 283.74, p value = 0.004, RMSE= 0.03817 Q = 0.6296, and Q^2 =0.8253. For acridinedione derivatives. Also QSAR model equation with High Square of correlation coefficient (R^2) was selected, group Model No: (11), R= 0.9011 R^2 = 0.812, RMSE=0.05156 Q = 0.7917, Q^2 = 0.6267, s = 0.021 , F = 34.511 , p = 0.0001

For polyhydroquinoline derivatives.

2.8. Designing of compounds

2.8.1. Designing of acridinedione derivatives

Acridinedione derivatives have attracted attention of medicinal Chemists for both with regard to heterocyclic and the pharmacological activities associated with them. In order to synthesize these derivatives expecting to possess biological activities against breast cancer, about 75 compounds were designed as anti-breast cancer and their predicted biological activities were Illustrated in table (3.1).

The proposed model (27) has all conditions to be considered as predictive model. It has correlation coefficient of cross-validation (Q^2) larger than 0.5, prediction (R^2) which is higher than 0.6 and excellent prediction in external validation (R^2 =1). Thus, this model was used to predict the in-vitro biological activity of designed N-substituted acridinedione derivatives from (C1-C75) against human breast cancer Cell Lines MCF-7, predicted biological activity of these compounds along with predicted descriptors were

tabulated in table (2.8). To select compounds for synthesis from designed one, the drugability of these compounds were evaluated through Lipinski‘s parameters rule of five which proposes that molecules with poor permeation and oral absorption have logP>5, molecular weight >500, more than 5 hydrogen-bond donor, and more than 10 acceptor groups.

The hydrogen bond donor and acceptor groups correlate to the capacity of intermolecular interactions, mainly with water molecules. The passage through cellular membrane becomes thermodynamically unfavorable with the increase of hydrogen bond count groups because desolvation is needed to enter in the lipidic environment (Yunta, 2017). All designed Accridinedione derivatives have acceptable number of hydrogen bond donor and acceptor groups see

The logP value is one of the most important descriptors to evaluate oral bioavailability because which indicates the lipophilicity and hydro solubility of a compound. As much lipophilicity is the compound, as better is the capacity to pass the lipidic-bilayer of the cellular membrane, and consequently, as high will be the bioavailability. The problem is that compounds excessively lipophilicity has difficult to dissolve in the water of organism, and then, it will not be absorbed the molecular weight describes the molecular size. Big molecules will have difficult to be absorbed because, the passage through biological membranes is unfavorable (Yunta, 2017).

The compounds that not passed in this criterion were compounds 34 and 36. But rest of these compounds are fit in rule of five can be classified as drug-like compounds, these compounds were selected for synthesis, other compounds were selected randomly for synthesis see table (2.10).

The selected compounds which showed low predicted PIC_{50} ranging from 4.27 to4.67 comparing with the rest of selected compounds showed high or

low predicted PIC_{50} (3.60 to 4.85), when comparing with compound C36. And Doxorubcin = PIC_{50} = 6.69.

Table 2.8. Designing of acridinedione derivatives and their predicted PIC_{50}

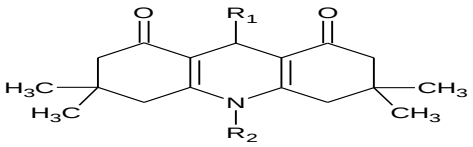

Com No.	R_1	R_2	AM1-IP	a-acc	a-don	TPSA	logP(o/w)	Weight	*predicted PIC_{50}
C1	H	H	8.28266	2	1	46.17	2.36	273.37	3.84
C2	CH_3	H	8.42256	2	1	46.17	2.73	287.40	3.89
C3	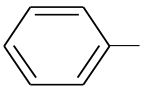	H	8.58666	2	1	46.17	4.01	349.47	4.04
C4	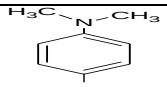	H	7.95074	2	1	49.41	3.92	392.54	4.06
C5	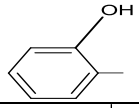	H	8.55518	3	2	66.40	3.734	365.47	4.21
C6	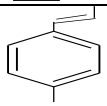	H	8.5106	2	1	46.17	4.649	375.51	4.11
C7	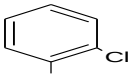	H	8.60739	2	1	46.17	4.595	383.91	4.10
C8	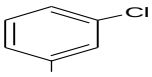	H	8.62309	2	1	46.17	4.634	383.91	3.69
C9	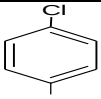	H	8.67126	2	1	46.17	4.597	383.91	3.62
C10	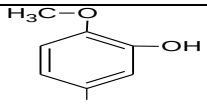	H	8.41111	4	2	75.63	3.688	395.49	4.29
C11	H	CH_3	8.19058	2	0	37.38	2.693	287.40	3.80
C12	CH_3	CH_3	8.29043	2	0	37.38	3.063	301.43	3.84

C13	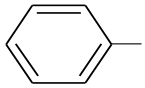	CH_3	8.50517	2	0	37.38	4.338	363.50	3.60
C14	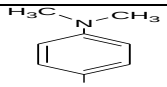	CH_3	7.94527	2	0	40.62	4.253	406.57	4.01
C15	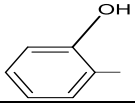	CH_3	8.50715	3	1	57.61	4.067	379.50	4.16
C16	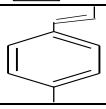	CH_3	8.39357	2	0	37.38	4.982	389.53	4.06
C17	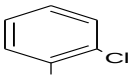	CH_3	8.38936	2	0	37.38	4.928	397.94	4.06
C18	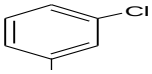	CH_3	8.60639	2	0	37.38	4.967	397.94	4.06
C19	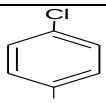	CH_3	8.53012	2	0	37.38	4.93	397.94	4.06
C20	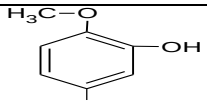	CH_3	8.40898	4	1	66.84	4.021	409.52	4.24
C21	H	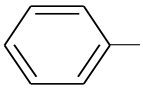	8.2156	2	0	37.38	4.347	349.47	3.99
C22	CH_3	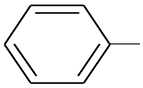	8.3064	2	0	37.38	4.717	363.50	4.03
C23	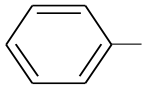	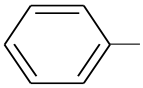	8.4354	2	0	37.38	5.992	425.57	4.18
C24	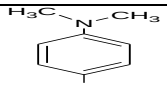	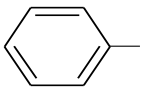	7.9581	2	0	40.62	5.907	468.64	4.20
*C25	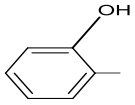	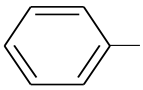	8.4654	3	1	57.61	5.721	441.57	4.34
*C26	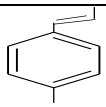	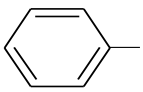	8.4154	2	0	37.38	6.636	451.61	4.25

C27	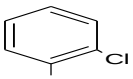	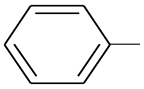	8.3442	2	0	37.38	6.582	460.01	4.25
C28	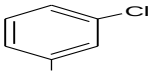	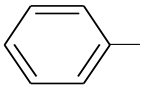	8.6348	2	0	37.8	6.621	460.01	4.25
C29	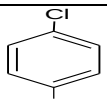	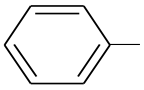	8.4972	2	0	37.38	6.584	460.01	4.25
C30	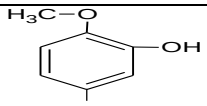	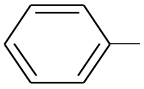	8.3644	4	1	66.81	5.675	471.59	4.44
C31	H	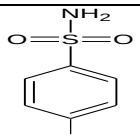	8.4572	4	1	97.54	2.775	428.55	4.40
C32	CH_3	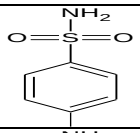	8.5476	4	1	97.54	3.145	442.58	4.45
C33	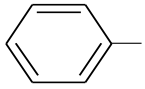	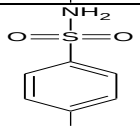	8.6418	4	1	97.54	4.42	504.65	4.60
*C34	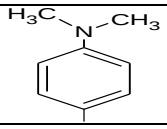	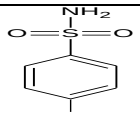	8.0675	4	1	100.78	4.335	547.72	4.62
*C35	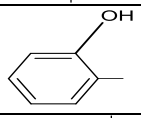	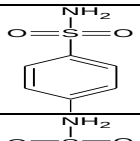	8.7304	5	2	117.77	4.149	520.65	4.77
*C36	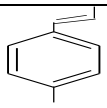	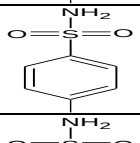	8.6884	4	1	97.54	5.064	530.68	4.67
C37	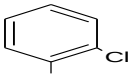	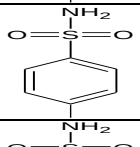	8.6583	4	1	97.54	5.01	539.09	4.66
C38	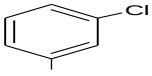	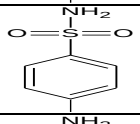	8.7366	4	1	97.54	5.049	539.09	4.67
C39	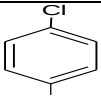	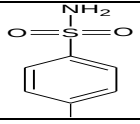	8.7937	4	1	97.54	5.012	539.09	4.66

C40	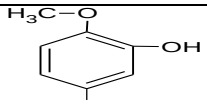	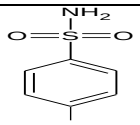	8.5620	6	2	127.00	4.103	550.67	4.85
C41	H	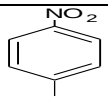	8.5919	2	0	83.20	4.282	394.47	4.44
C42	CH_3	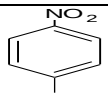	8.6881	2	0	83.20	4.652	408.49	4.48
C43	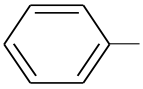	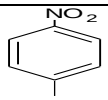	8.7867	2	0	83.20	5.927	470.56	4.63
C44	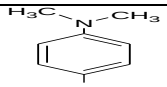	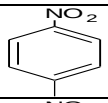	8.1069	2	0	86.44	5.842	513.63	4.65
C45	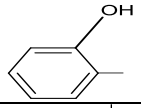	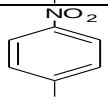	8.8929	3	1	103.43	5.656	486.56	4.80
C46	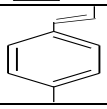	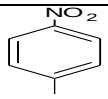	8.7410	2	0	37.38	6.571	496.60	4.25
C47	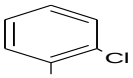	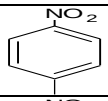	8.7302	2	0	37.38	6.517	505.01	4.25
C48	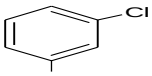	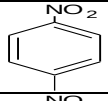	8.9146	2	0	37.38	6.556	505.01	4.25
C49	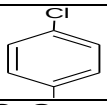	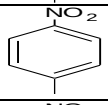	8.9259	2	0	40.62	6.519	505.01	4.27
C50	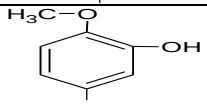	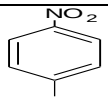	8.6014	4	1	57.61	5.61	516.59	4.34
C51	H	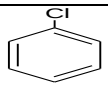	8.3023	2	0	37.38	4.939	383.91	4.06
C52	CH_3	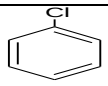	8.4093	2	0	37.38	5.309	397.94	4.10
C53	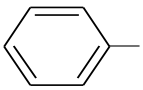	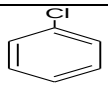	8.4754	2	0	37.38	6.584	460.01	4.25
C54	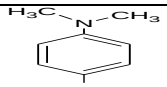	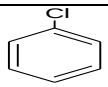	7.8682	2	0	37.38	6.499	503.08	4.24
C55	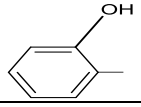	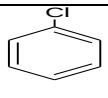	8.5787	3	1	66.84	6.313	476.01	4.51

C56	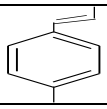	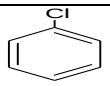	8.5064	2	0	37.38	7.228	486.05	4.32
C57	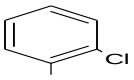	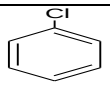	8.5387	2	0	37.38	7.174	494.46	4.32
C58	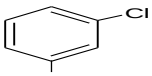	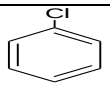	8.6247	2	0	37.38	7.213	494.46	4.32
C59	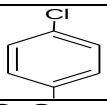	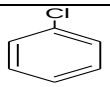	8.6555	2	0	40.62	7.176	494.46	4.35
C60	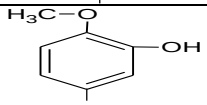	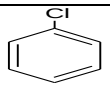	8.4597	4	1	57.61	6.267	506.04	4.41
C61	H	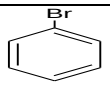	8.3237	2	0	37.38	5.145	428.37	4.08
C62	CH_3	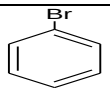	8.4274	2	0	37.38	5.515	442.39	4.12
C63	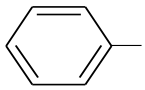	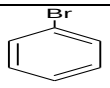	8.5567	2	0	37.38	6.79	504.46	4.27
C64	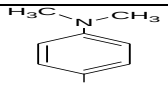	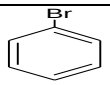	7.8898	2	0	40.62	6.705	547.53	4.29
C65	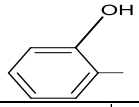	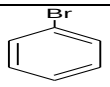	8.5820	3	1	57.61	6.519	520.46	4.44
C66	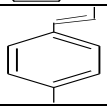	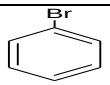	8.5087	2	0	37.38	7.434	530.50	4.35
C67	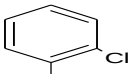	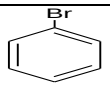	8.4584	2	0	37.38	7.38	538.91	4.34
C68	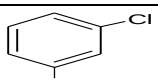	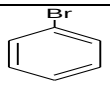	8.6215	2	0	37.38	7.419	538.91	4.35
C69	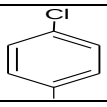	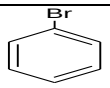	8.6250	2	0	37.38	7.382	538.91	4.34
C70	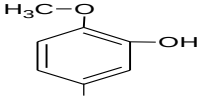	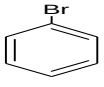	8.4342	4	1	66.84	6.473	550.49	4.53
C71	H	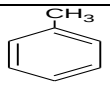	8.1777	2	0	37.38	4.645	363.50	4.02
C72	CH_3	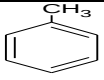	8.2828	2	0	37.38	5.015	377.52	4.07

C73	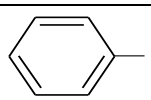	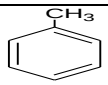	8.3603	2	0	37.38	6.29	439.59	4.21
C74	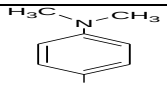	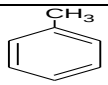	7.9349	2	0	40.62	6.205	482.66	4.24
C75	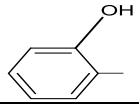	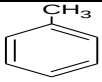	8.4204	3	1	57.61	6.019	455.59	4.38

* Based upon the QSAR model, and molecular docking the following compounds *C25, *C26, *C34, *C35, and *C36 were selected for synthesis. *predicted (PIC_{50}) were calculated from QSAR model equation, No. (27).

2.8.2. Designing of Polyhydroquinoline Derivatives

Polyhydroquinoline derivatives have been reported to possess some interesting biological properties. Their biological activities were predicted by using the obtained predictive QSAR model No. (11) R^2 = (0.81).

Designed compounds gave biological activity (PIC_{50}), ranging from 3.89 to 4.53 M less than standard drug Nicardepine (PIC_{50} = 4.08).

The drug ability of designed derivatives were also evaluated through Lipinski‘s parameters and all within acceptable ranges of parameters shown in table (3.8).

Table 2.9. Designing of polyhydroquinoline derivatives with their predicted PIC_{50}

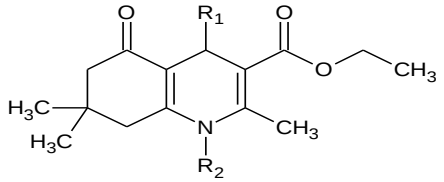

Com No.	R_1	R_2	AM1-IP	dipole	E	density	logP(o/w)	weight	LogP(o/w)	PM3-IP	TPSA	*predicted PIC_{50}
Q1	H	H	8.37727	1.3798	26.3462	0.711636	2.018	263.33	2.0180	8.5709	55.4000	3.93
Q2	CH_3	H	8.49747	1.2391	30.9363	0.703125	2.388	277.36	2.3880	8.6771	55.4000	3.95
Q3	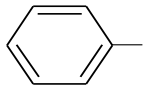	H	8.54577	1.3969	46.1071	0.69984	3.663	339.43	3.6630	8.7054	55.4000	4.14
Q4	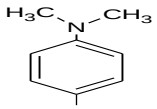	H	7.99826	1.3451	61.1472	0.693219	3.578	382.50	3.578	8.2703	58.6400	4.12
Q5	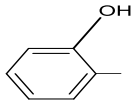	H	8.61446	1.4907	42.8922	0.720172	3.392	355.43	3.392	8.7542	75.6300	4.13
Q6	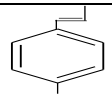	H	8.52635	1.3545	50.2682	0.692217	4.307	365.47	4.307	8.7069	55.4000	4.21

Q7	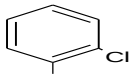	H	8.653791	1.7299	47.2940	0.746306	4.253	373.88	4.40	8.7198	55.4000	4.28
Q8	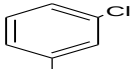	H	8.68946	1.8553	45.2881	0.746306	4.292	373.88	4.41	8.8013	55.4000	4.32
Q9	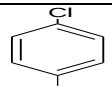	H	8.70191	1.6083	45.7186	0.746306	4.255	373.88	4.41	8.7793	55.4000	4.26
Q10	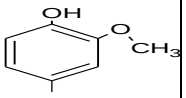	H	8.48757	0.6683	53.8830	0.729167	3.346	385.46	4.23	8.6583	84.8600	3.95
Q11	H	CH_3	8.28504	1.4557	35.0615	0.700256	2.351	277.36	4.04	8.3618	46.6100	3.99
Q12	CH_3	CH_3	8.4255	1.0667	39.2178	0.692933	2.721	291.39	4.13	8.4870	46.6100	3.95
Q13	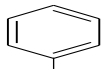	CH_3	8.43527	1.4704	55.2915	0.691621	3.996	353.46	4.31	8.5253	46.6100	4.20
Q14	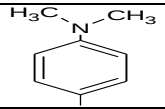	CH_3	7.96856	1.4402	70.4085	0.686248	3.911	396.53	4.15	8.2603	49.8500	4.18
Q15	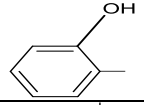	CH_3	8.5209	1.3817	51.6952	0.711069	3.725	369.46	4.29	8.5746	66.8400	4.15
Q16	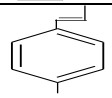	CH_3	8.45069	1.4634	58.9282	0.684994	4.64	379.5	4.40	8.5081	46.6100	4.27

Q17	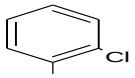	CH_3	8.38549	0.9990	55.5461	0.73604	4.586	387.90	4.38	8.4337	46.6100	4.18
Q18	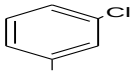	CH_3	8.51579	1.4968	53.8842	0.73604	4.625	387.90	4.41	8.6361	46.6100	4.28
Q19	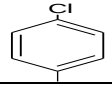	CH_3	8.58884	1.3836	54.3193	0.73604	4.588	387.90	4.43	8.6212	46.6100	4.25
Q20	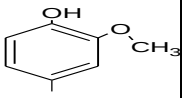	CH_3	8.43751	0.7595	61.4852	0.720217	3.679	399.48	4.26	8.4945	76.0700	4.01
Q21	H	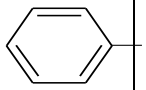	8.29026	1.2058	62.0470	0.697516	4.005	339.43	4.27	8.4341	46.6100	4.14
Q22	CH_3	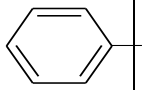	8.37146	1.2004	65.6887	0.691621	4.375	353.46	4.34	8.4434	46.6100	4.19
*Q23	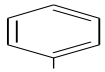	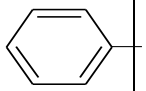	8.42195	1.2433	81.5941	0.690704	5.650	415.53	4.52	8.5507	46.6100	4.36
*Q24	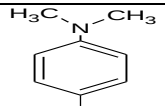	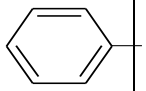	7.97589	1.2087	97.6824	0.686151	5.565	458.60	4.40	8.2378	49.8500	4.35

*Q25	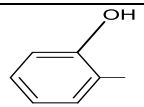	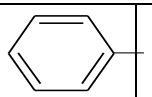	8.51627	1.3070	78.2524	0.707279	5.379	431.53	4.52	8.4694	66.8400	4.34
Q26	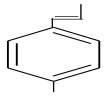	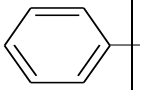	8.43818	1.1890	86.5120	0.685069	6.294	441.57	4.62	8.5500	46.6100	4.43
Q27	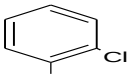	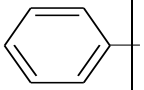	8.37494	0.7558	81.9823	0.728634	6.24	449.97	4.60	8.5012	46.6100	4.33
Q28	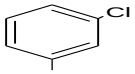	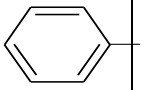	8.55014	0.9349	80.0269	0.728634	6.279	449.97	4.65	8.5229	46.6100	4.37
Q29	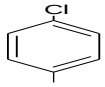	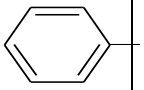	8.54258	1.3948	81.9230	0.728634	6.242	449.97	4.64	8.7918	46.6100	4.46
Q30	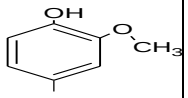	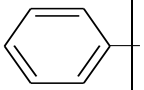	8.42585	0.5112	89.2226	0.715349	5.333	461.55	4.49	8.4587	76.0700	4.17
Q31	H	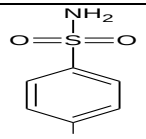	8.53858	0.9536	34.9903	0.775087	2.433	418.51	4.12	8.6767	106.7700	3.89

Q32	CH_3	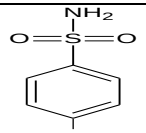	8.62384	0.8556	38.9657	0.766392	2.803	432.54	4.19	8.7726	106.7700	3.92
Q33	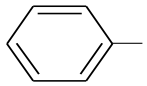	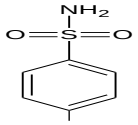	8.69417	1.0713	52.2527	0.755212	4.078	494.61	4.39	8.8123	106.7700	4.13
Q34	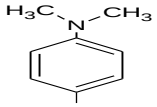	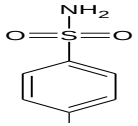	8.14064	1.0828	67.6231	0.745028	3.993	537.68	4.23	8.4047	110.0100	4.12
Q35	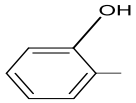	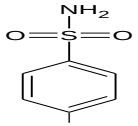	8.75897	1.0267	51.8444	0.769626	3.807	510.61	4.36	8.7516	127.0000	4.08
*Q36	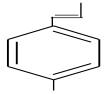	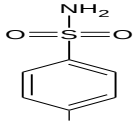	8.68812	0.8323	60.3337	0.746037	4.722	520.65	4.47	8.7574	106.7700	4.16
Q37	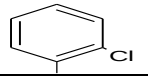		8.62517	0.8031	51.8396	0.788593	4.668	529.05				

		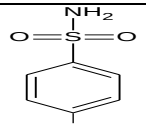							4.45	8.7485	106.7700	4.14
Q38	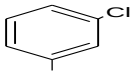	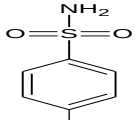	8.80085	1.1551	54.5289	0.788593	4.707	529.05	4.50	8.9233	106.7700	4.22
Q39	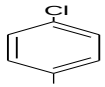	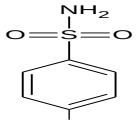	8.80326	1.1595	51.7898	0.788593	4.67	529.05	4.59	8.8035	106.7700	4.22
*Q40	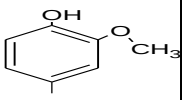	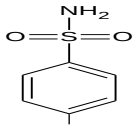	8.58614	0.6367	59.8400	0.773949	3.761	540.63	4.31	8.7167	136.2100	3.99
Q41	H	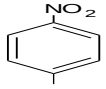	8.68457	0.3959	81.3324	0.752997	3.94	384.43	4.41	8.7167	92.4300	3.97
Q42	CH_3	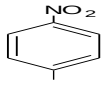	8.75281	0.5165	84.6398	0.744832	4.31	398.45	4.43	8.8092	92.4300	4.04

Q43	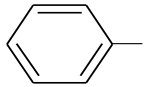	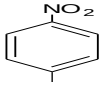	8.82567	0.3809	101.3183	0.736247	5.585	460.53	4.63	8.9247	92.4300	4.17
Q44	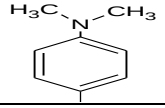	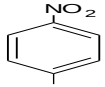	8.18467	0.5465	117.3811	0.727459	5.5	503.59	4.45	8.5145	95.6700	4.19
Q45	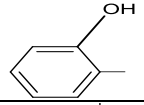	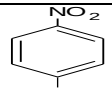	8.87235	0.4956	99.7244	0.751585	5.314	476.52	4.60	8.8893	112.6600	4.16
Q46	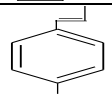	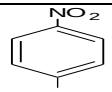	8.80126	0.4341	105.7087	0.727887	6.229	486.56	4.71	8.8083	92.4300	4.26
Q47	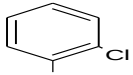	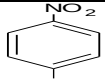	8.74856	0.8513	101.8137	0.771631	6.175	494.97	4.69	8.8490	92.4300	4.34
Q48	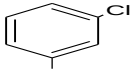	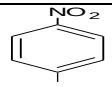	8.91539	0.7570	100.3599	0.771631	6.214	494.97	4.73	8.8764	92.4300	4.33
Q49	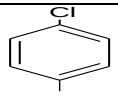	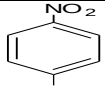	8.93196	0.4613	101.5985	0.771631	6.177	494.97	4.73	9.2007	92.4300	4.26
Q50	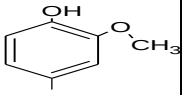	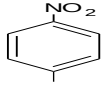	8.66471	1.0665	109.4942	0.757044	5.268	506.55	4.54	9.1467	121.8900	4.27
Q51	H	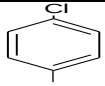	8.3844	0.7722	61.1060	0.743907	4.597	373.88	4.38	8.4953	46.6100	4.13

Q52	CH_3	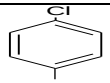	8.45168	0.5625	65.0014	0.73604	4.967	387.90	4.45	8.5806	46.6100	4.13
Q53	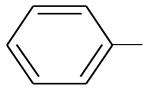	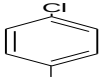	8.56441	0.7947	80.8529	0.728634	6.242	449.97	4.65	8.6175	46.6100	4.34
Q54	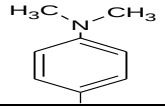	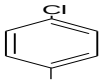	8.02615	0.8379	96.0482	0.720487	6.157	493.04	4.50	8.2860	49.8500	4.34
Q55	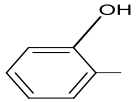	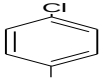	8.62003	0.8077	77.9675	0.74427	5.971	465.97	4.62	8.5905	66.8400	4.31
Q56	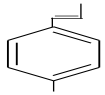	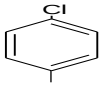	8.52486	0.7957	85.8037	0.720668	6.886	476.01	4.73	8.5552	46.6100	4.42
Q57	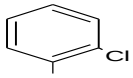	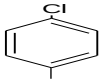	8.59715	1.1782	81.1142	0.764653	6.832	484.42	4.74	8.5629	46.6100	4.49
Q58	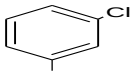	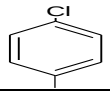	8.68287	1.1950	80.2742	0.764653	6.871	484.42	4.76	8.8738	46.6100	4.50
Q59	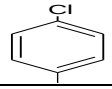	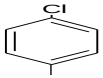	8.68787	0.9079	81.1566	0.764653	6.834	484.42	4.76	8.7438	46.6100	4.44
Q60	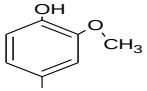	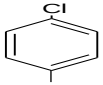	8.52096	0.2395	88.0860	0.750182	5.925	496.00	4.58	8.5274	76.0700	4.18

Q61	H	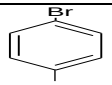	8.40535	0.8567	61.5583	0.811314	4.803	418.33	4.41	8.4374	46.6100	4.17
Q62	CH_3	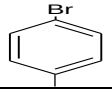	8.5076	0.6199	65.5362	0.800588	5.173	432.35	4.49	8.5927	46.6100	4.17
Q63	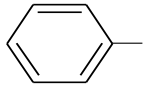	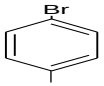	8.59185	0.8829	81.3626	0.784067	6.448	494.42	4.68	8.6247	46.6100	4.38
Q64	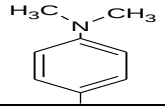	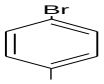	8.04034	0.8999	96.5257	0.770765	6.363	537.49	4.53	8.2923	49.8500	4.37
Q65	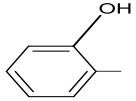	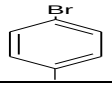	8.67524	1.0674	79.3476	0.798645	6.177	510.42	4.67	8.7477	66.8400	4.39
Q66	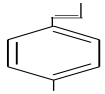	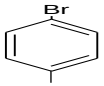	8.53671	0.8275	86.2440	0.77272	7.092	520.46	4.76	8.6633	46.6100	4.45
Q67	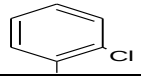	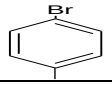	8.57977	1.2602	82.0484	0.817992	7.038	528.87	4.76	8.5991	46.6100	4.53
Q68	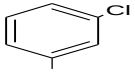	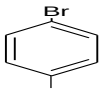	8.641851	1.3238	80.4079	0.817992	7.077	528.87	4.78	8.7263	46.6100	4.55
Q69	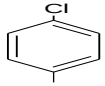	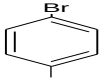	8.69667	1.0364	80.8270	0.817992	7.04	528.84	4.79	8.7113	46.6100	4.49

Q70	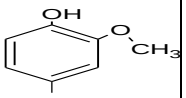	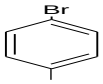	8.52428	1.5800	89.1305	0.801613	6.131	540.45	4.62	8.6376	76.0700	4.49
Q71	H	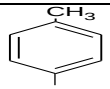	8.25994	1.2380	64.3087	0.691621	4.303	353.46	4.30	8.3578	46.6100	4.19
Q72	CH_3	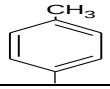	8.34693	1.0790	681369	0.686264	4.673	367.48	4.38	8.4664	46.6100	4.20
Q73	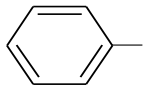	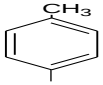	8.40922	1.2732	84.0115	0.686157	5.948	429.56	4.57	8.4442	46.6100	4.13
Q74	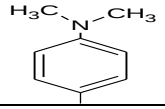	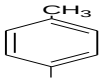	7.98061	1.2610	98.7393	0.682203	5.863	472.62	4.45	8.2348	49.8500	4.39
Q75	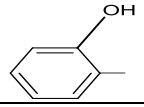	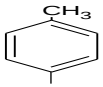	8.5271	1.3670	80.2150	0.702155	5.677	445.55	4.56	8.4032	66.8400	4.39

* Based upon the QSAR model, and molecular docking the following compounds *Q23, *Q24, *Q25, *Q36, and *Q40 were selected for synthesis.

*predicted (PIC_{50}) were calculated from QSAR model equation, No. (11).

2.9. Molecular docking

After drawing the target molecule, using suitable software the ligand is docked onto the receptor and the interactions were checked. The scoring function generates scores depending on which the ligand with the best is selected.

All the designed of N-substituted Acridinedione derivatives (C1-C75), were subjected to molecular docking studies in order to investigate their binding mechanisms with 5OM7 protein, which was downloaded from protein data bank (PDB).The designed polyhydroquinoline derivatives (Q1-Q75), were also subjected to docking studies, for another protein (4gdb) which was selected for this purpose and the results were listed in table (2.10), and (2.12). For 2D, 3D and ligand interaction see appendix.

Table 2.10. Molecular docking of designed acridinedione derivatives

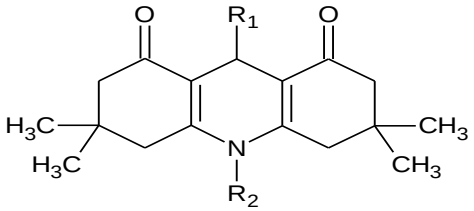

Entry	R1	R2	S	rmsd	Amino - acid	Group of interaction	Types of interaction	Length in (Å)
C1	H	H	-0.4843	1.83	SerA274	C=O	H-bond	2.98
C2	CH_3	H	22.85	1.33	SerA274	C=O	H-bond	2.97
C3	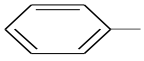	H	46.50	1.01	GluA278 TrpB388 PheA277	N-H Phenyl phenyl	H-bond π- bond π- bond	1.82 - -
C4	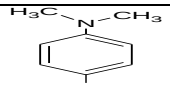	H	61.53	1.39	TrpB388	phenyl	π- bond	-

C5	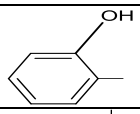	H	71.72	1.31	GluA278 TrpB388	O-H phenyl	H-bond π- bond	1.64 -
C6	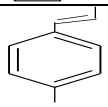	H	-15.83	1.95	TrpB388 PheA277	Phenyl phenyl	π- bond π- bond	- -
C7	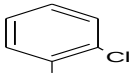	H	72.80	1.08	SerA274	C=O	H-bond	3.07
C8	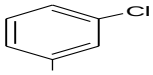	H	114.82	1.19	TrpB388 PheA277	Phenyl phenyl	π- bond π- bond	- -
C9	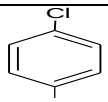	H	55.53	1.25	GluA278	N-H	H-bond	1.87
C10	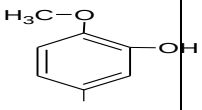	H	55.35	2.21	TrpB388 GluA278 SerA274	Phenyl O-H CH_3O	π- bond H-bond H-bond	- 1.91 3.19
C11	H	CH_3	0.77	1.18	SerA274	C=O	H-bond	2.98
C12	CH_3	CH_3	21.56	1.93	SerA274	C=O	H-bond	2.96
C13	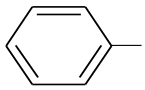	CH_3	65.51	1.44	TrpB388 TrpB388	Phenyl Phenyl	π- bond π- bond	- -
C14	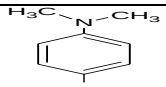	CH_3	85.72	1.33	SerA274 PheA277	C=O Phenyl	H-bond π- bond	2.54 -
C15	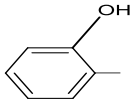	CH_3	94.83	2.04	GlnA278 SerA274	O-H O-H	H-bond H-bond	2.40 3.76
C16	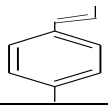	CH_3	-13.15	2.66	TrpB388 PheA277	Phenyl Phenyl	π- bond π- bond	- -
C17	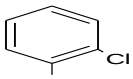	CH_3	-17.40	8.69	PheA277	Phenyl	π- bond	-
C18	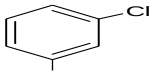	CH_3	-15.67	7.53	TrpB388 PheA277	Phenyl Phenyl	π- bond π- bond	- -
C19		CH_3	70.58	3.85	SerA274 TrpB388	C=O Phenyl	H-bond π- bond	2.47 -

	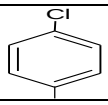				PheA277	Phenyl	π- bond	-
C20	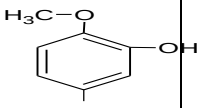	CH_3	83.75	1.45	SerA274 SerA274 GluA278 TrpB388	CH_3O O-H O-H Phenyl	H-bond H-bond H-bond π- bond	2.90 3.20 2.35 -
C21	H	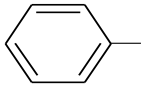	39.89	139	AsnB383 TrpB388	C=O Phenyl	H-bond π- bond	3.23 -
C22	CH_3	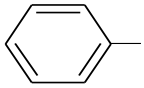	51.68	1.40	SerA274	C=O	H-bond	2.97
C23	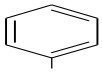	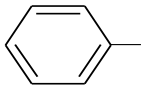	69.36	1.68	GlnA242 TrpB388	C=O Phenyl	H-bond π- bond	2.76 -
C24	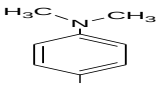	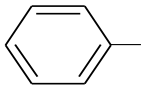	65.01	2.62	AsnB383 TrpB388	C=O Phenyl	H-bond π- bond	2.73 -
C25	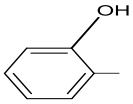	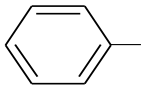	69.12	1.55	AsnB383 GlnA242 TrpB388	C=O C=O Phenyl	H-bond H-bond π- bond	2.77 3.75 -
C26	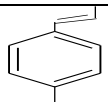	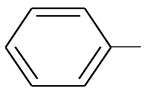	50.17	1.48	TrpB388 PheA277	Phenyl Phenyl	π- bond π- bond	- -
C27	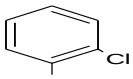	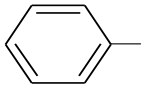	76.29	2.26	SerA274 TrpB388 PheA277	C=O Phenyl Phenyl	H-bond π- bond π- bond	3.16 - -
C28	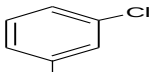	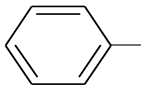	68.81	1.98	AsnB383 GlnA242 TrpB388	C=O C=O Phenyl	H-bond H-bond π- bond	3.73 2.86 -
C29	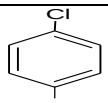	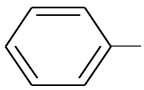	59.91	1.36	TrpB388 PheA277	Phenyl Phenyl	π- bond π- bond	- -

C30	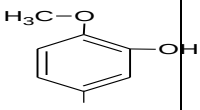	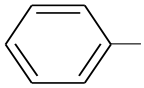	67.82	2.19	GlnA242 AsnB383 TrpB388	C=O C=O Phenyl	H-bond H-bond π- bond	2.73 5.05 -
C31	H	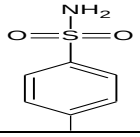	36.69	2.87	SerA274 TrpB388	S=O Phenyl	H-bond π- bond	2.85 -
C32	CH_3	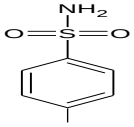	161.73	1.32	GlnA242 AspB383 PheA277 TrpB388	S=O S=O Phenyl Phenyl	H-bond H-bond π- bond π- bond	2.86 3.67 - -
C33	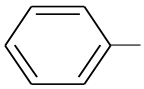	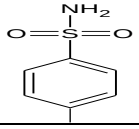	59.55	1.49	SerA274 GlnA242 TrpB388	S=O C=O Phenyl	H-bond H-bond π- bond	2.85 3.84 -
C34	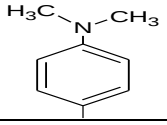	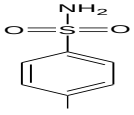	55.92	1.99	SerA274 GlnA242 TrpB388	N-H C=O Phenyl	H-bond H-bond π- bond	2.23 2.74 -
C35	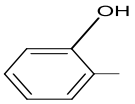	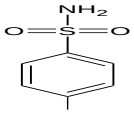	70.41	1.84	GlnA242 SerA274 TrpB388	O-H S=O Phenyl	H-bond H-bond π- bond	2.74 3.02 -
C36	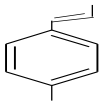	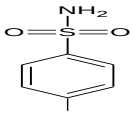	-17.49	6.42	TrpB388 PheA277 LeuA280	Phenyl Phenyl N-H	π- bond π- bond H-bond	- - 2.19
C37	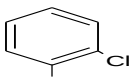	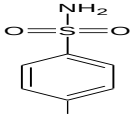	-19.16	9.03	PheA277	Phenyl	π- bond	-
C38	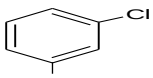	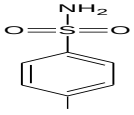	73.71	2.87	AsnB383 SerA277 TrpB388	S=O C=O Phenyl	H-bond H-bond π- bond	3.41 2.70 -
C39	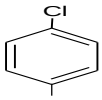	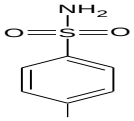	67.38	1.66	AsnB383 GlnA242 SerA274 TrpB388	C=O C=O S=O Phenyl	H-bond H-bond H-bond π- bond	2.86 2.72 2.67 -
					SerA274	O-H	H-bond	3.19

C40	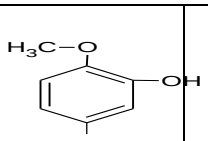	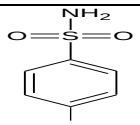	80.51	1.37	GluA278 SerA274 TrpB388	O-H CH_3O phenyl	H-bond H-bond π- bond	1.76 2.90 -
C41	H	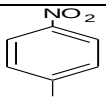	33.14	1.44	AsnB383 TrpB388	C=O Phenyl	H-bond π- bond	3.12 -
C42	CH_3	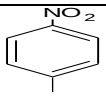	152.45	1.55	SerA274 PheA277	C=O Phenyl	H-bond π- bond	3.01 -
C43	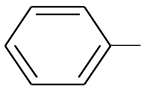	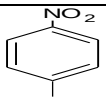	89.87	2.00	PheA277 TrpB388	Phenyl Phenyl	π- bond π- bond	- -
C44	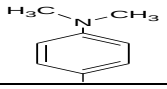	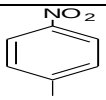	65.53	1.72	AsnB383 TrpB388	C=O Phenyl	H-bond π- bond	5.06 -
C45	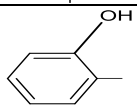	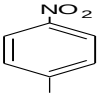	115.09	2.11	TrpB388 PheA277	Phenyl Phenyl	π- bond π- bond	- -
C46	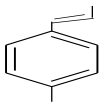	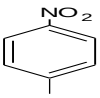	66.06	1.53	AsnB383 TrpB388	C=O Phenyl	H-bond π- bond	2.67 -
C47	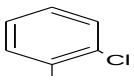	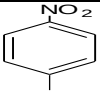	64.72	1.55	AsnB383 TrpB388	C=O Phenyl	H-bond π- bond	3.48 -
C48	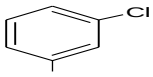	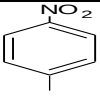	64.53	1.64	AsnB383 TrpB388	C=O Phenyl	H-bond π- bond	3.57 -
C49	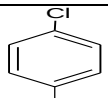	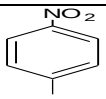	65.30	1.52	AsnB383 TrpB388	C=O Phenyl	H-bond π- bond	2.69 -
C50	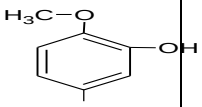	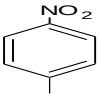	59.85	1.46	AsnB383 TrpB388	C=O Phenyl	H-bond π- bond	2.80 -
C51	H	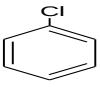	55.31	1.42	SerA274	C=O	H-bond	6.86
C52	CH_3	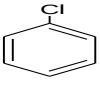	92.99	1.16	SerA274	C=O	H-bond	2.90

C53	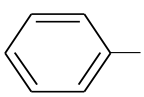	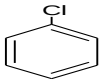	68.75	1.75	TrpB388	Phenyl	π- bond	-
C54	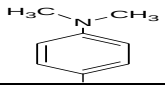	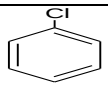	68.61	1.45	AsnB383 TrpB388	C=O Phenyl	H-bond π- bond	3.40 -
C55	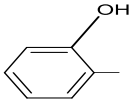	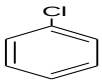	200.36	1.69	GlnA270 PheA277 TrpB388	O-H Phenyl Phenyl	H-bond π- bond π- bond	1.95 - -
C56	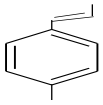	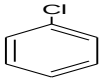	67.11	2.77	AsnB383 GlnA242 TrpB388	C=O C=O Phenyl	H-bond H-bond π- bond	5.56 2.74 -
C57	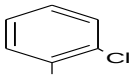	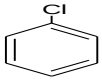	67.06	1.94	AsnB383 GlnA242 TrpB388	C=O C=O Phenyl	H-bond H-bond π- bond	2.82 2.75 -
C58	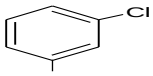	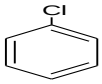	66.86	2.53	AsnB383 GlnA242 TrpB388	C=O C=O Phenyl	H-bond H-bond π- bond	2.85 2.75 -
C59	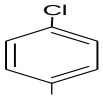	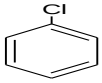	66.76	5.74	SerA274 TrpB388 PheA277	C=O Phenyl phenyl	H-bond π- bond π- bond	2.48 - -
C60	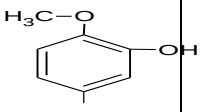	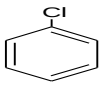	59.72	2.39	AsnB383 TrpB388	C=O Phenyl	H-bond π- bond	2.82 -
C61	H	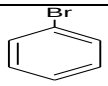	63.50	1.58	SerA274 PheA277	C=O Phenyl	H-bond π- bond	2.77 -
C62	CH_3	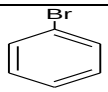	111.45	1.64	SerA274 PheA277	C=O Phenyl	H-bond π- bond	2.87 -
C63	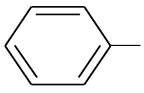	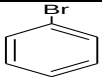	97.66	1.78	TrpB388 PheA277	Phenyl Phenyl	π- bond π- bond	- -
C64	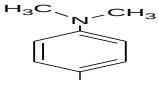	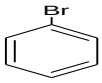	68.29	1.84	AsnB383 GlnA242 TrpB388	C=O C=O Phenyl	H-bond H-bond π- bond	2.81 2.70 -

C65	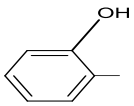	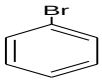	73.54	0.92	AsnB383 TrpB388 TrpB388	O-H O-H Phenyl	H-bond H-bond π- bond	2.89 2.62 -
C66	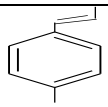	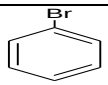	223.88	1.14	SerA274	C=O	H-bond	2.90
C67	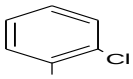	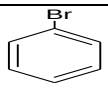	76.15	1.15	AsnB383 TrpB388	C=O Phenyl	H-bond π- bond	2.61 -
C68	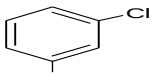	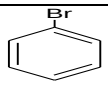	75.66	1.36	AsnB383 TrpB388	C=O Phenyl	H-bond π- bond	2.61 -
C69	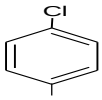	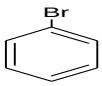	68.67	1.69	AsnB383 GlnA242 TrpB388	C=O O-H Phenyl	H-bond H-bond π- bond	2.84 2.72 -
C70	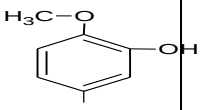	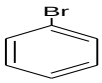	85.45	1.85	PheA277 PheA277 TrpB388	O-H Phenyl Phenyl	H-bond π- bond π- bond	1.96 - -
C71	H	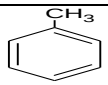	49.39	0.95	SerA274 TrpB388	C=O Phenyl	H-bond π- bond	2.72 -
C72	CH_3	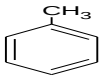	73.34	1.44	SerA274	C=O	H-bond	2.90
C73	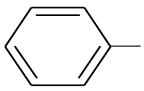	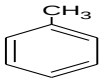	64.59	5.57	SerA274 TrpB388	C=O Phenyl	H-bond π- bond	2.43 -
C74	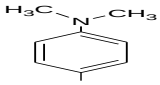	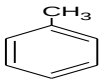	73.72	1.42	AsnB383 TrpB388	C=O Phenyl	H-bond π- bond	2.82 -
C75	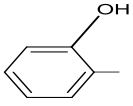	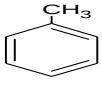	74.91	1.59	GluA278 PheA277 TrpB388	O-H Phenyl Phenyl	H-bond π- bond π- bond	2.21 - -

Table (2.11): structures, molecular docking of imidazolyl derivatives of 1, 8-acridinediones, the training sets, test set, and their reference drug (Doxorubicin) (Jamalian *et al.*, 2011):-

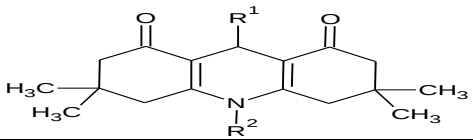

Entry	R1	R2	S	rmsd	Amino - acid	Group of interaction	Types of interaction	Length in (Å)
1	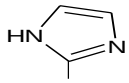	H	50.14	1.36	GluA278 TrpA256	N-H	H-bond	2.02
2	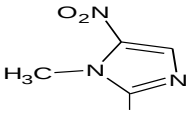	H	79.23	2.45	GluA278 GlnA242 PheA277	N-H N Imidazolyl ring	H-bond π- bond π- bond	2.30 2.81 -
3	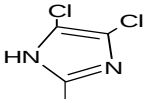	H	38.48	1.26	TrpA386 GluA278 TrpA386 PheA277	C=O N-H Imidazolyl ring Imidazolyl ring	H-bond H-bond π- bond π- bond	2.71 1.72 - -
4	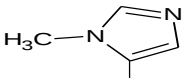	H	16.14	1.40	GluA278	N-H	H-bond	1.82
5	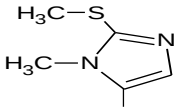	H	11.82	1.16	GluA278	N-H	H-bond	1.88
6	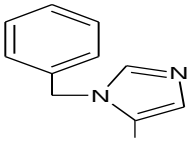	H	12.55	2.36	GluA278	N-H	H-bond	1.80

Doxorubicin (a reference drug)	-35.2941	LeuA280 PheA277 GlnA242 PheA277 TrpB386	N-H N-H OH	H-bond H-bond H-bond π-interaction π-interaction	2.41 1.88 2.15 - -

Table 2.12. Molecular docking of designed polyhydroquinoline derivatives

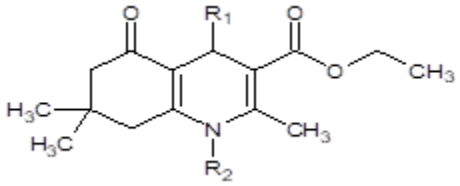

Entry	R1	R2	S	rmsd	Amino - acid	Group of interaction	Types of interaction	Length in (Å)
Q1	H	H	87.53	1.15	HisA74 TrpA98	C=O C=O	H-bond H-bond	2.53 2.82
Q2	-CH_3	H	95.25	0.94	HisA74	C=O	H-bond	2.64
Q3	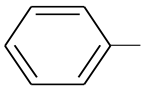	H	187.57	1.04	GluA101	N-H	H-bond	1.78
Q4	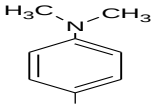	H	272.63	0.95	HisA74 TrpA98 Zn502	C=O Phenyl Phenyl	H-bond π- bond π- bond	2.46 - -
Q5	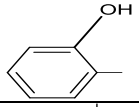	H	143.97	1.42	GluA101	N-H	H-bond	2.33
Q6	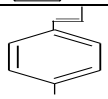	H	134.79	1.49	TrpA98	Phenyl	π- bond	-
Q7	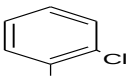	H	335.03	0.82	GluA101	N-H	H-bond	1.68
Q8	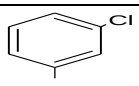	H	210.14	1.12	GluA101	N-H	H-bond	1.96

Q9	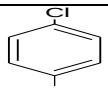	H	250.52	1.03	GluA101	N-H	H-bond	1.74
Q10	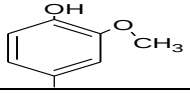	H	241.63	1.13	GluA101 GlyA192	N-H O-H	H-bond H-bond	1.69 1.79
Q11	H	CH_3	99.82	0.87	HisA194	C=O	H-bond	2.48
Q12	$-CH_3$	CH_3	107.16	1.11	HisA194	C=O	H-bond	2.49
Q13	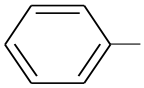	CH_3	205.44	1.12	HisA74 HisA221 AspA209 HisA221 HisA72 HisA74	C=O Phenyl Zn502	H-bond π- bond π- cation	3.01 - -
Q14	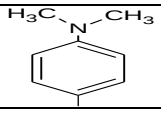	CH_3	235.74	1.23	TrpA98 TrpA98	C=O Phenyl	H-bond π- bond	2.66 -
Q15	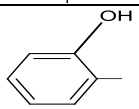	CH_3	347.50	1.09	GluA101 TrpA98 HisA74	O-H C=O Phenyl	H-bond H-bond π- bond	1.70 2.37 -
Q16	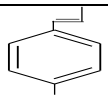	CH_3	216.83	1.25	TrpA98	C=O	H-bond	2.80
Q17	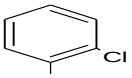	CH_3	229.07	1.11	HisA194 HisA194	C=O Phenyl	H-bond π- bond	1.35 -
Q18	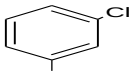	CH_3	255.11	1.45	HisA221 HisA72 HisA74 AspA309	Phenyl Zn502 C=O- Zn	π- bond π- cation	- -
Q19	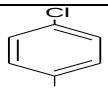	CH_3	241.58	0.99	HisA194	C=O	H-bond	2.14
Q20	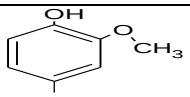	CH_3	309.54	0.87	GlyA192	O-H	H-bond	2.16
Q21	H	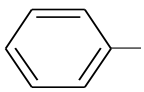	174.15	1.52	HisA194	Phenyl	π- bond	-

Q22	CH_3	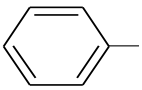	209.74	1.16	HisA258 HisA74 AspA309 HisA72 HisA221	C=O C=O- Zn	H-bond π- cation	2.58 - - - -
Q23	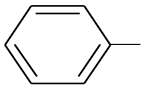	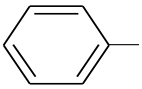	434.75	1.15	HisA221 Zn502	C=O Phenyl	H-bond π- cation	2.55 -
Q24	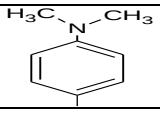	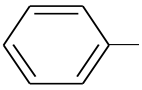	475.64	1.12	HisA194 HisA194	C=O Phenyl	H-bond π- bond	2.26 -
Q25	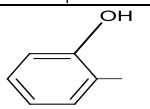	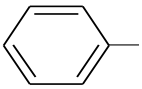	425.60	1.45	TrpA98 Zn502	Phenyl Phenyl	π- bond π- cation	- -
Q26	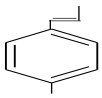	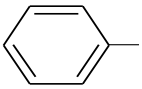	233.18	1.78	GluA101 TrpA98 GlyA192 Zn502 HisA255	Phenyl Phenyl Phenyl Phenyl Phenyl	π- bond π- bond π- bond π- bond π- bond	- - - - -
Q27	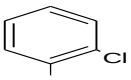	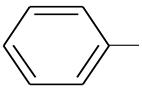	488.89	1.09	HisA194 HisA194	C=O Phenyl	H-bond π- bond	2.19 -
Q28	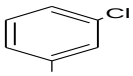	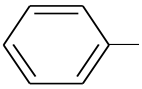	385.03	1.23	HisA194 HisA194	C=O Phenyl	H-bond π- bond	2.30 -
Q29	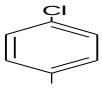	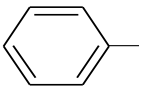	424.72	1.01	HisA194 HisA255 HisA194 HisA221	C=O C=O Phenyl Phenyl	H-bond H-bond π- bond π- bond	2.35 2.28 - -
Q30	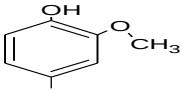	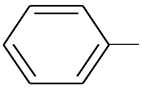	239.03	1.39	HisA255 GluA224 TrpA98 HisA255	CH_3O- O-H Phenyl Phenyl	H-bond H-bond π- bond π- bond	2.99 3.11 - -
Q31	H	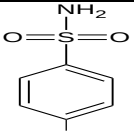	208.62	1.21	ProA180	N-H	H-bond	3.81

Q32	CH_3	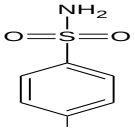	269.86	1.43	GluA101 TrpA98 HisA255 HisA194	N-H S=O C=O Phenyl	H-bond H-bond H-bond π- bond	1.98 2.79 2.49 -
Q33	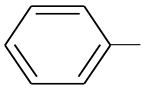	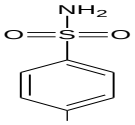	413.95	1.53	HisA194 HisA194 HisA72 HisA74 AspA309 HisA221	C=O Phenyl C=O- Zn	H-bond π- bond π- cation π- cation π- cation π- cation	2.38 - - - - -
Q34	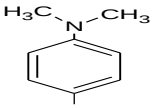	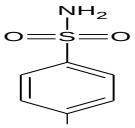	413.78	1.51	ProA180 TrpA98 HisA74 Zn502	N-H Phenyl Phenyl Phenyl	H-bond π- bond π- bond π- cation	6.66 - - -
Q35	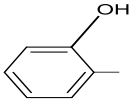	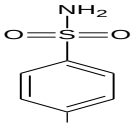	501.50	1.37	GluA101 SerA313 HisA255 GluA224 TrpA98 Zn502	O-H S=O S=O N-H Phenyl Phenyl	H-bond H-bond H-bond H-bond π- bond π- cation	2.90 2.83 2.63 2.35 - -
Q36	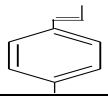	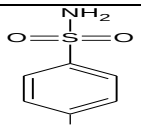	264.83	1.30	HisA221 Zn502	Phenyl Phenyl	π- bond π- cation	- -
Q37	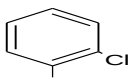	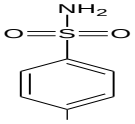	458.29	1.22	AspA309 GluA101 SerA313 SerA223 TrpA98 Zn502	N-H N-H S=O S=O S=O Phenyl	H-bond H-bond H-bond H-bond H-bond π- cation	1.77 2.14 2.37 2.25 2.78 -
Q38	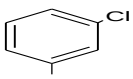	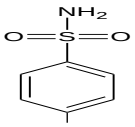	413.80	1.29	SerA223 AspA309 SerA313 SerA223 HisA221	N-H N-H S=O S=O Phenyl	H-bond H-bond H-bond H-bond π- bond	1.53 2.08 2.51 2.19 -

					Zn502	Phenyl	π- cation	-
Q39	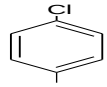	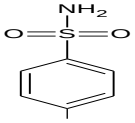	555.74	1.28	GluA101 SerA223 SerA223 SerA313 AspA309 Zn502	N-H N-H N-H S=O S=O Phenyl	H-bond H-bond H-bond H-bond H-bond π- cation	1.64 2.39 2.46 2.26 2.61 -
Q40	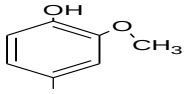	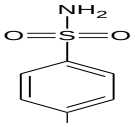	577.12	1.37	TyrA197 HisA255 SerA223 HisA255 HisA221 HisA72 HisA74 HisA221 AspA309	C=O CH_3O- CH_3O- O-H O-H Zn502 Zn502 Zn502 Zn502	H-bond H-bond H-bond H-bond H-bond π- cation π- cation π- cation π- cation	2.37 3.12 3.22 2.27 2.46 - - - -
Q41	H	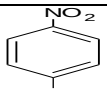	213.76	1.14	HisA194	C=O	H-bond	2.67
Q42	CH_3	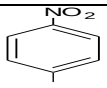	216.28	1.36	HisA255 HisA194	C=O Phenyl	H-bond π- bond	4.32 -
Q43	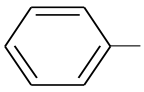	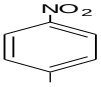	424.67	1.29	TyrA197 HisA255 HisA194	C=O Phenyl Phenyl	H-bond π- bond π- bond	2.71 - -
Q44	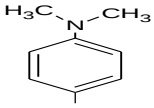	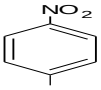	246.36	1.58	HisA221	Phenyl	π- bond	-
Q45	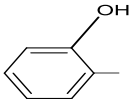	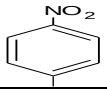	634.32	1.36	SerA213 HisA194	C=O Phenyl	H-bond π- bond	2.27 -
Q46	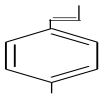	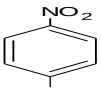	313.34	2.06	HisA221 HisA255 Zn502 TrpA98	Phenyl Phenyl Phenyl Phenyl	π- bond π- bond π- cation π- cation	- - - -
					HisA74	Phenyl	π- bond	-

Q47	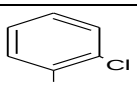	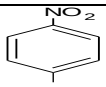	429.42	1.17	Zn502 TrpA98	Phenyl Phenyl	π- cation π- bond	- -
Q48	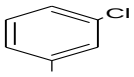	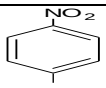	532.64	1.07	TrpA98 HisA74	Phenyl Phenyl	π- bond π- bond	- -
Q49	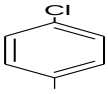	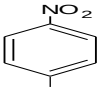	531.26	1.40	TrpA98 HisA221 Zn502	Phenyl Phenyl Phenyl	π- bond π- bond π- cation	- - -
Q50	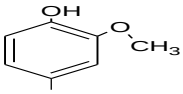	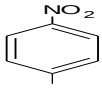	450.15	1.15	SerA313 SerA223 SerA223 HisA194 Zn502	O-H O-H CH_3O- Phenyl Phenyl	H-bond H-bond H-bond π- bond π- cation	3.30 1.71 3.06 - -
Q51	H	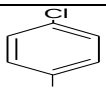	201.52	1.34	HisA74	Phenyl	π- bond	-
Q52	CH_3	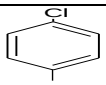	269.44	1.24	HisA194 HisA221	Phenyl Phenyl	π- bond π- bond	- -
Q53	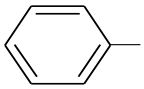	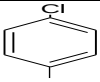	498.63	0.87	HisA194 HisA194	C=O Phenyl	H-bond π- bond	2.27 -
Q54	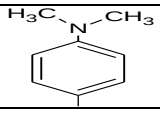	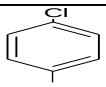	514.07	1.42	HisA194 HisA194	C=O Phenyl	H-bond π- bond	2.17 -
Q55	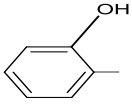	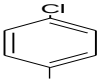	402.12	1.55	TrpA98 TrpA98 HisA194	O-H Phenyl Phenyl	H-bond π- bond π- bond	2.77 - -
Q56	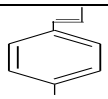	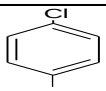	288.34	1.27	TrpA98 HisA255	Phenyl Phenyl	π- bond π- bond	- -
Q57	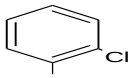	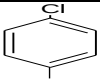	428.95	1.26	HisA221 Zn502	Phenyl Phenyl	π- bond π- bond	- -
Q58	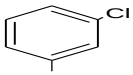	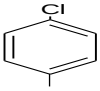	495.11	1.29	TrpA98 HisA221 HisA221 Zn502	C=O C=O Phenyl Phenyl	H-bond H-bond π- bond π- cation	2.47 2.71 - -
Q59	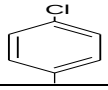	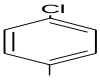	529.85	0.95	TyrA197 HisA194	C=O Phenyl	H-bond π- bond	2.57 -

Q60	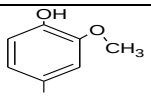	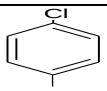	461.79	1.24	MetA122 HisA194	O-H Phenyl	H-bond π- bond	2.31 -
Q61	H	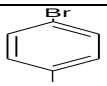	213.03	0.99	HisA194	C=O	H-bond	2.74
Q62	CH_3	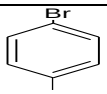	No interaction					
Q63	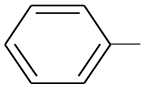	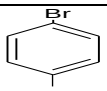	562.39	1.19	HisA221 HisA221	C=O Phenyl	H-bond π- bond	3.73 -
Q64	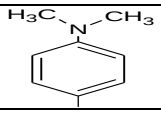	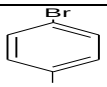	317.41	1.44	HisA74 Zn502	Phenyl Phenyl	π- bond π- cation	- -
Q65	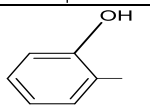	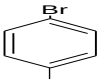	512.97	1.45	HisA194 HisA221 Zn502	O-H Phenyl Phenyl	H-bond π- bond π- bond	2.58 - -
Q66	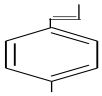	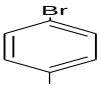	258.24	1.26	TrpA98 HisA221 Zn502	Phenyl Phenyl Phenyl	π- bond π- bond π- cation	- - -
Q67	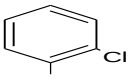	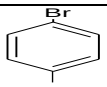	493.29	1.06	HisA221 Zn502	Phenyl Phenyl	π- bond π- cation	- -
Q68	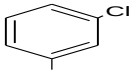	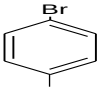	520.44	1.06	HisA221 HisA221 Zn502	C=O Phenyl Phenyl	H-bond π- bond π- cation	2.50 - -
Q69	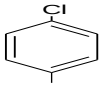	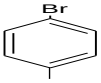	500.40	1.38	TrpA98 HisA221 Zn502	C=O C=O Phenyl	H-bond H-bond π- cation	2.77 2.50 -
Q70	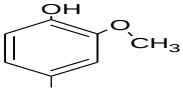	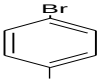	539.43	1.18	GluA101 TrpA98 HisA194 HisA194	O-H O-H C=O Phenyl	H-bond H-bond H-bond π- bond	2.08 3.01 3.98 -
Q71	H	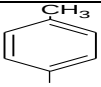	173.52	1.11	TrpA98	Phenyl	π- bond	-
Q72	CH_3	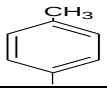	357.93	0.94	HisA255 SerA213	C=O C=O	H-bond H-bond	2.32 2.40

					HisA194	Phenyl	π- bond	-
Q73	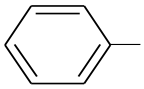	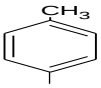	510.50	1.20	TrpA98 HisA221 Zn502	C=O Phenyl Phenyl	H-bond π- bond π- cation	2.58 - -
Q74	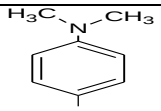	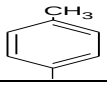	520.91	1.17	HisA194 HisA194	C=O Phenyl	H-bond π- bond	2.43 -
Q75	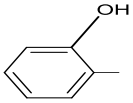	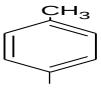	268.92	1.49	HisA74 Zn502	Phenyl Phenyl	π- bond π- cation	- -

Table (2.13): Docking studies 7- substituted hexahydroquinoline derivatives.

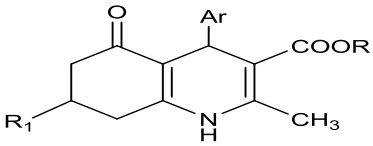

Entry	R	R_1	Ar	S Kcal/mol	rmsd	Amino acid	Group of interaction	Type of interaction	Length In (Å)
1	C_2H_5	CH_3	2,3-dichlorophenyl	262.26	1.10	AspA309 HisA194	N-H phenyl	H-bond π- bond -	2.10
2	C_2H_5	CH_3	2,4-dichlorophenyl	189.45	1.31	TrpA85	C=O phenyl	H-bond π- bond	2.82 -
3	CH_3	CH_3	2,5-dichlorophenyl	186.62	0.78	HisA194 SerA313 HisA221 HisA255	C=O C=O Phenyl Phenyl	H-bond H-bond π- bond π- bond	2.62 2.41 - -
4	C_2H_5	CH_3	2,5-dichlorophenyl	186.62	0.78	HisA194 SerA313 HisA221 HisA255	C=O C=O Phenyl Phenyl	H-bond H-bond π- bond π- bond	2.62 2.41 - -
5	CH_3	CH_3	2,6-dichlorophenyl	235.96	0.84	GluA101	N-H	H-bond	1.78
6	CH_3	C_6H_5	2,3-dichlorophenyl	235.95	0.84	GluA101	N-H	H-bond	1.79
7	CH_3	C_6H_5	2,5-dichlorophenyl	305.01	0.70	HisA74	Phenyl	π- bond	-

8	C_2H_5	C_6H_5	2,5-dichlorophenyl	177.52	0.92	HisA194 HisA194	C=O Phenyl	H-bond π- bond	2.38 -
9	CH_3	C_6H_5	2,6-dichlorophenyl	309.42	0.89	HisA221 - GluA101	Phenyl Phenyl N-H	π- bond π- bond H-bond	- - 3.25
10	C_2H_5	C_6H_5	2,6-dichlorophenyl	320.20	1.03	GluA101 -	N-H Zn^{2+} - cation	H-bond π- cation	2.16 -
11	C_2H_5	CH_3	2,6-dichlorophenyl	202.21	1.15	GluA101 -	N-H Zn^{2+} - cation	H-bond π- cation	1.97 -
12	C_2H_5	C_6H_5	2,3-dichlorophenyl	285.24	0.97	GluA101 HisA221 -	N-H Phenyl- Zn^{2+} cation	H-bond π- cation	2.25 - -
13	CH_3	CH_3	2,4-dichlorophenyl	195.94	1.39	GluA101 -	N-H Phenyl- Zn^{2+} cation	H-bond π- cation	1.77
14	CH_3	C_6H_5	2,4-dichlorophenyl	222.97	1.11	GluA101 HisA221 AspA309	N-H Phenyl Phenyl- Zn^{2+} cation	H-bond Π- bond π- cation π- cation	2.70 - - -
15	C_2H_5	C_6H_5	2,4-dichlorophenyl	309.32	1.13	GluA101 HisA221 -	N-H Phenyl Phenyl- Zn^{2+} cation	H-bond π- bond π- cation	2.41 - -
Nicardepine (a reference drug)			390.0632	1.2269	Trp-A85 His-A194 Trp-A85 Zn502		phenyl phenyl C=O C=O	π- bond π- bond H-bond π-cation	- - 5.10 -

2.10. Synthesis of acridinedione and hexahydroquinoline derivatives

2.10.1. General methods of preparation of acridinedione derivatives

2.10.1. 1.Method (A): preparation of 4-(9-(4-(dimethylamino)phenyl)-3,3,6,6-tetramethyl-1,8-dioxo-2,3,4,5,6,7,8,9-octahydroacridin-10(1H)-yl)benzenesulfonamide(I)

A mixture of aldehyde (1mmol), 5, 5-dimethyl-1, 3-cyclohexanedione (dimedone, 2mmol), sulfanilamide (1mmol) and Cetyl trimethyl ammonium bromide (CTAB) (0.1 mmol) in water (4ml) was vigorously stirred under reflux at 85^0C, for 6 hours. The workup procedure involved simple filteration and washing twice with water (10ml). The desired product of high purity was further achieved by recrystallization from an aqueous ethanol.

2.10.1.2. Method(B): preparation of 9-(2-hydroxyphenyl)-3,3,6,6-tetramethyl-10-phenyl-3,4,6,7,9,10-hexahydroacridine-1,8(2H,5H)-dione (II) and (E)-3,3,6,6-tetramethyl-10-phenyl-9-styryl-3,4,6,7,9,10-hexahydroacridine-1,8(2H,5H)-dione(III)

A mixture of aromatic aldehyde (1mmol), 5, 5-dimethyl, 1, 3-cyclohexanedione (dimedone, 2 mmol), Aniline, (1mmol) in water (4ml) equipped in round-bottomed flask fitted in refluxed condenser, the reaction mixture was stirred vigorously under reflux for three hours at degree of temperature about 98^0C. The reaction mixture was then completed after this period of time, as monitored by using TLC, the workup procedure involved simple filtration and washing cold ice water (10ml). The obtained pale yellow solid product of high purity was further achieved by recrystallization from aqueous ethanol.

2.10.1.3.Method(C):Preparationof4-(9-(2-hydroxyphenyl)-3,3,6,6-tetramethyl-1,8-dioxo-2,3,4,5,6,7,8,9-octahydroacridin-10(1H)-yl)benzenesulfonamide(IV) and (E)-4-(3,3,6,6-tetramethyl-1,8-dioxo-9-

styryl-2,3,4,5,6,7,8,9-octahydroacridin-10(1H)-yl)benzenesulfonamide(V)

A mixture of aromatic aldehyde (1mmol), dimedone, (2mmol), and sulfanilamide (1mmol). Ethanol: water 1: 1 system (5ml) was added to the mixture then stirred and refluxed at 70^0C, for 6 hours.

The reaction mixture was then completed after this period of time, as monitored by using TLC, the workup procedure involved simple filteration and washing with cold ice water (10ml). The obtained pale yellow solid product of high purity was further achieved by recrystallization from aqueous ethanol.

2.10.2. 1.General methods of preparation of hexahydroquinoline derivatives

2.10.2.2. Method(A): Preparation of ethyl 2, 7, 7-trimethyl-5-oxo-1, 4-diphenyl-1, 4, 5, 6, 7, 8-hexahydroquinoline-3-carboxylate(VI), ethyl 4-(2- hydroxyphenyl)-2,7,7-trimethyl-5-oxo-1-phenyl-1,4,5,6,7,8-hexahydroquinoline-3-carboxylate(VII)

A mixture of aromatic aldehyde, (1mmol), 5, 5-dimethyl, 1, 3-cyclohexanedione (dimedone, 1 mmol), Ethyl acetoacetate, (1mmol), and appropriate amine, (1 mmol), in water 4ml were equipped in round-bottom flask fitted with reflux condenser, the reaction mixture was stirred vigorously under reflux for three hours at Degree of temperature at 70^0C.

The reaction mixture was then completed after this period of time, as monitored by using TLC, the workup procedure involved simple filteration and washing with cold ice water (10ml). The obtained pale yellow solid product of high purity was further achieved by recrystallization from aqueous ethanol.

2.10.2.3.Method(B) peparation of ethyl 4-(3-hydroxy-4-methoxyphenyl)-2,7,7-trimethyl-5-oxo-1-(4-sulfamoylphenyl)-1,4,5,6,7,8-hexahydroquinoline-3-carboxylate(VIII),ethyl4-(4-(dimethylamino)phenyl)-2,7,7-trimethyl-5-oxo-1-phenyl-1,4,5,6,7,8-hexahydroquinoline-3-carboxylate(IX), and ethyl (E)-2,7,7-trimethyl-5-oxo-4-styryl-1-(4-sulfamoylphenyl)-1,4,5,6,7,8-hexahydroquinoline-3-carboxylate(X)

A mixture of Aldehyde, ethyl acetoacetate, dimedone, (any amine) ,and ethanol: water 1: 1 system 5ml was added to the mixture, then stirred and refluxed at 70^0C, for 6 hours. The reaction mixture was then completed after this period of time, as monitored by using TLC, the workup procedure involved simple filteration and washing with cold ice water (10ml). The obtained pale yellow solid product of high purity was further achieved by recrystallization from aqueous ethanol.

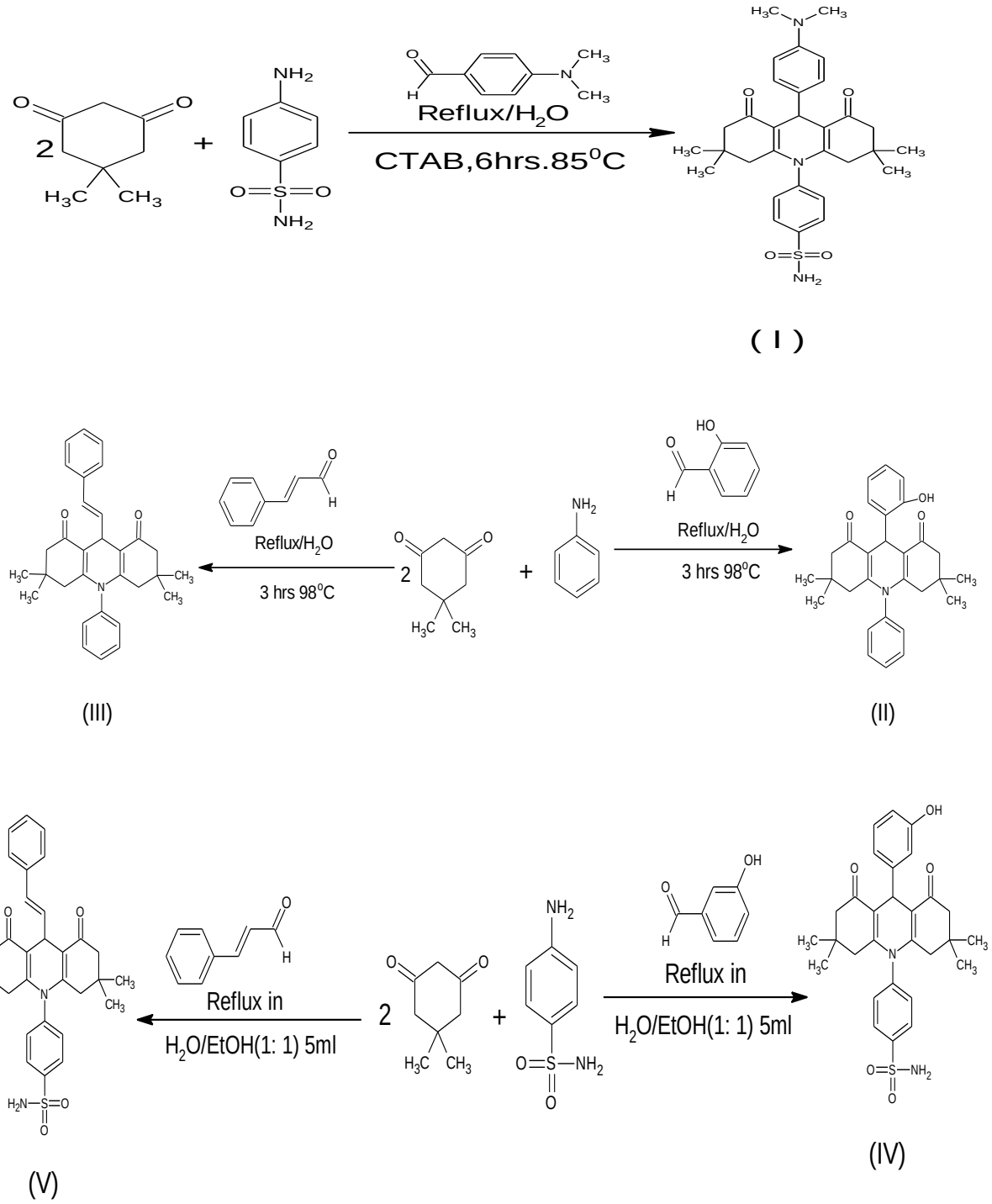

Scheme (2.1): Chemical structure of synthized acridinedione derivatives.

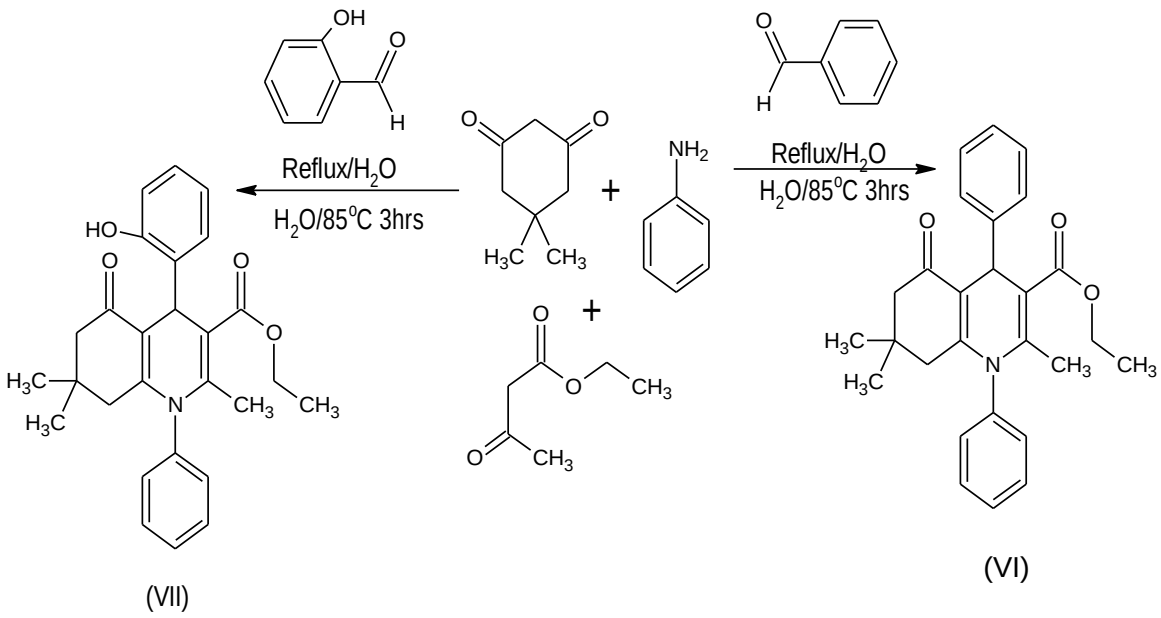

(VII) (VI)

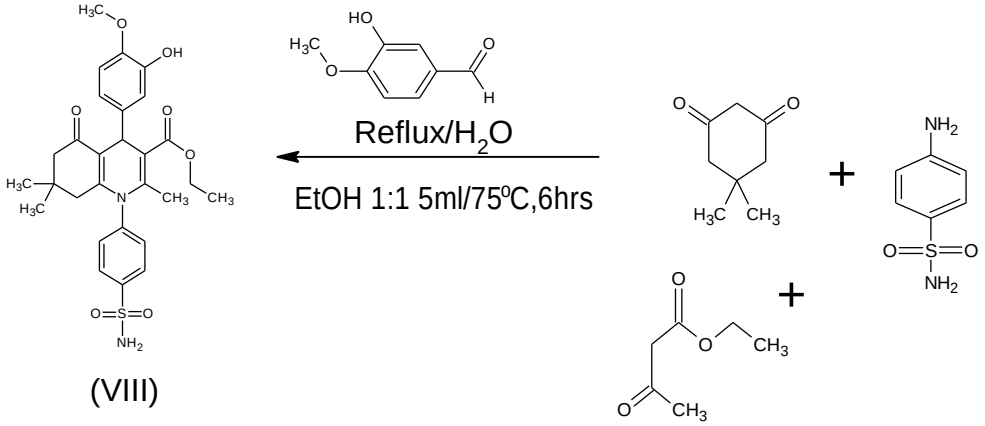

(VIII)

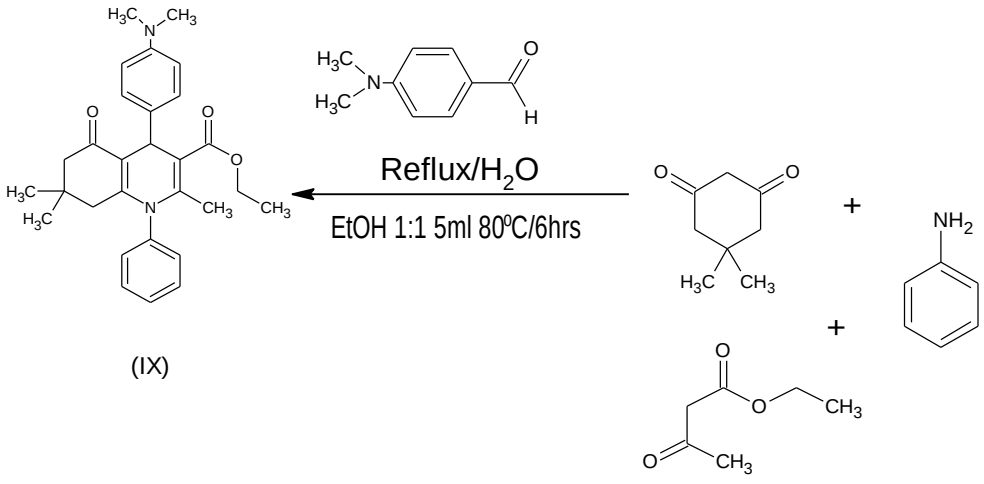

(IX)

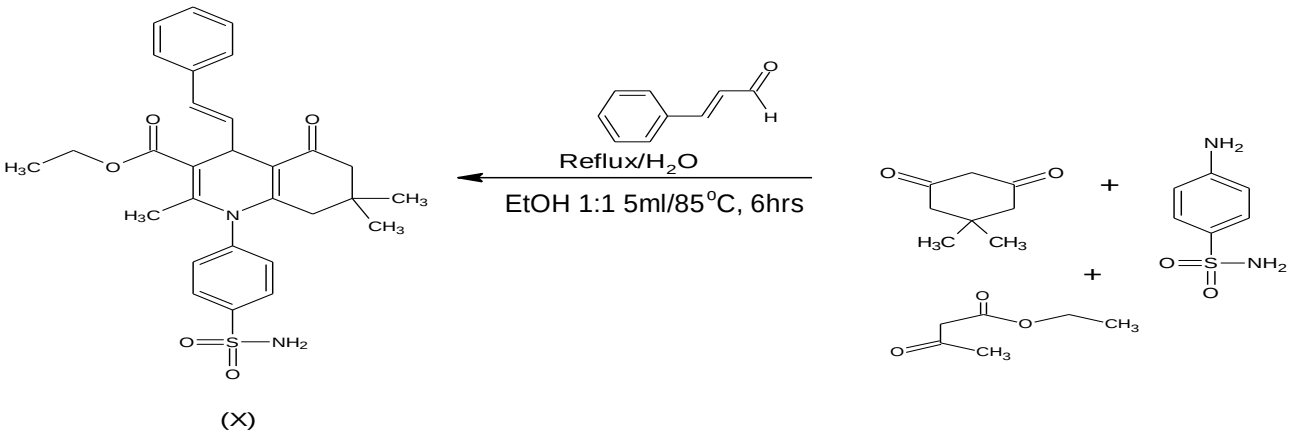

(X)

Scheme (2.2): Chemical structure of synthezed polyhydroquinoline derivatives.

Table (2.14): Chemical names of prepared acridinedione derivatives

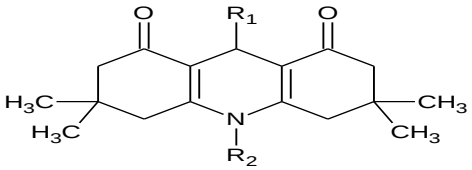

Compound No.	R_1	R_2	Chemical name
I	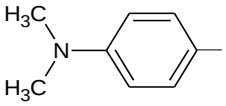	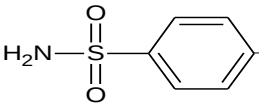	4-(9-(4- dimethyl amino) phenyl)- 3,3,6,6- tetramethyl- 1,8- dioxo- 2,3,4,5,6,7,8,9- ,octahydroacridin-10(1H)-yl) benzenesulfoneamide.
II	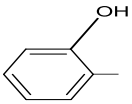	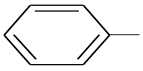	9-(2-hydoroxyphenyl)- 3,3,6,6- tetramethyl-10- phenyl-3,4,6,7,9,10- hexahydroacridin-1,8- (2H,5H)- dione.
III	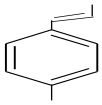	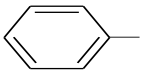	(E)- 3,3,6,6- tetramethyl-10- phenyl- 9- styryl- 3,4,6,7,9,10- hexahydroacridine- 1,8- (2H,5H)- dione.
IV	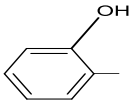	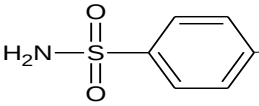	4-(9-(2- hydroxyphenyl)- 3,3,6,6- tetrmethyl- 1,8- dioxo- 2,3,4,5,6,7,8,9- octahydroacridin-10(1H)- yl)benzenesulfonamide.
V	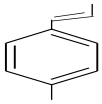	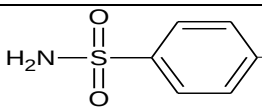	(E)- 4-(3,3,6,6- tetra methyl- 1,8-dioxo- 9- sryryl- 2,3,4,5,6,7,8,9- octahydroacridin-10(1H)-yl) benzenesulfonamide.

Table (2.15): Chemical names of polyhydroquinoline derivatives

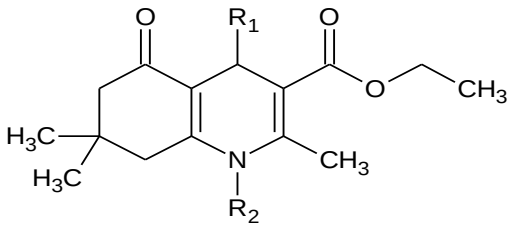

Compound No.	R_1	R_2	Chemical name
VI	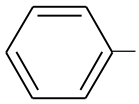	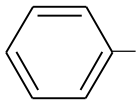	Ethyl -2, 7, 7-trimethyl-5-oxo-1, 4-diphenyl-1, 4, 5, 6, 7, 8-hexahydroquinoline-3-carboxylate.
VII	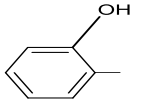	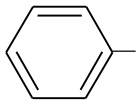	Ethyl-1-(2-hydroxyphenyl)-2, 7, 7-trimethyl-5-oxo-(phenyl)-1, 4, 5, 6, 7, 8-hexahydroquinoline-3-carboxylate.
VIII	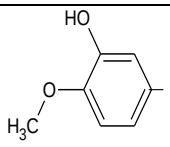	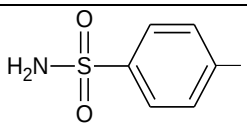	Ethyl-4-(3-hydroxy-4-methoxyphenyl)-2, 7, 7-trimethyl-5-oxo-1-(4-sulfamoyl)-1, 4, 5, 6, 7, 8-hexahydroquinoline-3-carboxylate.
IX	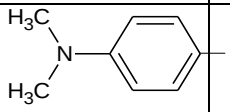	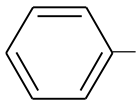	Ethyl-4-(4-dimethylaminophenyl)-2, 7, 7-trimethyl-5-oxo-1-phenyl-1, 4, 5, 6, 7, 8-hexahydroquinoline-3-carboxylate.
X	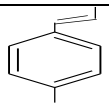	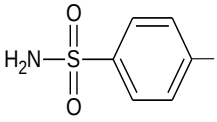	Ethyl (E)-2, 7, 7-trimethyl-5-oxo-4-styryl-1(-4-sulfamoylphenyl)-1, 4, 5, 6, 7, 8-hexahydroquinoline-3-carboxylate.

Table (2.16): Reaction conditions of the prepared acridinedione derivatives:

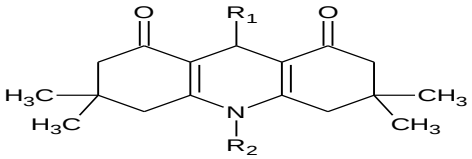

comp No.	R_1	R_2	solvent	Temp in ^0C	Weight/ g	Y%	Time in hrs	Recrys. Solvent	mp in ^0C	M.wt
I	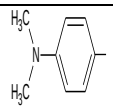	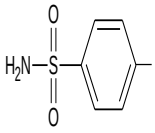	water	85	0.339	62	6	Aqueous Ethanol	200-202	547
II	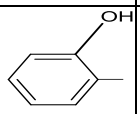	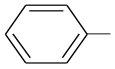	water	98	0.392	88.9	3	Aqueous Ethanol	183-185	441
III			water	98	0.418	92.7	3	Aqueous Ethanol	185-187	451
IV	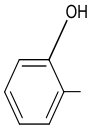	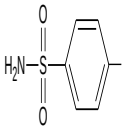	water: Ethanol 1:1	70	0.451	86.7	6	Aqueous Ethanol	192-194	520
V	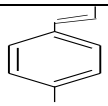	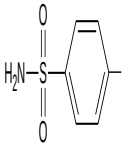	water: Ethanol 1:1	70	0.482	90.9	6	Aqueous Ethanol	179-180	530

Table (2.17): Reaction conditions of the prepared polyhydroquinoline derivatives

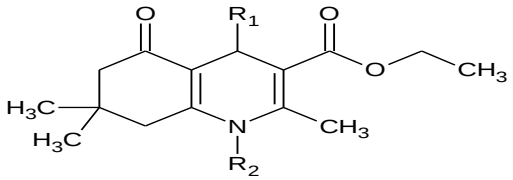

Com. No	R_1	R_2	solvent	Tempe. in ^0C	Weight/ g	Time in hrs	Y%	Recry. solvent	mp in ^0C	M.wt
VI			water	70	0.300	3	72.3	Aqueous Ethanol	168-170	415
VII	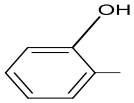		water	70	0.261	3	53.6	Aqueous Ethanol	161-163	431
VIII	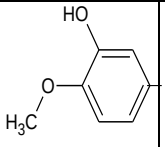	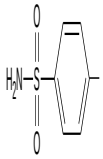	Ethanol: water 1:1	75	0.455	6	84.3	Aqueous Ethanol	198-200	540
IX	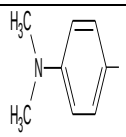	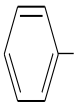	Ethanol: water 1:1	70	0.393	6	85.8	Aqueous Ethanol	180-182	458
X	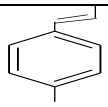	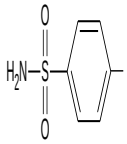	Ethanol: water 1:1	70	0.461	6	88.7	Aqueous Ethanol	188-191	520

Table (2.18): R_f values of the prepared acridinedione derivatives.

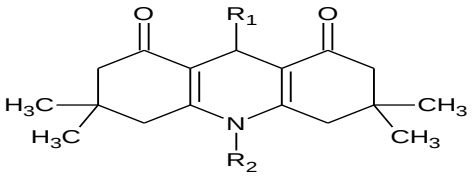

Compound No.	R_1	R_2	Solvent system	Ratio	R_f -value
I	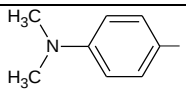	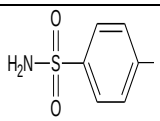	Chloroform: Methanol	9.5:0.5	0.92
II	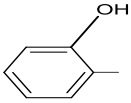	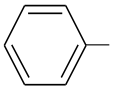	Chloroform: Methanol	9:1	0.90
III	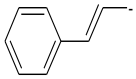	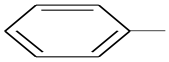	Chloroform: Methanol	9.5:0.5	0.80
IV	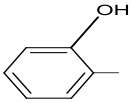	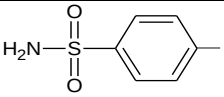	Chloroform: Methanol	9:1	0.60
V	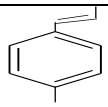	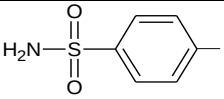	Chloroform: Methanol	9:1	0.67

Table (2.19): R_f values of the prepared polyhydroquinoline derivatives.

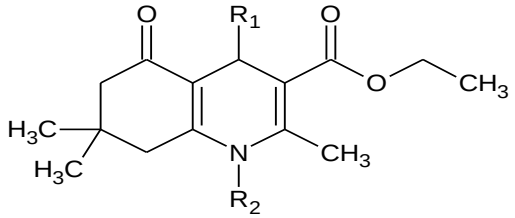

Compound No.	R_1	R_2	Solvent system	Ratio	R_f values
VI	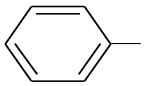	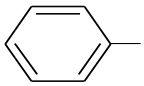	Chloroform: Methanol	9:1	0.89
VII	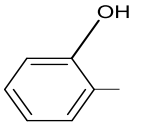	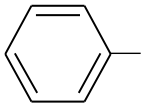	Chloroform: Methanol	9.5:0.5	0.96
VIII	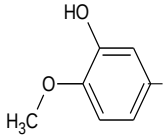	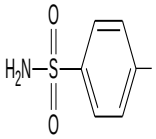	Hexane: Ethyl acetate	6:4	0.76
IX	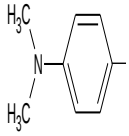	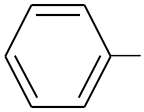	Hexane: Ethyl acetate	6:4	0.65
X	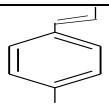	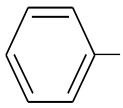	Hexane: Ethyl acetate	6:4	0.60

Table (2. 20): IR data for prepared acridinedione derivatives:

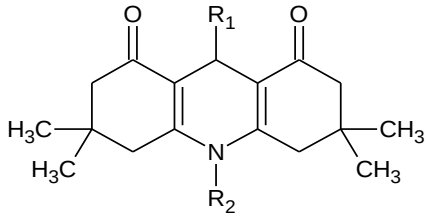

Com.No	R_1	R_2	C=O st.vib	C-H Arom	C-H Aliph	C=C st.vib	C-N st.vib	C-H bend deform. Ring	Others	N-H st.vib	N-H bend	C-O st.vib
I	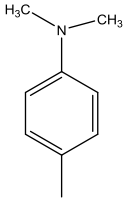	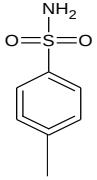	1593	-	2960	1521	1257	812	SO_2 asym,1369 sym.1311 OH (bonded) range 3200-3500	3446	1448	1232
II	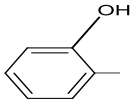	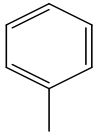	1640	-	2954	1588	1312	757	OH (bonded) range 3200-3500	-	1489	1235
III	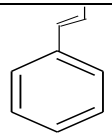	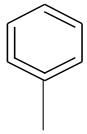	1616	3028	2964	1525	1269	835	-	-	1383	1152

IV	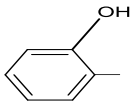	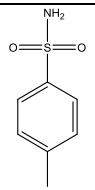	1641	-	2955	1590	1241	759	OH (bonded) range 3200-3500- SO_2 asym,1377 sym.1313	3192	1485	1156
V	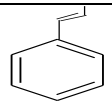	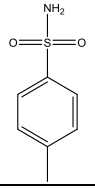	1604	-	2928	1457	1223	837	- SO_2 asym,1391 sym.1331	3367	1457	1151

Table (2.21): IR data (in Cm^{-1}) for the prepared polyhydroquinoline derivatives

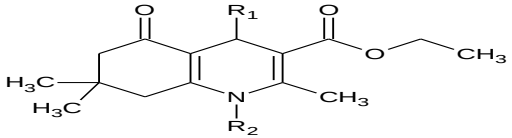

Compound No.	R_1	R_2	C=O st.vib	C-H Arom	C-H aliph	C=Cst.vib	C-Nst.vib	C-H bend deform. Ring	Others	N-H st.vib	N-H bend	C-O st.vib
VI	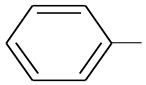	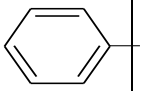	1727	-	2958	1591		860	-	-	1452	1230
VII	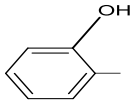	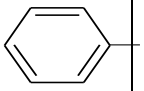	1723, 1640	-	2955	1453	1378	755	OH (bonded) range 3200-3500	-	1453	1233
VIII	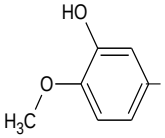	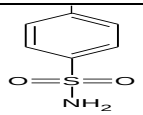	1731	-	2960	1590	1387	871	OH (bonded) range 3200-3500	3485	1464	1221
IX	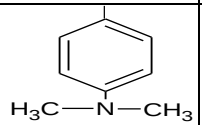	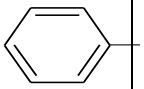	1716	-	2954	1614	1390	758	-	3423	1494	1223
X	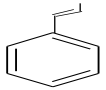	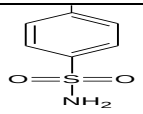	1714	-	2956	1630	1388	857	-	3421	-	1231

Table (2.22): [1]HNMR data of the prepared 4-(9-(4-(dimethylamino)phenyl)-3,3,6,6-tetramethyl-1,8-dioxo-2,3,4,5,6,7,8,9-octahydroacridin-10(1H)-yl)benzenesulfonamide

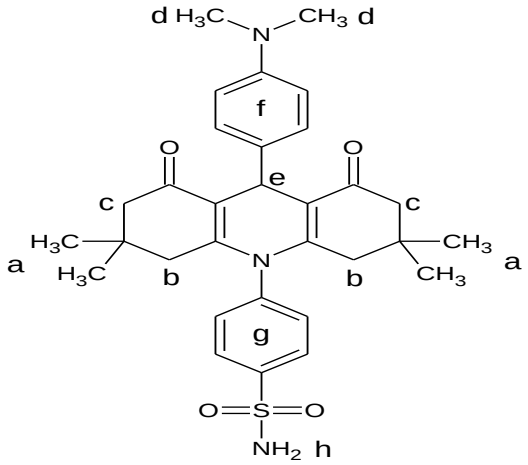

Compound No.	position	δ-value in (ppm)	Intensity	Multiplicity	Coupling J-constant
I	a	0.0967-1.099	6H	m	-
	b	2.27	2H	s	16.02
	c	2.32	2H	s	16.02
	d	2.46	6H	m	-
	e	5.47	1H	s	-
	f	7.38-7.059	4H	q	5.83
	g	7.136-7.74	4H	m	5.83
	h	6.98	2H	s	2.33

Table (2.23): [1]HNMR data of the prepare 9-(2-hydroxyphenyl)-3,3,6,6-tetramethyl-10-phenyl-3,4,6,7,9,10-hexahydroacridine-1,8(2H,5H)-dioned

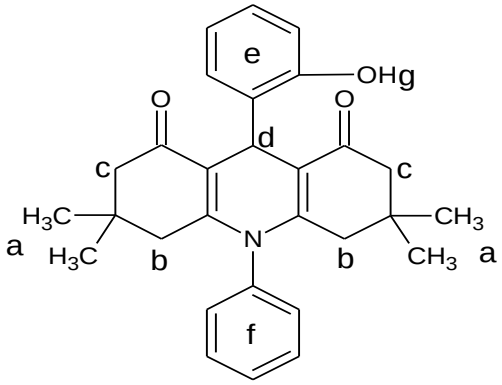

Compound No.	position	δ -value in (ppm)	Intensity	Multiplicity	Coupling J-constant
II	a	0.86-1.132	6H	m	-
	b	2.02	2H	s	15.37
	c	2.23	2H	s	15.37
	d	5.108	1H	s	7.49
	e	7.012-7.184	3H	q	-
	f	7.410-7.517	4H	m	-
	g	9.926	1H	s	-

Table (2.24): ^{1}HNMR data of the prepared (E)-3,3,6,6-tetramethyl-10-phenyl-9-styryl-3,4,6,7,9,10-hexahydroacridine-1,8(2H,5H)-dione

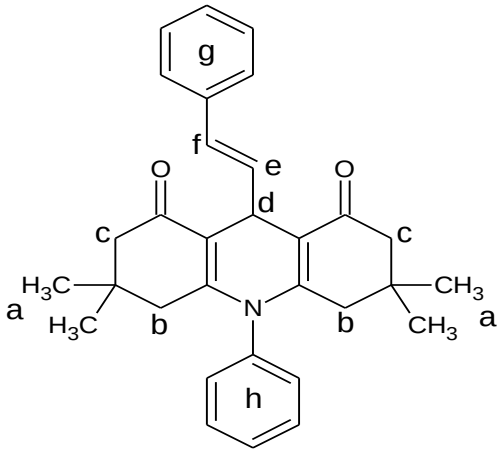

Compound No.	position	δ -value in (ppm)	Intensity	Multiplicity	Coupling J-constant
III	a	0.932-1.016	6H	s	-
	b	1.185-1.188	2H	s	-
	c	1.197-1.244	2H	s	-
	d	1.185	1H	s	-
	e	2.191	1H	s	-
	f	2.304	1H	s	-
	g	7.128-7.316	5H	m	-
	h	7.323-7.403	5H	m	-

Table (2.25): ^{1}HNMR data of the prepared 4-(9-(2-hydroxyphenyl)-3,3,6,6-tetramethyl-1,8-dioxo-2,3,4,5,6,7,8,9-octahydroacridin-10(1H)-yl)benzenesulfonamide

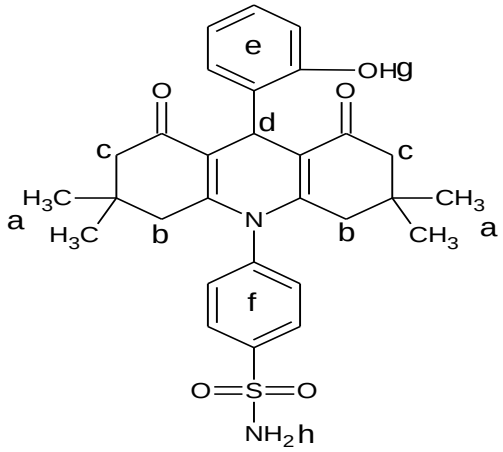

Compound No.	position	δ -value in (ppm)	Intensity	Multiplicity	Coupling J-constant
IV	a	1.14-1.32	6H	m	-
	b	2.05-2.13	2H	s	-
	c	2.22-2.63	2H	s	-
	d	4.69	1H	s	-
	e	7.039-7.17	4H	q	-
	f	7.168-7.28	4H	m	-
	g	11.353	1H	s	-
	h	6.942	2H	s	-

Table (2.26): ^{1}HNMR data of the prepared (E)-4-(3,3,6,6-tetramethyl-1,8-dioxo-9-styryl-2,3,4,5,6,7,8,9-octahydroacridin-10(1H)-yl)benzenesulfonamide

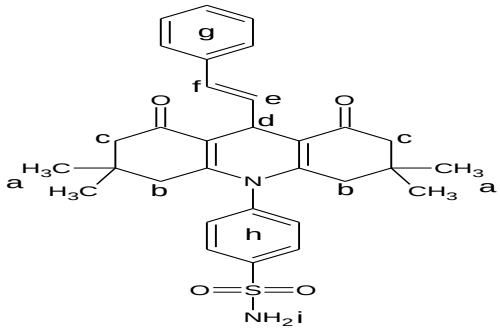

Compound No.	position	δ -value in (ppm)	Intensity	Multiplicity	Coupling J-constant
V	a	0.899-1.099	6H	m	-
	b	2.123-2.160	2H	s	-
	c	2.22-2.86	2H	s	-
	d	3.936	1H	s	-
	e	5.270	1H	s	-
	f	6.545	1H	s	-
	g	7.132-7.284	5H	m	-
	h	7.617-7.73	4H	q	-
	i	6.76	2H	s	-

Table (2.27): [1]HNMR data of the prepared ethyl 2, 7, 7-trimethyl-5-oxo-1, 4-diphenyl-1,4,5,6,7,8-hexahydroquinoline-3-carboxylate

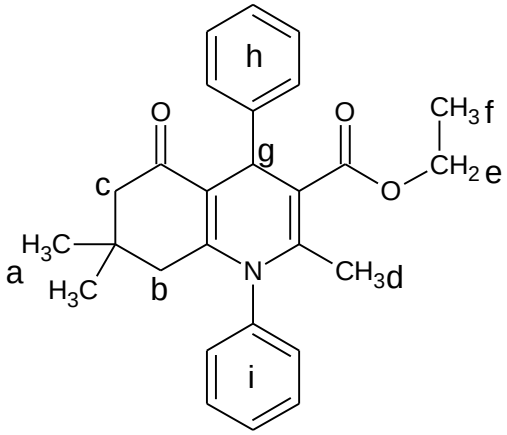

Compound No.	position	δ -value in (ppm)	Intensity	Multiplicity	Coupling J-constant
VI	a	0.191-1.176	6H	m	-
	b	2.242	2H	s	-
	c	1.010	2H	s	-
	d	1.852	3H	s	-
	e	5.56	2H	s	-
	f	2.242	3H		-
	g	5.303	1H	s	-
	h	7.113-7.190	5H	m	-
	i	7.284-7592	5H	m	-

Table (2.28): ^{1}HNMR data of the prepared ethyl 4-(2-hydroxyphenyl)-2, 7, 7-trimethyl-5-oxo-1-phenyl-1,4,5,6,7,8-hexahydroquinoline-3-carboxylate

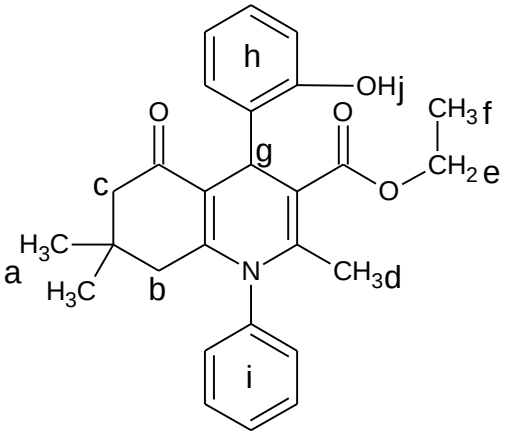

Compound No.	position	δ -value in (ppm)	Intensity	Multiplicity	Coupling J-constant
VII	a	0.858-1.045	6H	m	19.53
	b	2.007	2H	s	-
	c	2.22	2H	s	-
	d	1.23	3H	s	1.74
	e	2.27	2H	s	-
	f	2.33	3H	s	16.85
	g	2.48	1H	s	-
	h	7.02-7.22	4H	m	30.50
	i	7.23-7.43	5H	m	-
	j	13.055	1H	s	-

Table (2.29): [1]HNMR data of the prepared ethyl 4-(3-hydroxy-4-methoxyphenyl)-2,7,7-trimethyl-5-oxo-1-phenyl-1,4,5,6,7,8-hexahydroquinoline-3-carboxylate

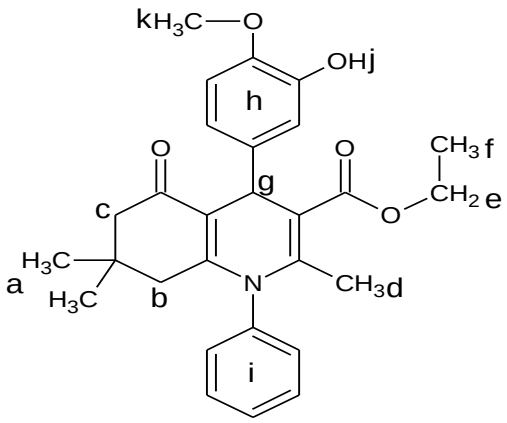

Compound No.	position	δ -value in (ppm)	Intensity	Multiplicity	Coupling J-constant
VIII	a	1.028-1.274	6H	m	19.56
	b	5.303	2H	s	-
	c	2.328	2H	s	-
	d	2.242	3H	s	1.32
	e	1.85	2H	s	-
	f	1.176	3H	s	-
	g	5.56	1H	s	-
	h	7.078-7.190	3H	m	5.32
	i	7.28-7.59	5H	m	3.31
	j	11.933	1H	s	-
	k	3.87	3H	s	3.08

Table (2.30): [1]HNMR data of the prepared ethyl 4-(4-(dimethylamino) phenyl)-2, 7, 7-trimethyl-5-oxo-1-phenyl-1,4,5,6,7,8-hexahydroquinoline-3-carboxylate

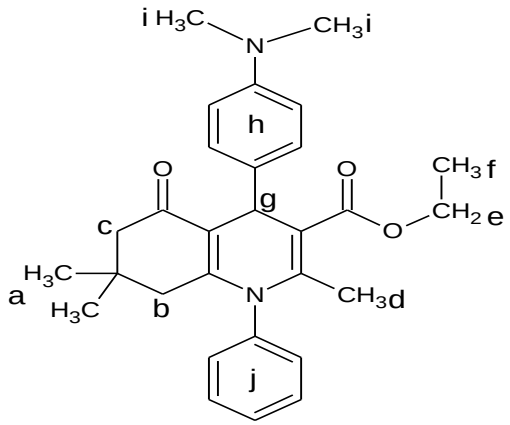

Compound No.	position	δ -value in (ppm)	Intensity	Multiplicity	Coupling J-constant
IX	a	0.907-1.025	6H	m	26.65
	b	2.268	2H	s	-
	c	2.307	2H	s	-
	d	2.275	3H	s	13.61
	e	2.32	2H	s	-
	f	2.24	3H	s	-
	g	2.17	1H	s	-
	h	7.123-7.189	4H	m	13.66
	i	2.259	6H	m	-
	j	7.304-7.37	5H		-

Table (2.31): [1]HNMR data of the prepared ethyl (E)-2,7,7-trimethyl-5-oxo-4-styryl-1-(4-sulfamoylphenyl)-1,4,5,6,7,8-hexahydroquinoline-3-carboxylate

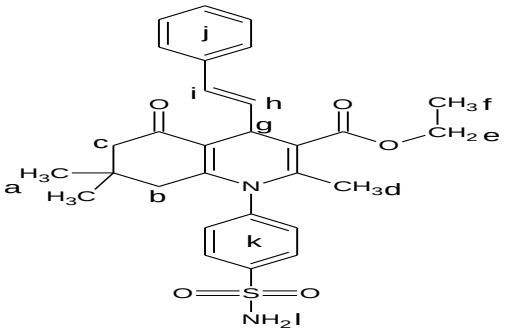

Compound No.	position	δ -value in (ppm)	Intensity	Multiplicity	Coupling J-constant
X	a	1.023-1.088	6H	m	9.25
	b	1.170	2H	s	-
	c	1.183	2H	s	-
	d	1.280	3H	s	-
	e	2.348	2H	s	-
	f	2.577	3H	s	-
	g	3.326	1H	s	-
	h	2.43	1H	s	-
	I	4.091	1H	s	-
	J	7.116-7.212	5H	m	11.93
	K	7.31-7.320	4H	q	4.94
	l	2.404	2H	s	2.36

Table (2.32): MS data of the prepared 4-(3,3,6,6-tetramethyl-1,8-dioxo-9-phenyl-2,3,4,5,6,7,8,9-octahydroacridin-10(1H)-yl)benzenesulfonamide (I)

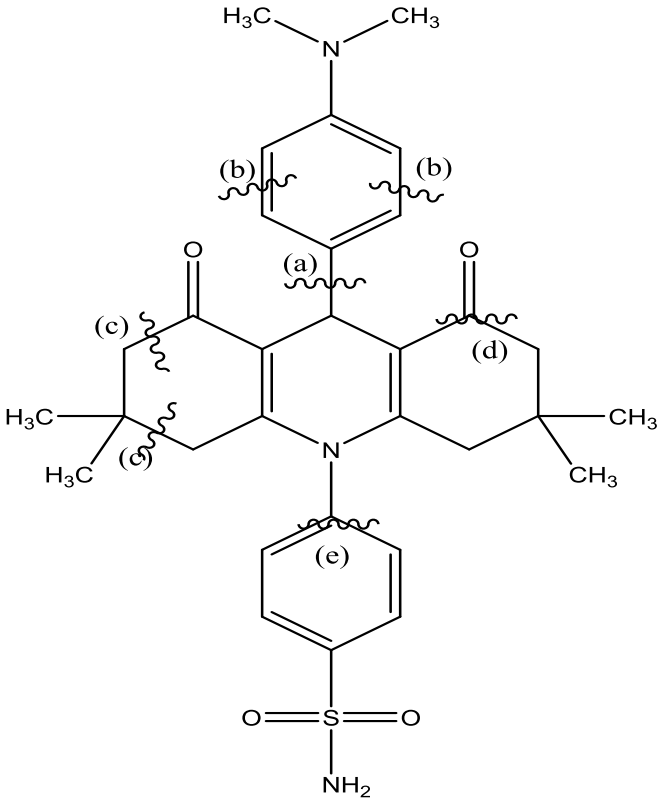

Compound No.	M. Formula	M. weight		Fragments m/z (RA %)				
				a	b	c	d	e
I	$C_{31}H_{37}N_3O_4S$	Cal	observed					
		547.72	547.90 548.90 549.90	120 (M+1) 121 (59.60)	82 M+1) 83 (79.1)	56 (52.81)	519 (M+4) 523	144 (17.83)

Table (2.33): MS data of the prepared 9-(2-hydroxyphenyl)-3,3,6,6-tetramethyl-10-phenyl-3,4,6,7,9,10-hexahydroacridine-1,8(2H,5H)-dione (II)

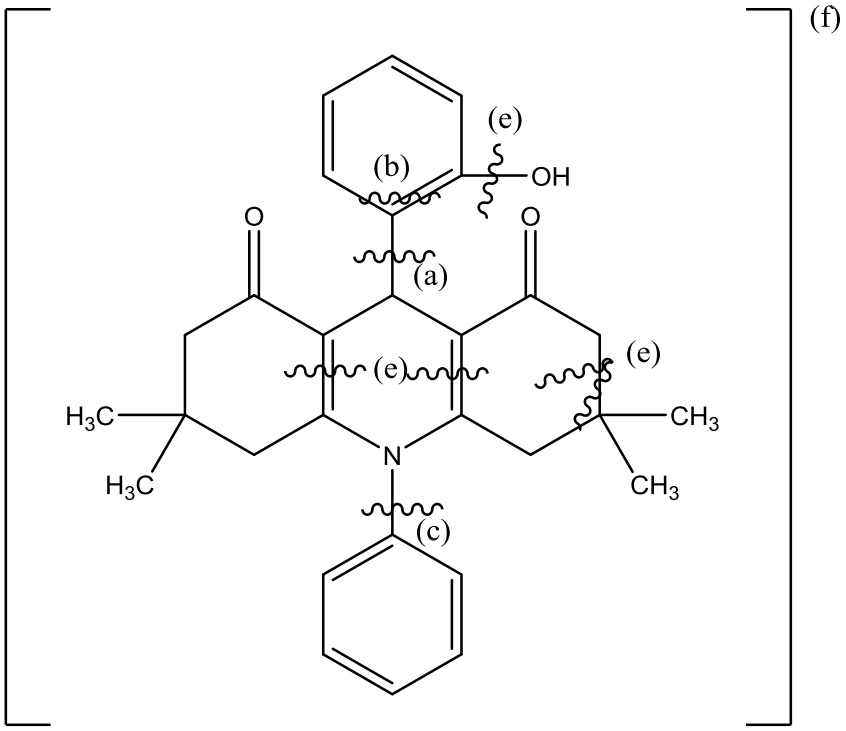

Compound No.	M. Formula	M. weight		Fragments m/z (RA %)					
				a	b	c	d	e	f
II	$C_{29}H_{31}NO_3$	Cal	observed						
		441	442.45 443.50	348 (4.60)	81 (M+2) 83 (35.88)	364 (M+2) 366 (82.70)	301 (M+1) 302 (0.16)	282 base peak (100%)	(M^+) 441 (1.53)

Table (2.34): MS data for the prepared 4-(9-(2-hydroxyphenyl)-3,3,6,6-tetramethyl-1,8-dioxo-2,3,4,5,6,7,8,9-octahydroacridin-10(1H)-yl)benzenesulfonamide (III)

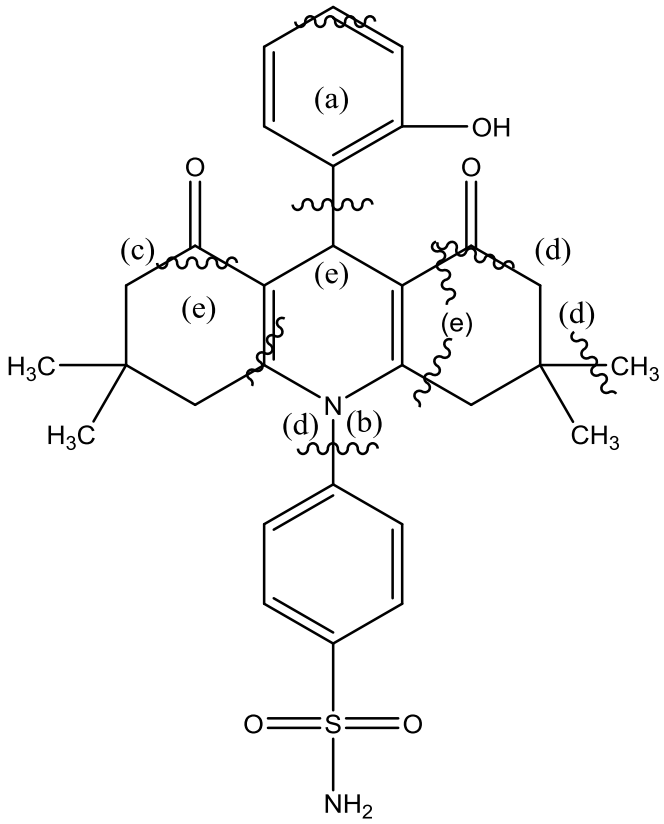

Compound No.	M. Formula	M. weight		Fragments m/z (RA %)				
				a	b	c	d	e
III	$C_{29}H_{32}N_2O_5S$	Cal	observed					
		451	469 (M+4)	80 (M+3) 83 Base peak (100%)	183 (M+2) 185 (0.13)	492 (0.32)	228 (M+4) 232 (0.30)	301 (M+1) 302 (1.86)

Table (2.35): MS data for the prepared (E)-4-(3,3,6,6-tetramethyl-1,8-dioxo-9-styryl-2,3,4,5,6,7,8,9-octahydroacridin-10(1H)-yl)benzenesulfonamide (IV)

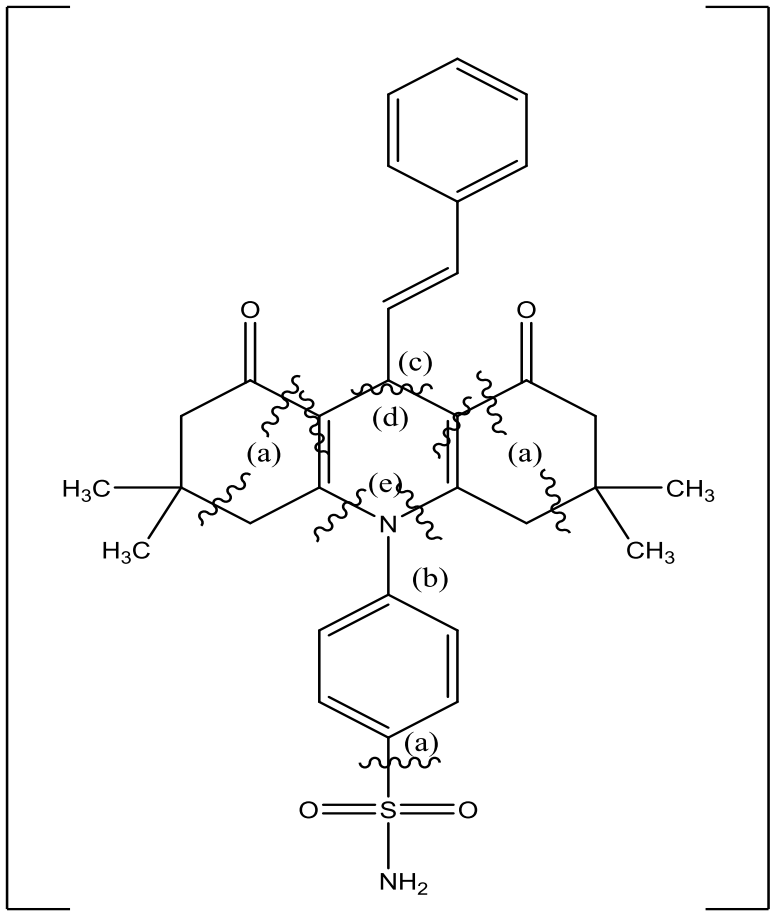

Compound No.	M. Formula	M. weight		Fragments m/z (RA %)					
				a	b	c	d	e	f
IV	$C_{31}H_{34}N_2O_4S$	Cal	observed						
		530	531 532 533 534	366 base peak (100%)	282 (54.83)	116 (M-1) 115 (29.23)	142 (M+1) 143 (5.48)	170 (M+1) 171 (0.11)	(M^+) 530 (M+3) 533 (0.07)

Table (2.36): MS data for the prepared (E)-3,3,6,6-tetramethyl-10-phenyl-9-styryl-3,4,6,7,9,10-hexahydroacridine-1,8(2H,5H)-dione (V)

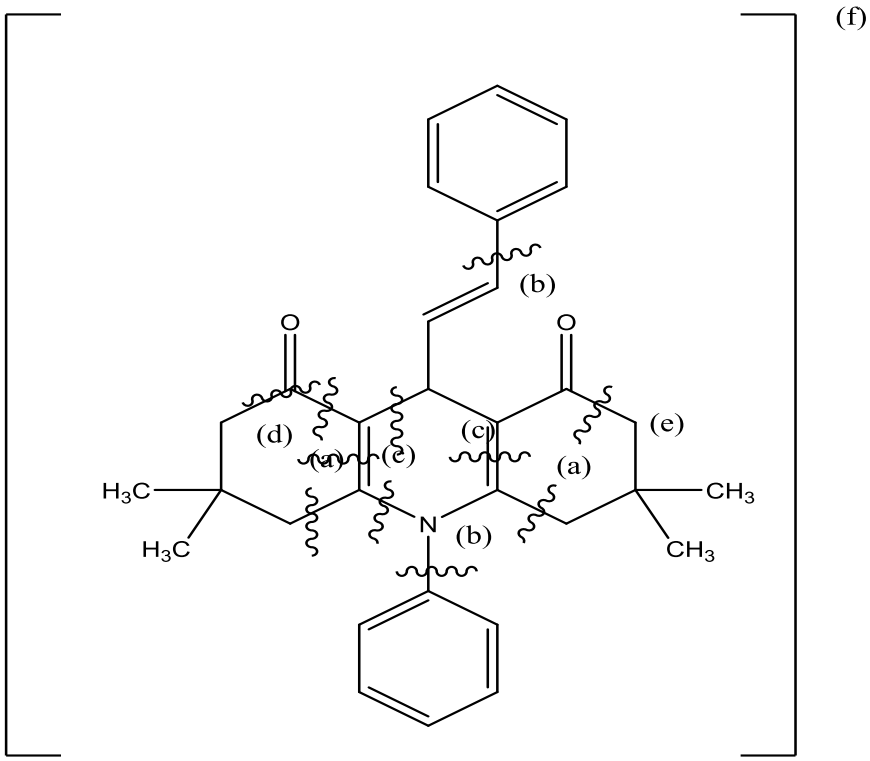

Compound No.	M. Formula	M. weight		Fragments m/z (RA %)					
		Cal	observed	a	b	c	d	e	f
V	$C_{31}H_{33}NO_2$	451	451.30 452.30 453.30	283 (M+1) 284(0.59)	254 (35.55)	129 (M-1) 128 (29.23) base peak (100%)	226 (M+3) 229 (3.36)	301 (M+2) 303 (1.82)	(M^+) 451 (2.01)

Table (2.37): MS data for the prepared ethyl 2, 7, 7-trimethyl-5-oxo-1, 4-diphenyl-1, 4, 5, 6, 7, 8-hexahydroquinoline-3-carboxylate (VI)

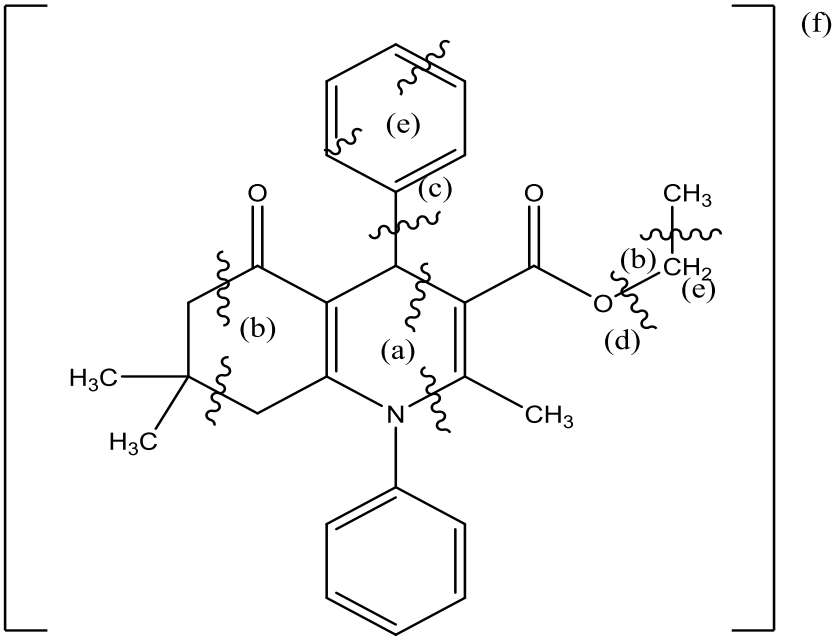

Compound No.	M. Formula	M. weight		Fragments m/z (RA %)					
				a	b	c	d	e	f
VI	$C_{27}H_{29}NO_3$	Cal	observed						
		415	425.50	303 (M+1) (4.20)	344 (M+4) 348 (1.38)	77 base peak (100%)	347 (M+1) 348 (1.38)	316 (11.64)	(M^+) 425 (14.68)

Table (2.38): MS data for the prepared ethyl 4-(2-hydroxyphenyl)-2, 7, 7-trimethyl-5-oxo-1-phenyl-1, 4, 5, 6, 7, 8-hexahydroquinoline-3-carboxylate (VII)

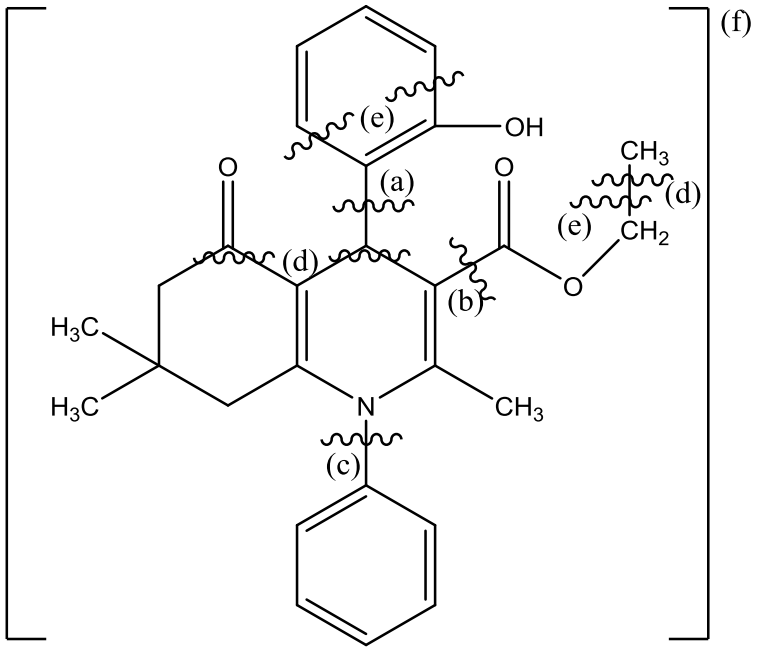

Compound No.	M. Formula	M. weight		Fragments m/z (RA %)					
				a	b	c	d	e	f
VII	$C_{27}H_{31}NO_4$	Cal	observed						
		431	431.40 432.40	93 (12.9)	358 (M+1) 359 (2.30)	77 (78.84)	282 (20.30)	363 (M+3) 366 (5.59)	(M^+) 431 (2.57)

Table (2.39): MS data for the prepared ethyl 4-(3-hydroxy-4-methoxyphenyl)-2, 7, 7-trimethyl-5-oxo-1-(4-sulfamoylphenyl)-1, 4, 5, 6, 7, 8-hexahydroquinoline-3-carboxylate (VIII)

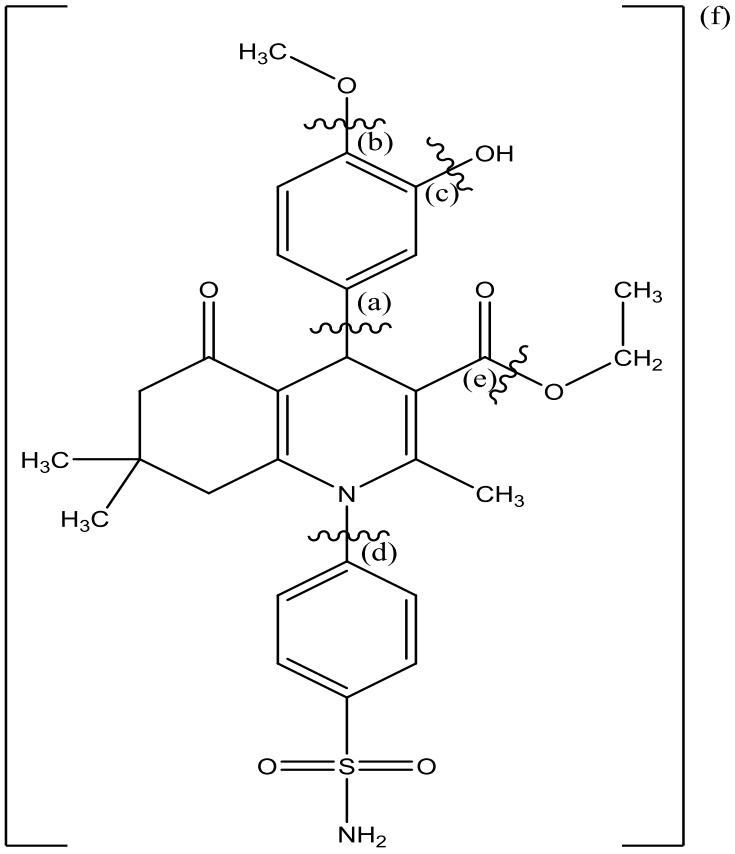

Compound No.	M. Formula	M. weight		Fragments m/z (RA %)					
				a	b	c	d	e	f
VIII	$C_{28}H_{32}N_2O_7S$	Cal	observed						
		540	540.40 541.40	417 (M-3) 414 (13.49)	509 (M+1) 510 (0.68)	523 (M+2) 525 (0.56)	156 (0.56)	495 (0.55)	(M^+) 540 (0.83)

Table (2.40): MS data for the prepared ethyl 4-(4-(dimethyl amino) phenyl)-2,7,7-trimethyl-5-oxo-1-phenyl-1,4,5,6,7,8-hexahydroquinoline-3-carboxylate (IX)

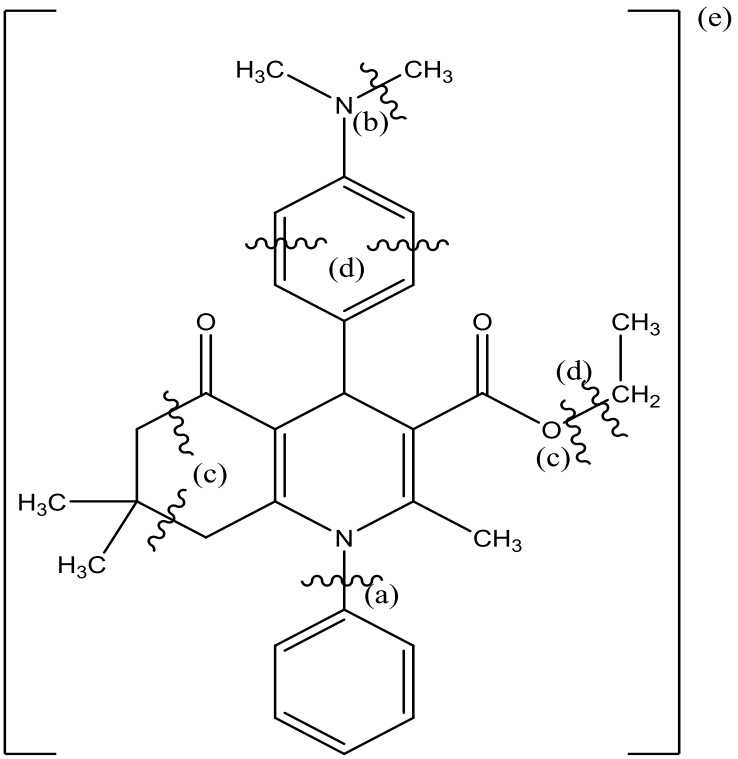

Compound No.	M. Formula	M. weight		Fragments m/z (RA %)				
				a	b	c	d	e
IX	$C_{29}H_{34}N_2O_3$	Cal	observed					
		458	459.30 460.30	77 (52. 9)	443 (M+2) 445 (1.19)	231 (M+1) 232 (3.25)	347 (M+2) 349 (1.11)	(M^+) (M+1) 459 (1.37)

Table (2.41): MS data for the prepared ethyl (E)-2,7,7-trimethyl-5-oxo-4-styryl-1-(4-sulfamoylphenyl)-1,4,5,6,7,8-hexahydroquinoline-3-carboxylate (X)

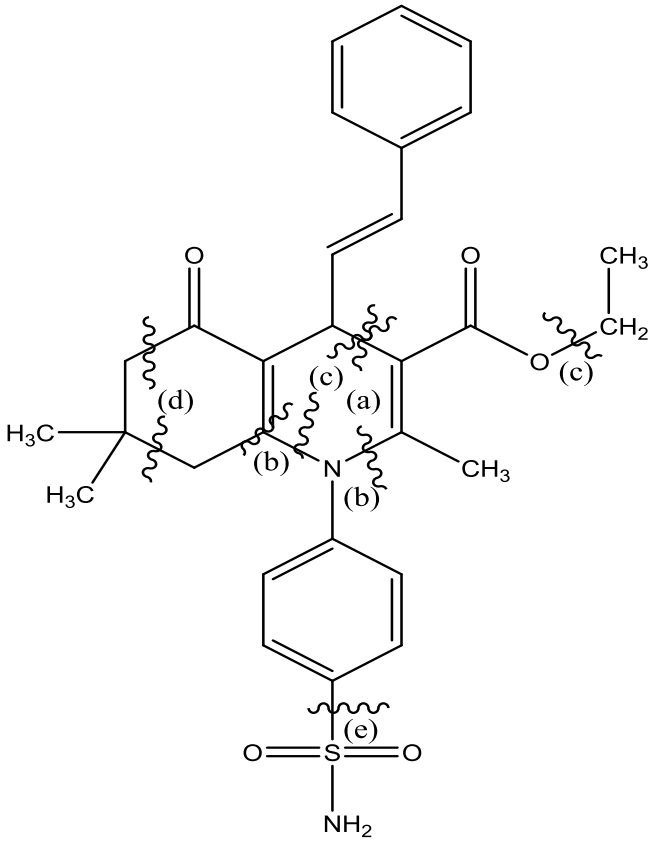

Compound No.	M. Formula	M. weight		Fragments m/z (RA %)				
				a	b	c	d	e
X	$C_{29}H_{34}N_2O_3$	Cal	observed					
		520	519.50 520.50	112 (M+3) 115 (28.40)	183 (M+1) 184 (0.87)	253 (M+1) 254 (12.70)	449 (M+2) 451 (0.08)	80 (M+3) 83 base peak (100%)

Table (2.42): UV. Vis data of the prepared acridinedione derivatives

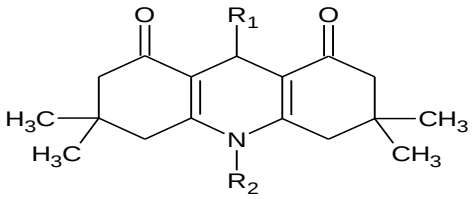

Compound No.	R_1	R_2	λ_{max} in (nm)
I	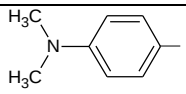	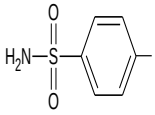	207, 258
II	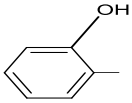	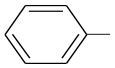	229, 272
III	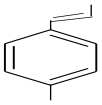	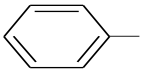	209, 260, 314
IV	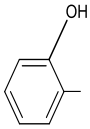	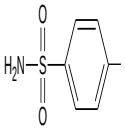	222, 271
V	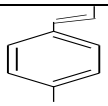	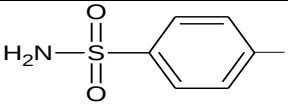	212, 265

Table (2.43): UV. Vis data of the prepared polyhydroquinoline derivatives

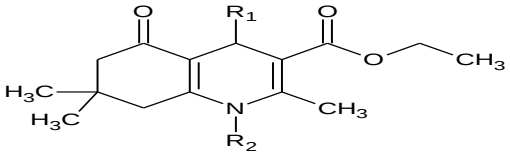

Compound No.	R_1	R_2	λ_{max} in (nm)
VI	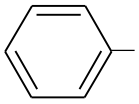	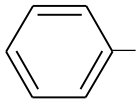	212, 258
VII	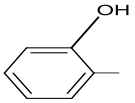		228, 273
VIII	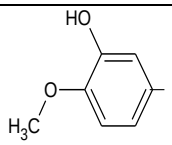	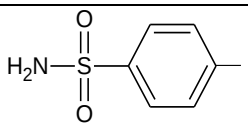	224, 271
IX	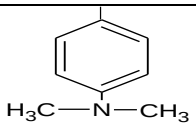	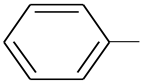	221, 260
X	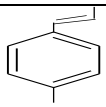	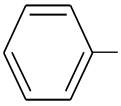	219, 273

3. Discussion

3.1. QSAR study

Among different derivatives of 1, 4-DHPs, 1, 8- acridinedione is a known scaffold with wide spectrum of biological effects (Jamalian *et al.*, 2011). Molecular descriptors play a fundamental role in developing models for chemistry. Molecular descriptors can be calculated from the chemical formula (1D descriptors), the 2D structure (2D descriptors), and the 3D conformation (3D descriptors) using a large number of methods based on atom types, molecular fragments, and the three-dimensional structure, respectively (Bajot, 2010).

In this work QSAR study was carried out for Imidazolyl derivatives of 1, 8-Acridinediones. Data set was collected from literature (Jamalian *et al.* 2011). Consist of 6 compounds table (2.1) which is then divided into two sub set. Training set containing 4 compounds and test set of two compounds. Total of 15 molecular descriptors for group(I), namely 2D descriptors such as Mw (Molecular Weight), logP (octanol/water) logP o/w), Mr (Molar refracticity), a-aac (Number of Hydrogen Bond acceptor atoms), a-don (Number of Hydrogen Bond doner atoms), Lip-acc (Lipinski acceptor count), Lip-don (Lipinski donor count), and TPSA (Topological Polar Surface Area). And 3D descriptors such as AMI-IP (Ionization Potential), E (Potential Energy), MNDO-IP (Potential Energy), PM3-IP (Potential Energy), MNDO-Ele (Electronic Energy), MNDO-HF (Heat of Formation), and MNDO-HOMO (Higher Occupied Molecular Orbital Energy). And total of 11 Molecular descriptors for group (II), 2D such as LogP(o/w), (octanol water partition coefficient), TPSA(Topological Polar Surface Area), Weight (Molecular Weight), Density (Mass Density), and Mr (Molar refractivity).

3D descriptors such as AMI-IP, (Ionization Potential), dipole (dipole moment), PM3-IP (Ionization Potential), E(Potential Energy), PM3-E (Total Energy), and PM3-HF(Heat of Formation). Were calculated for training set and test set in table (2.2).

All descriptors were calculated by using MOE and ACD/lab programmes.

For a statistically reliable model, the number of compounds and number of descriptors should bear a relation of at least 5:1. Thus, only two descriptors are required for 9 compounds in the training set to develop statistically reliable QSAR model. Selection of a set of appropriate descriptors from a large number of them requires a method, which is able to distinguish between the parameters.

Person correlation matrix has been performed for all selected descriptors by using MOE software see figure (2.1) and figure (2.2) in order to select appropriate sub set descriptors. The analysis of these matrixes revealed appropriate 15 descriptors for the training set compounds.

Multiple linear regression (MLR) is commonly used in QSAR due to its simplicity, transparency, reproducibility and easy interpretable (Roy *et al*. 2015).

QSAR models were developed during MLR analysis in training set with two descriptors and the best equation, (No.27), which showed high square correlation coefficient (R^2) and low root mean square error (RMSE), was considered as the best model with TPSA and logP (o/w), for acridinedione derivatives.

PIC_{50} =-3.20129+0.15696 * logP(o/w)+0.81590 * AM1-IP. Model No. (19).

PIC_{50} =2.97797+0.13501 * logP(o/w) +0.14800 * lip-acc . Model No. (22).

PIC_{50} = 3.11067+0.11632 * logP(o/w) +0.00995 * TPSA. Model No. (27).

PIC50 = -3.13167 + 0.00363 * Weight + 0.69421* AM1-IP. Model No. (61).

PIC50 =2.58357+0.00252 * Weight+0.00837 *TPSA. Model No. (69).

The best model for group (I), because, R^2 was very high than the other four models, see table (2.6).

For polyhydroquinoline derivatives.

PIC_{50}= 3.39051+0.20874*dipole+0.12501*LogP (o/w). Model (II). No. (11)

PIC_{50}= 3.13653+0.21581*dipole+0.00201*weight…….Model No. (14)

PIC_{50}= 3.29567+0.21574*dipole+0.06096*mr…….…...Model No. (17)

These two models are better than the model No. (11), but the best choice is model (11), because logP(o/w) is very important descriptor. See table (2.7).

The developed QSAR model equation (model No. 27) showed a relationship between *in-vitro* biological activities and correlated two descriptors TPSA and logP (o/w). It is indicated that from the model equation that the molecular descriptors, namely logP (o/w) partition coefficient and AM-IP are positively correlated with PIC_{50}, and positively correlated with PIC_{50}, logP (o/w) and dipole (model No.11).

Internal validation by training Validation is a crucial aspect of any QSAR analysis, this step achieved by set compounds (cross validation) and external validation by test set compounds.

The statistical fit of a QSAR can be assessed in many easily available statistical terms. The statistical quality of the resulting model is determined by R, $R^{2,}$ Q, Q^2, RMSE, S, F, and P value.

The correlation coefficient, (R) is the measure of the degree of linearity of the relationship. It signifies the quality of fit of the model and quantifies the variance in the data. In an ideal situation the correlation coefficient must be equal to or approach 1(Verma *et al*., 2010).

The Square Correlation Coefficient, (R^2) which gives an evaluation of the dispersion of theoretical values around the experimental data. The quality of

the model is improved when the points are close to the fitting line. The adjustment of the point to this line can be evaluated by correlation coefficient (N'guessan *et al*., 2017), that means if R^2 value closes to 1 the theoretical and experimental values will be assumed to correlate.

Cross-Validation Q^2 is the one of most extensively employed methods for the internal validation of a statistical model is estimated using a reduced set of structural data. Usually, one element of the set is extracted each time, and a new model is derived based on the reduced dataset, which is then employed to predict the activity of the excluded molecule. The procedure is repeated n number of times until all compounds have been excluded and predicted once. This is the (so called leave- one out) (LOO) method. The outcome of LOO procedure is criterion of both robustness and predictive ability of the model. It has been established that, in cases where test set with known values of biological activities were available for prediction, there existed no correlation between the Q^2 and R^2. Q^2 should be regarded as a measure of internal consistency of the derived model rather than a true indicator of the predictability. It should be noted that, since it is easier to fit the experimental data than to predict them from the QSAR model, R^2 of the model is always higher than Q^2 (Verma *et al*. 2010). For satisfactory model $Q>0.5$ and for an excellent model $Q^2 >0.9$. So, for a given training set a model will be performance if the acceptance criterion $R^2- Q^2< 0.3$ is respected (N'guessan *et al*., 2017).

The Fischer statistic (F-value) parameter is one of the several variance related that can be used as a measure of the level of statistical significance of the regression model. A higher F-value implies that a more significant correlation has been reached (Verma *et al*., 2010).

Root Mean Square Error (RMSE) has been used as a statistical metric to measure model performance in meteorology, air quality, and climate research studies (Chai and Draxler 2014). The lower its value the better the model.

Standard error of estimate (s), for good model, the standard error of estimate of Y should be low; it measures the dispersion of the observed values about the regression line. The smaller the value of (s) means higher reliability of the prediction (Roy *et al*., 2015).

P-value is defined as the probability under null distributions of the sample outcome equal to or more extreme than that observed (Gibbons and Pratt 1975).

The QSAR model represents robustness, with good internal and external predictive capabilities and this model is acceptable because all the values of statistical measures are found to be in the acceptable ranges, the training set compounds group(I), (acridinedione derivatives).

R=0.996	R^2 = 0.993	RMSE=0.124	Q= 0.3963
Q^2 = 0.990	S = 0.209	F= 283.74	p= 0.004

Polyhydroquinoline derivatives, group (II).

R=0.9011	R^2 = 0.812	RMSE=0.05156	Q= 0.7917
Q^2 = 0.6267	s = 0.021	F= 34.511	p= 0.0001

One of the important characteristics of a QSAR model is its predictive power, (the ability of a model to predict accurately the biological activity of the compounds that were not used for model development (external validation). Whereas, internal validation techniques described above can be

used to establish model robustness, they do not directly assess model predictivity. In principle, external validation is the only way to determine the true predictive power of a QSAR model. This type of assessment requires the use of an external test set, compounds which not used for the model development.

The predictivity of a regression model was estimated by comparing the predicted and observed experimental values of PIC_{50} for group (I) against breast cancer of training set and their cross-validation, the residual values were calculated and listed in table (2.1). And table (2.2), for group (II).

3. 2. Applicability domain

Activity of the entire universe of chemicals cannot be predicted even by a robust and validated QSAR model. The prediction of a modeled response using QSAR is valid only if the compound being predicted is within the applicability domain of the model. The applicability domain is a theoretical region of the chemical space, defined by the model descriptors and modeled response and, thus, by the nature of the training set of molecules. It is possible to check whether a new chemical lies within applicability domain using the leverage approach. A compound will be considered outside the applicability domain when the leverage value is higher than the critical value of 3p/n, where p is the number of model variables plus 1 and n is the number of objects used to develop the model (Veerasamy *et al.* 2011).

Modeling of acridinedione derivatives predicting the biological activity of designed compounds. The QSAR model, No. (19) .Was selected to predict the biological activity of designed acridinediones from 1 to 75 against human breast cancer MCF-7 cell lines, the result using their predicted chemical descriptors were measured or calculated and listed in appendixes.

The drug ability of designed compounds was evaluated by using Lipinski rule of five in order to select compounds for synthesis.

According to Lipinski rule of five, most drug-like molecules have logP ≥ 5, number of hydrogen acceptors ≤ 10, molecular weight ≤ 500, and number of hydrogen donors' ≤ 5. Molecules violating one or more of these rules may have problem with bioavailability (Baell *et al*. 2013). Therefore, 12 out of 150 compounds were selected for synthesis in the next step. Descriptors of selected compounds predicted PIC_{50} and Lipinski rules were calculated in Table (2.7).

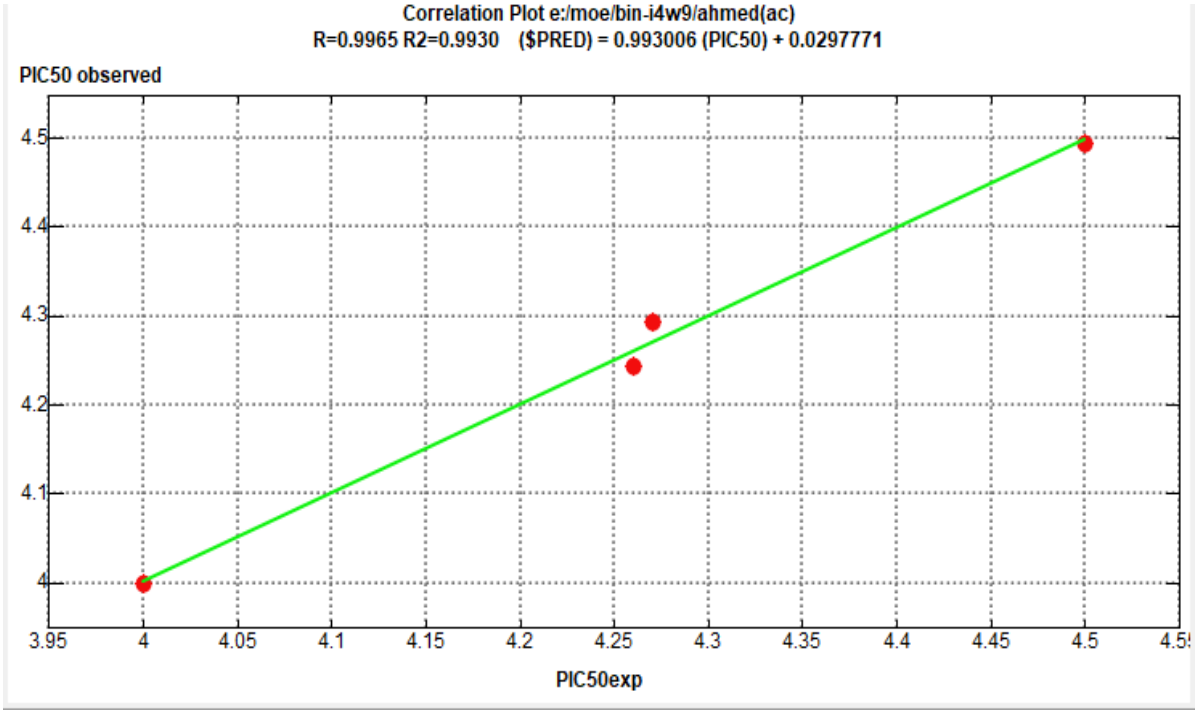

Figure (3.1): The plot of linear regression predicted PIC_{50} versus experimental values of the biological activity of training set compounds (validation) against human breast cancer MCF-7 cell lines.

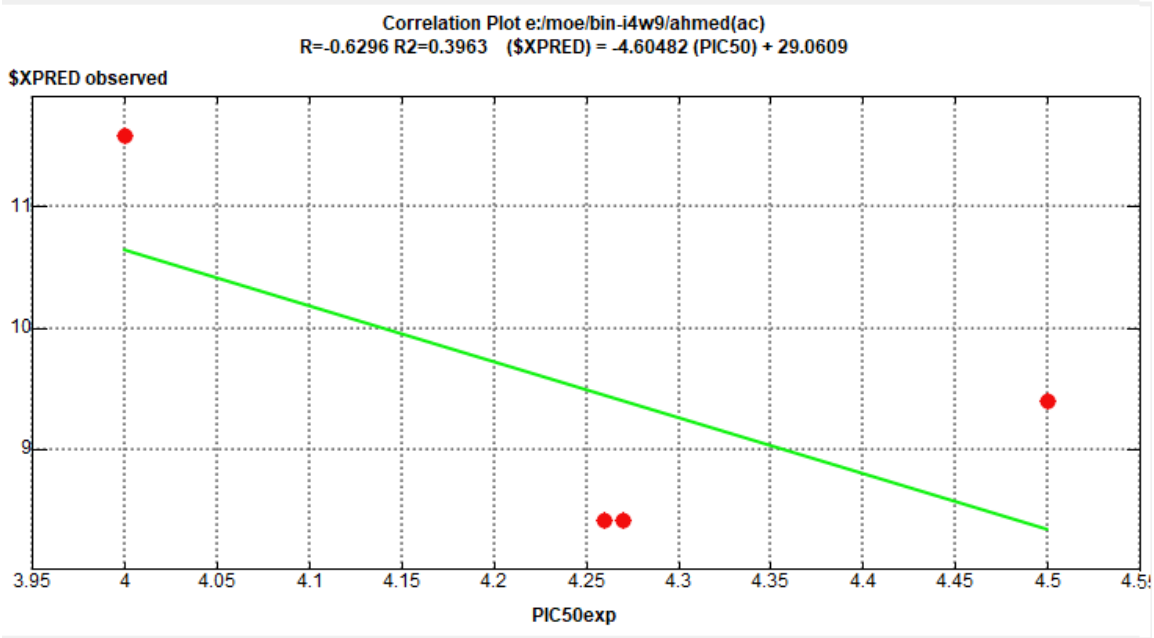

Figure (3.2): The plot of linear regression predicted PIC_{50} versus experimental values of the biological activity of training set compounds (cross-validation),

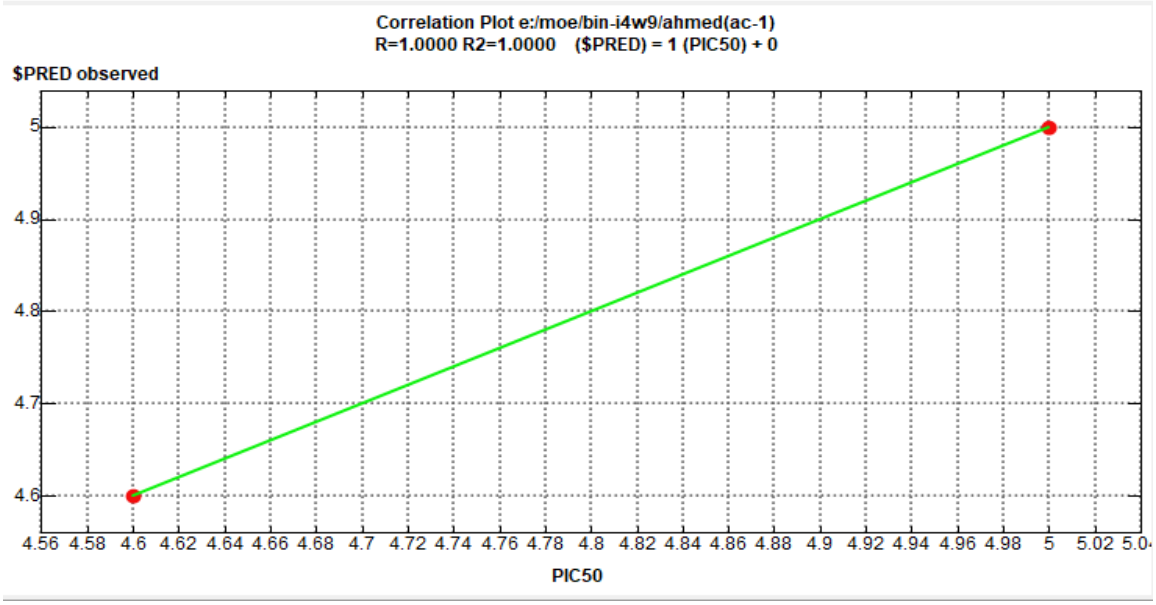

Figure (3.3): The plot of linear regression predicted PIC_{50} versus experimental values of the biological activity of test set compounds (validation). Group (I).

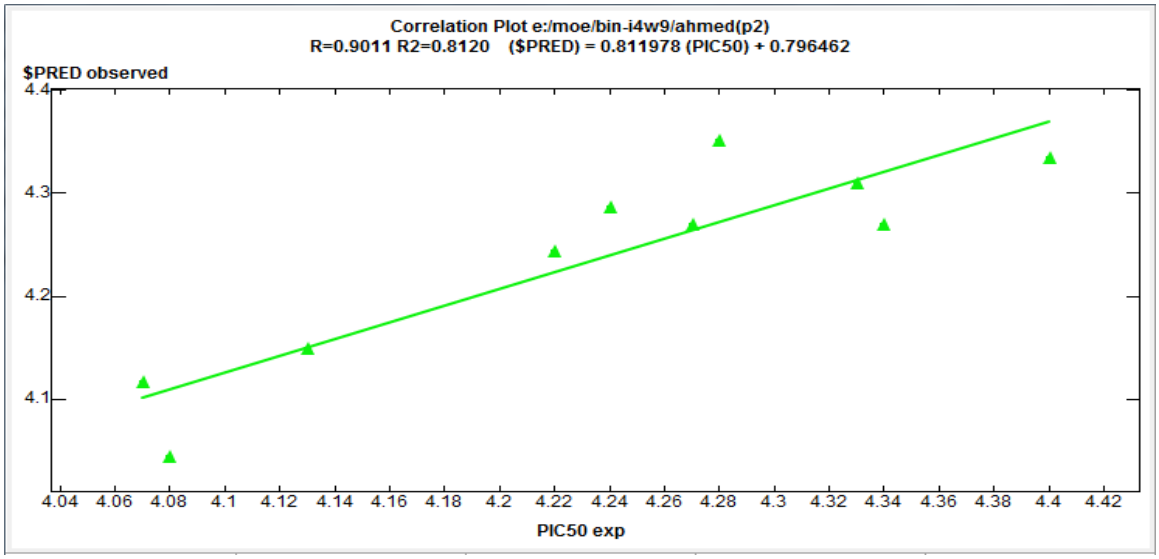

Figure (3.4): The plot of linear regression predicted PIC_{50} versus experimental values of the biological activity of training set compounds (validation), for group (II).

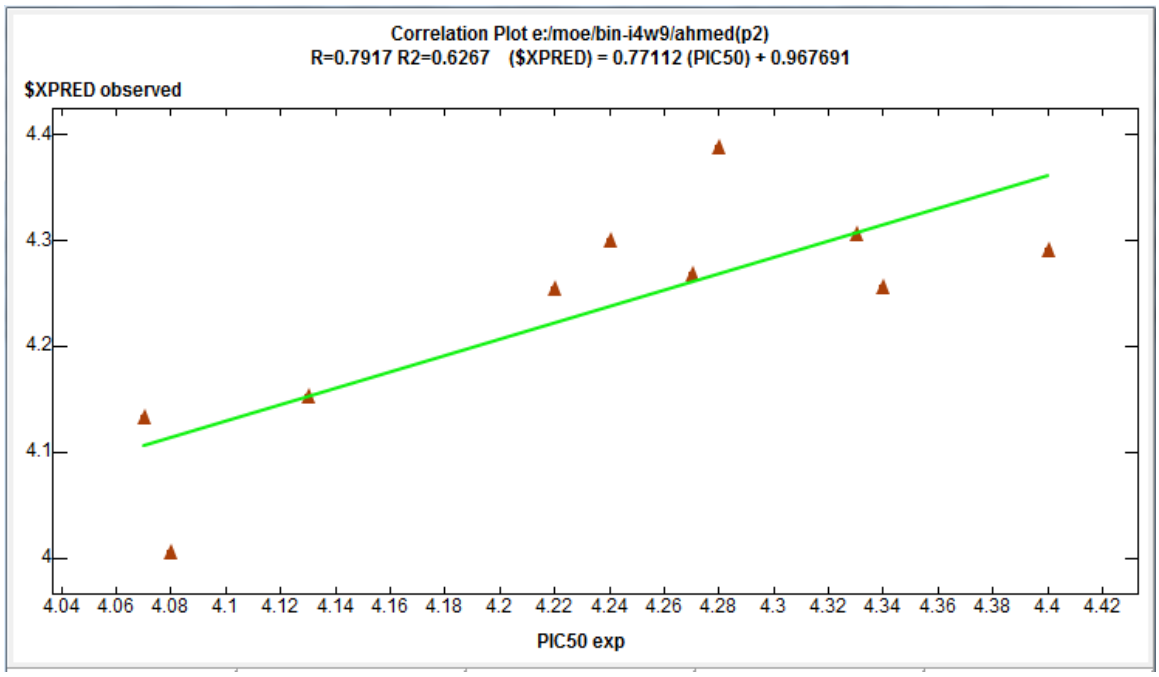

Figure (3.5): The plot of linear regression predicted PIC_{50} versus experimental values of the biological activity of training set compounds (cross-validation).

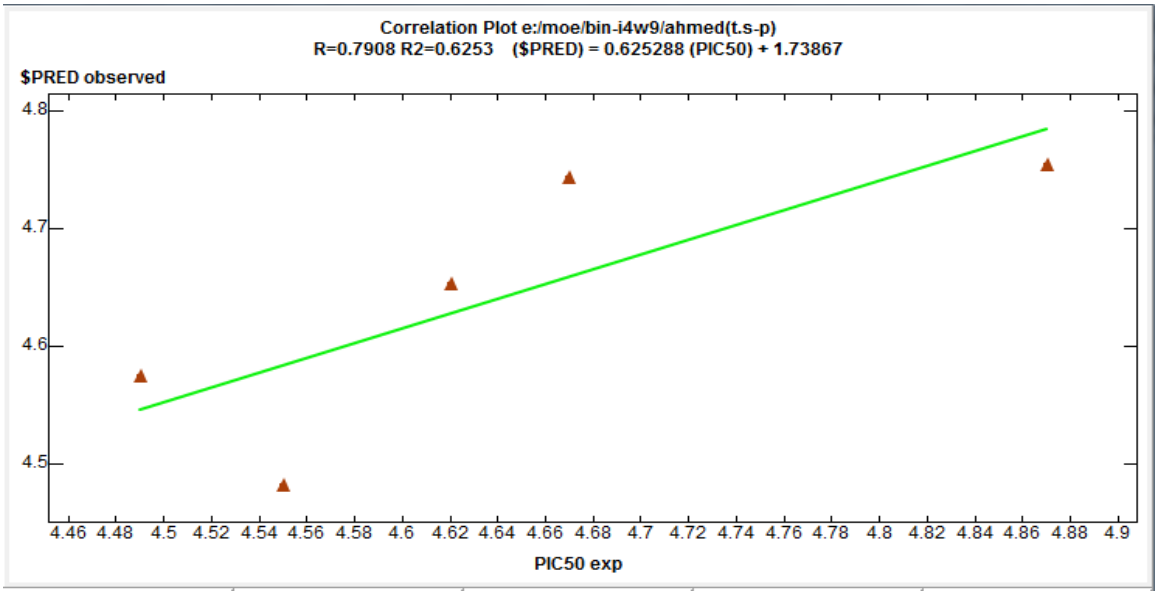

Figure (3.6): The plot of linear regression predicted PIC_{50} versus experimental values of the biological activity of test set compounds (validation).

The plots for QSAR model shows a good fit with R=0.9965 and R^2 which equal to 0.9930. And Q= 0.6296 Q^2 =0.3963 cross-validation for training set compounds.

And the plots for QSAR in the test set show a good fit with R= 1, R^2 =1(validation). And Q = 1, Q^2 =1 in (cross-validation), for group (I).

The plots for QSAR model shows a good fit with R=0.9011 and R^2 which equal to 0.8120. And Q= 0.7917 Q^2 =0.6267 cross-validation for training set compounds.

And the plots for QSAR in the test set show a good fit with R= 1, R^2 =1(validation). And Q = 0.7908, Q^2 =0.62053 in (cross-validation), for group (II). According to the results of QSAR, and docking studies of the designed compounds some of them were selected for synthesis.

3.4. Synthesis acridinediones and polyhydroquinolines derivatives

3.4.1. Synthetic design

The synthetic design of these derivatives of Acridinediones and Polyhydroquinolines in this part is based mainly upon retro-synthetic analysis. Standard C-C and C-N disconnections were followed; bear in mind the concepts of region and chemo- selectivity.

The retro synthetic direction is going backwards from a target molecule to the starting materials by way of retro-reaction or transformation.

Retro-synthesis is a technique of working backwards from a molecule to simpler ones for solving problems in synthesis planning, especially those presented by complex structures (Nadenla, 2002) .

Retro synthetic analysis (RSA), aid in the establishment of good synthetic scheme in (RSA), key steps are developed by examine important structure element in the final product and figuring out how specific reaction could lead to the product. The procedure is performed so that a complex final molecule is reduced to simpler intermediates. The advantage of such an approach is that it's greatly simplifies planning the synthesis of a complex product and readily leads to a convergent synthesis.

In performing (RSA), it may also be useful to disconnect a bond showing the fragment not as an electrophilic and nucleophilic (synthons).This may help bring to mind other reaction that can be used to reassemble the fragment (Hornback, 2005).

The disconnection approach is the current most widely used technique in designing organic synthesis. By such a technique, the bonds in the target molecule can logically be disconnected or interconverted to synthons, from which suitable or synthetic equivalents can be generated.

The disconnection approach has been adopted in this work, with the basic concepts of the synthetic methods.

The retro synthetic analysis of the prepared acridinediones are shown below by general structures of 3,3,6,6-tetramethyl-3,5,6,7,9,10-hexahydroacridine-1,8-(2H,5H)-dione derivatives.

The appropriate synthetic equivalent of the produced synthons may be:

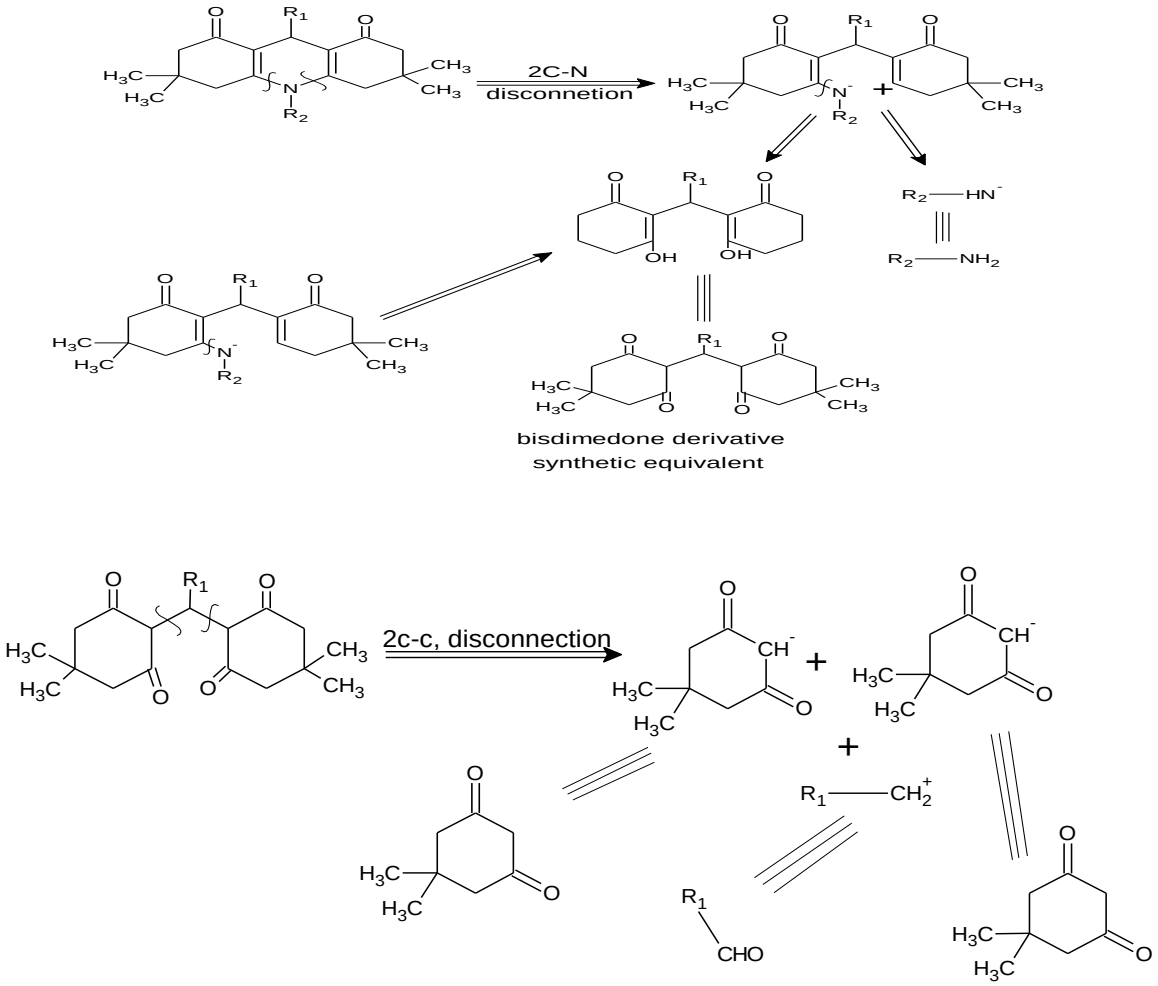

Figure (3.7): The retro-synthetic analysis of the prepared acridinedione derivative (I, II, III, IV and V).

Synthetic equivalent can account for the formation of the octahydroxanthenes from the corresponding bis dimedone derivatives.

The next step is the disconnection of 2C-C in the bis dimedone, the resulting of the synthetic equivalents were two molecules of dimedone and one mole of an aldehyde. Furthermore, the dimedone structure can be disconnected in the following manner:

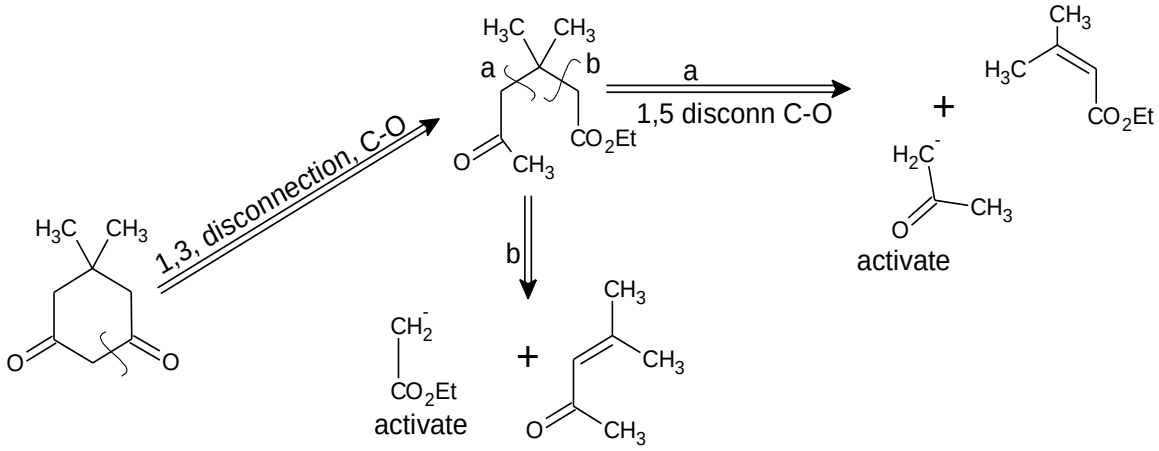

Similar disconnections can be seen in the case of polyhydroquinoline derivatives.

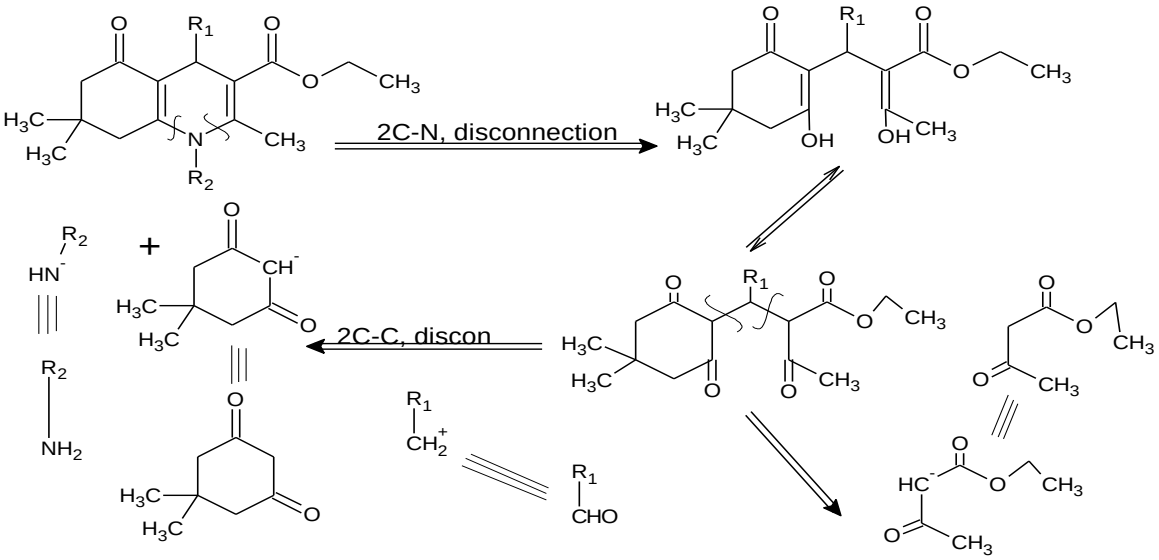

Figure (3.8): The retro-synthetic analysis of the prepared polyhydroquinoline derivatives.

In the above disconnection protocol in the case of polyhydroquinoline derivatives the synthetic equivalent is ethyl acetoacetate, and dimedone. Alongside, other synthetic equivalent such as an amine and aldehyde.

According to the disconnection protocols mentioned above suitable mechanisms for both Acridinedione and polyhydroquinoline could be formulated.

3.4.1.1: The proposed mechanism of formation of acridinedione derivatives

Formation of the hydroacridinediones may be rationalized by an intial formation of the imine from the condensation of the aromatic aldehydes with the appropriate amino alcohol on attacking of the enol form of dimedone to the imine could afford the formation of adduct which in turn underwent an internal arrangement to release amino alcohols and arylidenes .The released amino alcohols could react with another molecule of dimedone to give the amino which in turn could attack through its nucleophilic amino group into the electrophilic carbon atom of the former arylidine to obtain the new imine .The unstable imine could rearrange into the relativity stable structure of the hydroxyhydroacridinediones which ultimately could stabilized easily into the title structure of hydroacridinediones by elimination of a molecule of water (Abdelhamid *et al*., 2014).(see scheme 3.2a).

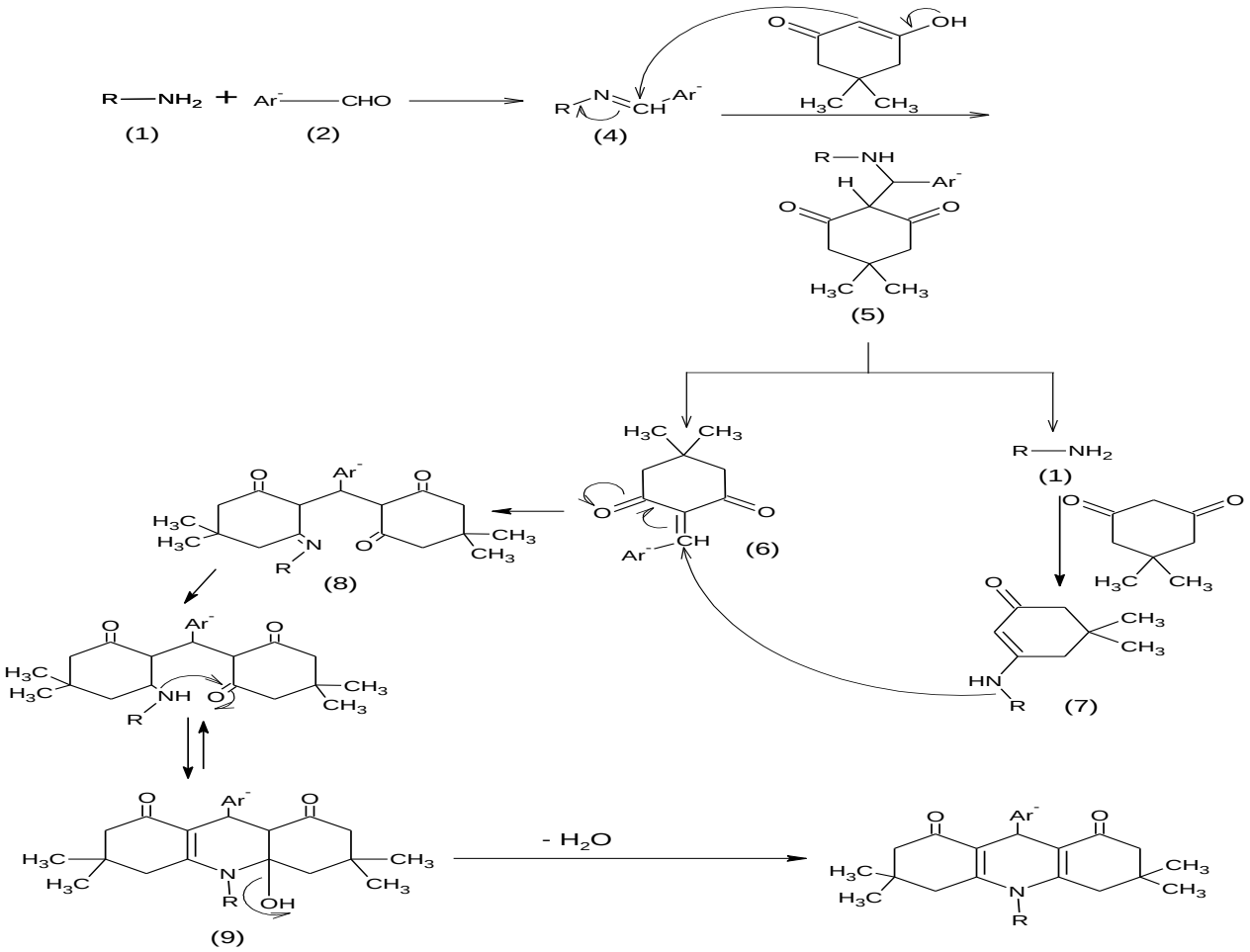

(Abdelhamid *et al*., 2014).

Figure (3.9): a proposed mechanism of the formation of acridinedione derivatives.

3.4.1.2: The proposed mechanism of the formation of poyhydroquinoline derivatives

The proposed mechanism,the poyhydroquinoline derivatives could be synthesized by two methods.The SBA-Pr-SO_3H catalyses subsequently the knoevenagel type coupling of aldehydes with active methylene compounds and then the Michael type addition of intermediates together to provide the products.

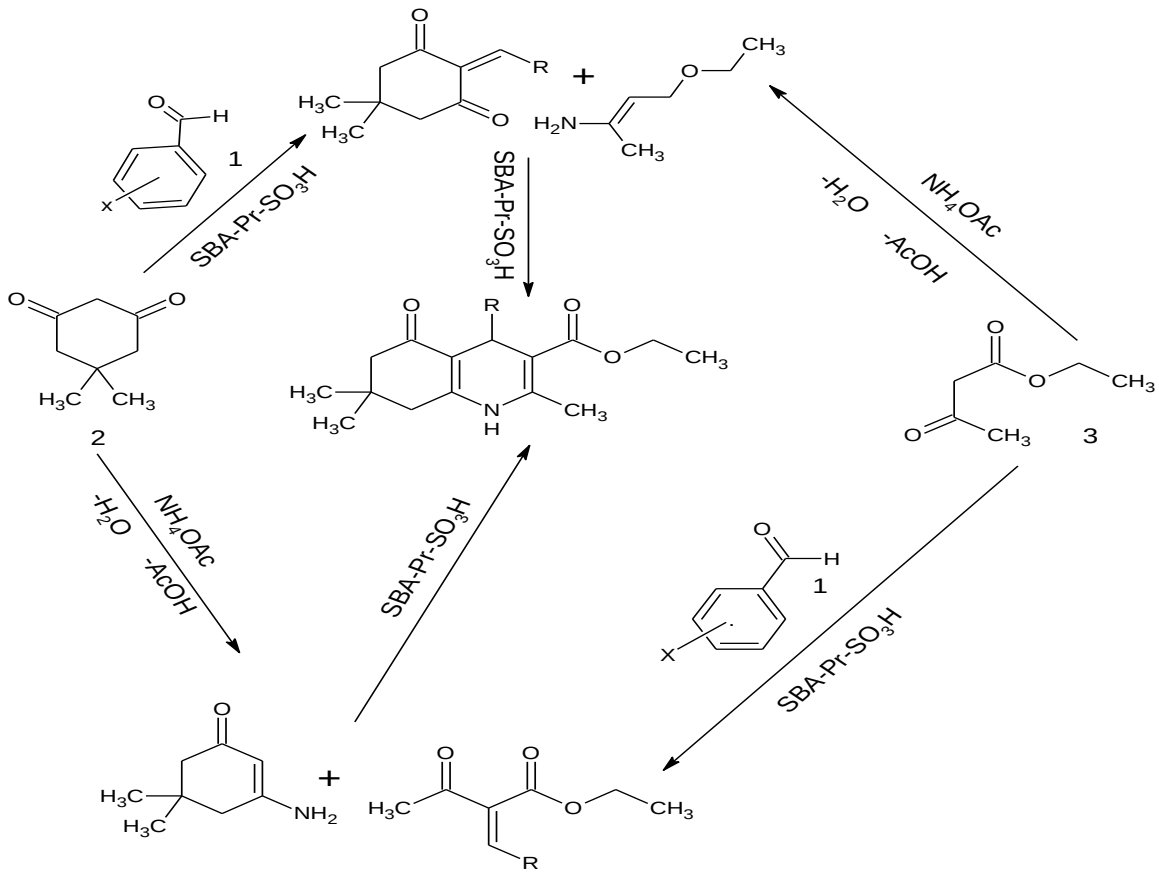

(Beck *et al*., 1992)

Figure (3.10): A proposed mechanism of the formation of Polyhydroquinoline derivatives.

3.5. The R_f-values

Thin layer chromatography is the method for analyzing the purity of the prepared compounds and monitoring of the reactions.

Chloroform and Methanol and other solvents were used as solvent systems, and the R_F values were recorded in table (2.2a) and (2.2b).

3.6. Spectroscopic data analysis for the prepared compounds

3.6.1. IR spectral data

Infra-red spectroscopy is one of the most important tools in structure elucidation, it provides an excellent means of identification of the different functional groups associated with an organic molecules.

Infra-red (IR) radiation refers broadly to that part of the electromagnetic spectrum between the visible and the microwave region of greatest practical use to the organic chemist, the limited portion between 4000 and 400 cm^{-1}. The spectra of the prepared compounds were recorded with FT-TR, 8400s instrument (SHIMADZU, Japan) using KBr disc. The results were tabulated in table (2.2a).

The characteristic peaks for Acridinedione derivatives were observed for aromatic ring, C-H aromatic which was observed at 3060$cm^{-1}$for compound no. (I) and compound No (IV) at 3028 cm^{-1}.And C-H aliphatic for these compounds were observed in the range between (2954-2964 cm^{-1}). Compound (I) was appeared at 2960 cm^{-1}, (II) at 2954 cm^{-1} and compound No. (III) .Was observed at 2964 cm^{-1} st.vib respectively.

The carbonyl group of these compounds was appeared at (1593-1640cm^{-1}) for compound No. (I) C=O which observed at 1593cm^{-1}, this abnormal absorption for C=O due to the presence of the keto-enol tautomarism and formation of enolic group (C=C-OH).

C=C st.vib in compound (I) was observed at 1521cm^{-1} st.vib, compound (III) at 1525cm^{-1} st.vib respectively.

C-N stretching vibration compound No. which observed at 1257cm^{-}, (II) at 1312cm^{-1} and (III) at 1269cm^{-1} respectively. C-H deforming ring for these compounds were appeared at 812cm^{-1}, 846 $cm^{-1,}$ 757 cm^{-1} and 835cm^{-1} respectively. The SO^{2} asymmetric for compound (I) which appeared at 1369 cm^{-1} and the symmetric one was appeared at 1311cm^{-1}.

OH group appeared at 3185 cm^{-1} in compound (II) the low absorption of the hydroxyl group due to hydrogen bonding. N-H st.vib for compound (I) appeared at 3446 cm^{-1}. N-H bending for compound (I) appeared typically at

1448 cm^{-1} , C-O st.vib for compound (I), (II) and (III) were observed at 1232 cm^{-1}, 1235 cm^{-1} and 1152 cm^{-1} respectively.

Compound (IV), C=O appeared at 1641 cm^{-1}, OH at 3192 cm^{-1}, CH_3 at 2955 cm^{-1}, C=C at 1590 cm^{-1}, C-O at 1156 cm^{-1}. Compound (V), C=O appeared at 1604 cm^{-1}, OH at 3367 cm^{-1}, CH_3 at 2928 cm^{-1}, C=C at 1457 cm^{-1} and C-O at 1151 cm^{-1}.

The IR spectra for the prepared compounds of polyhydroquinoline derivatives were observed as follows:

Compound (VI), the C-H aliphatic which was observed at 2968 cm^{-1} and for (VII) at 2955 cm^{-1} st.vib. The C=O for compound (VI), (VII), and (X) were observed at 1727 cm^{-1}, 1723 cm^{-1}, and 1728 cm^{-1} for carbonyl esters.

C=C for compound (VI) was observed at 1591 cm^{-1} st.vib and (VII) at 1640 cm^{-1}, and (IX) which appeared at 1583 cm^{-1}. C-N st.vib for compound (VII) was observed at 1387 cm^{-1} st.vib, and compound (VII) at 1369 cm^{-1}. C-H bending (ring) for these compounds was observed at 860 cm^{-1}, 755 cm^{-1}, and 902 cm^{-1}. The OH for compound No. (VII) Which was observed at 3280 cm^{-1} was due to hydrogen bonding. The C-O st.vib for (VI), (VII), (VIII) were observed at 1230 cm^{-1}, 1233 cm^{-1} and 1234 cm^{-1} respectively.

Compound (VIII), (IX) and (X). The C=O which appeared at 1731, 1716 and 1714 cm^{-1}. C=C, at 1590, 1614 and 1630 cm^{-1} respectively. S=O appeared at 1387, 1390 and 1388 cm^{-1}. CH_3 at 2960, 2954 and 2965 cm^{-1}. Compound (X), OH, appeared at 3244 cm^{-1}. Compound (VII), (IX) and (X), N-H bond appeared at 3485, 3423 and 3421 cm^{-1} respectively. Also, C-O for these compounds appeared at 1221, 1223 and 1231 cm^{-1} respectively.

3.6.2. Ultra violet Spectroscopic analysis

Most organic molecules and functional groups are transparent in the portions of the electromagnetic spectrum which we call the Ultra violet (UV) and

visible (VIS) regions that is, the regions where wavelengths range from 190nm to 800nm. Consequently, absorption rospectroscopy is of limited utility in this range of wavelengths. However, in some cases we can derive useful information from these regions of the spectrum. That information, when combined with the detail provides by infrared and nuclear magnetic resonance, can led to valuable structural proposals (Pavia *et al*., 2002.

The UV-VIS spectra of these derivatives recorded in ethanol exhibit an intense absorption band which is attributed to the π- π* or n- π* in carbonyl group. Also, the polyhydroquinoline derivatives exhibit an intense absorption band which is attributed to the same transition of the double bond in phenyl ring or carbonyl group. The absorption maxima (λ_{max}) wavelength was observed in the range of (207 to 314nm) table (2.42) and (2.43).

An n- π* transition in these compounds represent the transition of one electron of a lone-pair, a non-bonding pair of electrons, to an anti-bonding π-orbital.

3.6.3. ^{1}HNMR-Spectroscopy

Proton nuclear magnetic resonance spectroscopy (^{1}HNMR) is a very important technique for structure elucidation of the prepared compounds (Williams, 1980; Finar, 1975).

Mass spectroscopy (MS) is a technique for measuring the mass, and therefore, the molecular weight (M.wt) of the molecule. In addition, it is often possible to gain structural information about a molecule by measuring the masses of the fragments produced when molecules are broken apart (McMurry, 2000).

3.6.3.1. 4-(9-(4-(dimethylamino)phenyl)-3,3,6,6-tetramethyl-1,8-dioxo-2,3,4,5,6,7,8,9-octahydroacridin-10(1H)-yl) benzenesulfonamide (I)

^{1}H-NMR($CDCl_3$ (CH_3 ,6H,s), 0.0967-1.099; (CH_2), 2.27; (CH_2), 2.32; (CH_3 ,6H,m), 2.46; (CH, 1H), 5.47; Phenyl ring, (4Hq), 7.38-7.059; Phenyl ring, (4Hq), 7.136-7.74; (2H, NH_2), 6.98.

3.6.3.2. 9-(2-hydroxyphenyl)-3,3,6,6-tetramethyl-10-phenyl-3,4,6,7,9,10-hexahydroacridine-1,8(2H,5H)-dioned(II)

^{1}H-NMR($CDCl_3$ (CH_3 ,6H,s), 0.86-1.132; (CH_2), 2.02; (CH_2), 2.23; (CH, 1H), 5.108; Phenyl ring, (3Hq); 7.012-7.184; Phenyl ring, (4Hq), 7.410-7.517; OH(1H), 9.926.

3.6.3.3.4-(9-(2-hydroxyphenyl)-3,3,6,6-tetramethyl-1,8-dioxo-2,3,4,5,6,7,8,9-octahydroacridin-10(1H)-yl)benzenesulfonamide(III)

^{1}H-NMR($CDCl_3$ (CH_3 ,6H,s), 1.14-1.32; (CH_2), 2.05-2.13; (CH_2), 2.22-2.63; (CH, 1H), 4.69; Phenyl ring, (4Hq), 7.039-7.17; Phenyl ring, (4Hq), 7.168-7.28; OH(1H), 11.353; (2H, NH_2), 6.942.

3.6.3.4.(E)-4-(3,3,6,6-tetramethyl-1,8-dioxo-9-styryl-2,3,4,5,6,7,8,9-octahydroacridin-10(1H)-yl)benzenesulfonamide(IV)

^{1}H-NMR($CDCl_3$ (CH_3 ,6H,s), 0.899-1.099; (CH_2), 2.123-2.160; (CH_2), 2.22-2.86; (CH, 1H), 3.936; (CH, 1H), 5.270; (CH, 1H), 6.545; Phenyl ring, (5H,m), 7.132-7.284; Phenyl ring, (4H,q), 7.617-7.73; (2H, NH_2), 6.76.

3.6.3.5.(E)-3,3,6,6-tetramethyl-10-phenyl-9-styryl-3,4,6,7,9,10-hexahydroacridine-1,8(2H,5H)-dione (V)

^{1}H-NMR($CDCl_3$ (CH_3 ,6H,s), 0.932-1.016; (CH_2), 1.185-1.188; (CH_2 1.197-1.244; (CH, 1H), 1.185; (CH, 1H), 2.191; (CH, 1H), 2.304; Phenyl ring, (5H,m), 7.128-7.316; Phenyl ring, (5H,m), 7.323-7.403.

3.6.3.6.Ethyl2,7,7-trimethyl-5-oxo-1,4-diphenyl-1,4,5,6,7,8-hexahydroquinoline-3-carboxylate(VI)

^{1}H-NMR($CDCl_3$ (CH_3 ,6H,s), 0.191-1.176; (CH_2), 2.242; (CH_2), 1.010; (CH_3 ,3H,m), 1.852; (CH, 1H), 5.303; Phenyl ring, (5Hm).,7.113-7.190; Phenyl ring, (5Hm), 7.284-7592.

3.6.3.7.Ethyl4-(2-hydroxyphenyl)-2,7,7-trimethyl-5-oxo-1-phenyl-1,4,5,6,7,8-hexahydroquinoline-3-carboxylate(VII)

^{1}H-NMR($CDCl_3$ (CH_3 ,6H,s), 0.858-1.045; (CH_2), 2.007; (CH_2), 2.22; (CH, 1H), 2.48; Phenyl ring, (4Hq); 7.02-7.22; Phenyl ring, (5Hm), 7.23-7.43; OH(1H), 13.055.

3.6.3.8. Ethyl 4-(3-hydroxy-4-methoxyphenyl)-2,7,7-trimethyl-5-oxo-1-phenyl-1,4,5,6,7,8-hexahydroquinoline-3-carboxylate(VIII)

^{1}H-NMR($CDCl_3$ (CH_3 ,6H,s), 1.028-1.274; (CH_2), 5.303; (CH_2), 2.328; (CH, 1H), 4.69; (CH_3 ,3H,m), 2.242, Phenyl ring, (3Ht), 7.078-7.190; Phenyl ring, (5Hm), 7.28-7.59; OH(1H), 11.933; (CH_3 ,3H,s), 3.87.

3.6.3.9. Ethyl 4-(4-(dimethyl amino) phenyl) - 2, 7, 7-trimethyl-5-oxo-1-phenyl-1,4,5,6,7,8-hexahydroquinoline-3-carboxylate(IX)

^{1}H-NMR($CDCl_3$ (CH_3 ,6H,s), 0.907-1.025; (CH_2), 2.268; (CH_2), 2.307; (CH_3 ,3H,m), 2.24 ; (CH, 1H), 2.17. (CH_3, 6H, s), 2.259; Phenyl ring, (4H, m), 7.123-7.189; Phenyl ring, (5H, m), 7.304-7.37.

3.6.3.10. (E)-2, 7, 7-trimethyl-5-oxo-4-styryl-1-(4-sulfamoylphenyl)-1, 4, 5, 6, 7, 8-hexahydroquinoline-3-carboxylate(X)

^{1}H-NMR($CDCl_3$ (CH_3 ,6H,s), 1.023-1.088; (CH_2), 1.170; (CH_2 1.183; (CH, 1H), 1.185; (CH_3, 3H, s), 1.280; (CH_2), 2.348; (CH_3, 3H, s), 2.577; (CH, 1H), 3.326; (CH, 1H), 2.43; (CH, 1H), 4.091; Phenyl ring, (5H,m), 7.116-7.212; Phenyl ring, (5H,m), 7.31-7.320; (NH_2, 2H), 2.404.

3.6.4. Mass Spectroscopic Analysis

In its simplest form, the mass spectrometer has five components. The first component of the mass spectrometer is the sample inlet, which brings the sample from the laboratory environment. The sample inlet leads to the ion source, where the sample molecules are transformed into gas phase ions.The ions are then accelerated by an electromagnetic field. Next, the mass

analyzer separates the sample ions based on their mass-to-charge (m/z) ratio. The ions then are counted by the detector, and the signal is recorded and processed by the data system. The output from the data system in the mass spectrum-graph of the number of ions detected as a function of their m/z ratio (Pavia *et al*., 2002).

Mass spectrometry (MS) was used to determine the molecular weights of synthesized compounds of acridinedione derivatives. Compound (I) shows, fragments at m/z at 55, 56, 83, 101, 121, 129, 144, 159, 172, 272, 411, 450, 456, 477, 492, and 538. Compound (II) shows, fragments at m/z at 55, 56, 91, 101, 115, 128, 143, 155, 171, 227, 240, 282, 366, 423, and 441. Compound (III) shows, fragments at m/z at 55, 56, 83, 91, 102, 115, 128, 141, 165, 185, 205, 215, 222, 244, 278, 288, 302, 316, 329, 348, 368, 404, 419, 441, 451, 469, 526, and 536. Compound (IV) shows, fragments at m/z at 55, 56, 83, 102, 115, 128, 143, 155, 171, 227, 240, 265, 282, 366, 418, 430, 452, 477, 501, 510, 519, and 533. Compound (V) shows, fragments at m/z at 55, 56, 83, 92, 102, 115, 128, 141, 156, 170, 183, 204, 220, 239, 254, 266, 284, 410, 434, 441, and 451.

The compounds of polyhydroquinoline derivatives. Compound (VI) shows, fragments at m/z at 55, 56, 77, 93, 102, 155, 131, 144, 159, 171, 183, 199, 220, 227, 241, 256, 269, 292, 303, 316, 332, 348, 350, 368, 382, 401, 415, and 425. Compound (VII) shows, fragments at m/z at 55, 56, 77, 93, 104, 115, 128, 143, 155, 171, 185, 198, 211, 227, 259, 265, 267, 282, 302, 310, 327, 348, 359, 366, 383, 396, 407, and 431. Compound (VIII) shows, fragments at m/z at 55, 56, 83, 92, 108, 112, 133, 156, 172, 187, 203, 217, 231, 243, 257, 273, 287, 302, 315, 329, 339, 359, 390, 414, 431, 442, 461, 477, 495, 510, 525 and 540. Compound (IX) shows, fragments at m/z at 55, 56, 77, 83, 91, 105, 115, 128, 141, 165, 191, 221, 232, 241, 252, 268, 288,

316, 330, 349, 356, 368, 383, 403, 417, 433, 445 and 459. Compound (X) shows, fragments at m/z at 55, 56, 83, 84, 102, 115, 128, 141, 155, 170, 184, 198, 221, 237, 254, 273, 284, 295, 309, 333, 361, 376, 394, 410, 426, 436, 450, 451, 462, 487, 503, and 513.

A molecular ion peak (M^+) with their relative abundances was observed for acridinediones 547 (0.61%), 441 (1.53%), 526 (0.59%), 533 (0.07%), and 551 (2.01%). And for polyhydroquinoline derivatives, 425 (14.68%), 431 (2.57%), 540 (0.83%), 459 (1.37%), and (520), (0.06%). Was observed in their respective mass spectra and with their structures. Compounds I, II, III, IV and V showed base peaks at 272, 282, 83, 366, and 128, (100%), for acridinedione derivatives. Compounds VI, VII also showed base peaks at 77, 115, whereas VIII, IX, X showed same base peaks at 83 (100%), for polyhydroquinoline derivatives.

The M+1 and M+2 isotope peaks was also observed in all synthesized derivatives. The M+1 occur due to the presences of isotopes ^{2}H or ^{13}C observed with a relative abundance ranging from (1.09- 5.69%).

M+2 the isotope peak of oxygen atom appears due to the presence of C=O or O-H groups. With a relative abundance between (3.25- 65.07%).

M+3 occurred due to the presence of may be isotopes of ^{13}C or ^{18}O in these derivatives.

M+4 were also occurred due to the presence of ^{18}O or ^{34}S atoms in compounds which contain sulphoneamide moiety. The fragmentation pattern of the synthesized compounds acridinediones or polyhydroquinolines was shown in schemes (3.1) to (3.10) respectively.

The common fragmentation pattern involves some rearrangement with the removal of simple and smaller molecules such as C=O or O-H groups and sometimes $–CH_2-$ group.

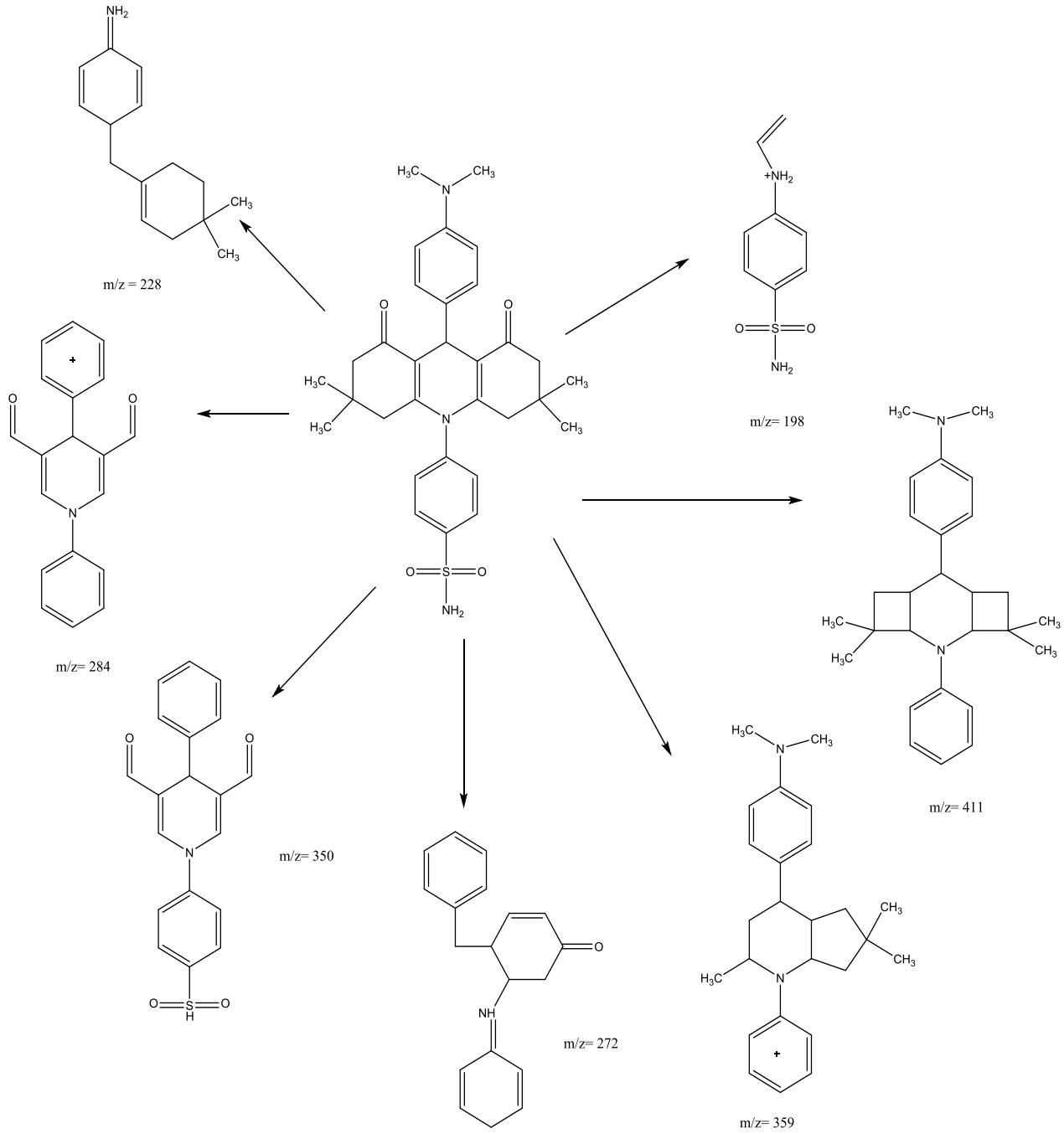

Scheme (3.1): Mass fragmentation of 4-(9-(4-(dimethylamino)phenyl)-3,3,6,6-tetramethyl-1,8-dioxo-2,3,4,5,6,7,8,9-octahydroacridin-10(1H)-yl)benzenesulfonamide(I)

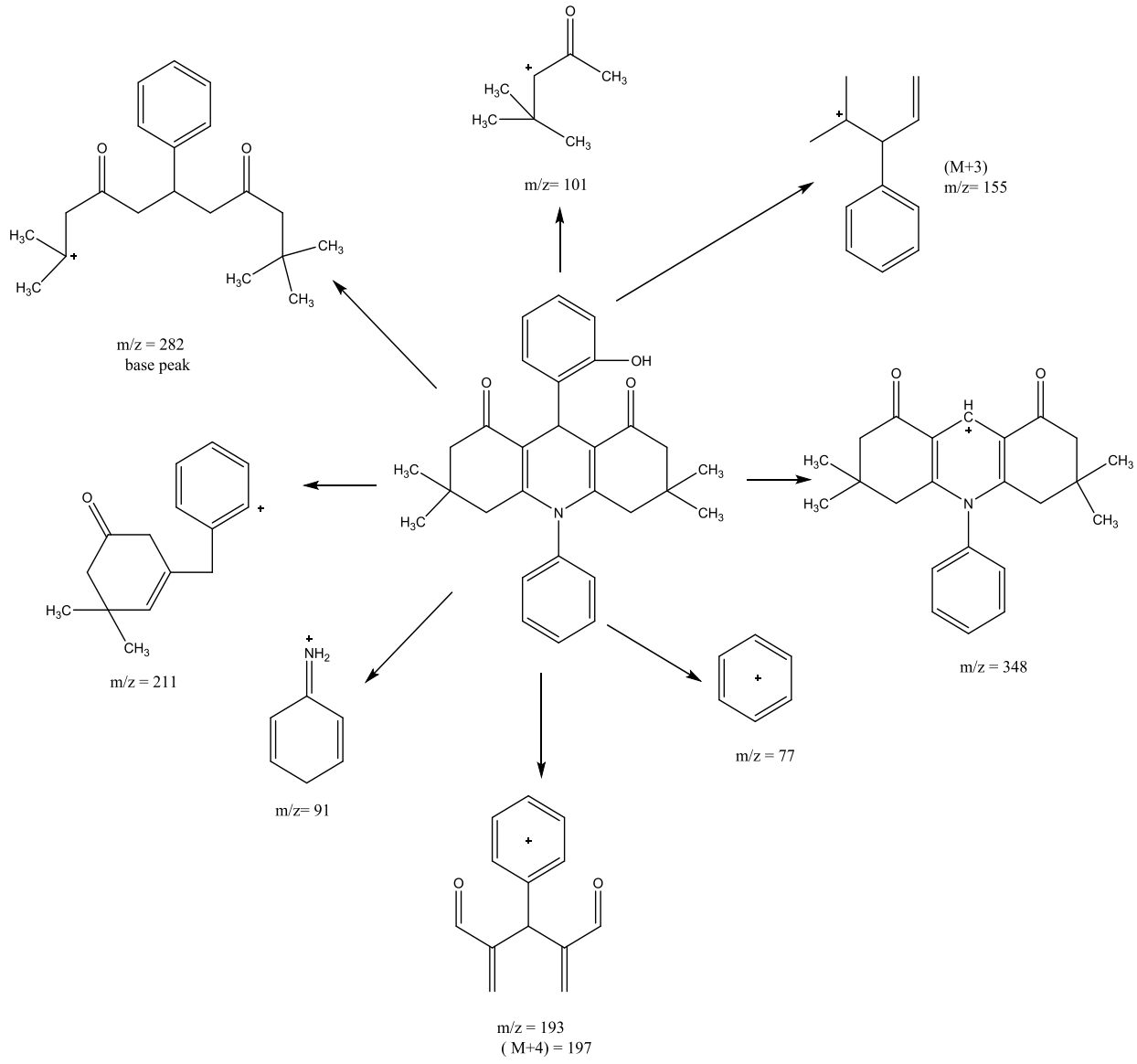

Scheme (3.2): Mass fragmentation of 9-(2-hydroxyphenyl)-3,3,6,6-tetramethyl-10-phenyl-3,4,6,7,9,10-hexahydroacridine-1,8(2H,5H)-dioned (II)

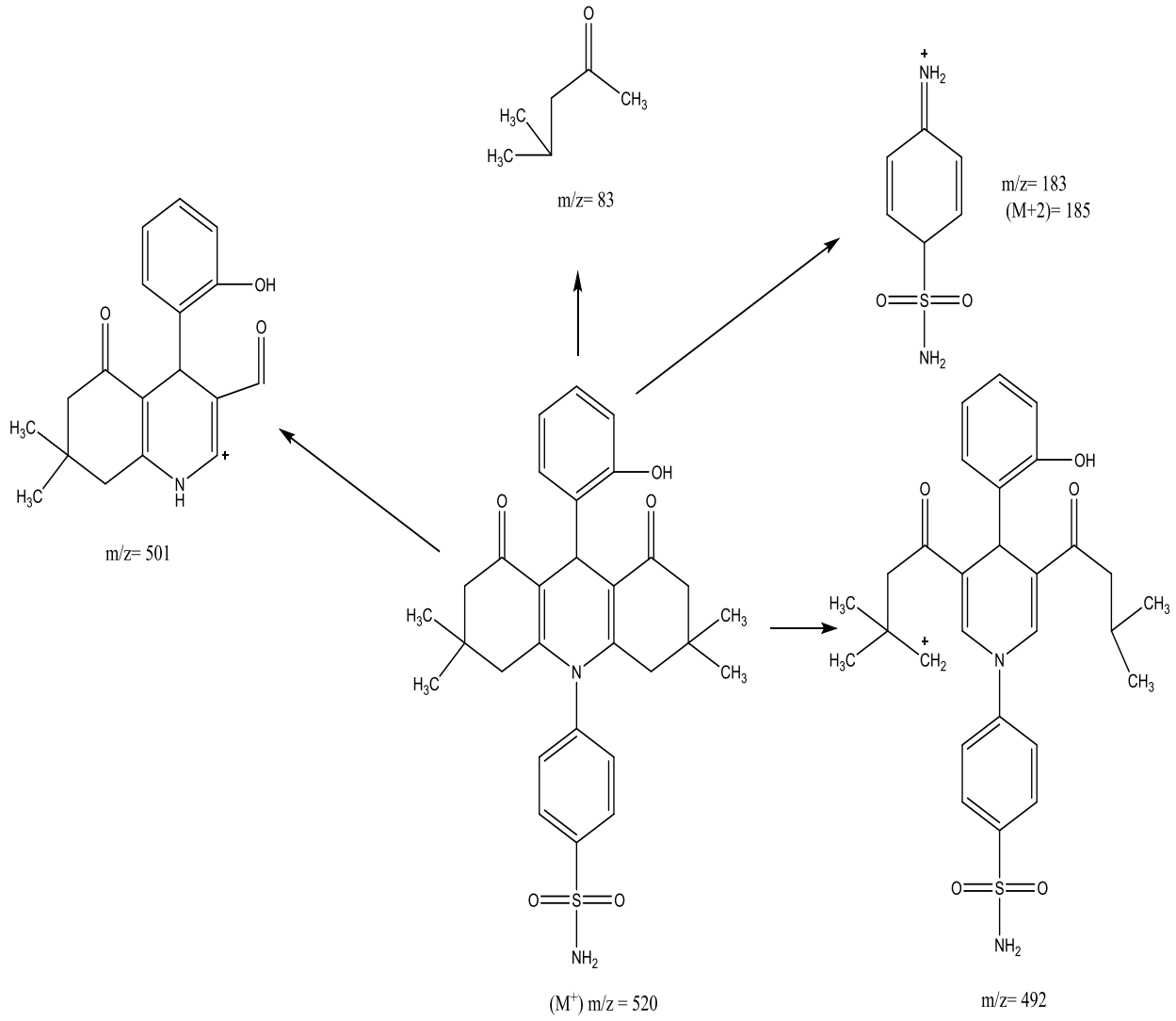

Scheme (3.3): Mass fragmentation of 4-(9-(2-hydroxyphenyl)-3,3,6,6-tetramethyl-1,8-dioxo-2,3,4,5,6,7,8,9-octahydroacridin-10(1H)-yl)benzenesulfonamide (III)

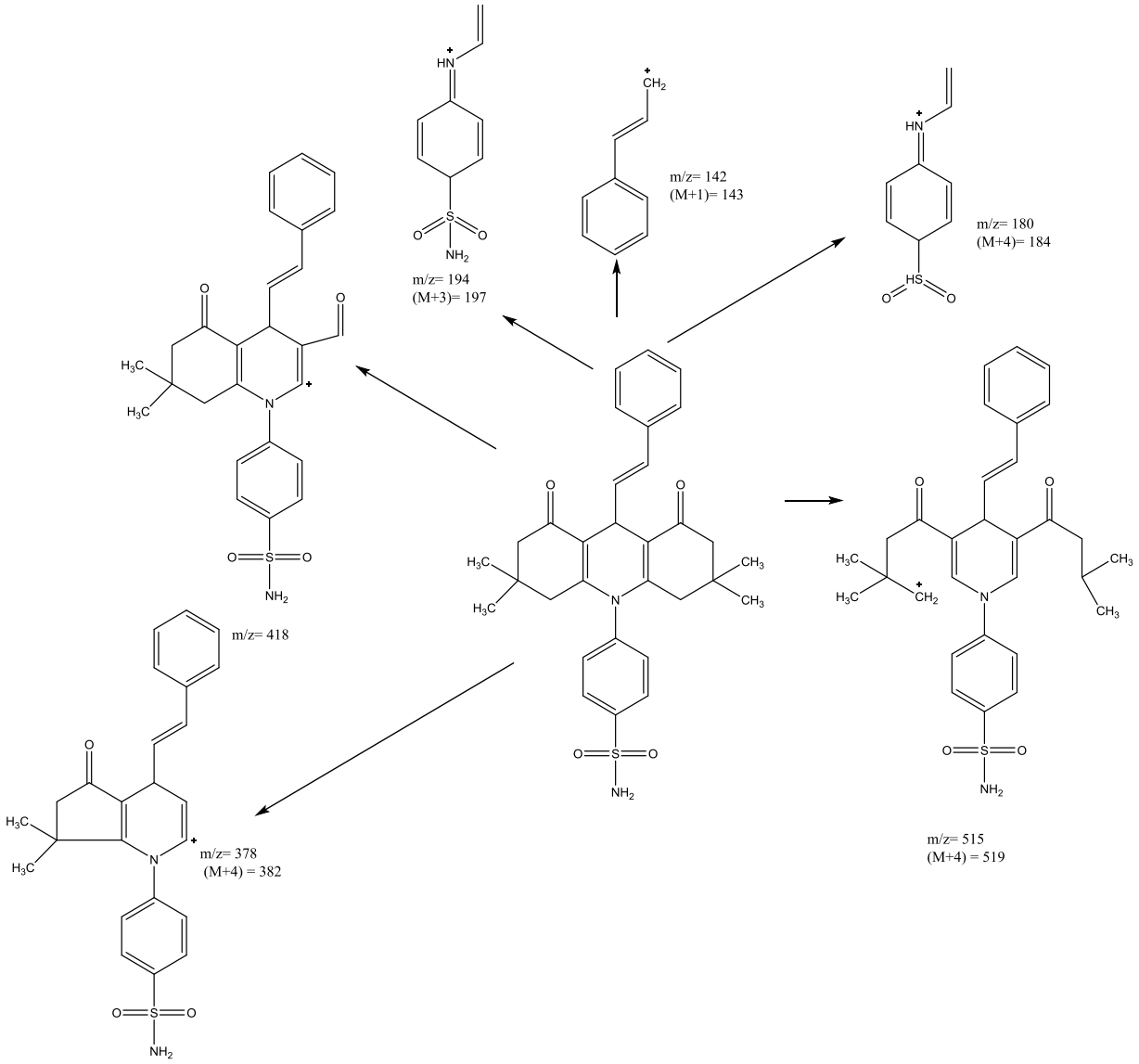

Scheme (3.4): Mass fragmentation of (E)-4-(3,3,6,6-tetramethyl-1,8-dioxo-9-styryl-2,3,4,5,6,7,8,9-octahydroacridin-10(1H)-yl)benzenesulfonamide (IV)

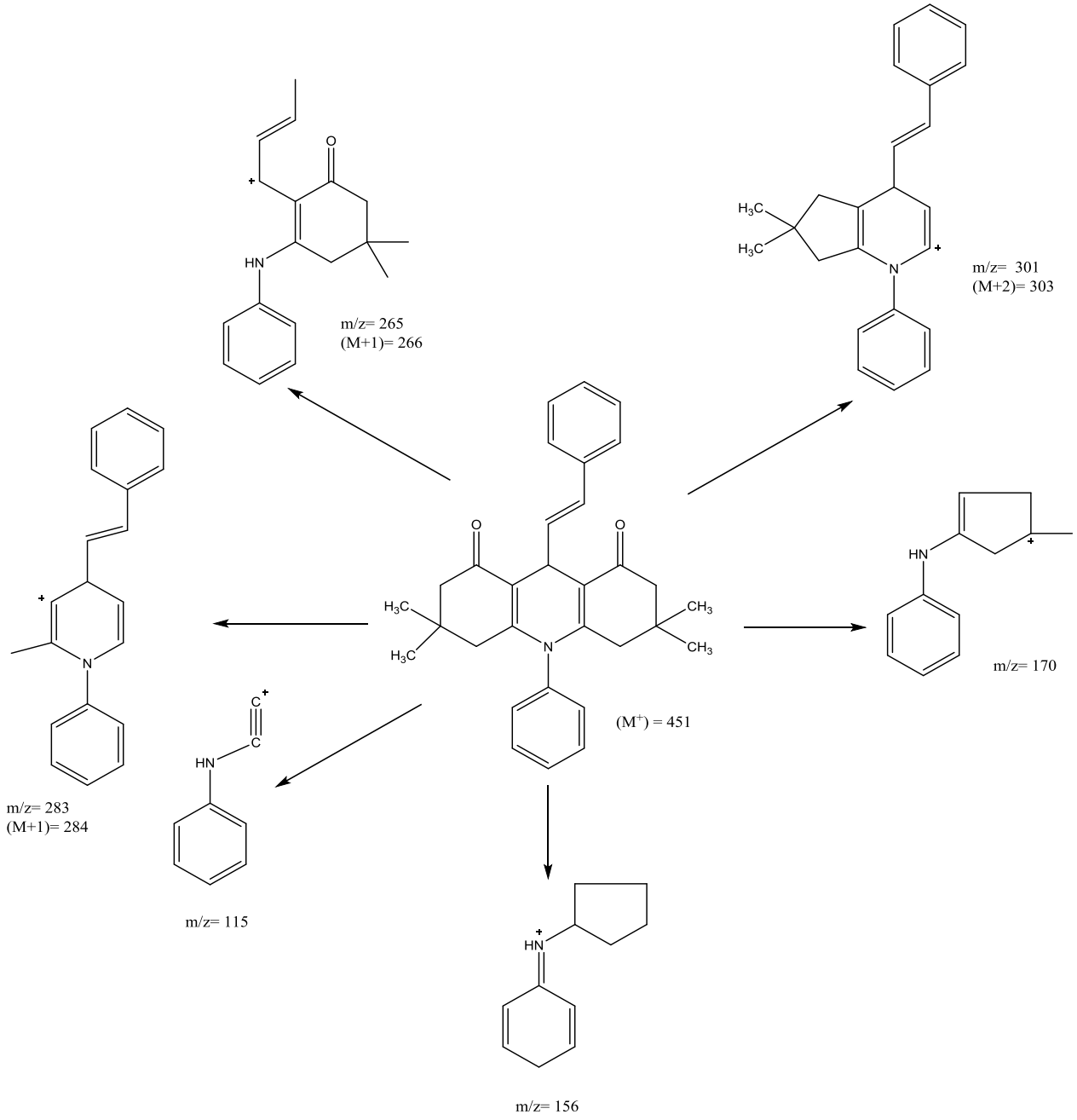

Scheme (3.5): Mass fragmentation of (E)-3,3,6,6-tetramethyl-10-phenyl-9-styryl-3,4,6,7,9,10-hexahydroacridine-1,8(2H,5H)-dione (V)

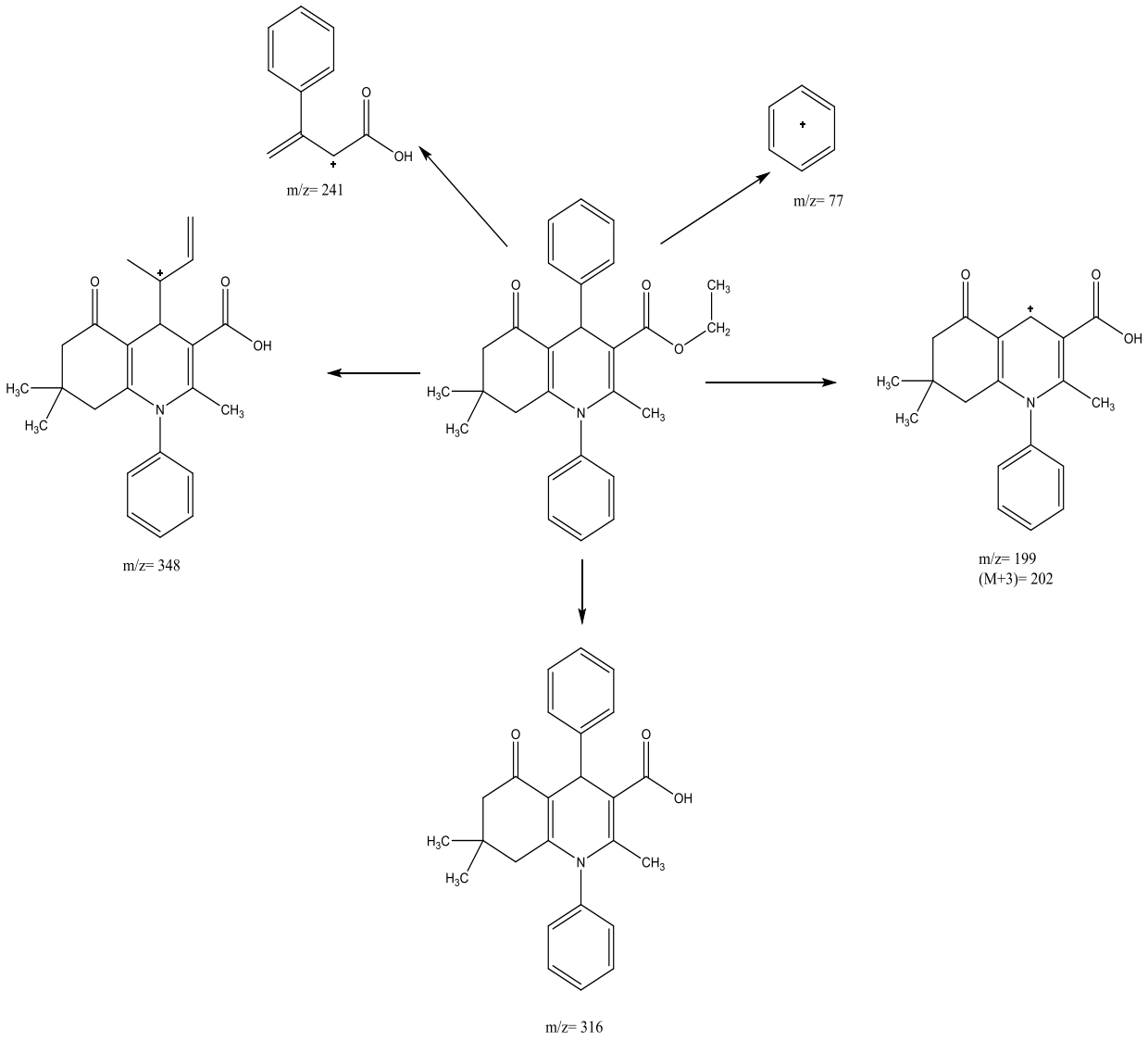

Scheme (3.6): Mass fragmentation of ethyl 2, 7, 7-trimethyl-5-oxo-1, 4-diphenyl-1, 4, 5, 6, 7, 8-hexahydroquinoline-3-carboxylate (VI)

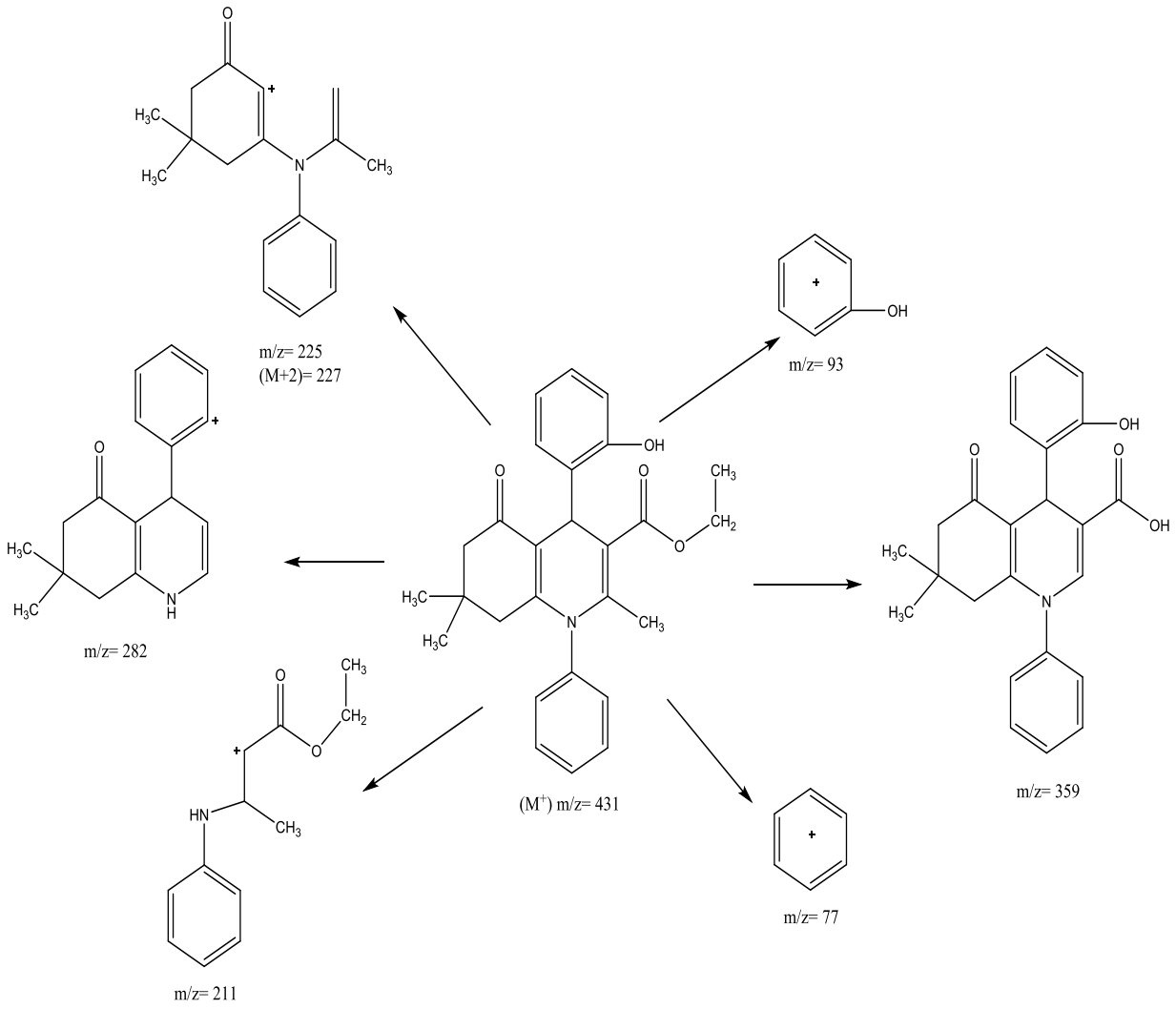

Scheme (3.7): Mass fragmentation of 9-(2-hydroxyphenyl)-3,3,6,6-tetramethyl-10-phenyl-3,4,6,7,9,10-hexahydroacridine-1,8(2H,5H)-dioned (VII)

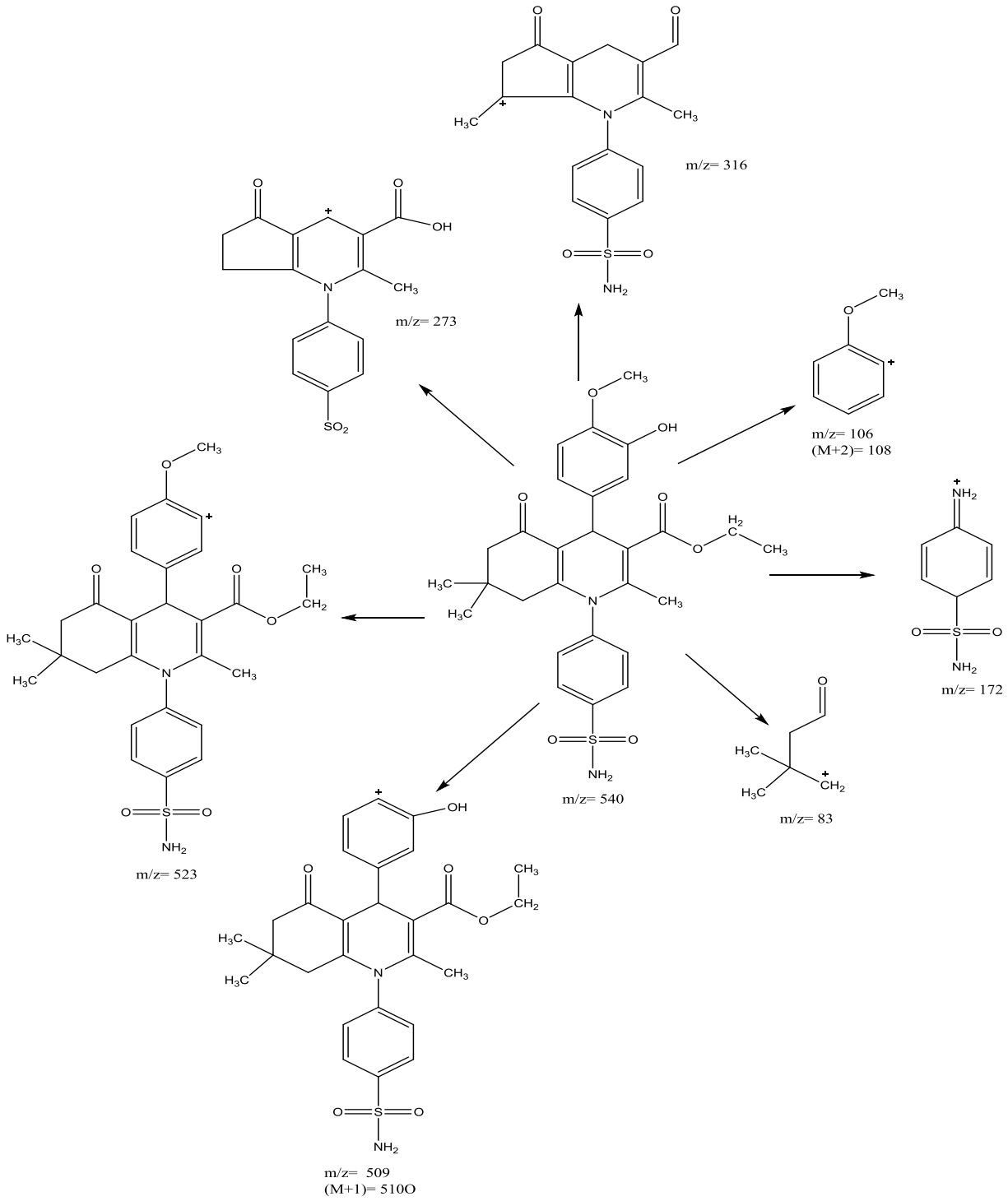

Scheme (3.8): Mass fragmentation of ethyl 4-(3-hydroxy-4-methoxyphenyl)-2,7,7-trimethyl-5-oxo-1-phenyl-1,4,5,6,7,8-hexahydroquinoline-3-carboxylate (VIII)

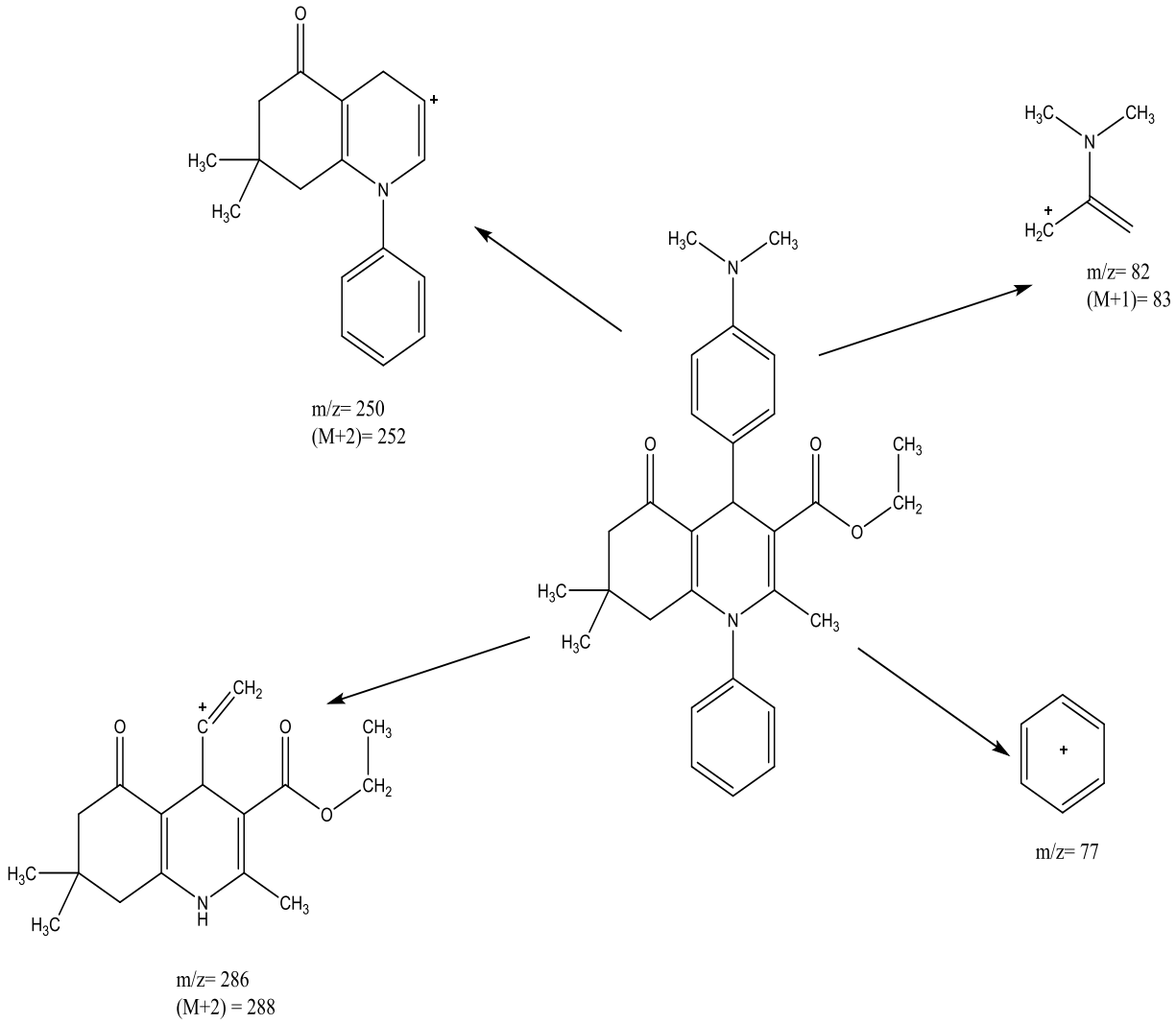

Scheme (3.9): Mass fragmentation of ethyl 4-(4-(dimethylamino) phenyl)-2, 7, 7-trimethyl-5-oxo-1-phenyl-1,4,5,6,7,8-hexahydroquinoline-3-carboxylate (IX)

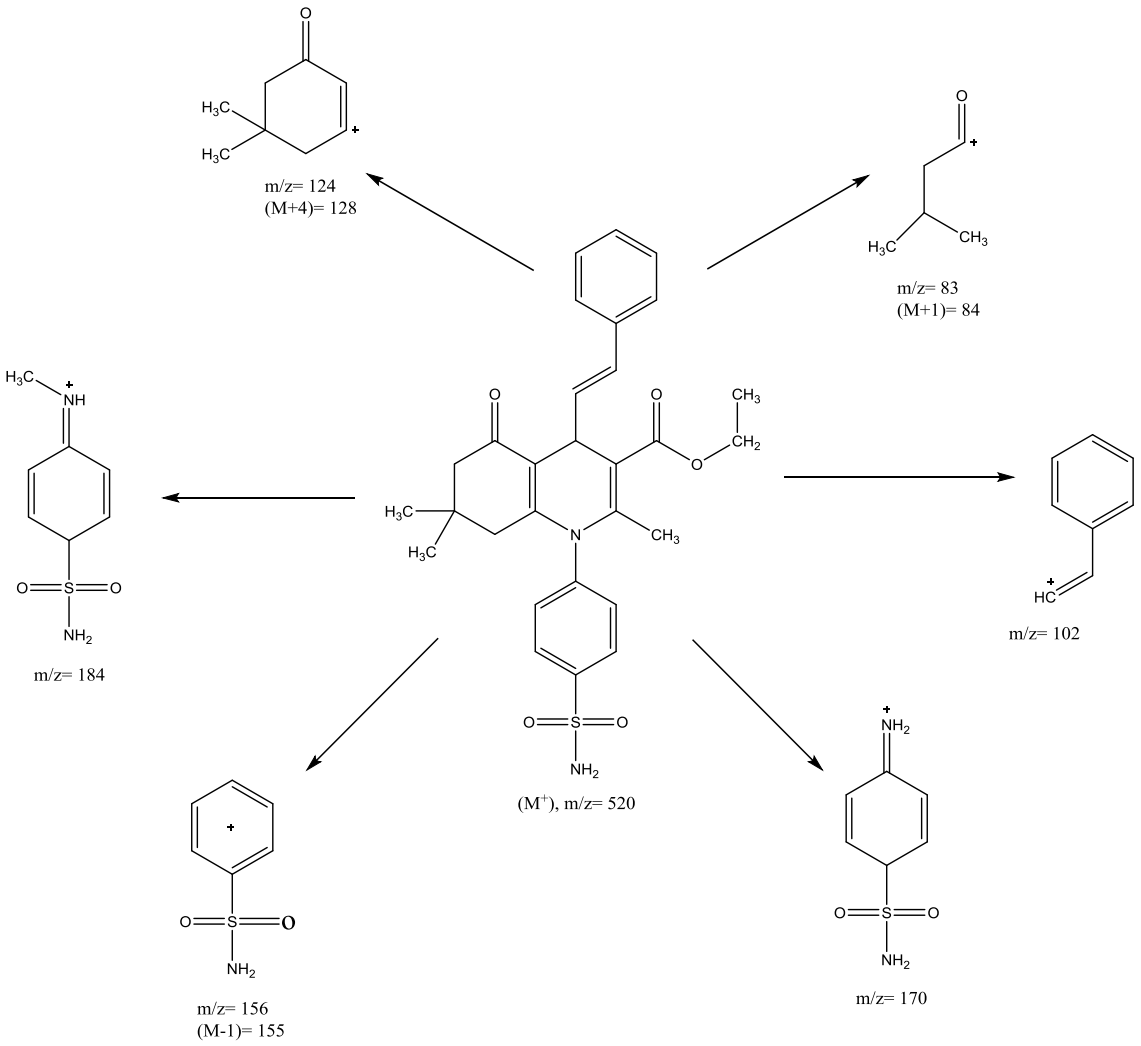

Scheme (3.10): Mass fragmentation of ethyl (E)-2,7,7-trimethyl-5-oxo-4-styryl-1-(4-sulfamoylphenyl)-1,4,5,6,7,8-hexahydroquinoline-3-carboxylate (X)

3.7. Docking study

Docking of molecules is not an easy task. The difficulties are mainly associated with the choice of the crystallographic structure of a target protein. Some molecules may have a specific mechanism of chemical behavior associated with their unique binding properties. For instance, some molecules may have multiple binding modes resulting in higher overall interaction energies in comparison with molecules with a single binding

mode. Such a molecule can be attractive as a potential drug.Alkylating agents have been found no doubt as potent anti-cancer agents (Gowramma *et al.*, 2009). Most of synthesized derivatives of N-substituted acridinedione and polyhydroquinoline were tabulated in table (2) and table (2.), revealed promising biological activity against human breast cancer MCF-7 cell lines. Thus, it was interesting to perform molecular docking to study the differences in docking patterns and amino acids interactions for the newly synthesized derivatives. The protein 5OM7 which was used to download the protein structure. All docking procedures were achieved by using MOE (Molecular operating environment) software, the docking protocol was verified by re-docking of the co-crystallized ligand (Doxorubicin) in the vicinity of the active site of the protein with energy score(s) = -35.4348kcal/mol, rmsd- refine = 1.5227.

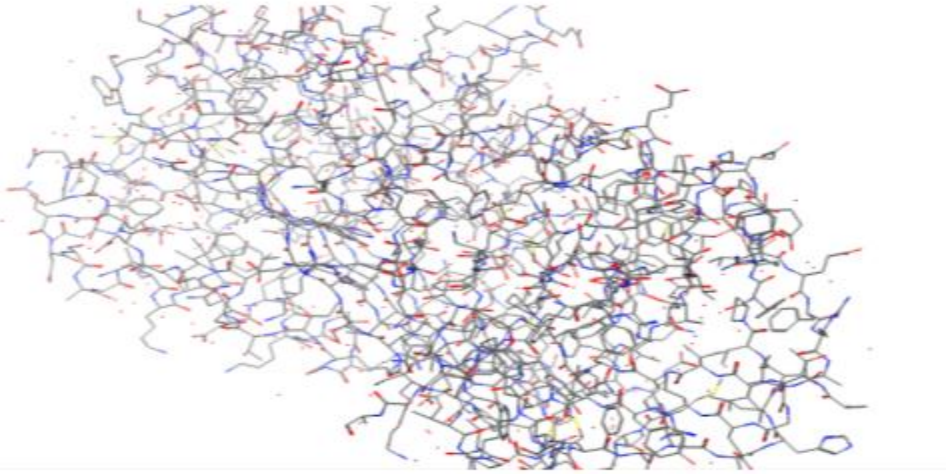

Figure (3.11): The 3D structure of 5OM7 that was imported from PDB.

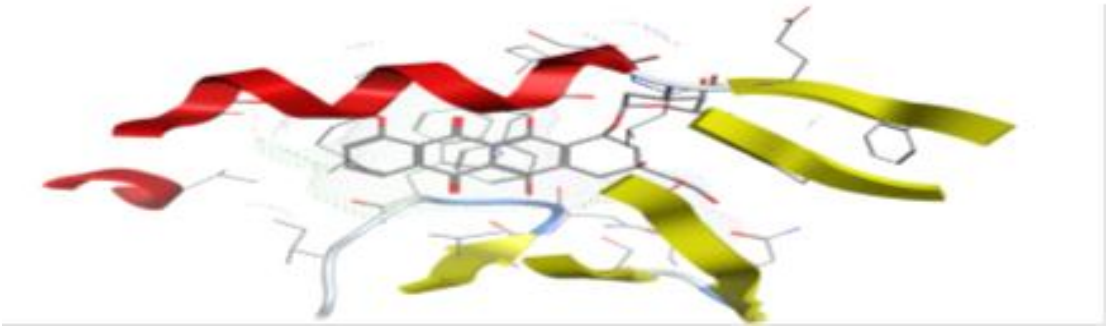

Figure (3.12): The structure of 5OM7 pocket after preparation and 2D and 3D, interaction of doxorubicin inside the active site of 5OM7 protein.

Figure (3.13): The structure of 5OM7 pocket and ligand after preparation and 2D and 3D, interaction of doxorubicin inside the active site of 5OM7 protein.

Docking on the active site of 5OM7 was performed for all synthesized derivatives of acridinedione and polyhydroquinoline; the results were tabulated in table (2.9) and table (2.10).

Compounds of Acridinediones showed low docking scores which ranging from -12.3358 to -13.0118 kcal/mol comparing with compounds that carrying sulfonanilamide moiety which showed proper fitting to the active site of 5OM7 with high energy scores ranging from -12.3358 to -13.0118 kcal/mol. The observation of these sulfonamides, the best docking score was assigned to compound no (X). (21) (58.415kcal/mol. Compound (IX) failed to show any interaction with the amino acid in the docking study.

In the further look to the docking results side by side to QSAR results when predicted the PIC_{50} for these synthesized derivatives, we can observed that the more active compound PIC_{50} = 4.67M respectively have shown good docking score -13.0118 Kcal/mol.

Also these derivatives were capable of forming a pi bond interactions with the amino acids such as pheA277.

Amino acid interactions of the active compounds are illustrated in figures (3.15 to 3.49)

These results merit further investigation of these compounds which carried sulfonamide moiety as potential anti-tumor agents.

Beside these interactions mentioned above, one π-cations interaction was revealed between Trp-residue with phenyl ring of sulfonamide moiety see figure (3.14).

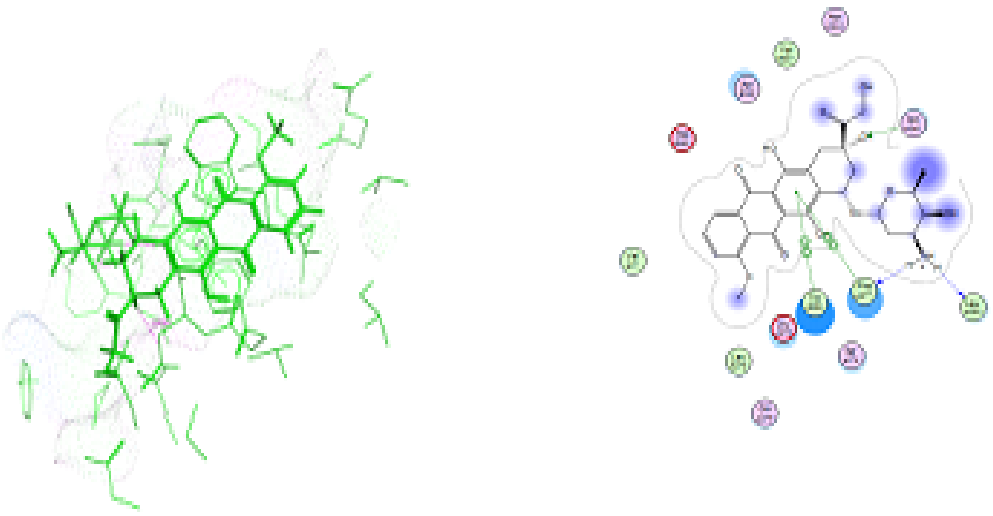

Figure: (3.14) 3D and 2D, interaction of doxorubicin inside the active site of 5OM7 protein.

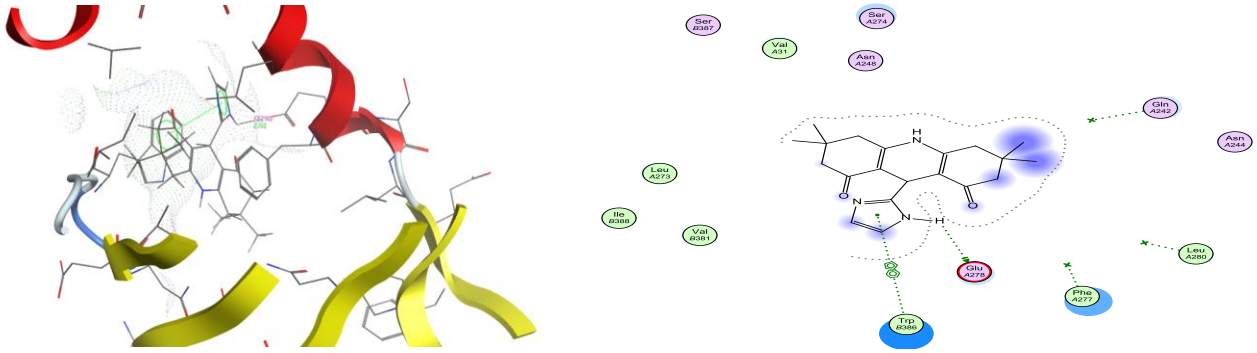

Figure: (3.15) 3D and 2D, interaction of 9-(1H-imidazol-2-yl)-3,3,6,6-tetramethyl-3,4,6,7,9,10-hexahydroacridine-1,8(2H,5H)-dione(1) inside the active site of 5OM7 protein.

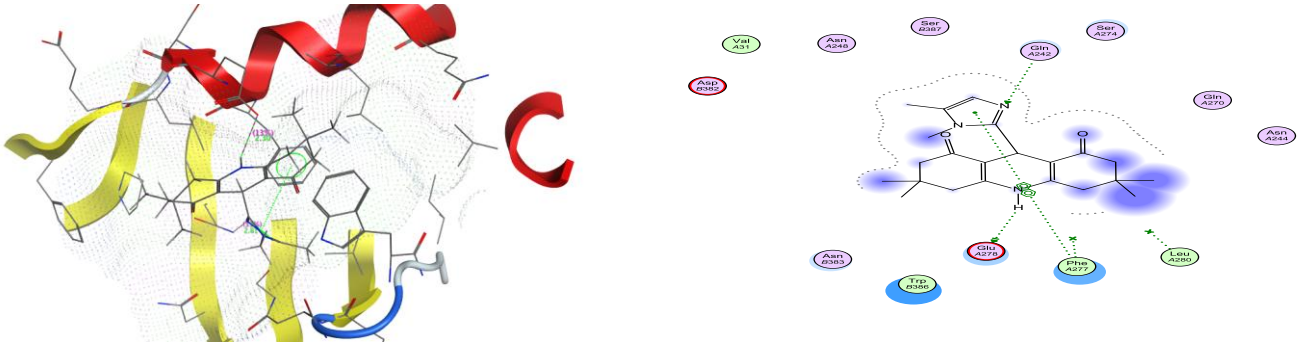

Figure: (3.16) 3D and 2D, interaction of 9-(1,5-dimethyl-1H-imidazol-2-yl)-3,3,6,6-tetramethyl-3,4,6,7,9,10-hexahydroacridine-1,8(2H,5H)-dione (2) inside the active site of 5OM7 protein**.**

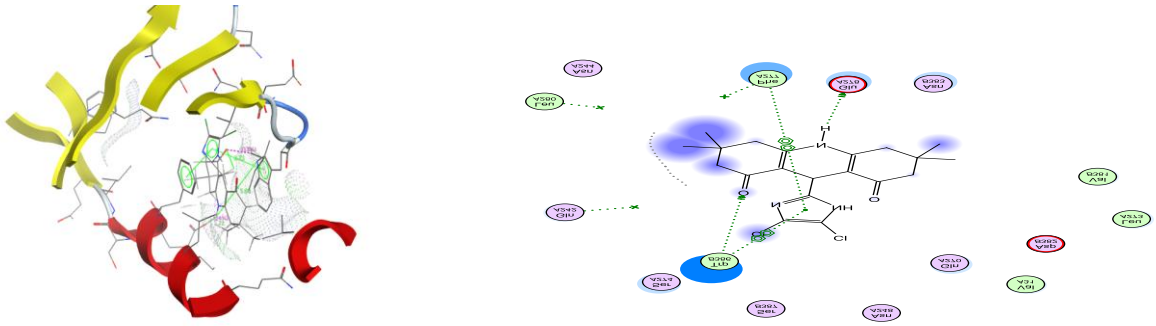

Figure: (3.17) 3D and 2D, interaction of 9-(4,5-dichloro-1H-imidazol-2-yl)-3,3,6,6-tetramethyl-3,4,6,7,9,10-hexahydroacridine-1,8(2H,5H)-dione(3) inside the active site of 5OM7 protein.

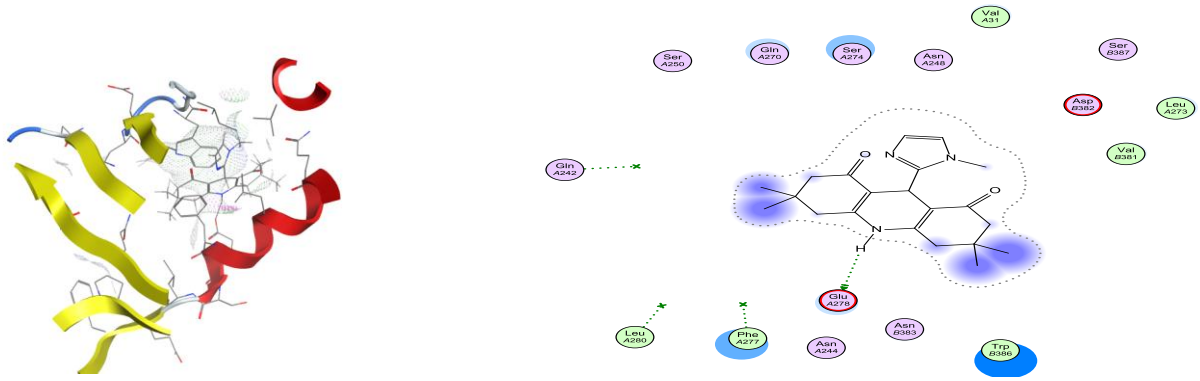

Figure: (3.18) 3D and 2D, interaction of 3,3,6,6-tetramethyl-9-(1-methyl-1H-imidazol-2-yl)-3,4,6,7,9,10-hexahydroacridine-1,8(2H,5H)-dione(4) inside the active site of 5OM7 protein.

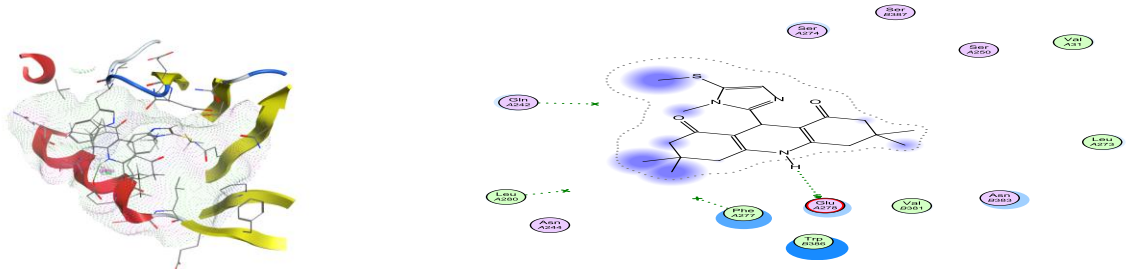

Figure: (3.19) 3D and 2D, interaction of 3,3,6,6-tetramethyl-9-(1-methyl-5-(methylthio)-1H-imidazol-2-yl)-3,4,6,7,9,10-hexahydroacridine-1,8(2H,5H)-dione(5) inside the active site of 5OM7 protein.

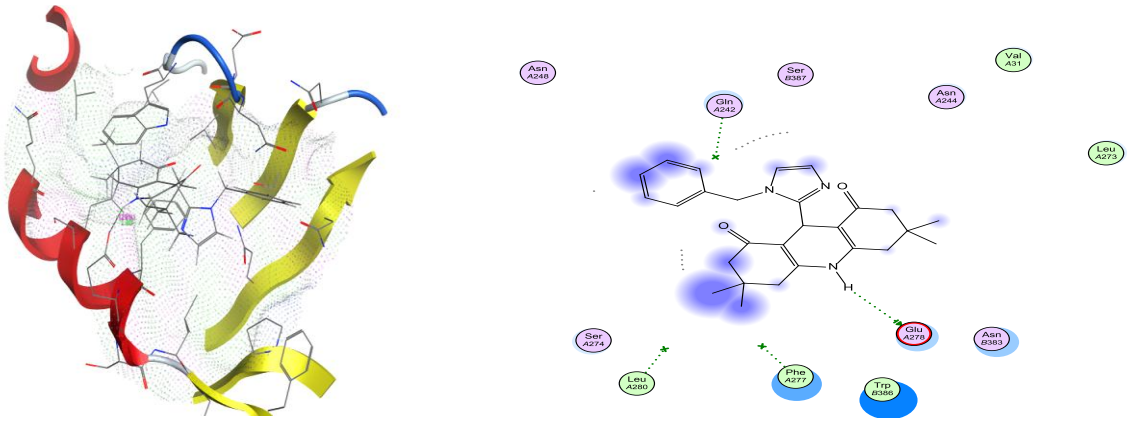

Figure: (3.20) 3D and 2D, interaction of 9-(5-benzyl-1H-imidazol-2-yl)-3,3,6,6-tetramethyl-3,4,6,7,9,10-hexahydroacridine-1,8(2H,5H)-dione(6) inside the active site of 5OM7 protein.

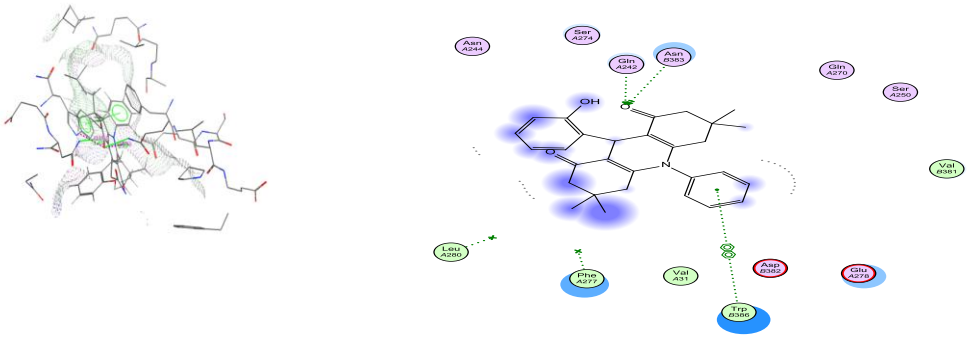

Figure: (3.21) 3D and 2D, interaction of 9-(2-hydroxyphenyl)-3,3,6,6-tetramethyl-10-phenyl-3,4,6,7,9,10-hexahydroacridine-1,8(2H,5H)-dione **C25/II** inside the active site of 5OM7 protein.

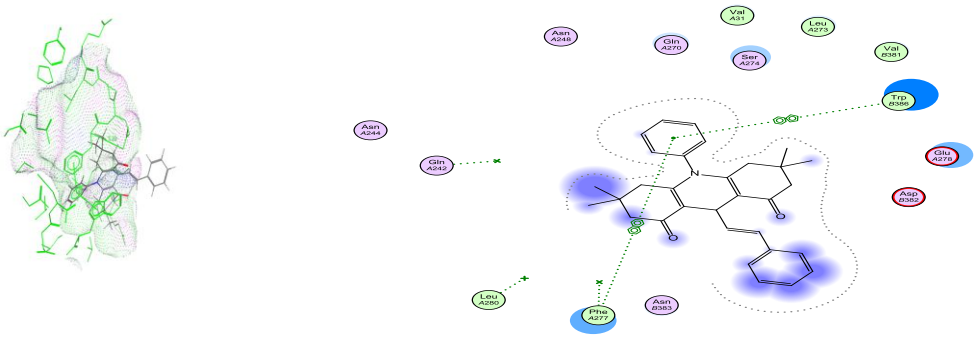

Figure: (3.22) 3D and 2D, interaction of (E)-3,3,6,6-tetramethyl-10-phenyl-9-styryl-3,4,6,7,9,10-hexahydroacridine-1,8(2H,5H)-dione **C26/V** inside the active site of 5OM7 protein.

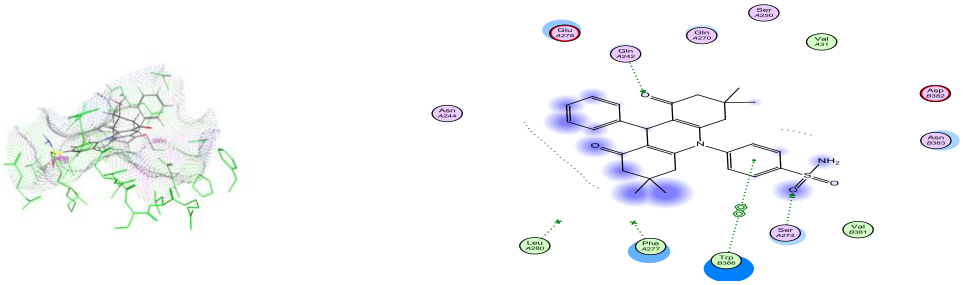

Figure: (3.23) 3D and 2D, interaction of 4-(3,3,6,6-tetramethyl-1,8-dioxo-9-phenyl-2,3,4,5,6,7,8,9-octahydroacridin-10(1H)-yl)benzenesulfonamide **C33** inside the active site of 5OM7 protein.

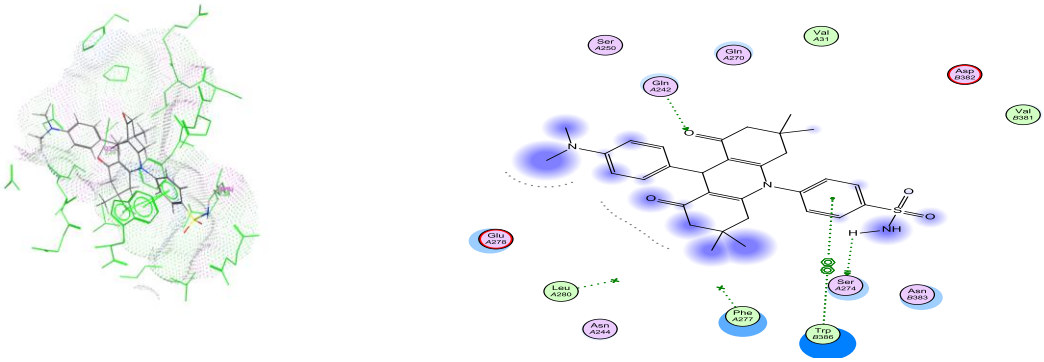

Figure: (3.24) 3D and 2D, interaction of 4-(9-(4-(dimethylamino)phenyl)-3,3,6,6-tetramethyl-1,8-dioxo-2,3,4,5,6,7,8,9-octahydroacridin-10(1H)-yl)benzenesulfonamide **C34/I** inside the active site of 5OM7 protein.

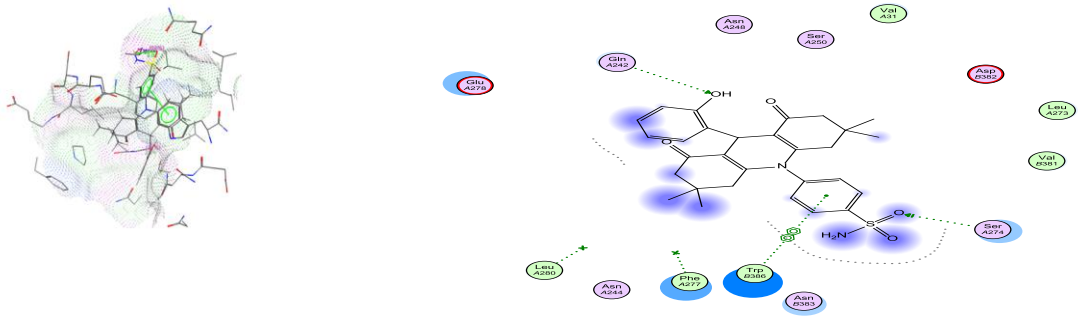

Figure: (3.25) 3D and 2D, interaction of 4-(9-(2-hydroxyphenyl)-3,3,6,6-tetramethyl-1,8-dioxo-2,3,4,5,6,7,8,9-octahydroacridin-10(1H)-yl)benzenesulfonamide **C35/ III** inside the active site of 5OM7 protein.

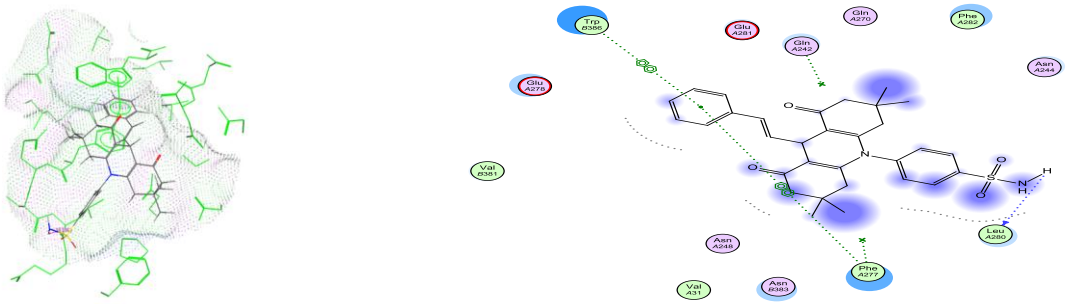

Figure: (3.26) 3D and 2D, interaction of (E)-4-(3,3,6,6-tetramethyl-1,8-dioxo-9-styryl-2,3,4,5,6,7,8,9-octahydroacridin-10(1H)-yl)benzenesulfonamide **C36/IV** inside the active site of 5OM7 protein.

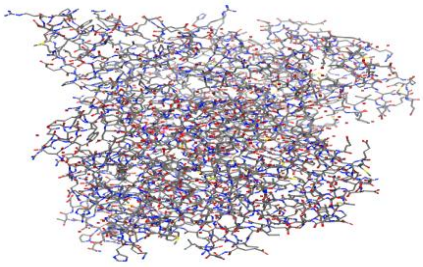

Figure (327): The 3D structure of 4gbd that was imported from PDB.

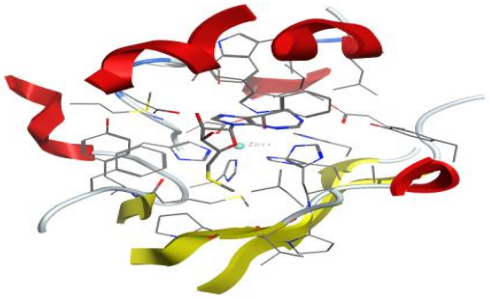

Figure (3.28): The structure of 4gbd pocket and ligand after preparation and 2D and 3D, interaction of doxorubicin inside the active site of 4gbd protein.

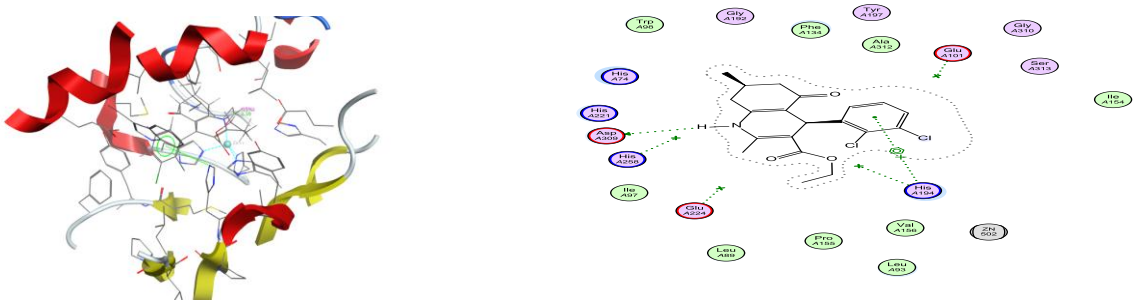

Figure (3.29) 3D and 2D, interaction of ethyl 4-(2, 3-dichlorophenyl)-2, 7-dimethyl-5-oxo-1, 4, 5, 6, 7, 8-hexahydroquinoline-3-carboxylate (1) inside the active site of 4gdb protein.

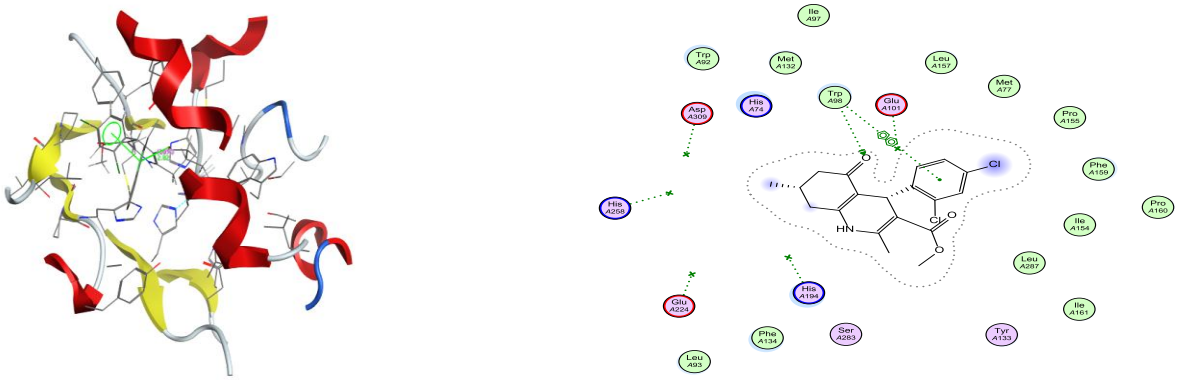

Figure (3.30) 3D and 2D, interaction of methyl 4-(2, 4-dichlorophenyl)-2,7-dimethyl-5-oxo-1,4,5,6,7,8-hexahydroquinoline-3-carboxylate(2) inside the active site of 4gdb protein.

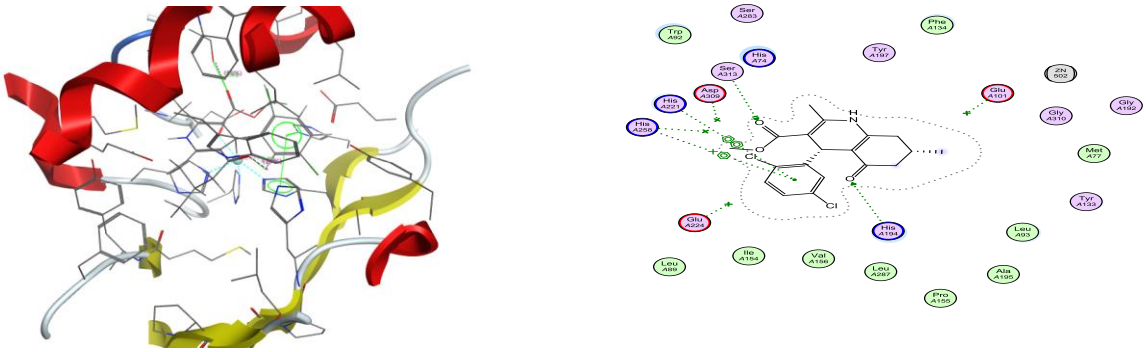

Figure (3.31) 3D and 2D, interaction of methyl 4-(2, 5-dichlorophenyl)-2, 7-dimethyl-5-oxo-1, 4, 5, 6, 7, 8-hexahydroquinoline-3-carboxylate (3) inside the active site of 4gdb protein.

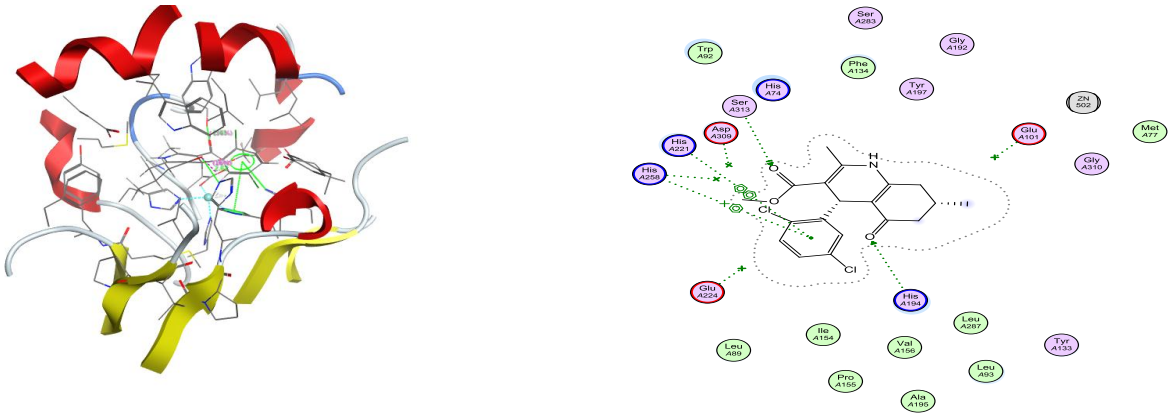

Figure (3.32) 3D and 2D, interaction of. ethyl 4-(2,5-dichlorophenyl)-2,7-dimethyl-5-oxo-1,4,5,6,7,8-hexahydroquinoline-3-carboxylate(4) inside the active site of 4gdb protein.

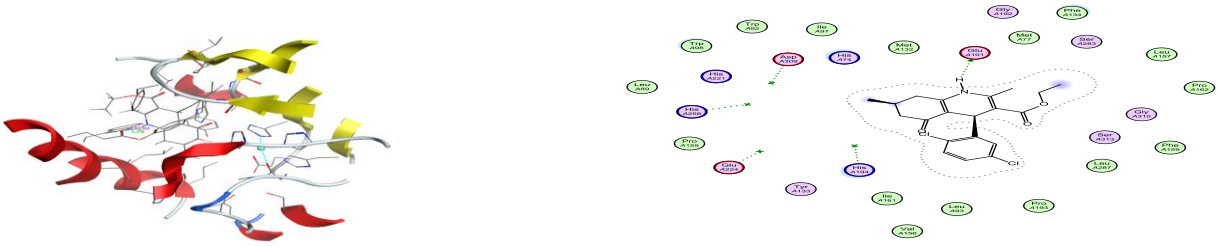

Figure (3.33) 3D and 2D, interaction of. methyl 4-(2,5-dichlorophenyl)-2,7-dimethyl-5-oxo-1,4,5,6,7,8-hexahydroquinoline-3-carboxylate(5) inside the active site of 4gdb protein.

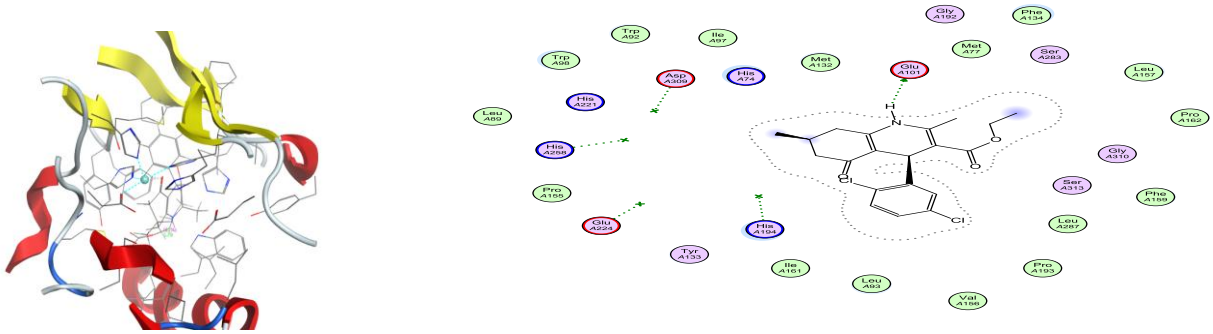

Figure (3.34) 3D and 2D, interaction of ethyl 4-(2, 5-dichlorophenyl)-2, 7-dimethyl-5-oxo-1, 4, 5, 6, 7, 8-hexahydroquinoline-3-carboxylate (6) inside the active site of 4gdb protein.

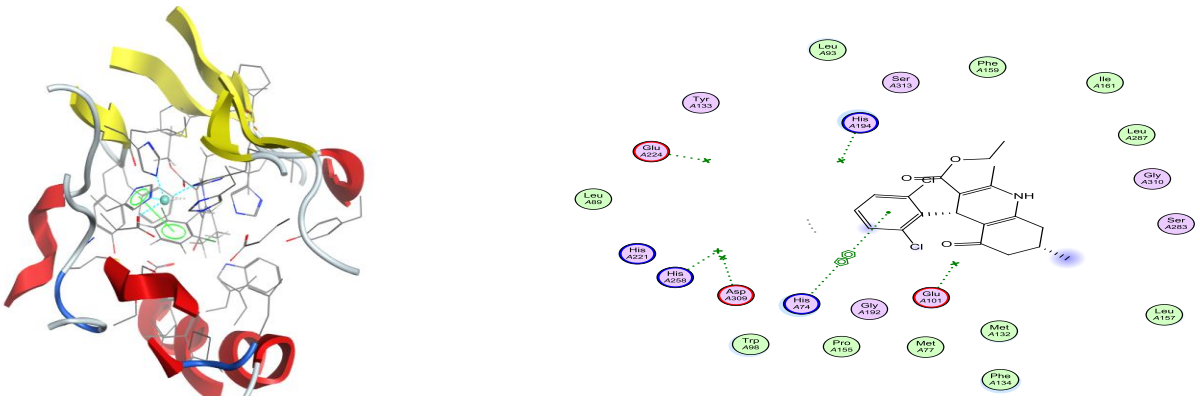

Figure (3.35) 3D and 2D, interaction of ethyl 4-(2-chloro-6-methylphenyl)-2, 7-dimethyl-5-oxo-1, 4, 5, 6, 7, 8-hexahydroquinoline-3-carboxylate (7) inside the active site of 4gdb protein.

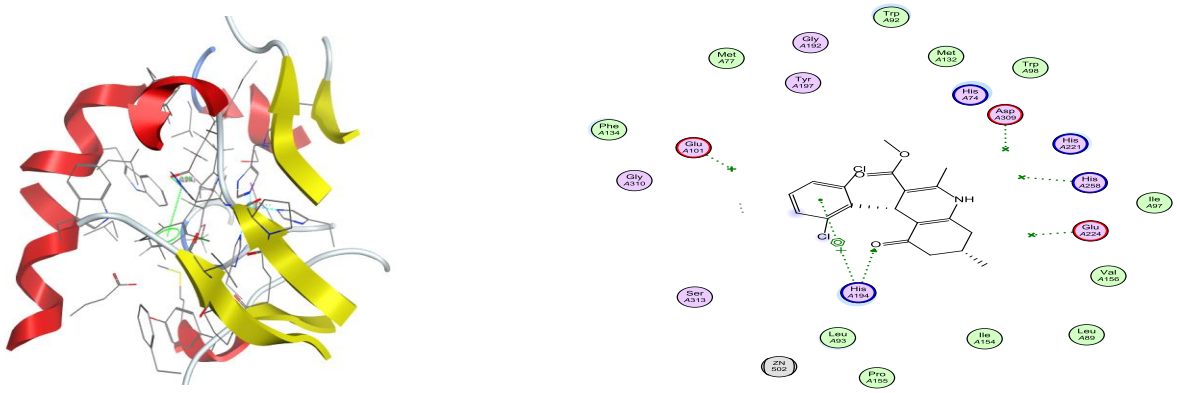

Figure (3.36) 3D and 2D, interaction of methyl 4-(2-chloro-6-methylphenyl)-2, 7-dimethyl-5-oxo-1, 4, 5, 6, 7, 8-hexahydroquinoline-3-carboxylate (8) inside the active site of 4gdb protein.

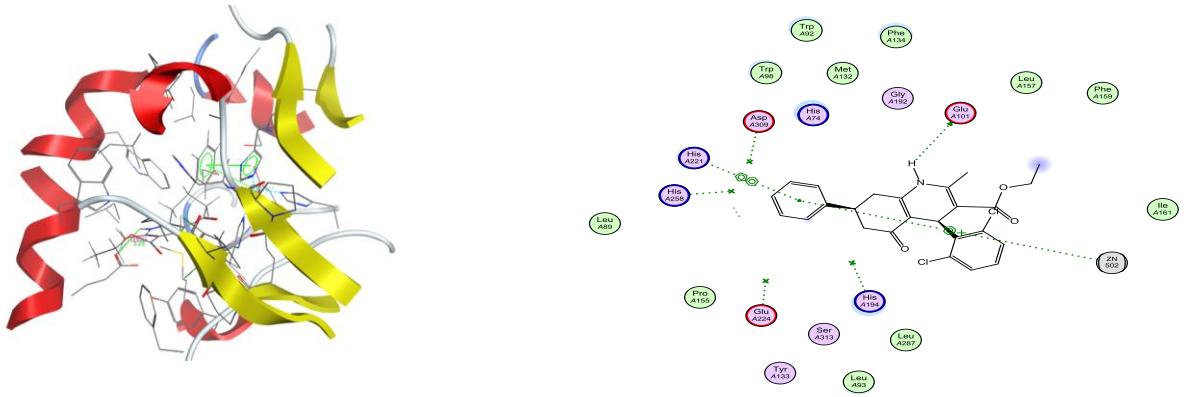

Figure (3.37) 3D and 2D, interaction of ethyl4-(2,6-dichlorophenyl)-2-methyl-5-oxo-7-phenyl-1,4,5,6,7,8-hexahydroquinoline-3-carboxylate(9) inside the active site of 4gdb protein.

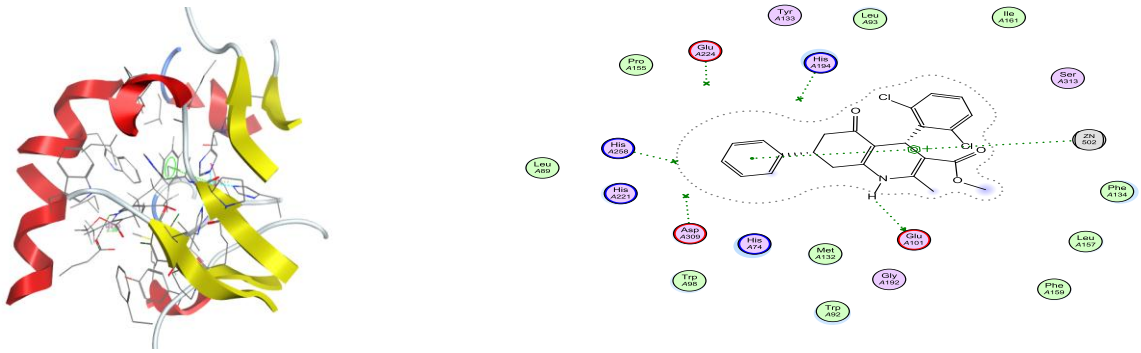

Figure (3.38) 3D and 2D, interaction of methyl 4-(2,6-dichlorophenyl)-2-methyl-5-oxo-7-phenyl-1,4,5,6,7,8-hexahydroquinoline-3-carboxylate(10) inside the active site of 4gdb protein.

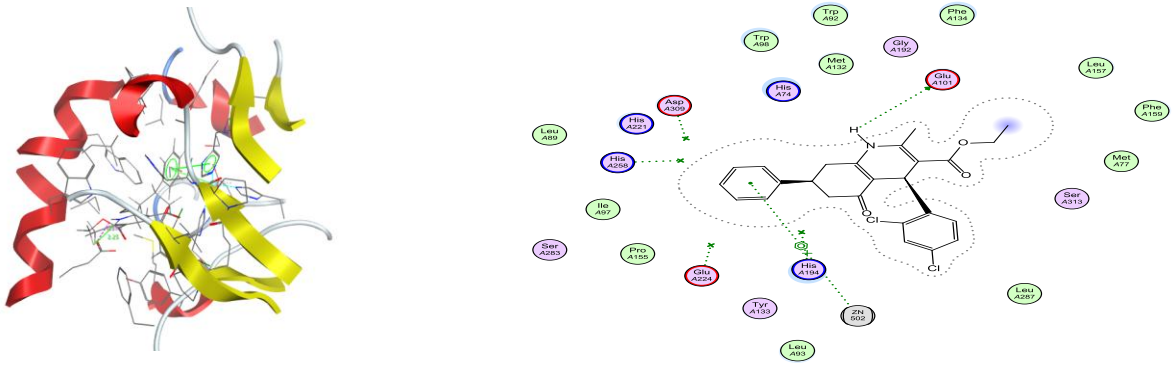

Figure (3.39) 3D and 2D, interaction of ethyl 4-(2, 4-dichlorophenyl)-2-methyl-5-oxo-7-phenyl-1,4,5,6,7,8-hexahydroquinoline-3-carboxylate(11) inside the active site of 4gdb protein.

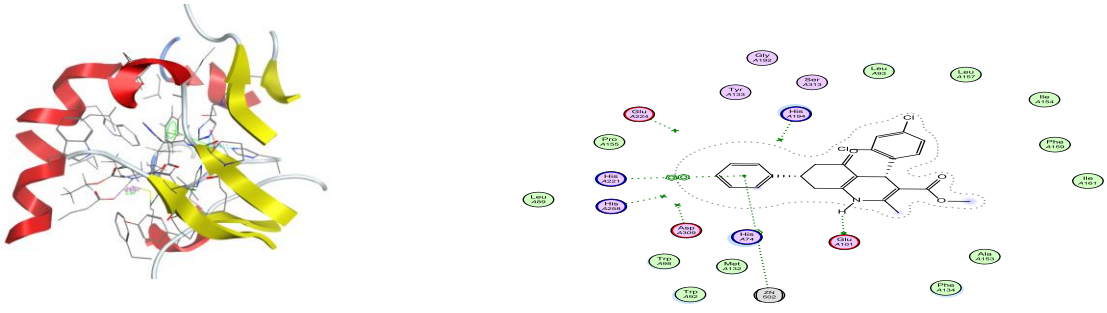

Figure (3.40) 3D and 2D, interaction of methyl 4-(2, 4-Dichlorophenyl)-2-methyl-5-oxo-7-phenyl-1, 4, 5, 6, 7, 8-hexahydroquinoline-3-carboxylate (12) inside the active site of 4gdb protein.

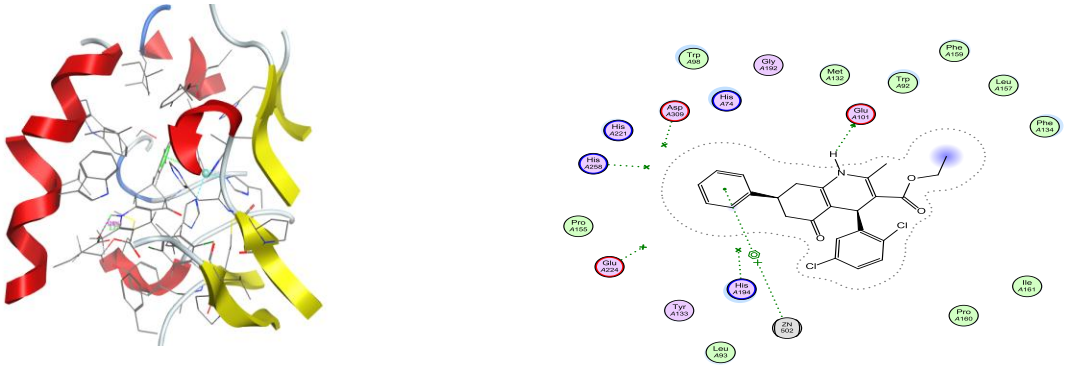

Figure (3.41) 3D and 2D, interaction of ethyl 4-(2, 5-dichlorophenyl)-2-methyl-5-oxo-7-phenyl-1, 4, 5, 6, 7, 8-hexahydroquinoline-3-carboxylate (13) inside the active site of 4gdb protein.

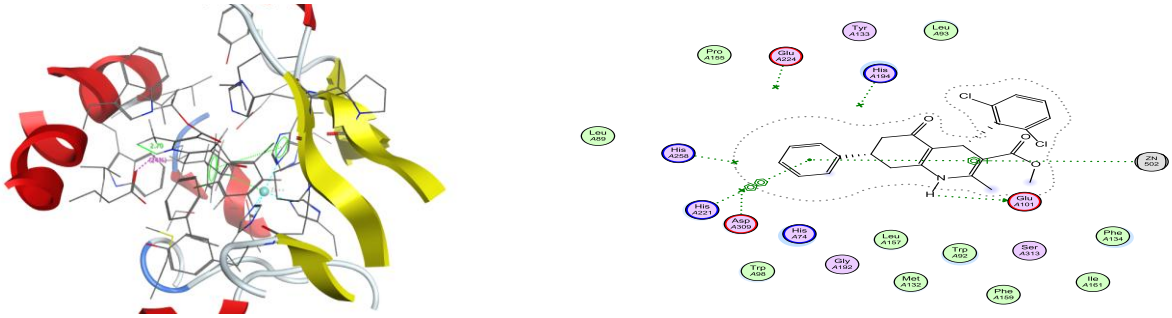

Figure (3.42) 3D and 2D, interaction of methyl 4-(2, 6-dichlorophenyl)-2-methyl-5-oxo-7-phenyl-1, 4, 5, 6, 7, 8-hexahydroquinoline-3-carboxylate (14) inside the active site of 4gdb protein.

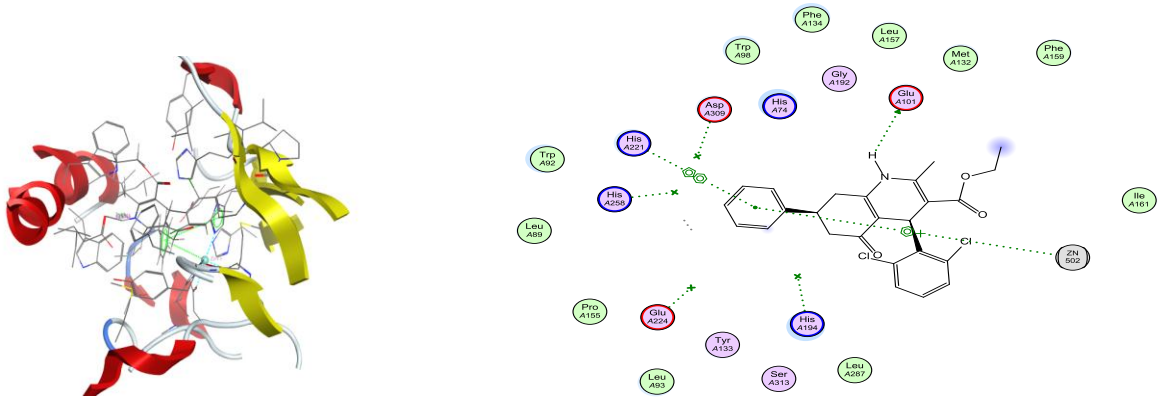

Figure (3.43) 3D and 2D, interaction of ethyl 4-(2, 6-dichlorophenyl)-2-methyl-5-oxo-7-phenyl-1, 4, 5, 6, 7, 8-hexahydroquinoline-3-carboxylate (15) inside the active site of 4gdb protein

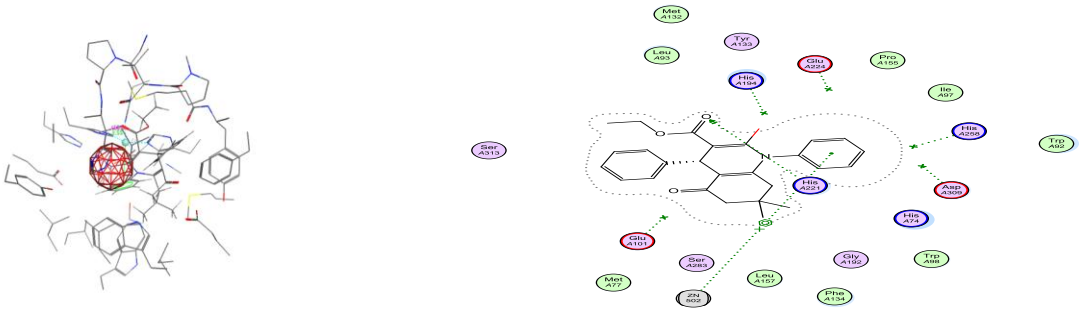

Figure (3.44) 3D and 2D, interaction of - Ethyl 2,7,7-trimethyl-5-oxo-1,4-diphenyl-1,4,5,6,7,8-hexahydroquinoline-3-carboxylate **Q23/VI** inside the active site of 4gdb protein.

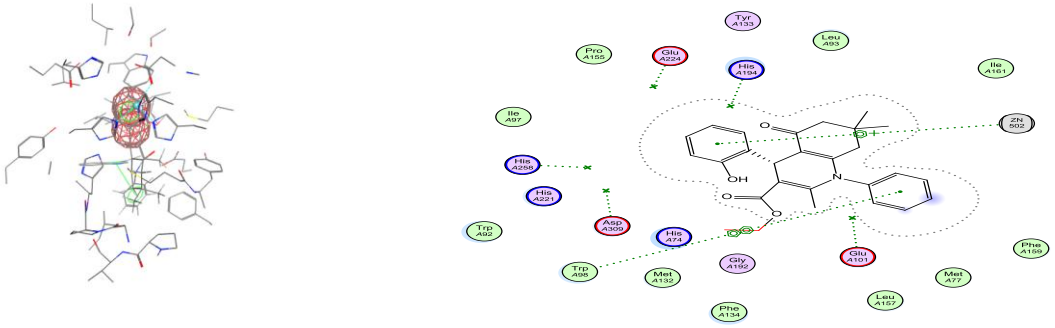

Figure (3.45) 3D and 2D, interaction of - Ethyl 4-(2-hydroxyphenyl)-2, 7, 7-trimethyl-5-oxo-1-phenyl-1, 4, 5, 6, 7, 8-hexahydroquinoline-3-carboxylate **Q25/VII** inside the active site of 4gdb protein.

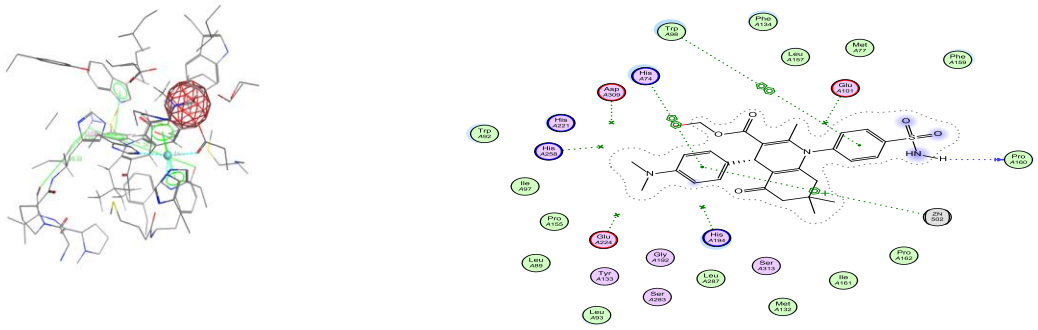

Figure (3.46) 3D and 2D, interaction of - Ethyl 4-(4-(dimethylamino)phenyl)-2,7,7-trimethyl-5-oxo-1-(4-sulfamoylphenyl)-1,4,5,6,7,8-hexahydroquinoline-3-carboxylate **Q34** inside the active site of 4gdb protein.

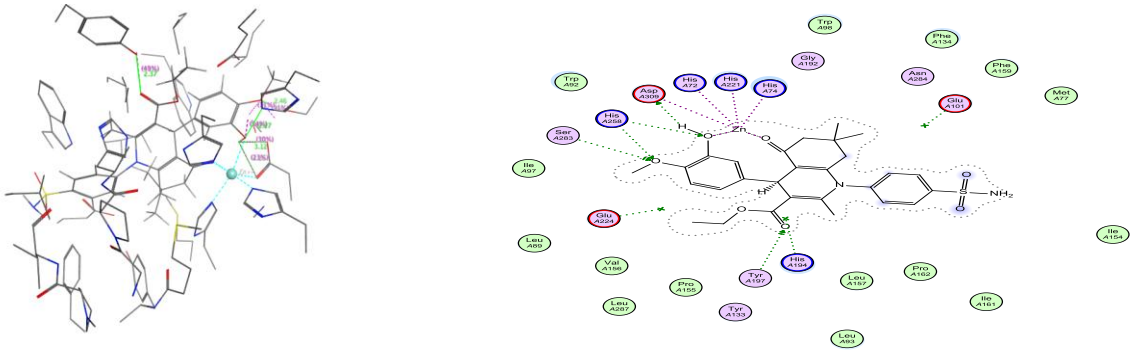

Figure (3.47) 3D and 2D, interaction of - Ethyl 4-(3-hydroxy-4-methoxyphenyl)-2, 7, 7-trimethyl-5-oxo-1-(4-sulfamoylphenyl)-1, 4, 5, 6, 7, 8-hexahydroquinoline-3-carboxylate **Q40/VIII** inside the active site of 4gdb protein.

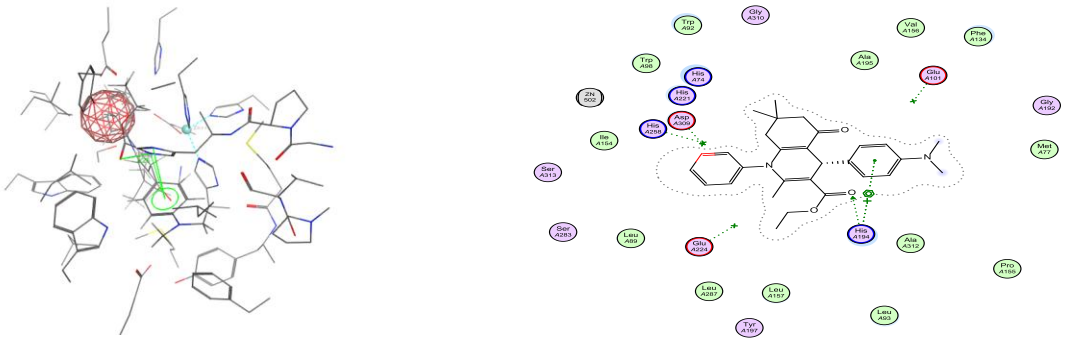

Figure (3.48) 3D and 2D, interaction of - Ethyl 4-(4-(dimethylamino) phenyl)-2, 7, 7-trimethyl-5-oxo-1-phenyl-1, 4, 5, 6, 7, 8-hexahydroquinoline-3-carboxylate **Q24/IX** inside the active site of 4gdb protein.

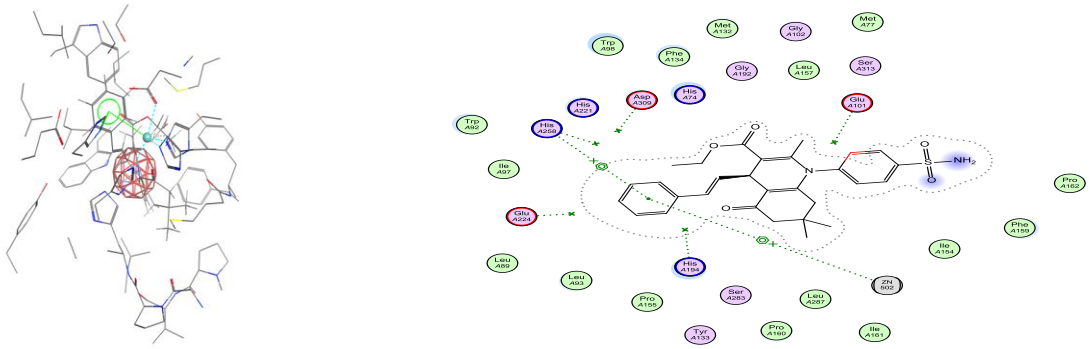

Figure (3.49) 3D and 2D, interaction of - Ethyl (E)-2,7,7-trimethyl-5-oxo-4-styryl-1-(4-sulfamoylphenyl)-1,4,5,6,7,8-hexahydroquinoline-3-carboxylate **Q36/X** inside the active site of 4gdb protein.

3.8. Conclusions and Recommendations

In summary, the following points can be concluded and/or recommended according to this study:

- ✓ At present work QSAR models can be obtained in order to predict the biological activity of the synthesized compounds.
- ✓ Two QSAR models were developed, and they were statistically significant and predictive, and could be used for the design and synthesis of new anti-cancer compounds against human breast cancer MCF-7 Cell lines.

- ✓ The first model showed that the anti-cancer activity model equation that the molecular descriptors, namely logP (o/w) partition coefficient and TPSA (topological polar surface area) are positively correlated with PIC_{50}. This model was used to predict the anti-cancer activity of designed 75 acridinedione derivatives.
- ✓ The second model showed that there is positive correlation between PIC_{50} with namely logP (o/w) partition coefficient and dipole moment. The developed model was used to predict the activity of designed 75 polyhydroquinoline derivatives as Calcium channel modulators.
- ✓ 5 out of 75 designed acridinedione derivatives and the same number of polyhydroquinoline derivatives were selected for synthesis based upon Lipiniski's rule of five or according to QSAR results, and docking study.
- ✓ The reactions of synthesized derivatives were followed by TLC, and their structures were characterized using spectroscopic analysis such as IR, UV, GC-MS and ^{1}HNMR.
- ✓ Molecular docking studies were carried out to investigate the interaction between the cancer proteins and synthesized acridinedione and polyhydroquinoline derivatives.
- ✓ There was good correlation between QSAR and docking results.
- ✓ ACD/lab in organic synthesis so as to design these compounds, because this programme provides vital informations which saves time and effort.
- ✓ This recommended that another programmes should be used with such these compounds to design new synthesized derivatives for both

acridinedione and polyhydroquinoline derivatives, such as modern Cambridge Chem draw.

- ✓ It is highly recommended that the anti-inflammatory action of some of these derivatives is to be tested in experimental animal models.
- ✓ Other spectroscopic techniques such as X-Ray crystallography for the compounds should as be reported.
- ✓ From the synthetic point of view the retro synthetic analysis adopted in this work proved to be correct and good in accordance with the proposed mechanisms.
- ✓ Further research can be carried out on synthesized derivatives of acridinedione (I, II, III, IV and V) to investigate them *in vitro* anti-cancer activity against breast cancer MCF-7 Cell lines.

3.9. References

Abdelhamid, A. A., S. Mohamed, S.K., Moharamov, A., Khalilov, A., and Allhaverdiev,M.,(2014). Facile and efficient synthesis of acridinediones from primary amino alcohols via three-component condensation reactions assisted by microwave irradiation. Journal of Saudi Chemical Society 18(5): 474-478.

Abdel-llah, L. Elma Veljovic, Leja Gurbeta, and Almir Badnjevic.(2017). Applications of QSAR Study in Drug Design. International Journal of Engineering Research and Technology. (6); 6, 582-587.

Acheson, A. (1956). Acridines, (148) Interscience Division,first edition. John Wiley and Sons, New York.

Alajarín, R., J. J. Vaquero, Navio.I.G. Builla, J.A, (1992). Synthesis of 1, 4-dihydropyridines under microwave irradiation.Thieme e. Journal. (4): 297-298.

Alvala, M., S. Bhatnagar, S., Ravi, A., jeankumar, Vu, Manjashetty, TH, Yogeswary, P., Sriramd, D., (2012). Novel acridinedione derivatives : design, synthesis, SIRT1 enzyme and tumor cell growth inhibition studies.Bioorg. Med. Chem Lett. 22(9): 3256-3260.

Ashraf, M. A., Z. Liu, (2020). New Copper Complex on Fe 3 O 4 Nanoparticles as a Highly Efficient Reusable Nanocatalyst for Synthesis of Polyhydroquinolines in Water.Springer 150(3): 683-701.

Baell, J., M. Congreve, Paul Leeson, Celerno Abad-Zapatero. (2013). Ask the experts: past, present and future of the rule of five. Future medicinal chemistry. 5(7): 745-752.

Bajot, F. (2010). The use of QSAR and computational methods in drug design. Recent advances in QSAR studies, Springer**:** 261-282.

Bano, S., M. S. Alam, M.S., Javed.; K.; Dudeja, M.; Das, A.K., and Dhulap, A., (2015). Synthesis, biological evaluation and molecular docking of some substituted pyrazolines and isoxazolines as potential antimicrobial agents." European journal of medicinal chemistry 95: 96-103.

Banothu, J., R. Bavantula,and PeterA.,(2013). Poly (4-vinylpyridinium) hydrogen sulfate catalyzed an efficient and ecofriendly protocol for the one-pot multicomponent synthesis of 1, 8-acridinediones in aqueous medium . Journal of Chemistry. Article. ID 850254. (6 Pages).

Bazargan, L., S. Fouladdel, L.S.; FFouladdel, Shafiee, A. Amini, M.; Ghaffari, S.M.; Azizi,F., (2008). Evaluation of anticancer effects of newly synthesized dihydropyridine derivatives in comparison to verapamil and doxorubicin on T47D parental and resistant cell lines in vitro. Cell Biology and Toxicology. 24(2): 165-174.

Beck, J. S., J. Vartuli, Mc Cullen S.B.; Higgins J., Schlenker J.L, (1992). "A new family of mesoporous molecular sieves prepared with liquid crystal templates. Journal of the American Chemical Society 114(27): 10834-10843.

Borhade, A. V., Uphade, B. K. Anil Gorakshnath.(2015. Efficient, solvent-free synthesis of acridinediones catalyzed by CdO nanoparticles. Research on Chemical Intermediates, 41(3): 1447-1458.

Boyd, D. B. (1990). Aspects of molecular modeling. Reviews in Computational Chemistry 1: 321-351.

Cameron, Adrian; Trivedi, and Provin K. (2005). Microeconometrics; methods and applications. Cambridge New York: Cambridge University press. ISBN 978052 1848053.

Chai, T. and R. R. Draxler (2014). Root mean square error (RMSE) or mean absolute error (MAE). Geoscientific Model Development Discussions. 7(1): 1525-1534.

Cronin, M. T. (2010). Quantitative structure–activity relationships (QSARs)–applications and methodology. Recent Advances in QSAR Studies ،Springer**:** 3-11.

Domoling. (2004). Multi-component Reactions. Organic Chemistry Highlights. Special Topics, 2004.

Domling, A., Wang، WComb, A.J, and Kan Wang. (2012). Chemistry and biology of multicomponent reactions. J. Chem. Rev.112(6): 3083-3135.

Ellis, G.P.(2009). The Chemistry of Heterocyclic Compounds, synthesis of fused heterocycles. Part: 2. Page (1284). John Wiley and sons.

Finar, I.L, (1967); Organic Chemistry, Pyrrole and its derivatives, (792-793).5th Edition, vol. (1). Longman House, BurntMill, Hallow, Essex, England.

Finar, I.L, (1975); Organic Chemistry, Stereochemistry and the Chemisrty of Natural Products Physical properties and Chemical constitution, UV-Spectroscopy, (16-19), 5th Edition, vol. (2). Longman House, BurntMill, Hallow, Essex, England.

Fujita, T., Iwasa J, andHansch, C,(1964). A new substituent constant, π, derived from partition coefficients. Journal of the American Chemical Society. 86(23): 5175-51.٨،

Gadaleta, D.,. Mangiatordi, G. F Catto,M., Caratti, A, and Nicolotti, O. (2016). "Applicability domain for QSAR models: where theory meets reality. International journal_of quantitative structure-property relationships (IJQSPR) 1(1): 45-63.

Giacomini, K. M., Huang, S.-M.;Tweedie D.J.; Benet,, L.Z.; Brouwer, K.L.; Chu,; X.; Dahalin, A.; Evers, R.; Fischer, V.; Hillgreen, K.M.; Hillgreen,V. Hoffimaster, K.M.; Ishikawa, K.A.; Keppler T.; Kim, D.; Lee.; R.B.; Niemi, C.A.; Polli, M.; Sugiyama, J.W.; Swaan, Y.; Wane, P.W.; Wrhigt, J.A.; Yee, S.H.; Zamek, S.W.; Glisazanynki, Zhang, M.J.L. (2010). Membrane transporters in drug development. Nature reviews Drug discovery. 9(3): 215.

Gibbons, J. D. and J. W. Pratt (1975). P-values: interpretation and methodology. The American Statistician. 29(1): 20-25.

Gowramma, B., S. Jubie, S.; Kalirajan, R.; Gomathy, S, and Elango, K.(2009). "Synthesis, anticancer activity of some 1-(Bis N, N-(Chloroethyl)-amino acetyl)-3, 5-disubstituted 1, 2-pyrazolines. Int J Pharm Tech Res. 1(2): 347-352.

Greenland, S. (1989). Modeling and variable selection in epidemiologic analysis. American journal of public health. 79(3): 340-349.

Gröger, H. J. C. r. (2003). Catalytic enantioselective Strecker reactions and analogous syntheses. ACS Publications. 103(8): 2795-28.٢٨.

Guan-wu Wang, Chun-Bao Miao, (2006); Synthesis of Acridinedione derivatives in solvent-free and aqueous conditions. Green Chemistry, (12). 8.1080-1085.

Gündüz, M. G., Celebi, Dogan A.E., Simsek R., Erol K. and Safak C.(2009). 7-Substituted hexahydroquinoline derivatives and their calcium channel modulator effects. Lat. Am. J. Pharm 28(6): 922-926.

Guven, M., Yasar, K. O.B Karaca, A.A.,Hayalo. (2005). The effect of inulin as a fat replacer on the quality of set-type low-fat yogurt manufacture." International Journal of Dairy Technology 58(3): 180-184.

Hansch, C. (1979). QSAR in cancer chemotherapy. Il Farmaco; edizione scientifica. 34(1): 89-104.

Hansch, C., E. Lien, Steward, A.R., Anderson, S.M. and Bentley, D.L., (1968). Structure-activity correlations in the metabolism of drugs. Archives of biochemistry and biophysics 128(2): 319-330.

Hantzsch, A. (1881). Condensationsprodukte aus Aldehydammoniak und ketonartigen Verbindungen. Journal of Europian Society. 14(2): 1637-1638.

Hardman, R. J. E. h. p. (2006). A toxicologic review of quantum dots: toxicity depends on physicochemical and environmental factors.Journal Environ Health Perespect. 114(2): 165-172.

Heravi, M. M., M. Hosseini, Hossien, A., Oskooie, Bita Bagharnejad, and Farzaneh, F. (2010). Efficient synthesis of polyhydroquinolines via the hantzsch reaction using iron loaded mesoporous materials. Chinese Journal of Chemistry. 28(10): 2045-2048.

Hornback, J.M. (2005) Organic Chemistry, second edition, chapter 23, the synthesis of organic compounds, Cengage learning, 1024.

Ishikawa, T., Hirano, H., Saito, H., Sano, K., Ikegami, Y., Yamaotsu, N. and Hirono, S., 2012. Quantitative structure-activity relationship (QSAR) analysis to predict drug-drug interactions of ABC transporter ABCG2. *Mini reviews in medicinal chemistry*, *12*(6), pp.505-514.

Jacek, K., H. Popielarska, Anna Myka, Beata Drabinka, Marek K. Bernard,(2012). The log P Parameter as a Molecular Descriptor in the Computeraided Drug Design–an Overview. Computational_Methods in Science and Technology.18 (2): 81-88.

Jadhvar, S., C. Kasraliker, H.M.; Goswami, S.V.; Chakrawar, A.V.; Bhuare, S.R.(2017). One-pot synthesis and evaluation of anticancer activity of polyhydroquinoline derivatives catalyzed by [Msim] Cl. Research on Chemical Intermediates. 43(12): 7211-7221.

Jalali-Heravi, M., M. Asadollahi-Baboli, et al. (2008). QSAR study of heparanase inhibitors activity using artificial neural networks and Levenberg–Marquardt algorithm. European journal of medicinal chemistry. 43(3): 548-556.

Jamalian, A.,Miri, R.; Firuzi, O.; Amini, M.; Moosavi-Movahedi, A.A.; and Shafiee, A. (2011). Synthesis, cytotoxicity and calcium antagonist activity of novel imidazolyl derivatives of 1, 8-acridinediones. Journal of the Iranian Chemical Society. 8(4): 983-991.

Joseph rajan, Ramakrishnan,T.,V.,Kathiravan. G, and Muthumary.J. (2005). Synthesis and antimicrobial studies of some acridinediones and their thiourea derivatives. Arkovic. 11: 124-136.

Joule, J.A., and Mills, K. (2013). Heterocyclic Chemistry, unsymmetrical 1,4- dihydropyridines, page (159). 5th Edition. John Wiley and sons.

Julien, C., D. Florence. (2005). Synthesis and antileishmanial activities of 4, 5-di-substituted acridines as compared to their 4-mono-substituted homologues.Bioorganic and Medicinal Chemistry. 13(19): 5560-5568.

Karade, N. N., V. H. Budhewar, Vshnu H; Shinde, Sandeep V; Jadhav, Wamanyaon.(2007). L-proline as an efficient organo-catalyst for the synthesis of polyhydroquinoline via multicomponent Hantzsch reaction. Letters in Organic Chemistry. 4(1): 16-19.

Kaur, B. and Kumar, C. S.(2013). Methyltrioctylammonium chloride catalysed sonochemical synthesis of acridine diones. 125(5): 989-992.

Khabazzadeh, H., E. T. Kermani, Daryush Af Zadi, Ashgar Amiri, Arman Jalaladini.(2012). Efficient one-pot synthesis of polyhydroquinoline derivatives using Cs2. 5H0. 5PW12O40 as a heterogeneous and reusable catalyst in molten salt media.Arabian Journal of Chemistry. 5(2): 167-172.

Khan, A. U. (2016). Descriptors and their selection methods in QSAR analysis: paradigm for drug design. Drug discovery today 21(8): 1291-1302.

Kolossov, E. and R. Stanforth (2007). The quality of QSAR models: problems and solutions. SAR and QSAR in Environmental Research. 18(1-2): 89-100.

Kruithof, A., E. Ruijter, R.VA. Orru. (2011). Microwave-assisted multicomponent synthesis of heterocycles.Journal of Current Organic Chemistry. 15(2): 204-236.

Kumar, A. and R. A. J. S. Maurya (2008). Efficient synthesis of Hantzsch esters and polyhydroquinoline derivatives in aqueous micelles.Synlett. 2008(06): 883-885.

Kumar, N., S. Verma, and Suman L. (2012). Combined Thiourea Dioxide–Water: An Effective Reusable Catalyst for the Synthesis of Polyhydroquinolines via Hantzsch Multicomponent Coupling.The Chemical Society of Japan Chemistry Letters. 41(9): 920-922.

Kumar, P. S. V., L. Suresh, L., Bhargavi, G, Srinivas Basvoju, and Chandraomoudi, G.V.P.,(2015). Ionic liquid-promoted green protocol for the synthesis of novel naphthalimide-based acridine-1, 8-dione derivatives via a multicomponent approach. Acs Sustainable Chem. Eng. American Chemical Society. 3(1.٢٩٥٠-٢٩٤٤ :(١

Kursanov, D., M. Gonikberg.B.M. Dubnin, M.I. Kabachinik, E.D. , N.D. Sokolov, R.Kh. Freidina, and E.N. Prilezhaeva. (1952). The present state of the chemical structural theory. ACS. Publications. 29(1): 2.

Lambat, T., S. Deo, and Tomblesh Kumar., Deshmukh.(2014). Sulphamic acid assisted synthesis of polyhydroquinolines via Hantzsch multicomponent reaction: a green approach. Journal of Chemical and Pharmaceutical Research. 6(4): 888-892.

Leach, A. R. and V. J. Gillet (2007). Molecular descriptors. An introduction to chemoinformatics: 53-74.

Leov, N. M. J. J. o. t. A. U. L. and L. Association (1965). Jacques le fataliste, poème parabolique.Jacques le Fataliste et Son maitre-Wikipedea. 2.٤٨-٢٤ :(١)٣.

Mahama, O.,. Aboudramane, K, Kone Soleymane, and Collet Sylvain. (2020). Anticancer Activities and QSAR Study of Novel Agents with a Chemical Profile of Benzimidazolyl-Retrochalcone. Open Journal of Medicinal Chemistry. 10(03): 113.

McMurray, J. (2000); Organic Chemistry, Mass Spectrometry and Infra-red Spectroscopy, (440-474), 5th Edition, by Brooks/cole.

Mekheimer, R. A., Hameed, A. A. Afaf Abdel Hameed, and Kamal Usef Sadek.(2008). Solar thermochemical reactions: four-component synthesis of polyhydroquinoline derivatives induced by solar thermal energy.Green Chemistry. 10(5): 592-593.

Mohammmedi, Z. G., A. R. Badiei,. Ali Reza; Khaniania, Yeganeh, Haddadpour, Mahbobeh.(2010). One pot synthesis of polyhydroquinolines catalyzed by sulfonic acid functionalized SBA-15 as a new nanoporous acid catalyst under solvent free conditions. Iran Journal of Chemistry. Chem. Eng. 29. (2).

Mukesh, B. and K. Rakesh. (2011). Molecular docking: a review. Int J Res Ayurveda Pharm. 2(6): 1746-1751.

N'guessan, K. N., M. G.-R. Koné., M.G.; Bamba, K.; Patrice, O.W. and Ziao, N. (٢٠١٧) Quantitative structure anti-cancer activity relationship (QSAR) of a series of ruthenium complex azopyridine by the density functional theory (DFT) method. Computational Molecular Bioscience. **7**(2): 19-31.

Nadenla, R. (2002). Role of Antioxidant in Human Diseases-An Overview. The Times Of India. 34.

Nantasenamat, C., C. Isarankura-Na-Ayudhya, C.I.; Naenna, T. and Prachayasittikal, V.(2009). A practical overview of quantitative structure-activity relationship; Excli Journal, 8, 74-88.

Nikpassand, M., M. Mamaghani, M., and Tabataba, K.,(2009). An efficient one-pot three-component synthesis of fused 1, 4-dihydropyridines using HY-zeolit.Molecules. 14(4): 1468-1474.

Nirmal, J. P., P. V. Dadhaniya, Manish P. Patel, and Ranjan G. Patel, (2010). A facile four component one-pot synthesis of polyhydroquinoline derivatives catalyzed by ionic liquid via modified Hantzsch reaction. Indian Journal of Chemistry 49B: 587- 592.

Nishiya, Y., N. Kosaka, et al. (2002). A potent 1, 4-dihydropyridine L-type calcium channel blocker, benidipine, promotes osteoblast differentiation. National Library of Medicine. National Center for Biotechnology Information. 70(1): 30-39.

Panda, S.S.; Khanna, L.(2012). Bigineli Reaction. A green prespect. Current Organic Chemistry. 16. (4): 507-520.

Patel, H. M., M. N. Noolvi, M.N.; Sharma, P.; Jaiswal, V.; Bansal, S.; Lohan, S.; Kumar, S.S.; Abbot, P.; Dhiman, S. and Bhardwaj, V.(2014). Quantitative structure–activity relationship (QSAR) studies as strategic approach in drug discovery. Medicinal chemistry research. 23(12): 4991-5007.

Patny, A., P.. Desai, V., Akashy. (2006). Homology modeling of G-protein-coupled receptors and implications in drug design. Current medicinal chemistry. 13(14): 1667-1691.

Pavia, D.L.; Lambman, G.M.; Kriz, G.S, and Vyvyan J.R. (2002); Introduction to Spectroscopy, 4th edition, CENGAGE Learning. USA.

Perkins, R., H. Fang, Tong, W., Welsh W.(2003) (Quantitative structure-activity relationship methods: Perspectives on drug discovery and toxicology. Environmental Toxicology and Chemistry: An International Journal. 22(8): 1666-1679.

Purandhar, K., V. Jyothi, P., Prakap Reddy M. Adharvana Chari, and K. Mukkanti.(2012). Aluminum phosphate [AlPO4 (H)]: A mild and efficient recyclable catalyst for one-pot synthesis of polyhydroquinoline via the Hantzsch reaction under solvent-free conditions. Journal of Heterocyclic Chemistry. 49(1): 232-236.

Puri, S., B. Kaur, Anupama Parmar, and Harish Kumar.(2011). Copper perchlorate hexahydrate: an efficient catalyst for the green synthesis of polyhydroquinolines under ultrasonication. Organic Chemistry, Article ID948685, 4 pages. (2011).

Puzyn, T., J .Leszczynski, Jerzy, Cronin,and Mark T. (2010). Recent advances in QSAR studies: methods and applications. Springer. 978-1-4020-9783-6.

Raether, W., B. Enders, B., Hofmam J., Schwannecke U., Sedenath H., Hanel H. and Uphoff M., (1989). Antimalarial activity of new floxacrine-related acridinedione derivatives: studies on blood schizontocidal action of potential candidates against P. berghei in mice and P. falciparum in vivo and in vitro. National Library of Medicine. National Center for Biotechnology Information. 75(8): 619-626.

Roy, K., S. Kar, S. and Das, R.N.(2015). Statistical methods in QSAR/QSPR. A primer on QSAR/QSPR modeling, Springer**:** 37-59.

Safari, J ،.S. H. Banitaba, S.H, and Khalili, S.D.(2011). Cellulose sulfuric acid catalyzed multicomponent reaction for efficient synthesis of 1, 4-dihydropyridines via unsymmetrical Hantzsch reaction in aqueous media. J.Mol. Catal. A. Chem., 335(1-2): 46-50.

Sapkal, S. B., K. F. Shelke, Bapuaro B. Schingate, Murlidhr S. Shingare. (2009). Nickel nanoparticle-catalyzed facile and efficient one-pot synthesis of polyhydroquinoline derivatives via Hantzsch condensation under solvent-free conditions. Tetrahedron Letters. 50(15): 1754-1756.

Selassie, C. and R. P. Verma (2003). History of quantitative structure–activity relationships. Burger's medicinal chemistry and drug discovery: 1-96.

Sharma, V. K. and S. K. J. R. a. Singh (2017). Synthesis, utility and medicinal importance of 1, 2-& 1, 4-dihydropyridines. Royal Society of Chemistry. **7**(5): 2682-2732.

Singh, S. K. and K. N. J. J. o. H. C. Singh (2011). Eco-friendly and facile one-pot multicomponent synthesis of acridinediones in water under microwave. Journal of Heterocyclic Chemistry. 48(1): 69-73.

Sirisha, K., Achaiah, G. Vanga Malla Reddy.(2010). Facile Synthesis and Antibacterial, Antitubercular, and Anticancer Activities of Novel 1, 4-Dihydropyridines. Archiv der Pharmazie. 343(6): 342-352.

Srividya, N., P. Ramamurthy, (1996). Synthesis, characterization, and electrochemistry of some acridine-1, 8-dione dyes.Organic Chemistry. 61(15): 5083-5089.

Sudha, S., and Pasha, M.A.,(2013); Synthesis of an assembly of structurally important N-H and N-substituted acridine-1,8-diones by CAN (Ceric Ammonium Nitrate) Catalyzed one-pot four component reaction. The scientific world Journal, 10, 787-930.

Sullivan, J.J., Jones, A.D. and Tanji, K.K., (2000); QSAR treatment of electronic substituent effects using frontier orbital theory and topological parameters. Journal of Chemical information and computer Sciences. 40 (5), 1113-1127.

Torres, P. H., Sodero, A. C. Paula Jofily, and Floriano P. (2019). Key topics in molecular docking for drug design. International journal of molecular sciences. 20(18): 4574.

Tropsha, A. (2010). Best practices for QSAR model development, validation, and exploitation. Molecular informatics. 29(6-7): 476-488.

Tropsha, A., P. Gramatica, P., and Gombar, V.K., (2003). The importance of being earnest: validation is the absolute essential for successful application and interpretation of QSPR models. QSAR & Combinatorial Science. 22(1): 69-77.

Ugi, I., S. Heck, J. C. C. (2001). The multicomponent reactions and their libraries for natural and preparative chemistry. National Library of Medicine. National Center for Biotechnology Information. 4(1): 1-34.

Vaidya, S. S., H. Vinaya ،H. and Mahajan, S.S., (2012). Microwave-assisted synthesis, pharmacological evaluation, and QSAR studies of 1, 3-diaryl-2-propen-1-ones. Medicinal Chemistry Research. 21(12): 4311-4323.

Van der Lee, R., M. Pfaffendorf, P.A.; Van Zwieten.(2000). The differential time courses of the vasodilator effects of various 1, 4-dihydropyridines in isolated human small arteries are correlated to their lipophilicity. Journal of hypertension. 18(11): 1677-1682.

Veerasamy, R., H. Rajak, Abhishek Jain, Shalini Sivadasan, Christapher P.Varghese and Ram Kishore Agrawal.(2011). Validation of QSAR models-strategies and importance. Int. J. Drug Des. Discov. **3**: 511-519.

Verma, J., V. M. Khedkar, V.M. and Coutinho, E.C.(2010). 3D-QSAR in drug design-a review. Current topics in medicinal chemistry. 10(1): 95-115

Waki, M. and J. J. J. o. t. A. C. S. Meienhofer (1977). Peptide synthesis using the four-component condensation (Ugi reaction). Journal of American Chemical Society.99(18): 6075-6082.

Wang, G.-W., Xiu, J.-J. Miao, L.B.,Wu,X.L.(2006). Environmentally friendly and efficient synthesis of various 1, 4-dihydropyridines in pure water. Bull. Chem. Sos. JPn. 79(3): 454-459.

Wang, K., D. Kim, et al. (2010). Cyanoacetamide MCR (III): Three-component Gewald reactions revisited. Journal of American Chemical Society. 12(1): 111-118.

Wang, L.-M., J. Sheng, J., Zhang L., Han J.-W., Fan Z., Tian H., Qian C.-T., (2005). Facile Yb $(OTf)_3$ promoted one-pot synthesis of polyhydroquinoline derivatives through Hantzsch reaction .Tetrahedron :(٦)٦١ -١٥٣٩ -1543.

Williams, O.H, and Fleming, J., (1980); Spectroscopic Methods in Organic Chemistry, Ultra-violet and visible spectra, (135-153), McGraw-Hill Book company (UK), limited, England.

Wilson,W.(1992). Tumour hypoxia: challenges for cancer chemotherapy. The Search for New Anticancer Drugs, Springer**:** 87-131.

Wróblewska, A., Huta, O.M., Patsy I.O., Petryshyn R.S. and Blazejowski. (2004).Addition of nucleophiles to the 9-cyano-10-methylacridinium cation: utilization in their chemiluminescent assay. Analytica Chemica Acta. 50**7**(2): 229-236.

Yunta, M. (2017). It is important to compute intramolecular hydrogen bonding in drug design. Am. J. Model. Optim. **5**(1): 24-57.

Zhu, J. and H. Bienayme. (2006). Multicomponent reactions, John Wilely and Sons.

Figures (C1-C75). Showed 3D and 2D, interaction of Docking of acridinedione derivatives inside the active site of 5OM7 protein.

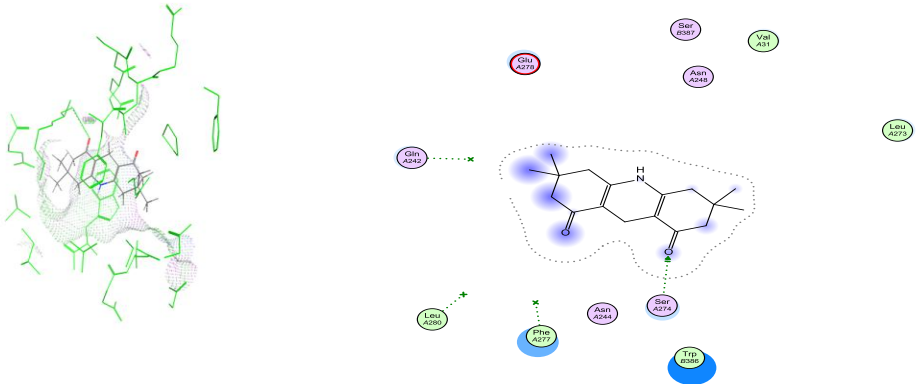

C1/ 3,3,6,6-tetramethyl-3,4,6,7,9,10-hexahydroacridine-1,8(2H,5H)-dione

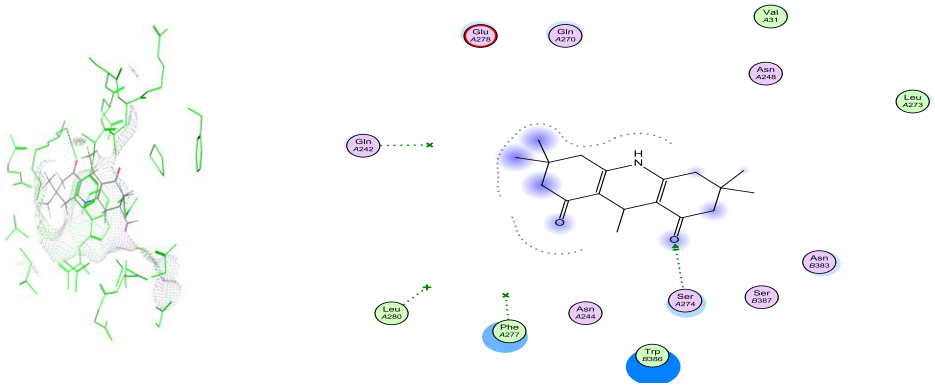

C2/ 3,3,6,6,9-pentamethyl-3,4,6,7,9,10-hexahydroacridine-1,8(2H,5H)-dione

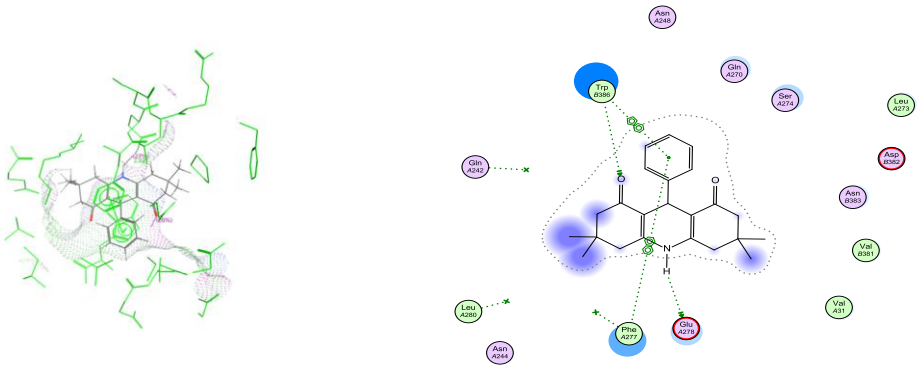

C3/ 3,3,6,6-tetramethyl-9-phenyl-3,4,6,7,9,10-hexahydroacridine-1,8(2H,5H)-dione

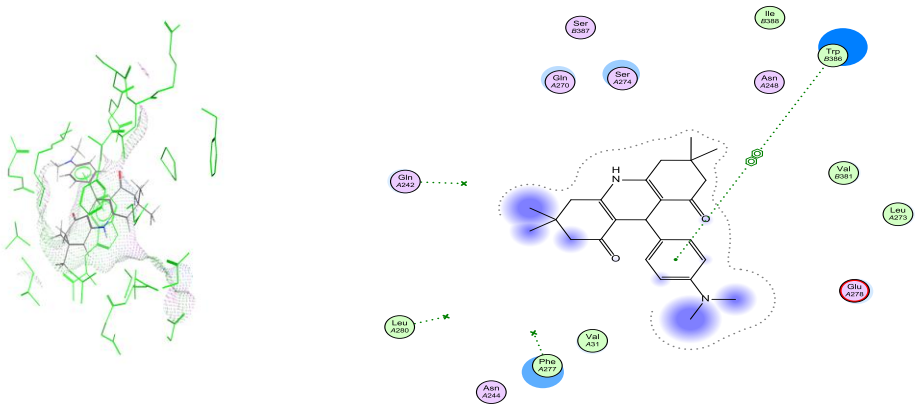

C4/ 9-(4-(dimethylamino)phenyl)-3,3,6,6-tetramethyl-3,4,6,7,9,10-hexahydroacridine-1,8(2H,5H)-dione

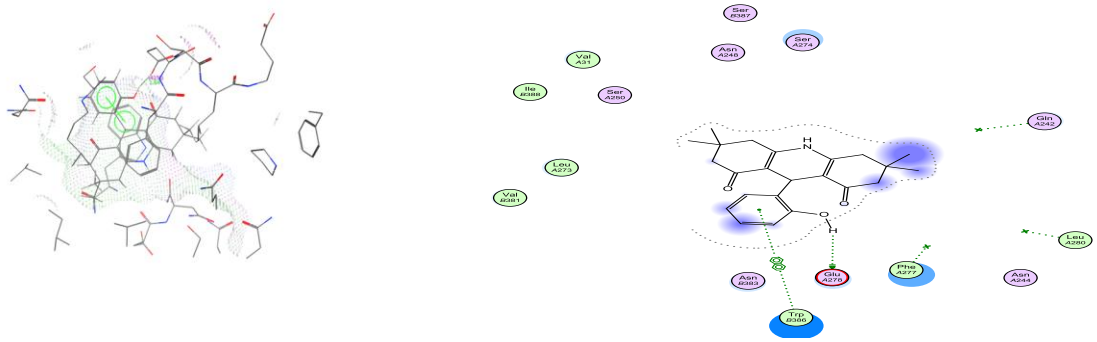

C5/ 9-(2-hydroxyphenyl)-3,3,6,6-tetramethyl-3,4,6,7,9,10-hexahydroacridine-1,8(2H,5H)-dione

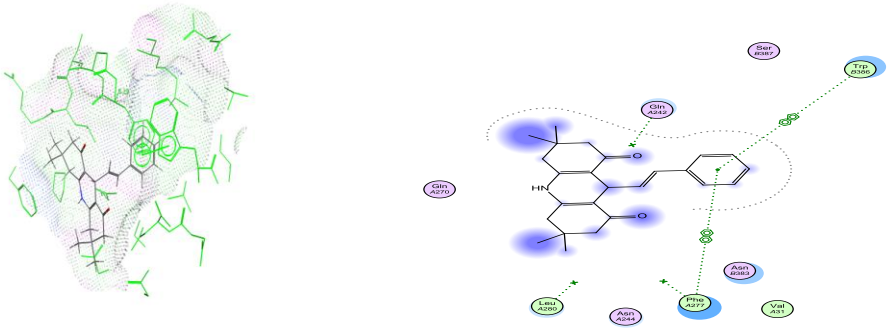

C6/ (E)-3,3,6,6-tetramethyl-9-styryl-3,4,6,7,9,10-hexahydroacridine-1,8(2H,5H)-dione

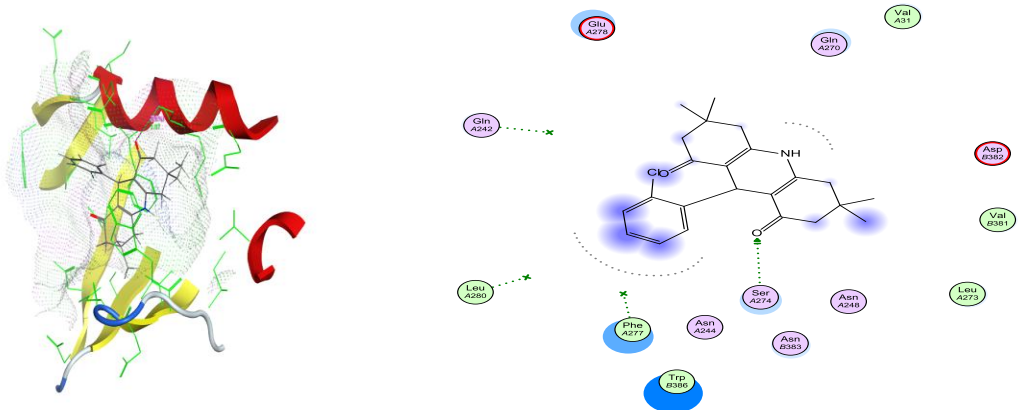

C7/9-(2-chlorophenyl)-3,3,6,6-tetramethyl-3,4,6,7,9,10-hexahydroacridine-1,8(2H,5H)-dione

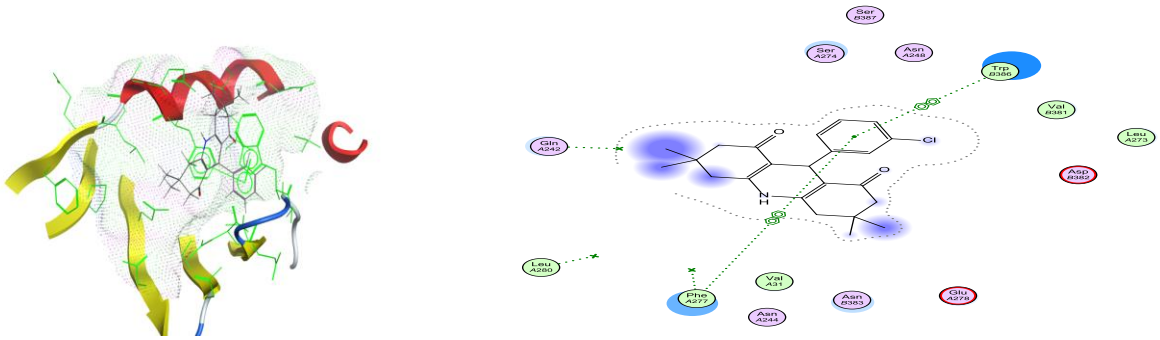

C8/ 9-(3-chlorophenyl)-3,3,6,6-tetramethyl-3,4,6,7,9,10-hexahydroacridine-1,8(2H,5H)-dione

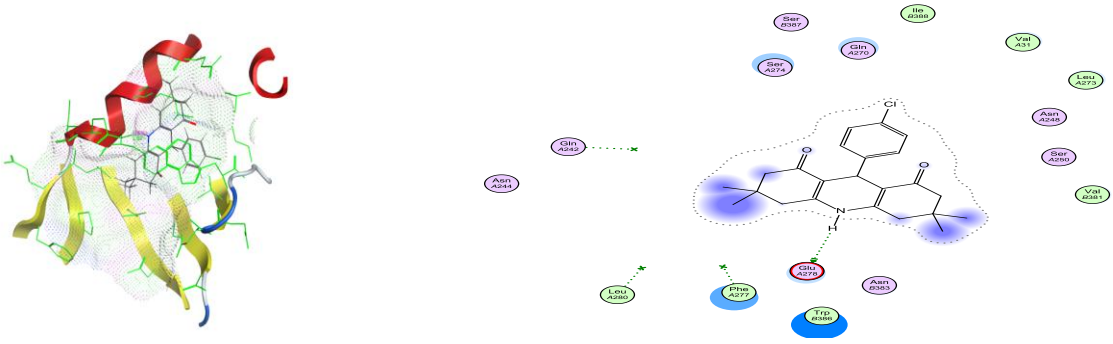

C9/ 9-(4-chlorophenyl)-3,3,6,6-tetramethyl-3,4,6,7,9,10-hexahydroacridine-1,8(2H,5H)-dione

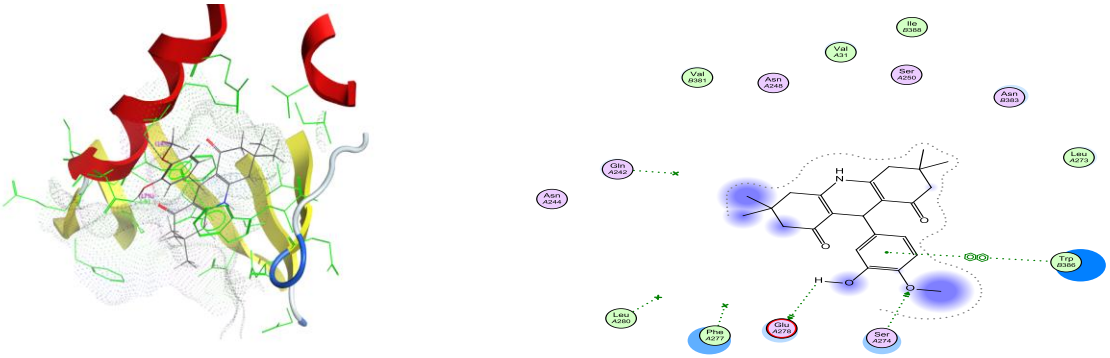

C10/ 9-(3-hydroxy-4-methoxyphenyl)-3,3,6,6-tetramethyl-3,4,6,7,9,10-hexahydroacridine-1,8(2H,5H)-dione

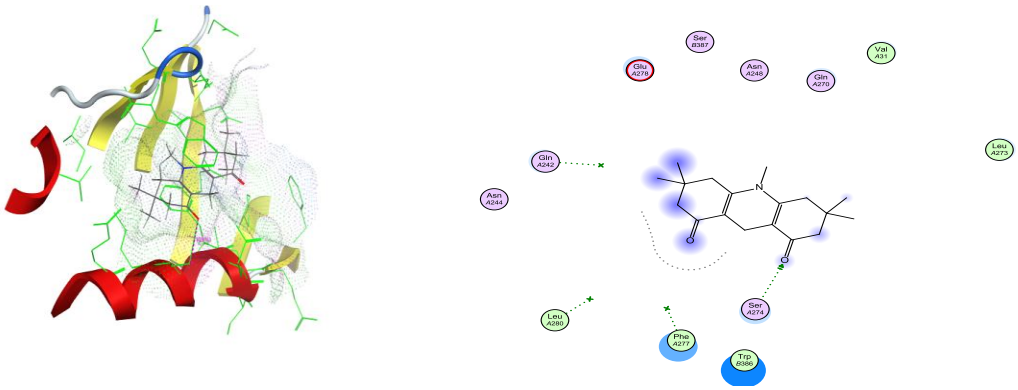

C11/ 3,3,6,6,10-pentamethyl-3,4,6,7,9,10-hexahydroacridine-1,8(2H,5H)-dione

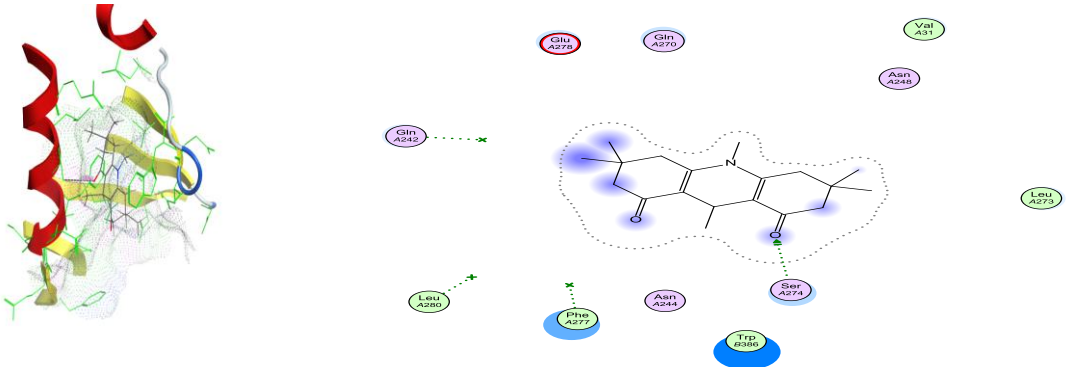

C12/ 3,3,6,6,9,10-hexamethyl-3,4,6,7,9,10-hexahydroacridine-1,8(2H,5H)-dione

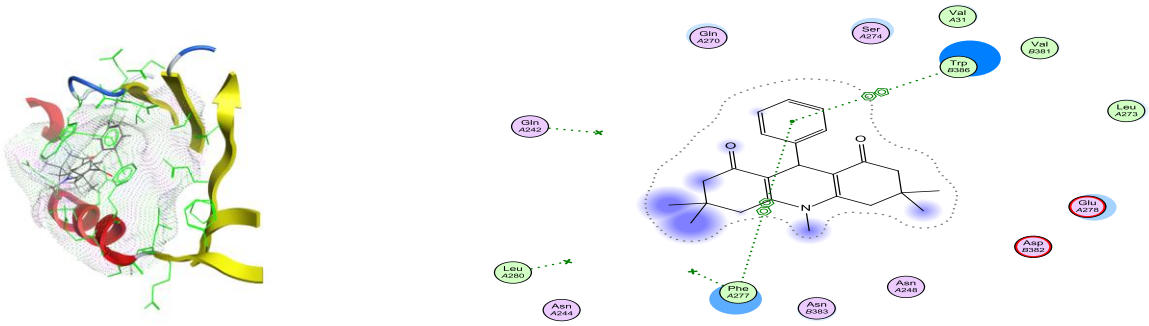

C13/ 3,3,6,6,10-pentamethyl-9-phenyl-3,4,6,7,9,10-hexahydroacridine-1,8(2H,5H)-dione

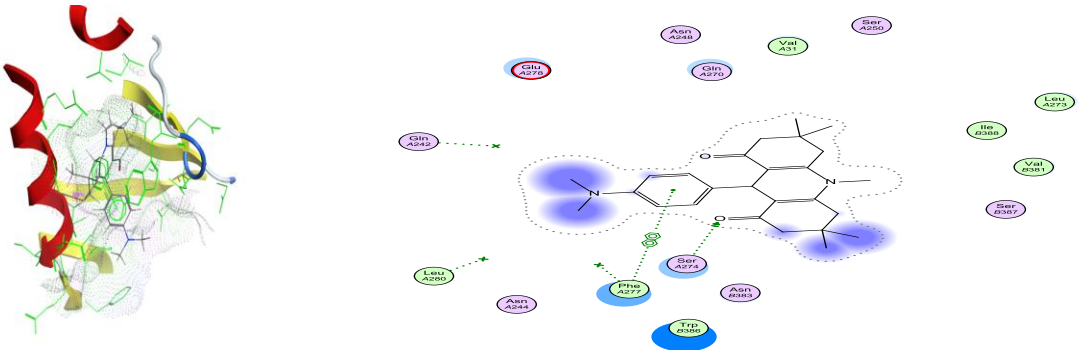

C14/ 9-(4-(dimethylamino)phenyl)-3,3,6,6,10-pentamethyl-3,4,6,7,9,10-hexahydroacridine-1,8(2H,5H)-dione

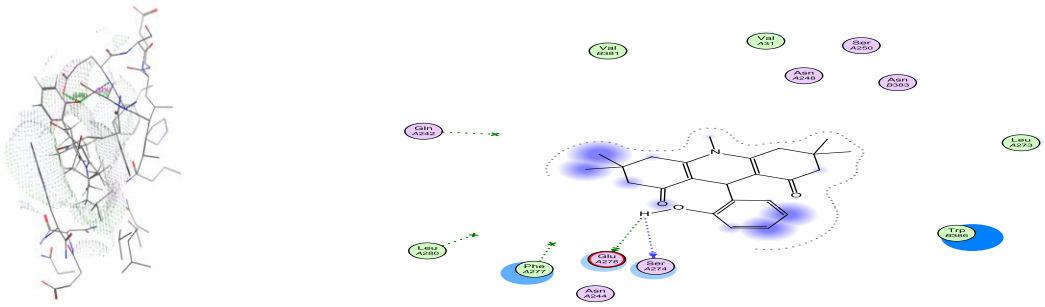

C15/ 9-(2-hydroxyphenyl)-3,3,6,6,10-pentamethyl-3,4,6,7,9,10-hexahydroacridine-1,8(2H,5H)-dione

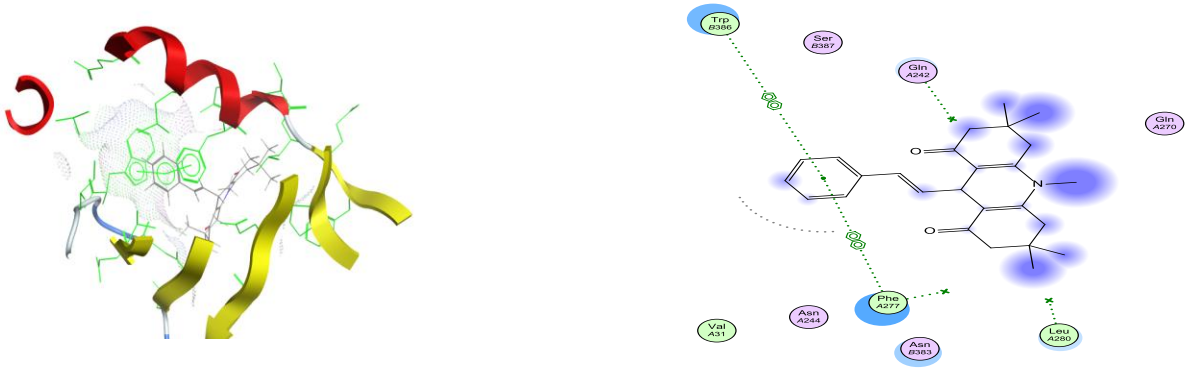

C16/ (E)-3,3,6,6,10-pentamethyl-9-styryl-3,4,6,7,9,10-hexahydroacridine-1,8(2H,5H)-dione

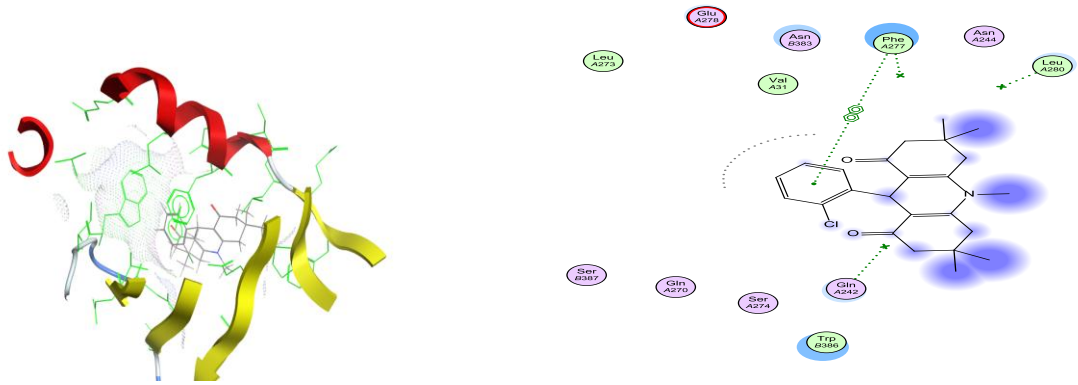

C17/ 9-(2-chlorophenyl)-3,3,6,6,10-pentamethyl-3,4,6,7,9,10-hexahydroacridine-1,8(2H,5H)-dione

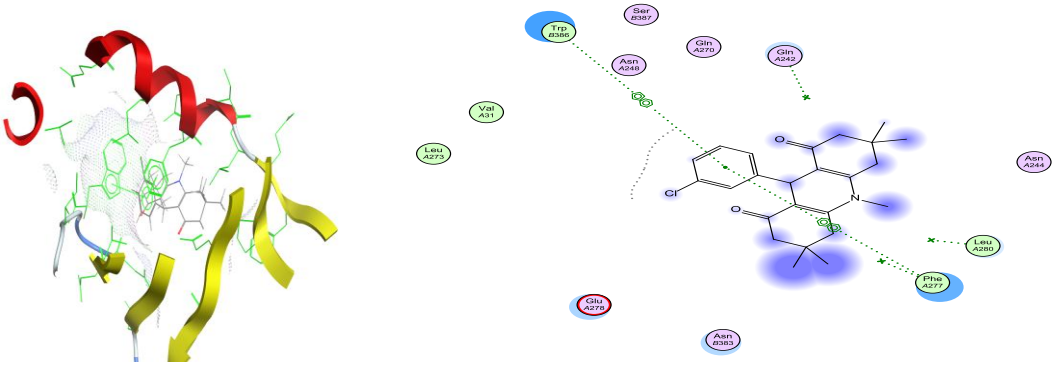

C18/ 9-(3-chlorophenyl)-3,3,6,6,10-pentamethyl-3,4,6,7,9,10-hexahydroacridine-1,8(2H,5H)-dione

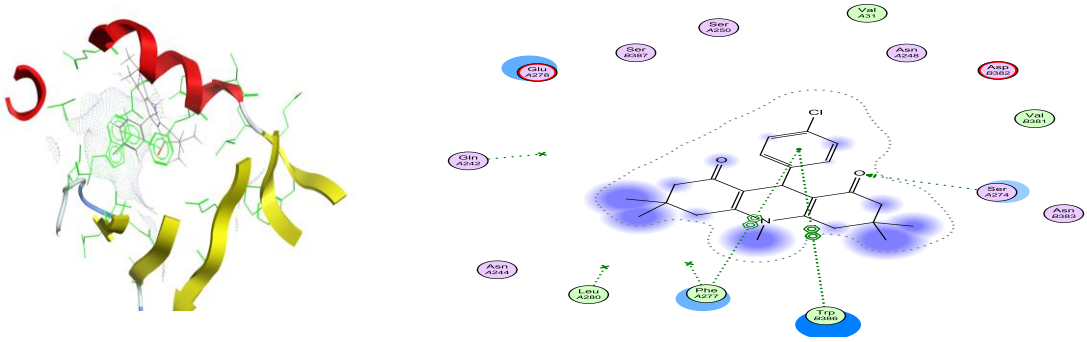

C19/ 9-(4-chlorophenyl)-3,3,6,6,10-pentamethyl-3,4,6,7,9,10-hexahydroacridine-1,8(2H,5H)-dione

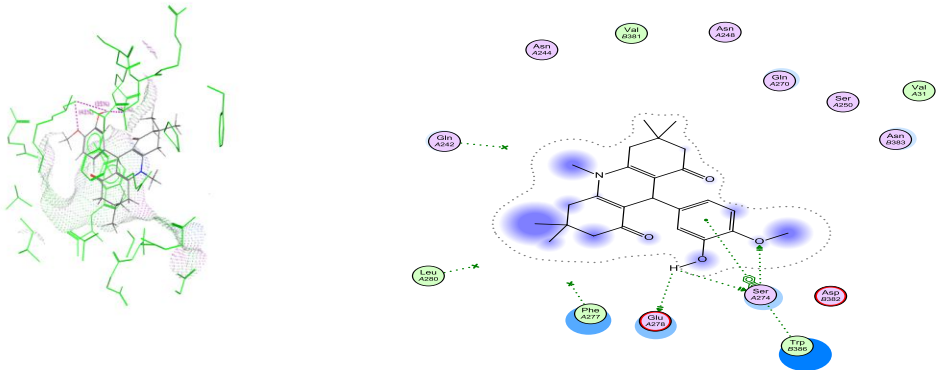

C20/ 9-(3-hydroxy-4-methoxyphenyl)-3,3,6,6,10-pentamethyl-3,4,6,7,9,10-hexahydroacridine-1,8(2H,5H)-dione

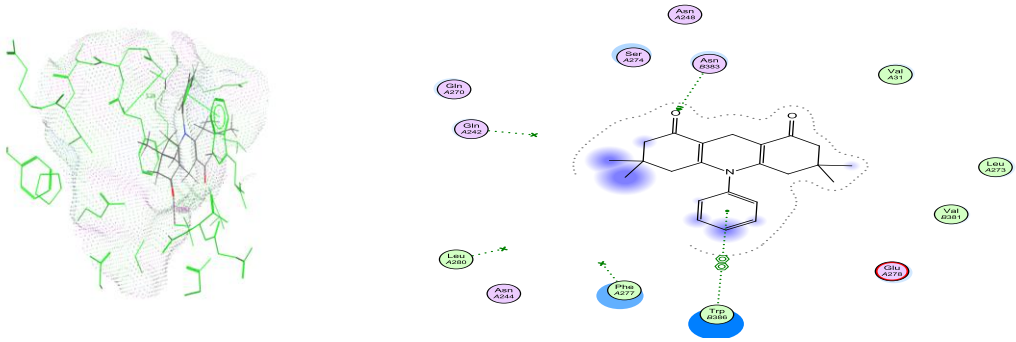

C21/ 3,3,6,6-tetramethyl-10-phenyl-3,4,6,7,9,10-hexahydroacridine-1,8(2H,5H)-dione

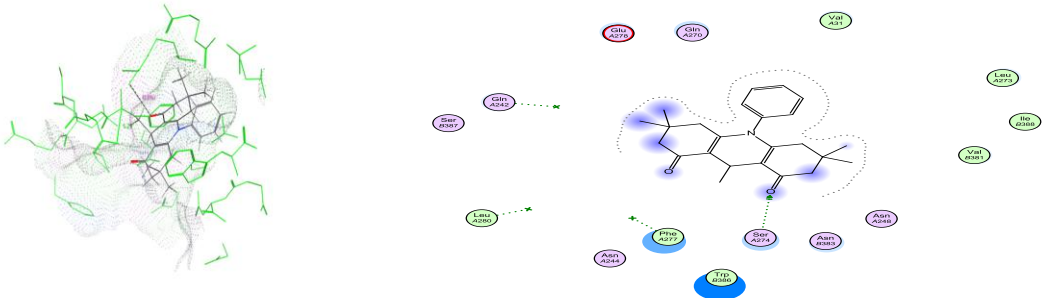

C22/ 3,3,6,6,9-pentamethyl-10-phenyl-3,4,6,7,9,10-hexahydroacridine-1,8(2H,5H)-dione

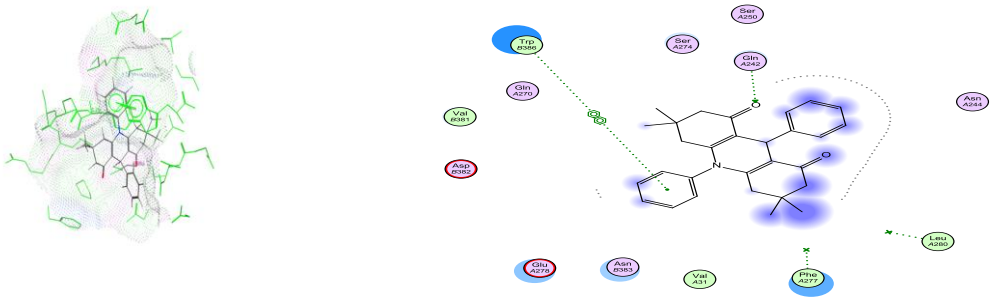

C23/ 3,3,6,6-tetramethyl-9,10-diphenyl-3,4,6,7,9,10-hexahydroacridine-1,8(2H,5H)-dione

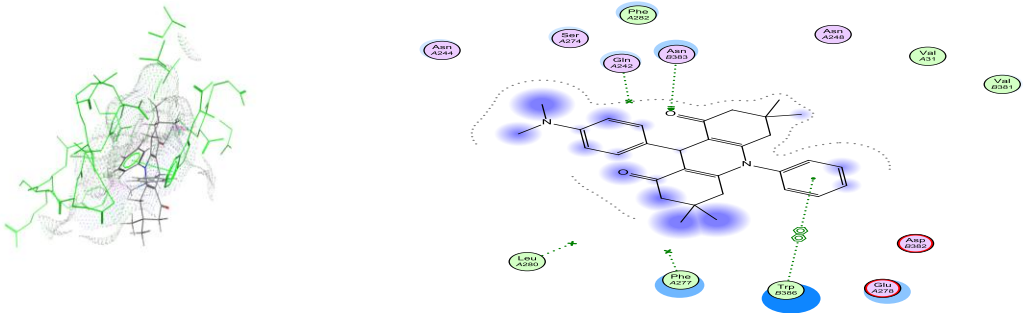

C24/ 9-(4-(dimethylamino)phenyl)-3,3,6,6-tetramethyl-10-phenyl-3,4,6,7,9,10-hexahydroacridine-1,8(2H,5H)-dione

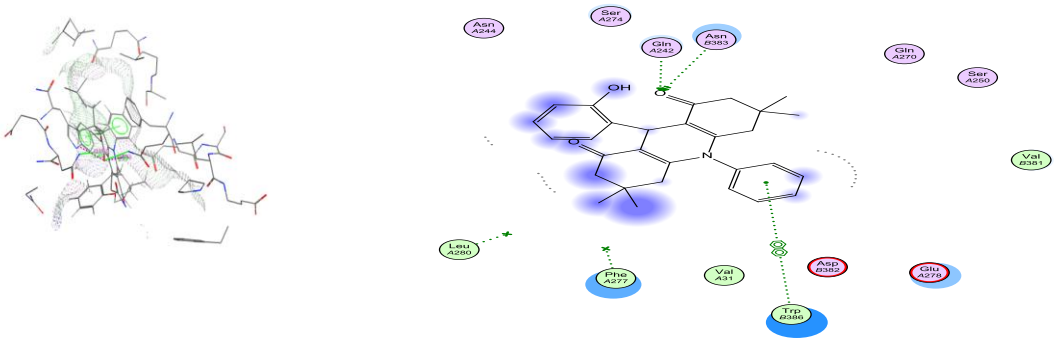

C25/ 9-(2-hydroxyphenyl)-3,3,6,6-tetramethyl-10-phenyl-3,4,6,7,9,10-hexahydroacridine-1,8(2H,5H)-dione

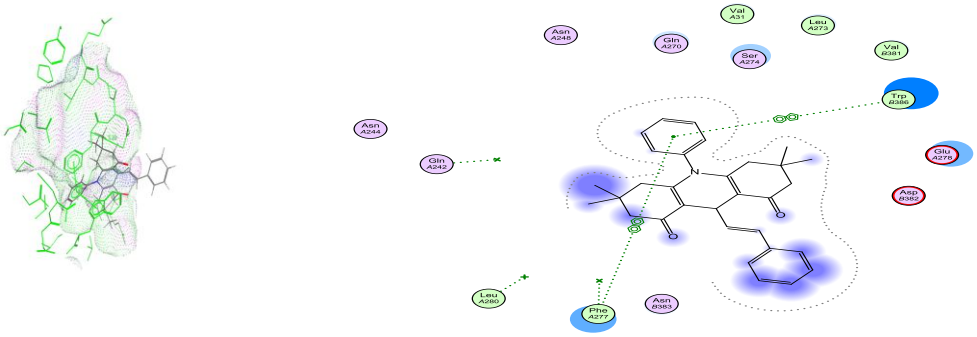

C26/ (E)-3,3,6,6-tetramethyl-10-phenyl-9-styryl-3,4,6,7,9,10-hexahydroacridine-1,8(2H,5H)-dione

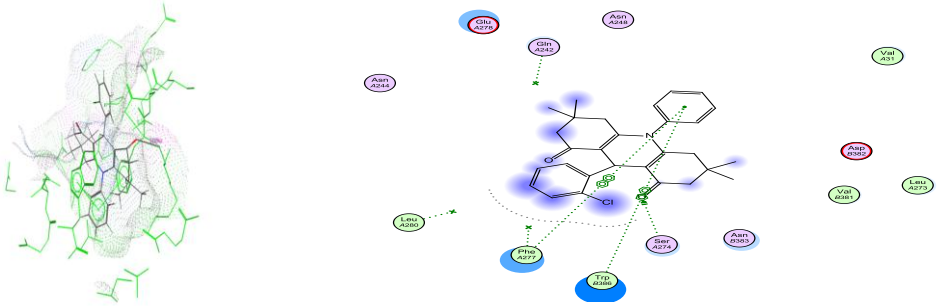

C27/ 9-(2-chlorophenyl)-3,3,6,6-tetramethyl-10-phenyl-3,4,6,7,9,10-hexahydroacridine-1,8(2H,5H)-dione

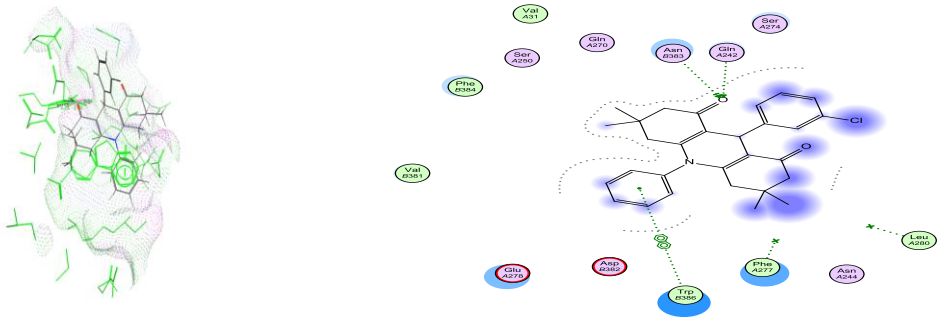

C28/ 9-(3-chlorophenyl)-3,3,6,6-tetramethyl-10-phenyl-3,4,6,7,9,10-hexahydroacridine-1,8(2H,5H)-dione

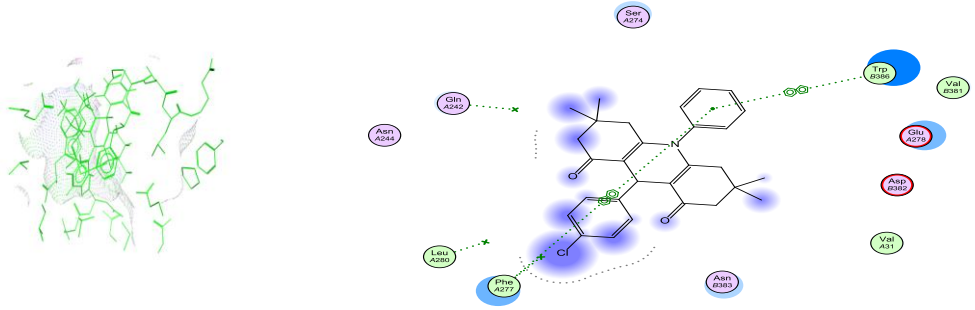

C29/ 9-(4-chlorophenyl)-3,3,6,6-tetramethyl-10-phenyl-3,4,6,7,9,10-hexahydroacridine-1,8(2H,5H)-dione

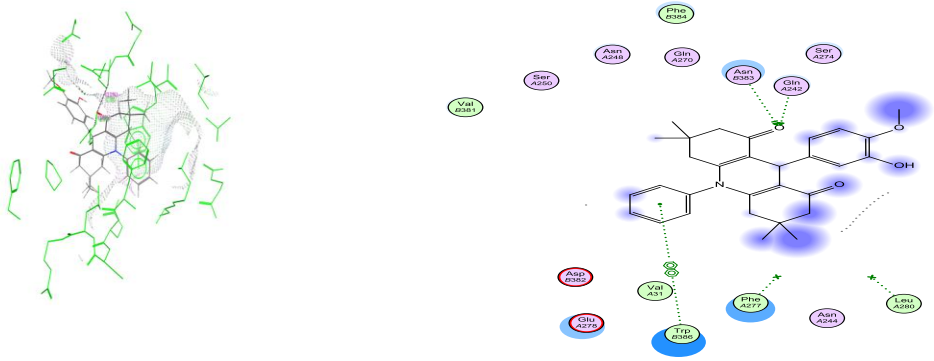

C30/ 9-(3-hydroxy-4-methoxyphenyl)-3,3,6,6-tetramethyl-10-phenyl-3,4,6,7,9,10-hexahydroacridine-1,8(2H,5H)-dione

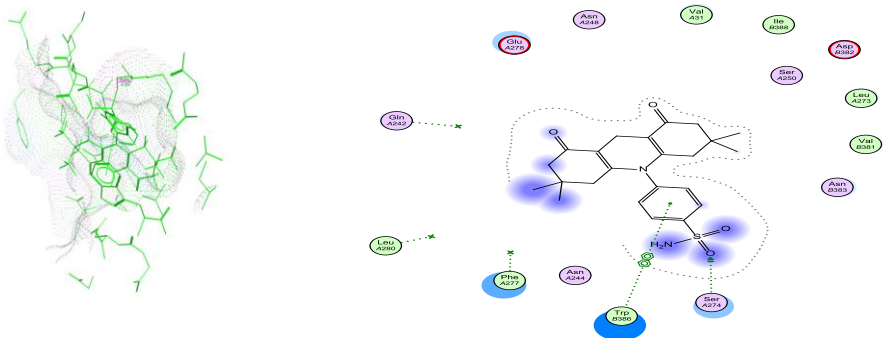

C31/ 4-(3,3,6,6-tetramethyl-1,8-dioxo-2,3,4,5,6,7,8,9-octahydroacridin-10(1H)-yl)benzenesulfonamide

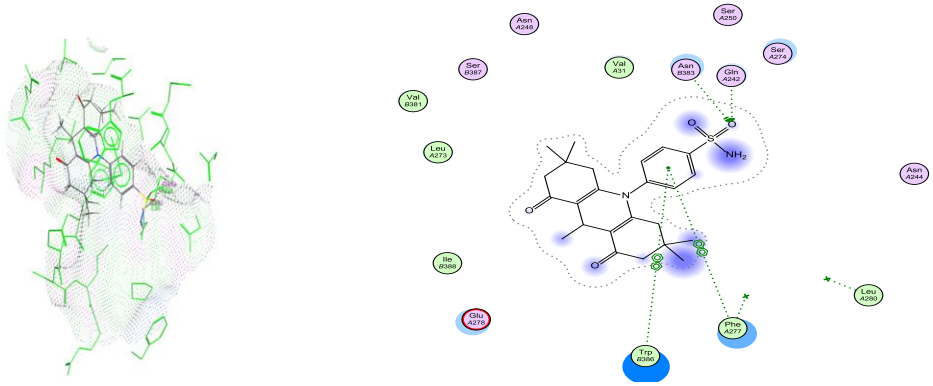

C32/ 4-(3,3,6,6,9-pentamethyl-1,8-dioxo-2,3,4,5,6,7,8,9-octahydroacridin-10(1H)-yl)benzenesulfonamide

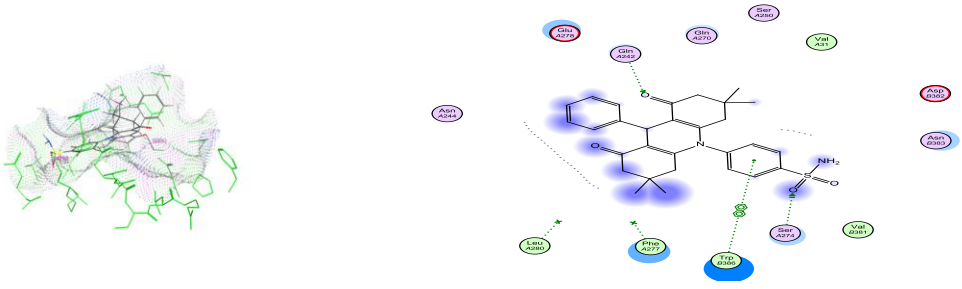

C33/ 4-(3,3,6,6-tetramethyl-1,8-dioxo-9-phenyl-2,3,4,5,6,7,8,9-octahydroacridin-10(1H)-yl)benzenesulfonamide

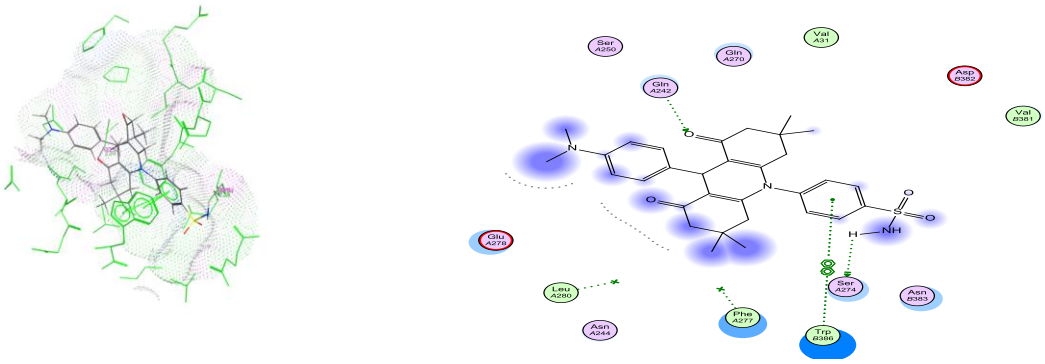

C34/ 4-(9-(4-(dimethylamino)phenyl)-3,3,6,6-tetramethyl-1,8-dioxo-2,3,4,5,6,7,8,9-octahydroacridin-10(1H)-yl)benzenesulfonamide

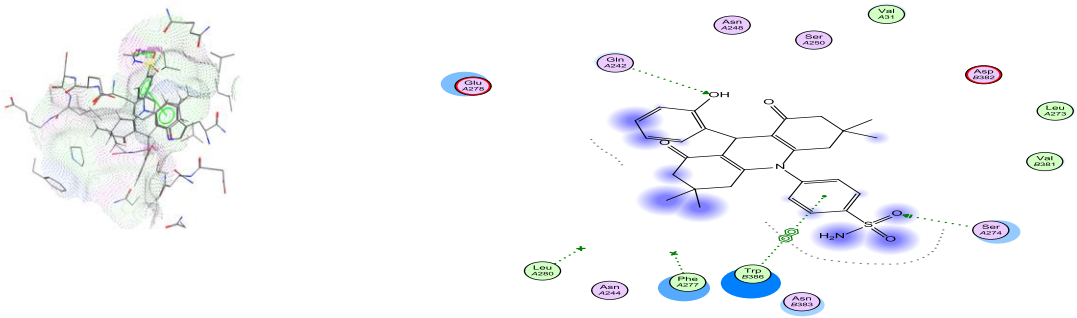

C35/ 4-(9-(2-hydroxyphenyl)-3,3,6,6-tetramethyl-1,8-dioxo-2,3,4,5,6,7,8,9-octahydroacridin-10(1H)-yl)benzenesulfonamide

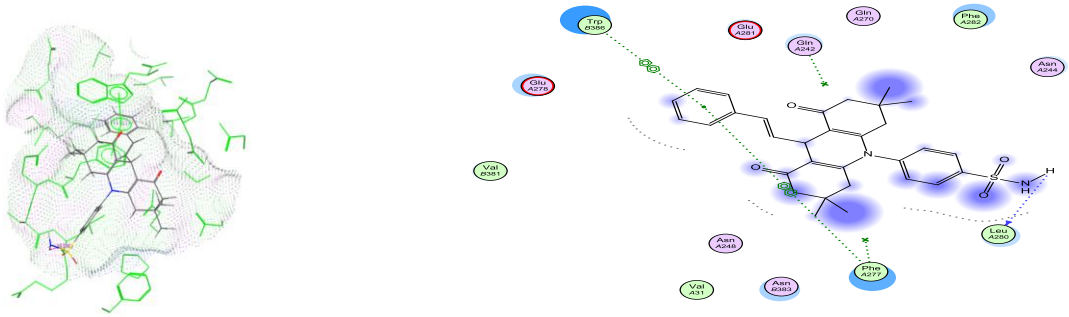

C36/ (E)-4-(3,3,6,6-tetramethyl-1,8-dioxo-9-styryl-2,3,4,5,6,7,8,9-octahydroacridin-10(1H)-yl)benzenesulfonamide

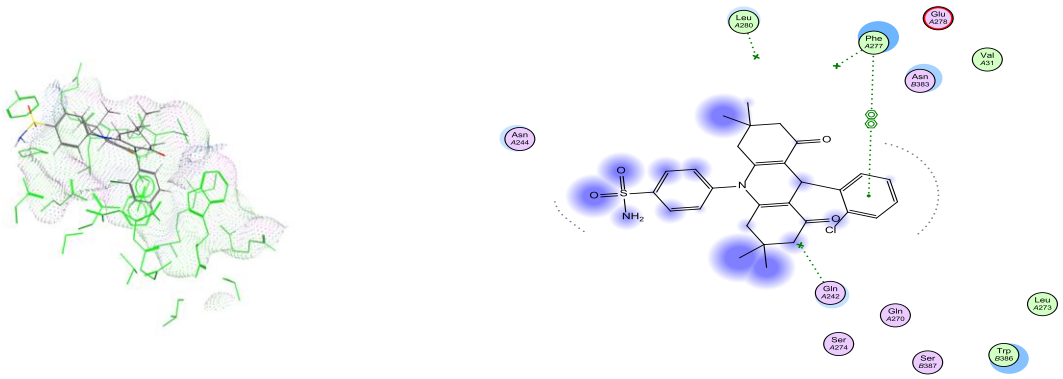

C37/ 4-(9-(2-chlorophenyl)-3,3,6,6-tetramethyl-1,8-dioxo-2,3,4,5,6,7,8,9-octahydroacridin-10(1H)-yl)benzenesulfonamide

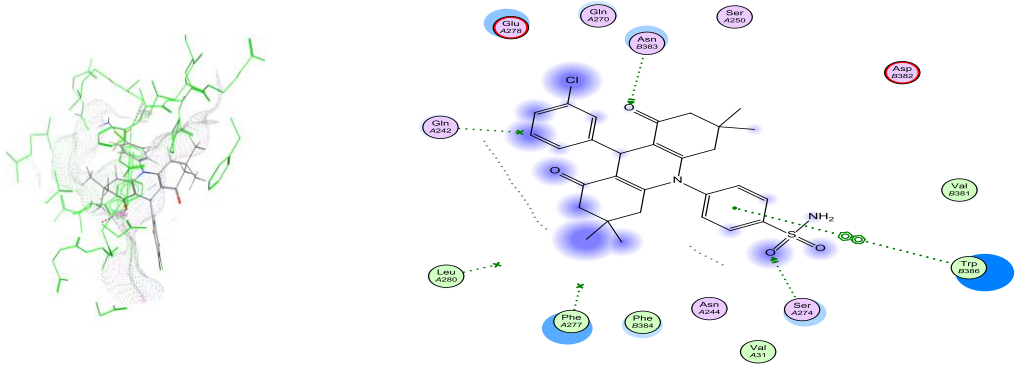

C38/ 4-(9-(3-chlorophenyl)-3,3,6,6-tetramethyl-1,8-dioxo-2,3,4,5,6,7,8,9-octahydroacridin-10(1H)-yl)benzenesulfonamide

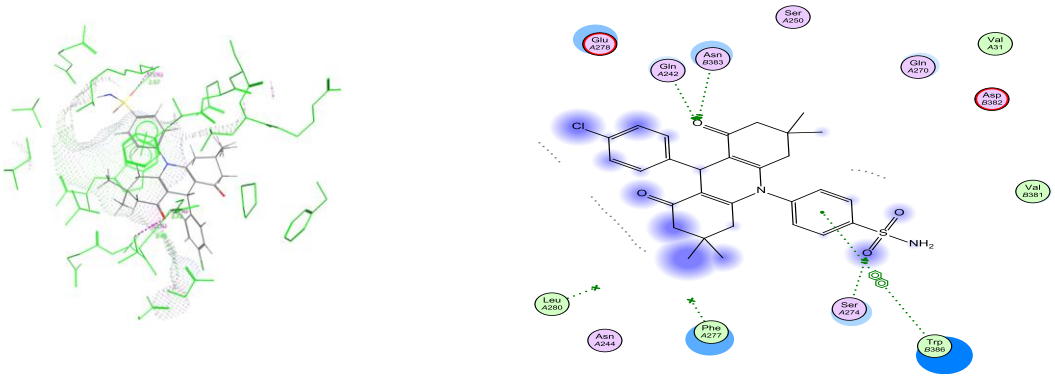

C39/ 4-(9-(4-chlorophenyl)-3,3,6,6-tetramethyl-1,8-dioxo-2,3,4,5,6,7,8,9-octahydroacridin-10(1H)-yl)benzenesulfonamide

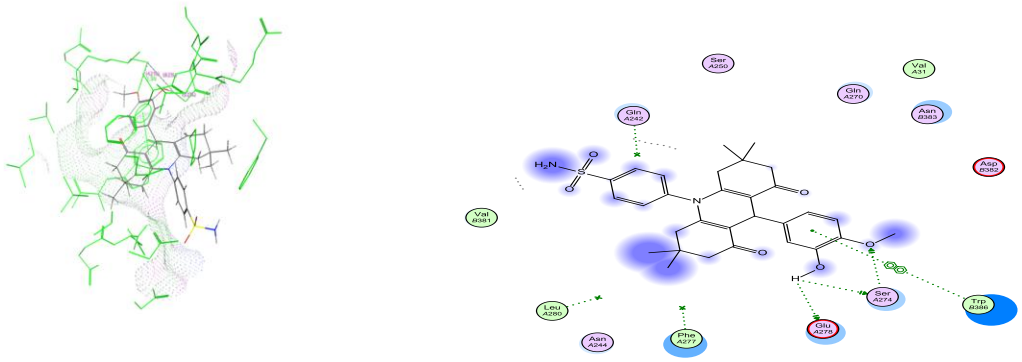

C40/ 4-(9-(3-hydroxy-4-methoxyphenyl)-3,3,6,6-tetramethyl-1,8-dioxo-2,3,4,5,6,7,8,9-octahydroacridin-10(1H)-yl)benzenesulfonamide

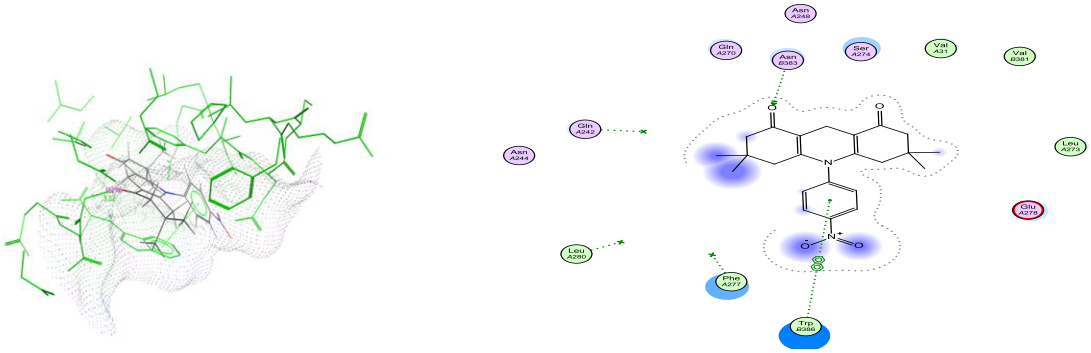

C41/ 3,3,6,6-tetramethyl-10-(4-nitrophenyl)-3,4,6,7,9,10-hexahydroacridine-1,8(2H,5H)-dione

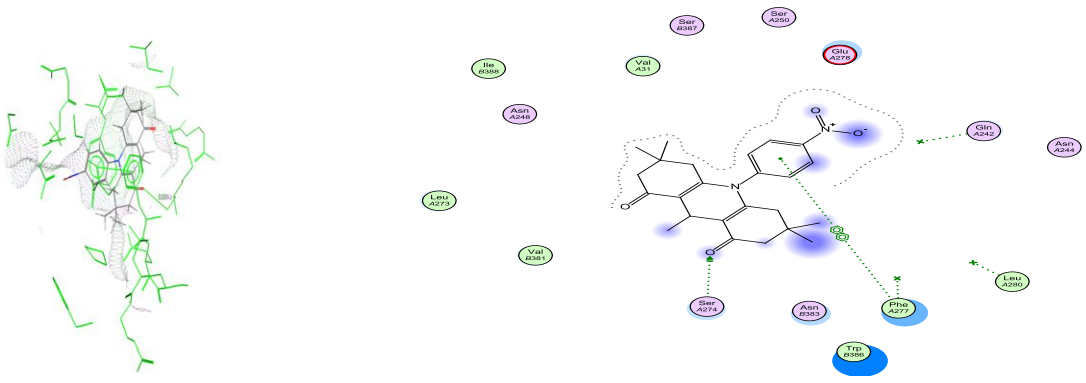

C42/ 3,3,6,6,9-pentamethyl-10-(4-nitrophenyl)-3,4,6,7,9,10-hexahydroacridine-1,8(2H,5H)-dione

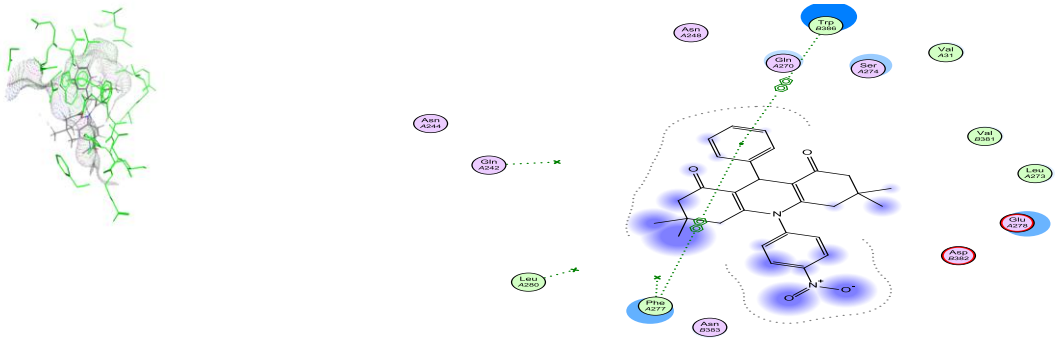

C43/ 3,3,6,6-tetramethyl-10-(4-nitrophenyl)-9-phenyl-3,4,6,7,9,10-hexahydroacridine-1,8(2H,5H)-dione

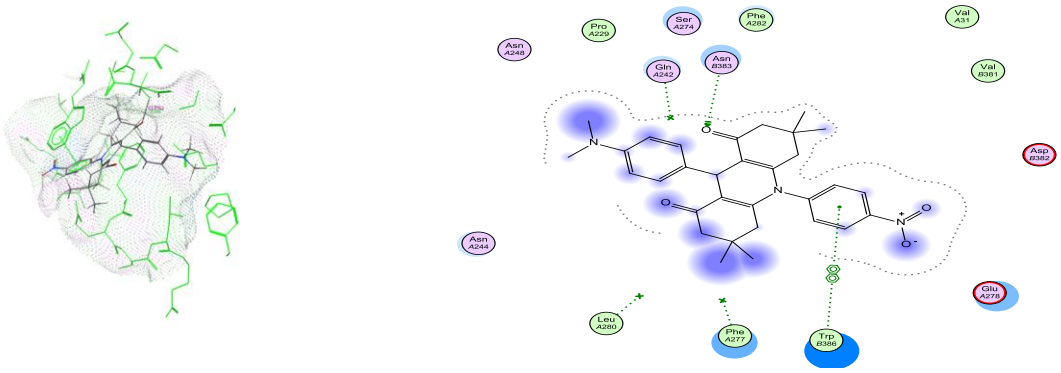

C44/ 9-(4-(dimethylamino)phenyl)-3,3,6,6-tetramethyl-10-(4-nitrophenyl)-3,4,6,7,9,10-hexahydroacridine-1,8(2H,5H)-dione

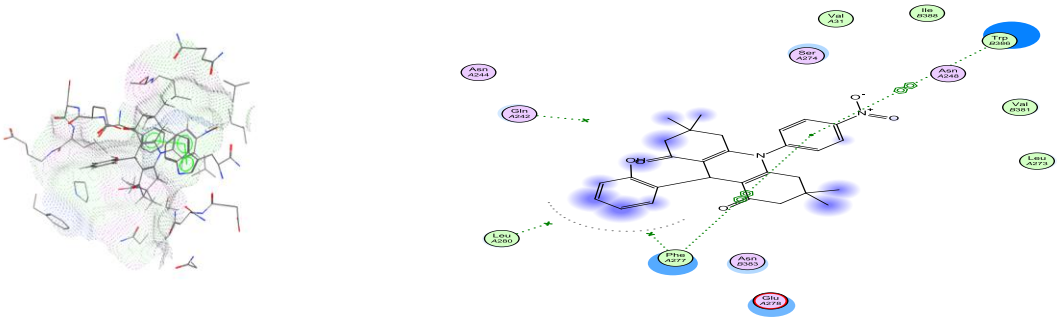

C45/ 9-(2-hydroxyphenyl)-3,3,6,6-tetramethyl-10-(4-nitrophenyl)-3,4,6,7,9,10-hexahydroacridine-1,8(2H,5H)-dione

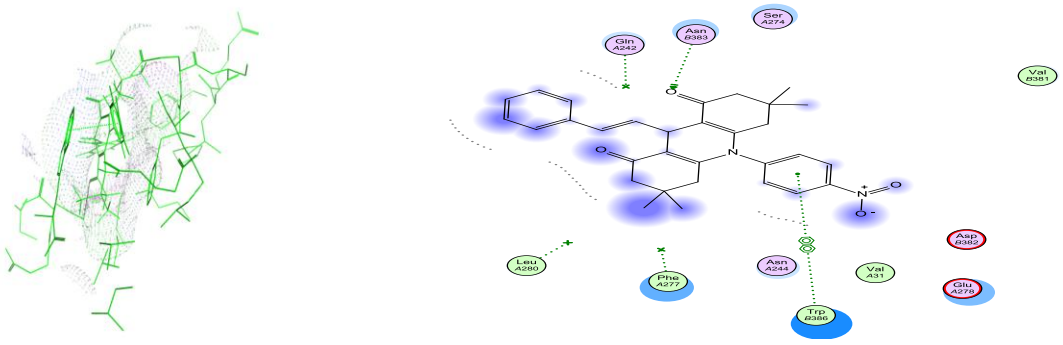

C46/ (E)-3,3,6,6-tetramethyl-10-(4-nitrophenyl)-9-styryl-3,4,6,7,9,10-hexahydroacridine-1,8(2H,5H)-dione

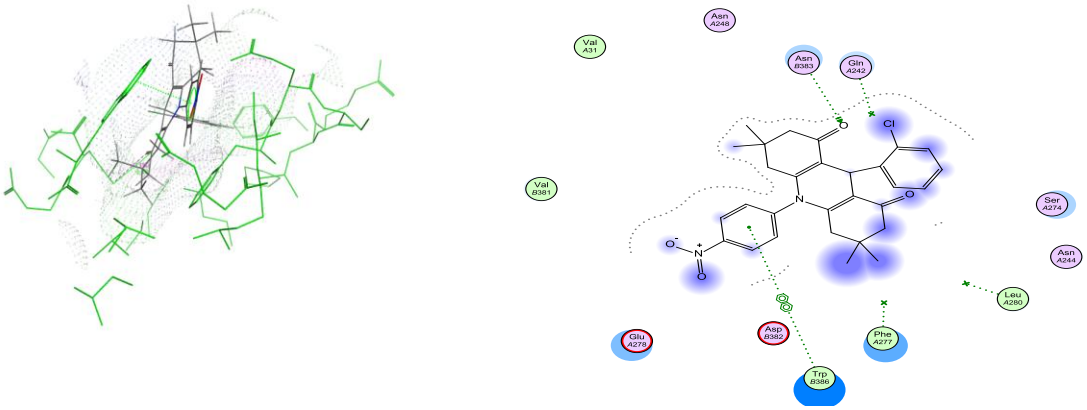

C47/ 9-(2-chlorophenyl)-3,3,6,6-tetramethyl-10-(4-nitrophenyl)-3,4,6,7,9,10-hexahydroacridine-1,8(2H,5H)-dione

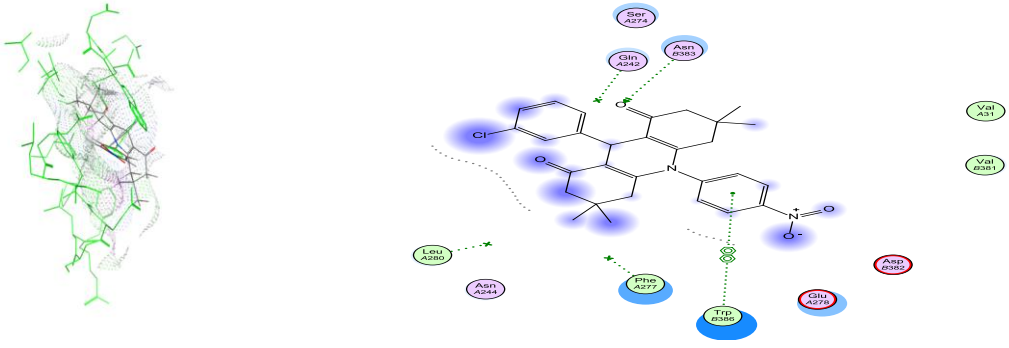

C48/ 9-(3-chlorophenyl)-3,3,6,6-tetramethyl-10-(4-nitrophenyl)-3,4,6,7,9,10-hexahydroacridine-1,8(2H,5H)-dione

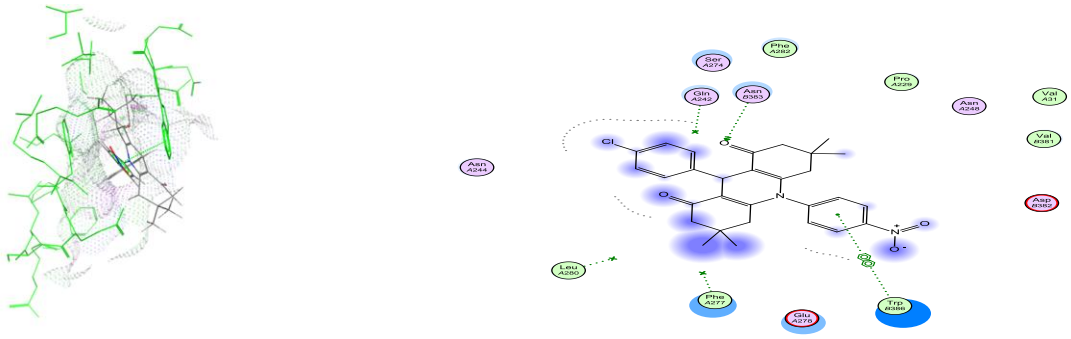

C49/ 9-(4-chlorophenyl)-3,3,6,6-tetramethyl-10-(4-nitrophenyl)-3,4,6,7,9,10-hexahydroacridine-1,8(2H,5H)-dione

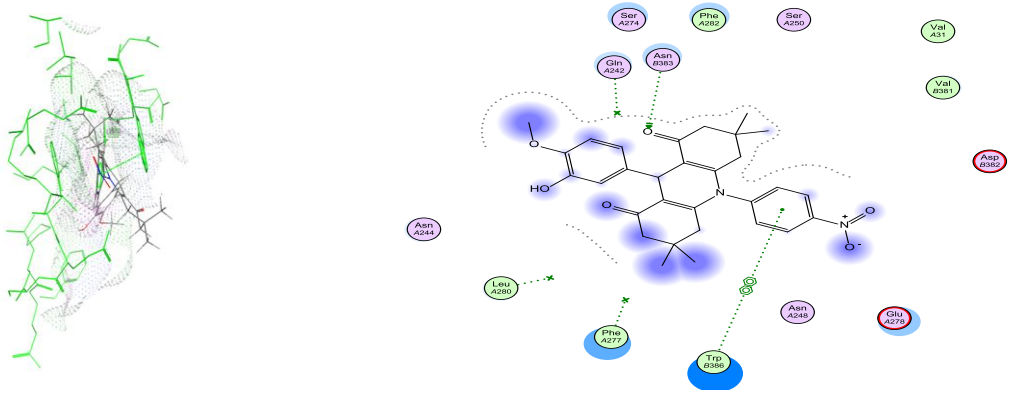

C50/ 9-(3-hydroxy-4-methoxyphenyl)-3,3,6,6-tetramethyl-10-(4-nitrophenyl)-3,4,6,7,9,10-hexahydroacridine-1,8(2H,5H)-dione

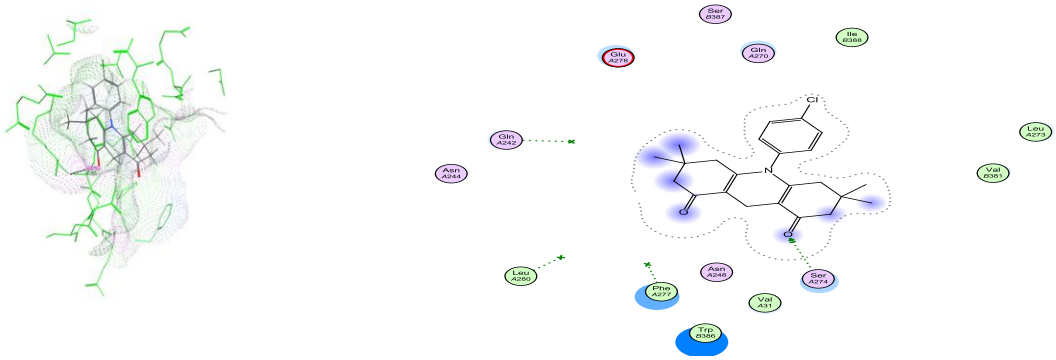

C51/ 10-(4-chlorophenyl)-3,3,6,6-tetramethyl-3,4,6,7,9,10-hexahydroacridine-1,8(2H,5H)-dione

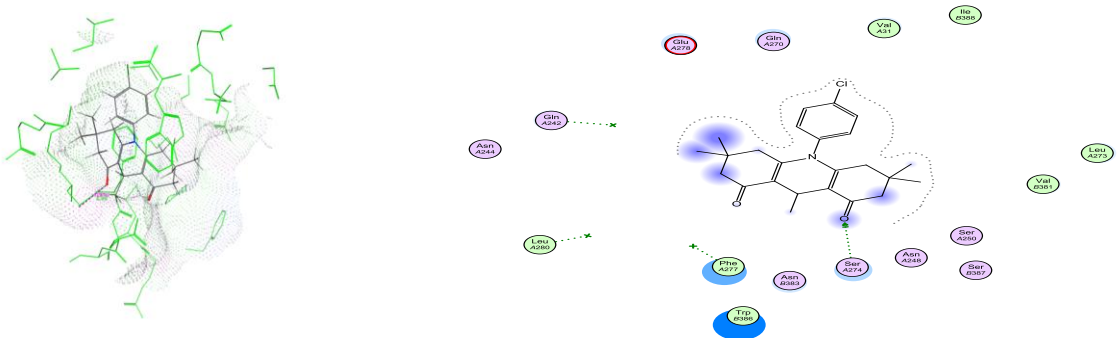

C52/ 10-(4-chlorophenyl)-3,3,6,6,9-pentamethyl-3,4,6,7,9,10-hexahydroacridine-1,8(2H,5H)-dione

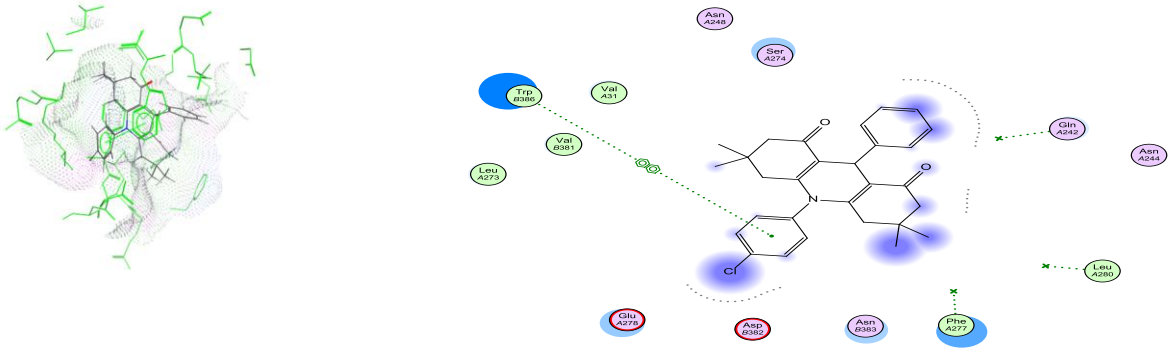

C53/ 10-(4-chlorophenyl)-3,3,6,6-tetramethyl-9-phenyl-3,4,6,7,9,10-hexahydroacridine-1,8(2H,5H)-dione

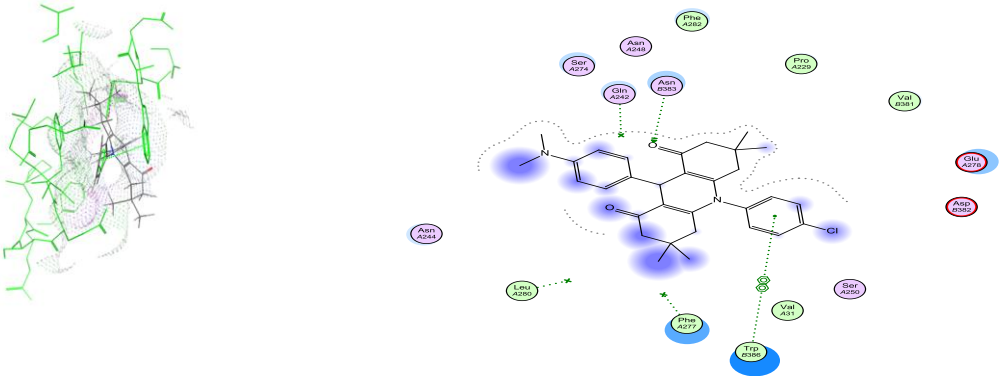

C54/ 10-(4-chlorophenyl)-9-(4-(dimethylamino)phenyl)-3,3,6,6-tetramethyl-3,4,6,7,9,10-hexahydroacridine-1,8(2H,5H)-dione

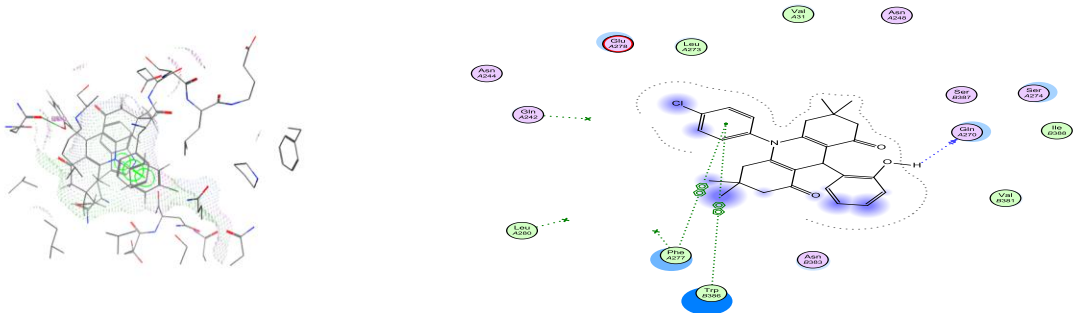

C55/ 10-(4-chlorophenyl)-9-(2-hydroxyphenyl)-3,3,6,6-tetramethyl-3,4,6,7,9,10-hexahydroacridine-1,8(2H,5H)-dione

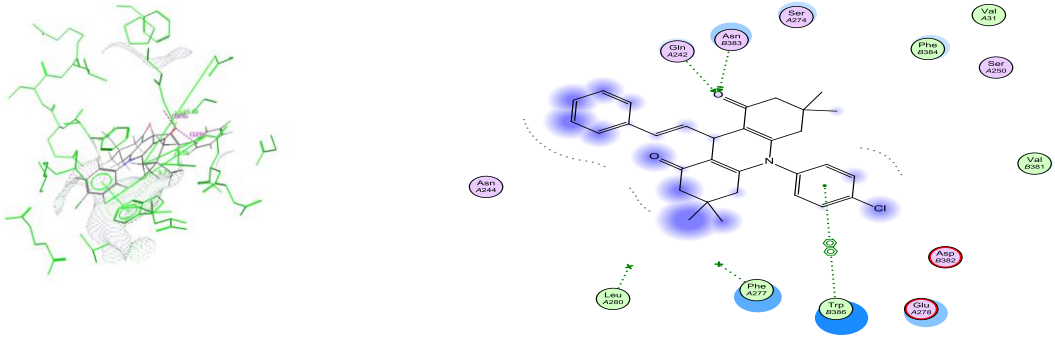

C56/ (E)-10-(4-chlorophenyl)-3,3,6,6-tetramethyl-9-styryl-3,4,6,7,9,10-hexahydroacridine-1,8(2H,5H)-dione

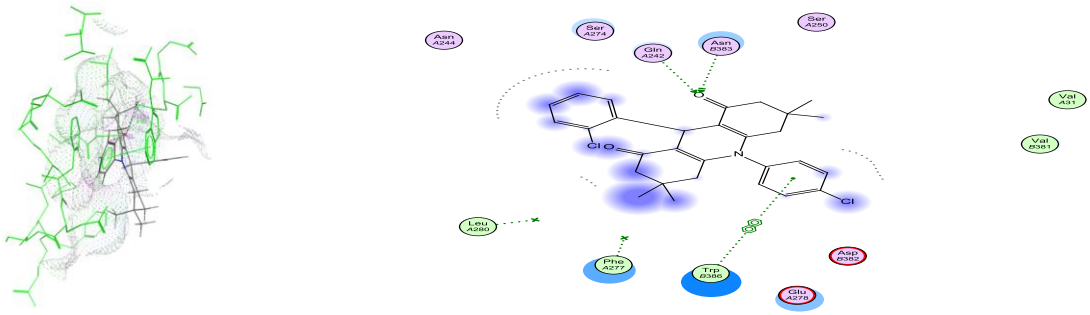

C57/ 9-(2-chlorophenyl)-10-(4-chlorophenyl)-3,3,6,6-tetramethyl-3,4,6,7,9,10-hexahydroacridine-1,8(2H,5H)-dione

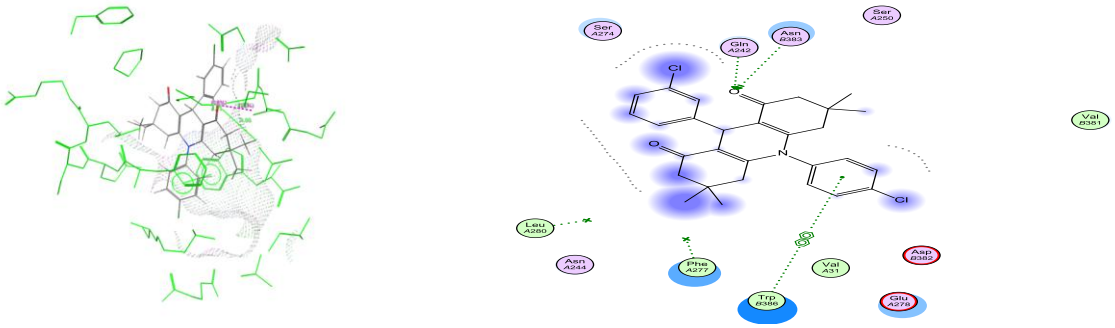

C58/ 9-(3-chlorophenyl)-10-(4-chlorophenyl)-3,3,6,6-tetramethyl-3,4,6,7,9,10-hexahydroacridine-1,8(2H,5H)-dione

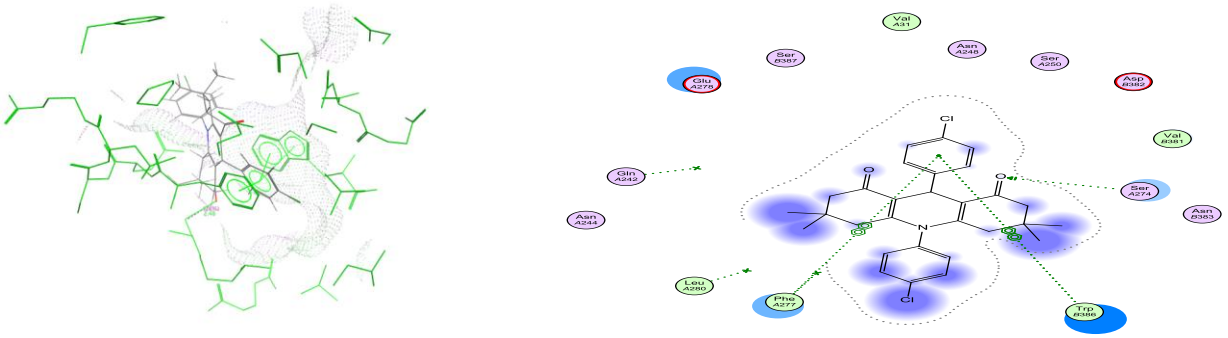

C59/ 9,10-bis(4-chlorophenyl)-3,3,6,6-tetramethyl-3,4,6,7,9,10-hexahydroacridine-1,8(2H,5H)-dione

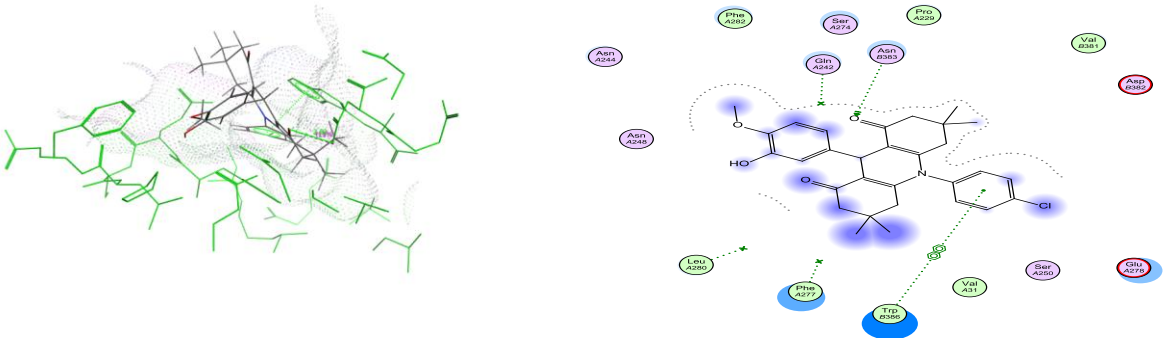

C60/ 10-(4-chlorophenyl)-9-(3-hydroxy-4-methoxyphenyl)-3,3,6,6-tetramethyl-3,4,6,7,9,10-hexahydroacridine-1,8(2H,5H)-dione

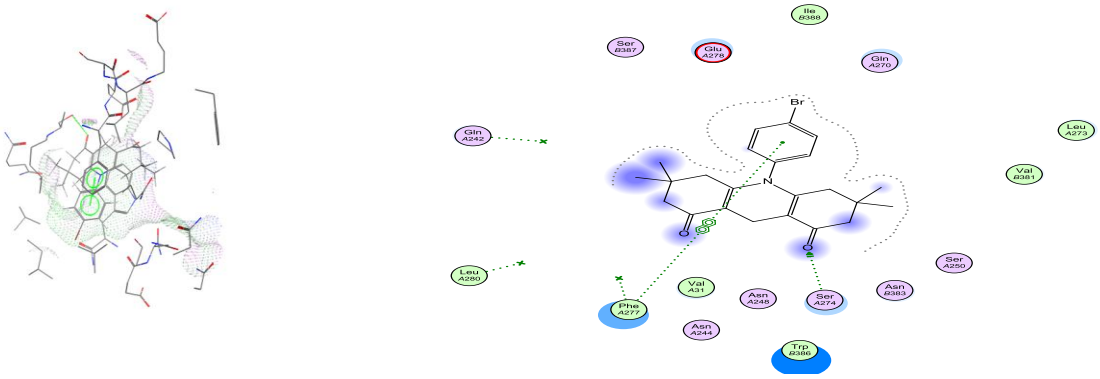

C61/ 10-(4-bromophenyl)-3,3,6,6-tetramethyl-3,4,6,7,9,10-hexahydroacridine-1,8(2H,5H)-dione

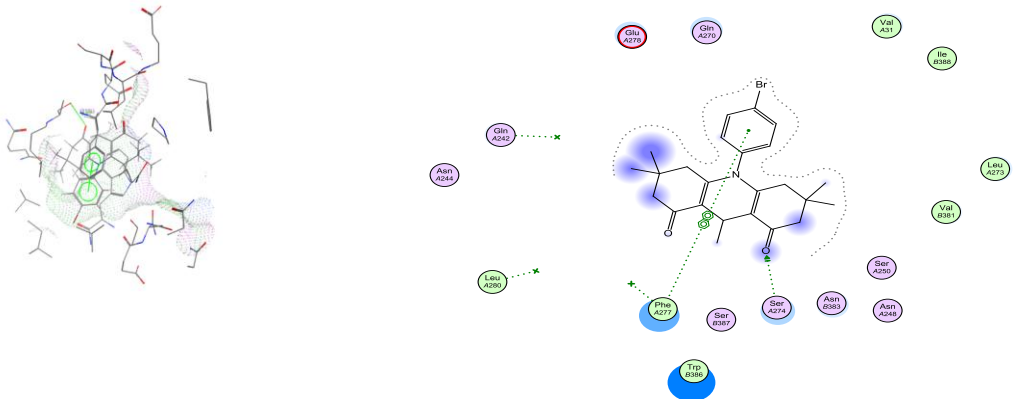

C62/ 10-(4-bromophenyl)-3,3,6,6,9-pentamethyl-3,4,6,7,9,10-hexahydroacridine-1,8(2H,5H)-dione

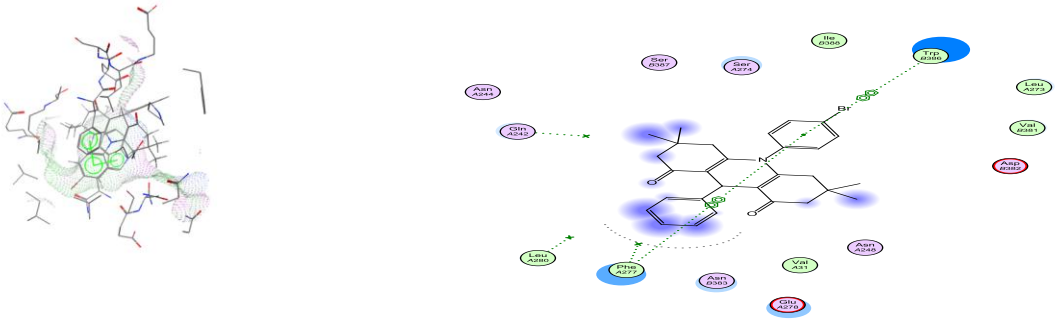

C63/ 10-(4-bromophenyl)-3,3,6,6-tetramethyl-9-phenyl-3,4,6,7,9,10-hexahydroacridine-1,8(2H,5H)-dione

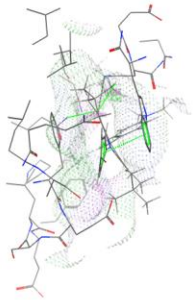

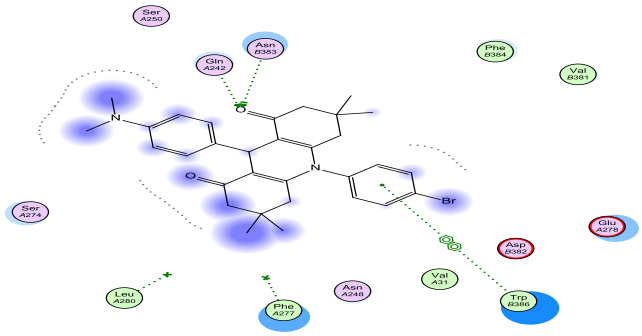

C64/ 10-(4-bromophenyl)-9-(4-(dimethylamino)phenyl)-3,3,6,6-tetramethyl-3,4,6,7,9,10-hexahydroacridine-1,8(2H,5H)-dione

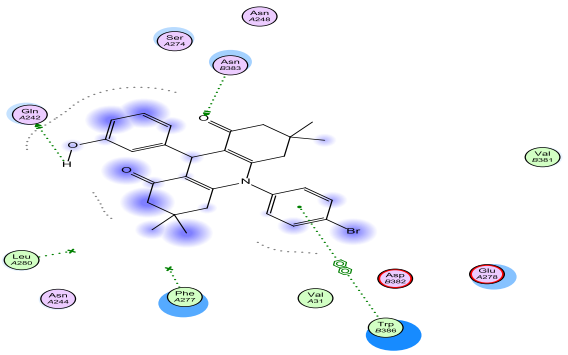

C65/ 10-(4-bromophenyl)-9-(2-hydroxyphenyl)-3,3,6,6-tetramethyl-3,4,6,7,9,10-hexahydroacridine-1,8(2H,5H)-dione

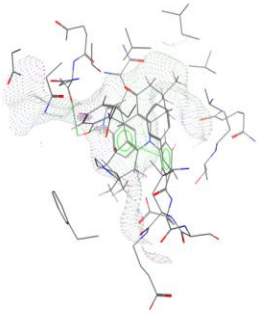

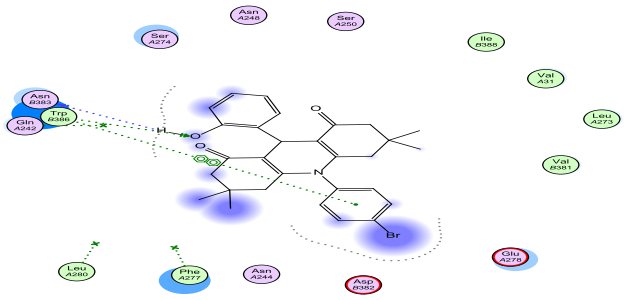

C66/ (E)-10-(4-bromophenyl)-3,3,6,6-tetramethyl-9-styryl-3,4,6,7,9,10-hexahydroacridine-1,8(2H,5H)-dione

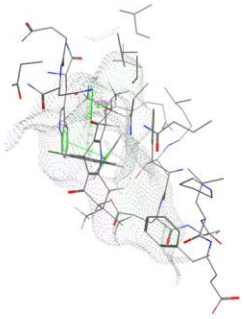

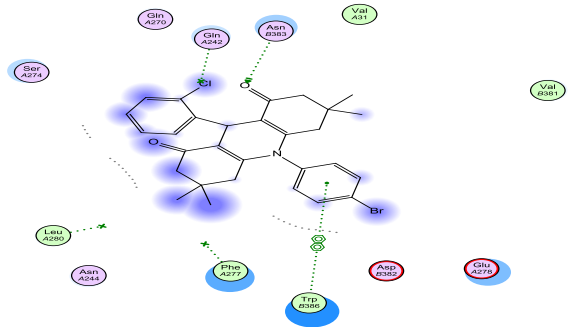

C67/ 10-(4-bromophenyl)-9-(2-chlorophenyl)-3,3,6,6-tetramethyl-3,4,6,7,9,10-hexahydroacridine-1,8(2H,5H)-dione

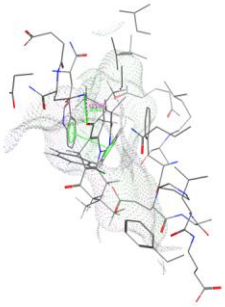

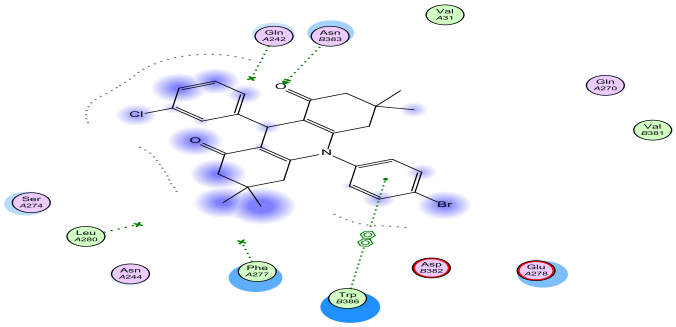

C68/ 10-(4-bromophenyl)-9-(3-chlorophenyl)-3,3,6,6-tetramethyl-3,4,6,7,9,10-hexahydroacridine-1,8(2H,5H)-dione

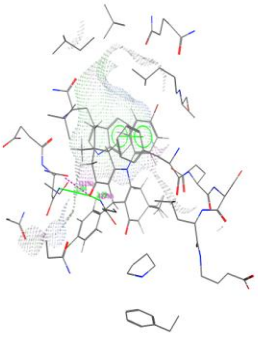

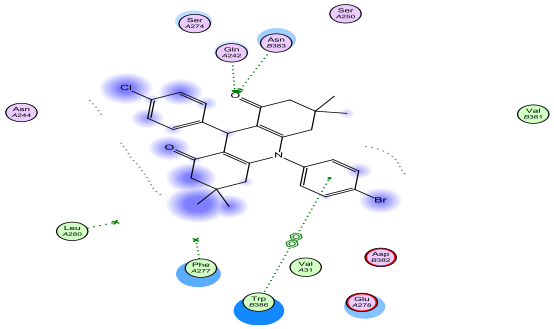

C69/ 10-(4-bromophenyl)-9-(4-chlorophenyl)-3,3,6,6-tetramethyl-3,4,6,7,9,10-hexahydroacridine-1,8(2H,5H)-dione

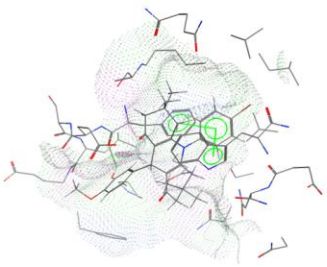

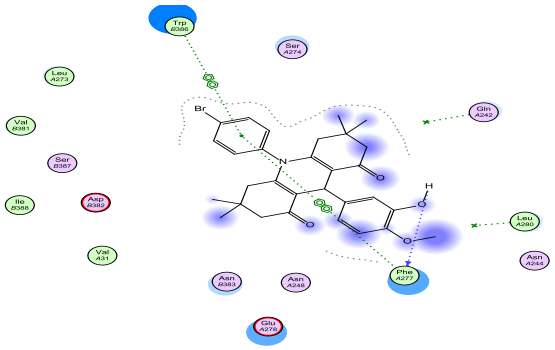

C70/ 10-(4-bromophenyl)-9-(3-hydroxy-4-methoxyphenyl)-3,3,6,6-tetramethyl-3,4,6,7,9,10-hexahydroacridine-1,8(2H,5H)-dione

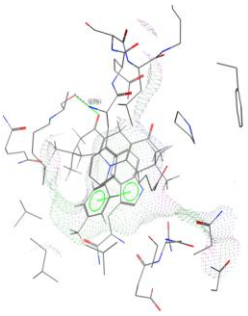

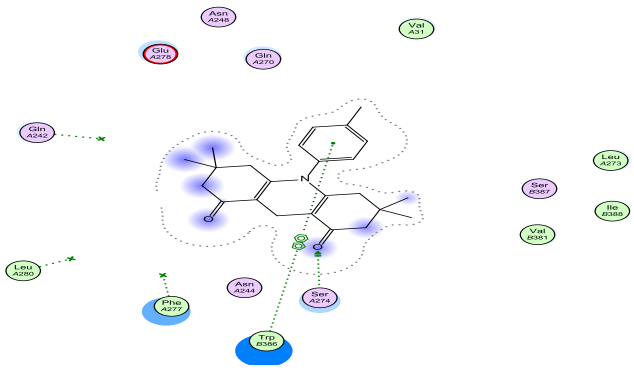

C71/ 3,3,6,6-tetramethyl-10-(p-tolyl)-3,4,6,7,9,10-hexahydroacridine-1,8(2H,5H)-dione

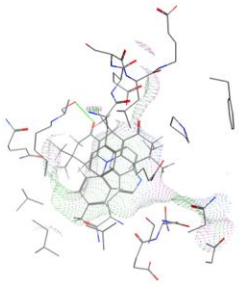

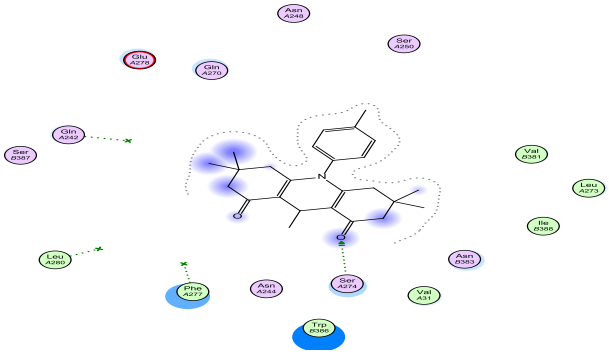

C72/ 3,3,6,6,9-pentamethyl-10-(p-tolyl)-3,4,6,7,9,10-hexahydroacridine-1,8(2H,5H)-dione

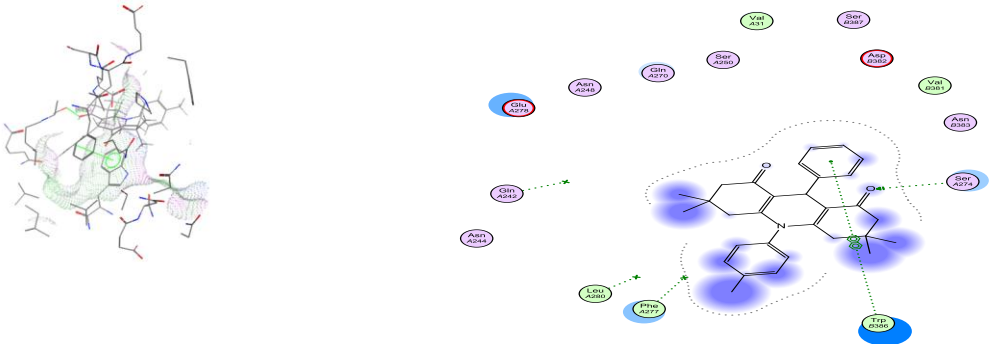

C73/ 3,3,6,6-tetramethyl-9-phenyl-10-(p-tolyl)-3,4,6,7,9,10-hexahydroacridine-1,8(2H,5H)-dione

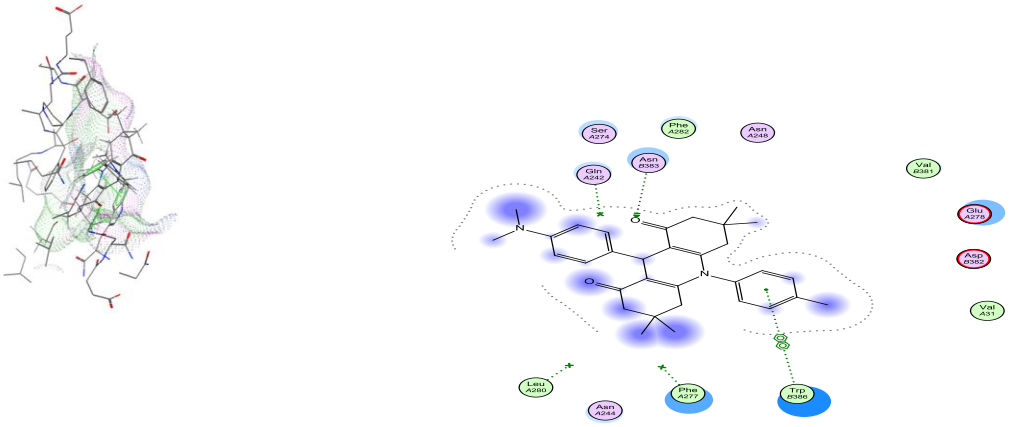

C74/ 9-(4-(dimethylamino)phenyl)-3,3,6,6-tetramethyl-10-(p-tolyl)-3,4,6,7,9,10-hexahydroacridine-1,8(2H,5H)-dione

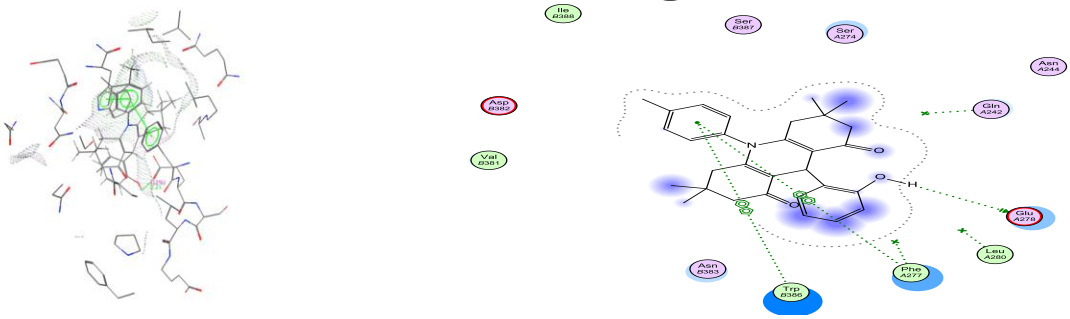

C75/ 9-(2-hydroxyphenyl)-3,3,6,6-tetramethyl-10-(p-tolyl)-3,4,6,7,9,10-hexahydroacridine-1,8(2H,5H)-dione.

***Figures (Q1-Q75).** Showed 3D and 2D, interaction of Docking of polyhydruquinoline derivatives inside the active site of 4gdb protein.

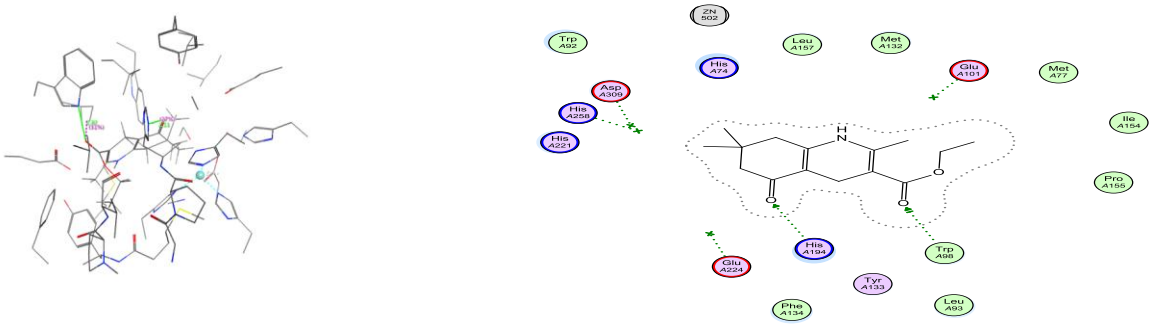

Q1 . Ethyl 2,7,7-trimethyl-5-oxo-1,4,5,6,7,8-hexahydroquinoline-3-carboxylate.

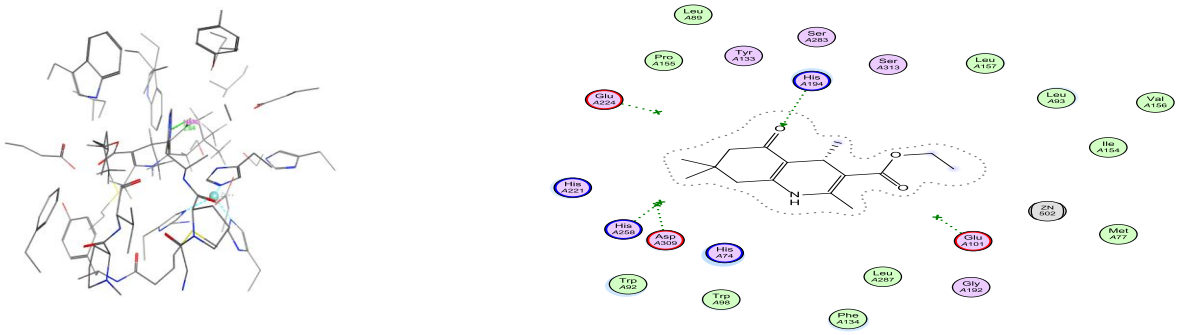

Q2 . Ethyl 2,4,7,7-tetramethyl-5-oxo-1,4,5,6,7,8-hexahydroquinoline-3-carboxylate.

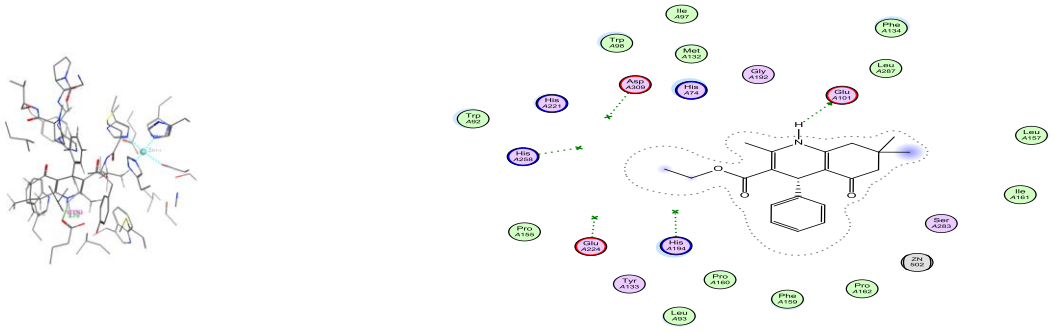

Q3 . Ethyl 2,7,7-trimethyl-5-oxo-4-phenyl-1,4,5,6,7,8-hexahydroquinoline-3-carboxylate.

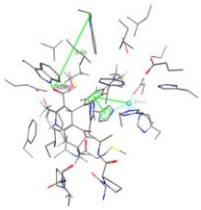

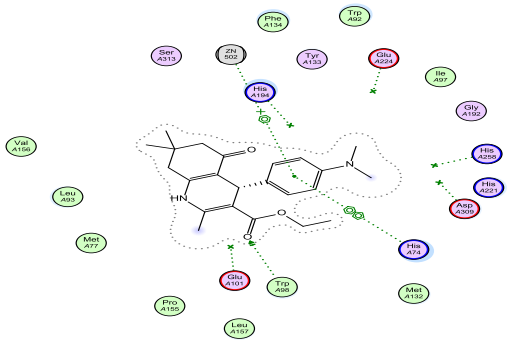

Q4 . Ethyl 4-(4-(dimethylamino)phenyl)-2,7,7-trimethyl-5-oxo-1,4,5,6,7,8-hexahydroquinoline-3-carboxylate.

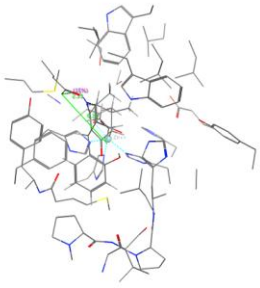

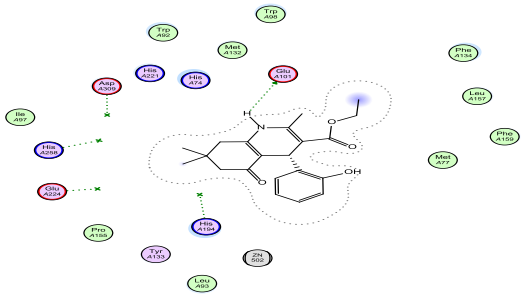

Q5. Ethyl 4-(2-hydroxyphenyl)-2,7,7-trimethyl-5-oxo-1,4,5,6,7,8-hexahydroquinoline-3-carboxylate.

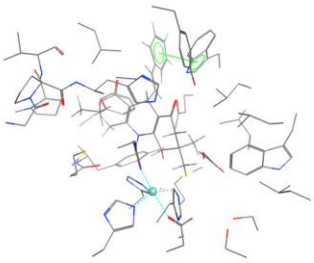

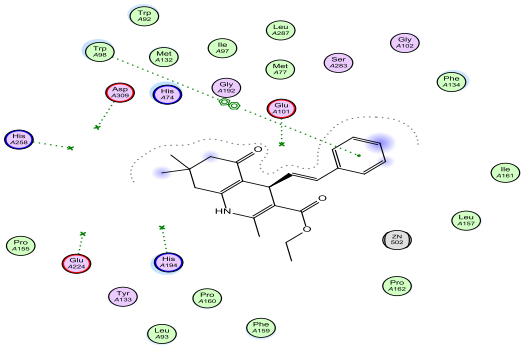

Q6. Ethyl 4-(3-hydroxyphenyl)-2,7,7-trimethyl-5-oxo-1,4,5,6,7,8-hexahydroquinoline-3-carboxylate .

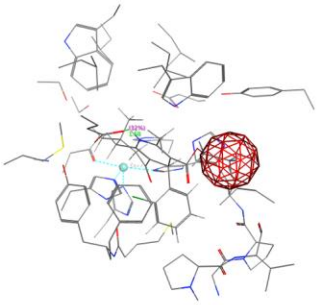

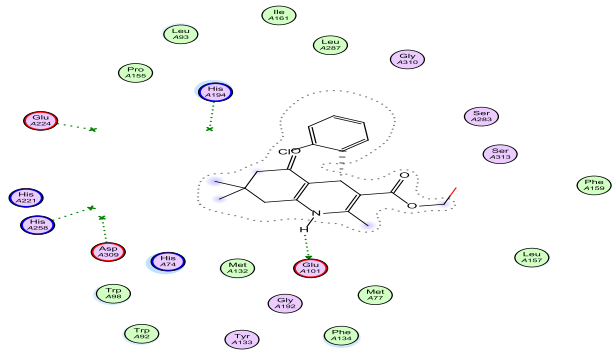

Q7. Ethyl 4-(2-chlorophenyl)-2,7,7-trimethyl-5-oxo-1,4,5,6,7,8-hexahydroquinoline-3-carboxylate .

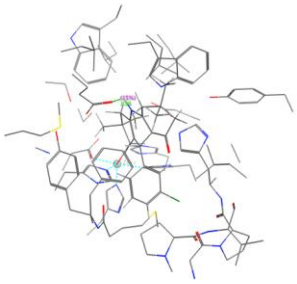

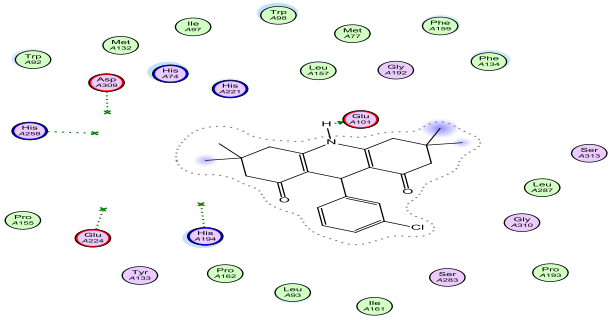

Q8. Ethyl 4-(3-chlorophenyl)-2,7,7-trimethyl-5-oxo-1,4,5,6,7,8-hexahydroquinoline-3-carboxylate.

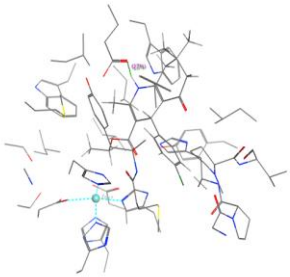

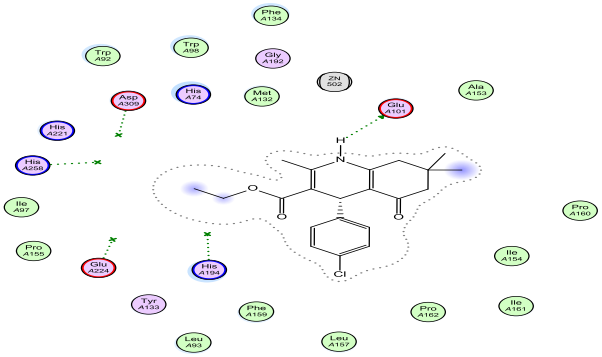

Q9. Ethyl 4-(4-chlorophenyl)-2,7,7-trimethyl-5-oxo-1,4,5,6,7,8-hexahydroquinoline-3-carboxylate.

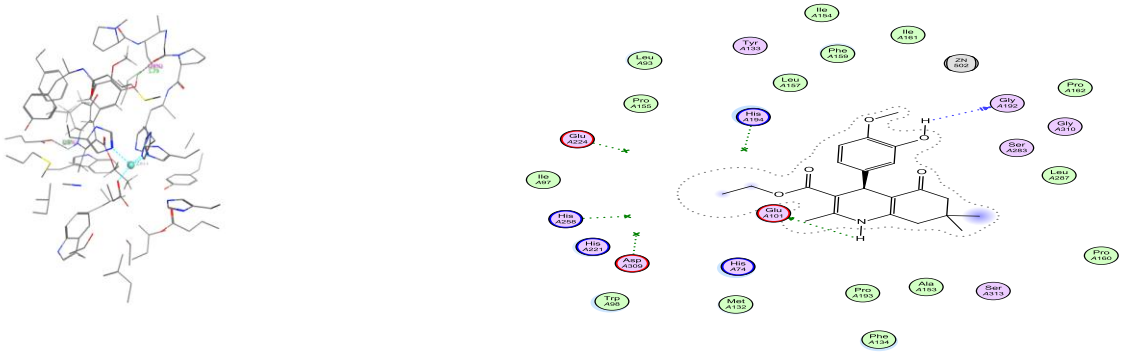

Q10. Ethyl 4-(3-hydroxy-4-methoxyphenyl)-2,7,7-trimethyl-5-oxo-1,4,5,6,7,8-hexahydroquinoline-3-carboxylate.

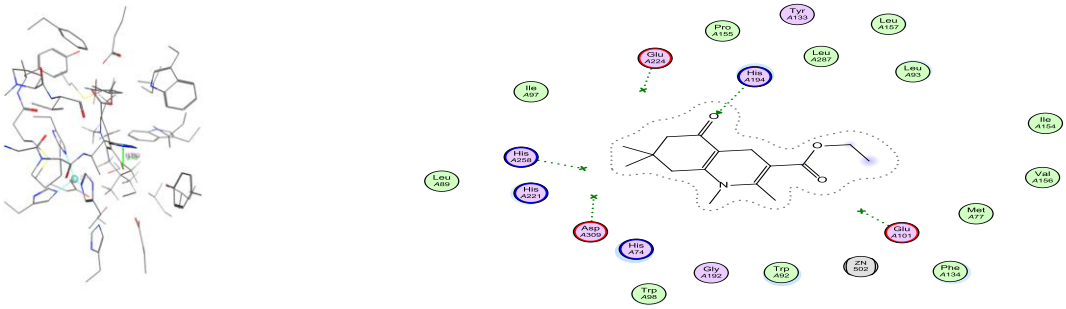

Q11. Ethyl 1,2,7,7-tetramethyl-5-oxo-1,4,5,6,7,8-hexahydroquinoline-3-carboxylate.

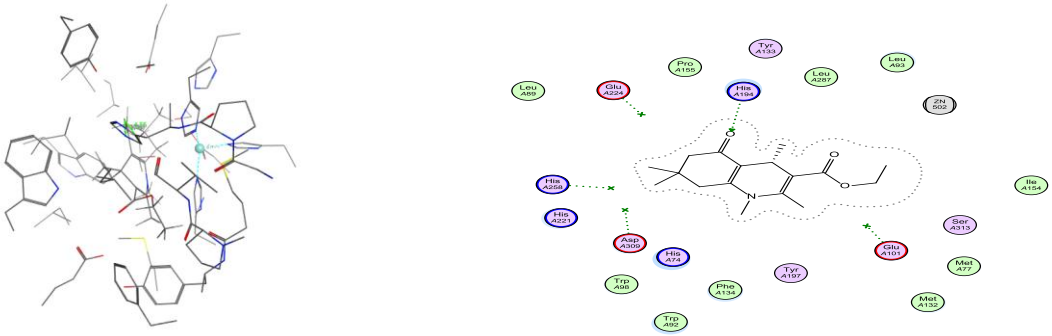

Q12. Ethyl 1,2,4,7,7-pentamethyl-5-oxo-1,4,5,6,7,8-hexahydroquinoline-3-carboxylate.

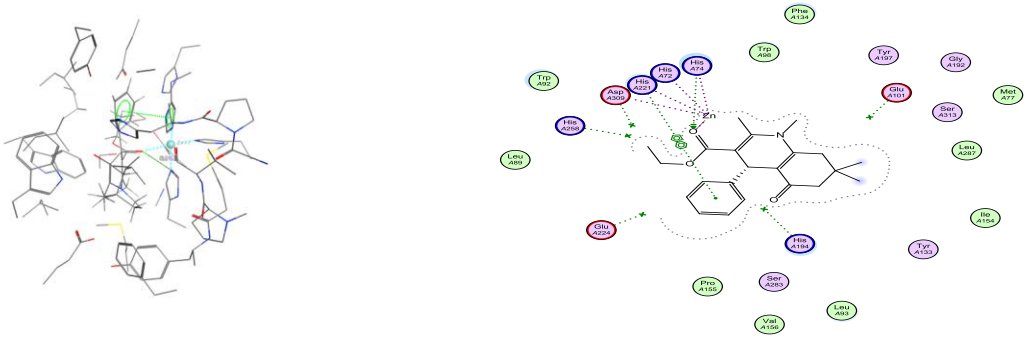

Q13. Ethyl 1,2,7,7-tetramethyl-5-oxo-4-phenyl-1,4,5,6,7,8-hexahydroquinoline-3-carboxylate.

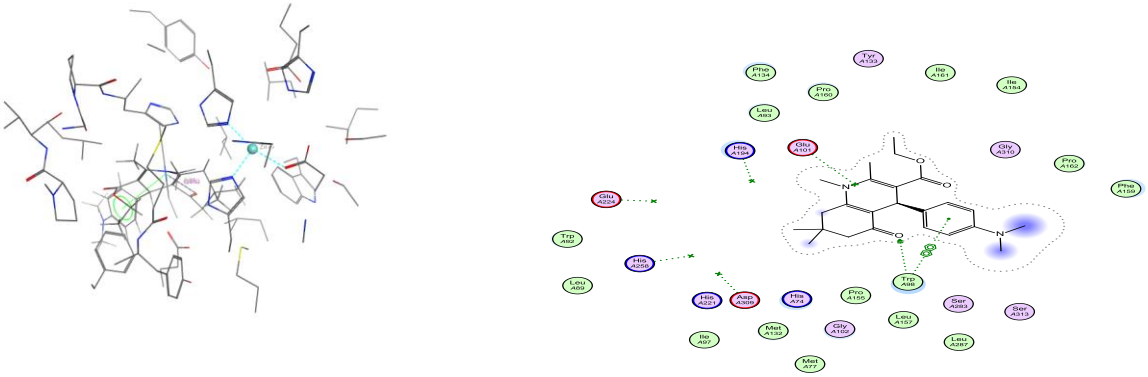

Q14. Ethyl 4-(4-(dimethylamino)phenyl)-1,2,7,7-tetramethyl-5-oxo-1,4,5,6,7,8-hexahydroquinoline-3-carboxylate.

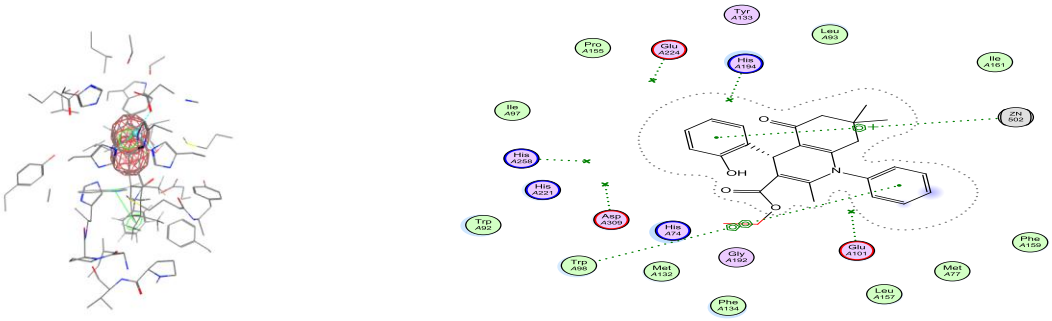

Q15. Ethyl 4-(2-hydroxyphenyl)-1,2,7,7-tetramethyl-5-oxo-1,4,5,6,7,8-hexahydroquinoline-3-carboxylate.

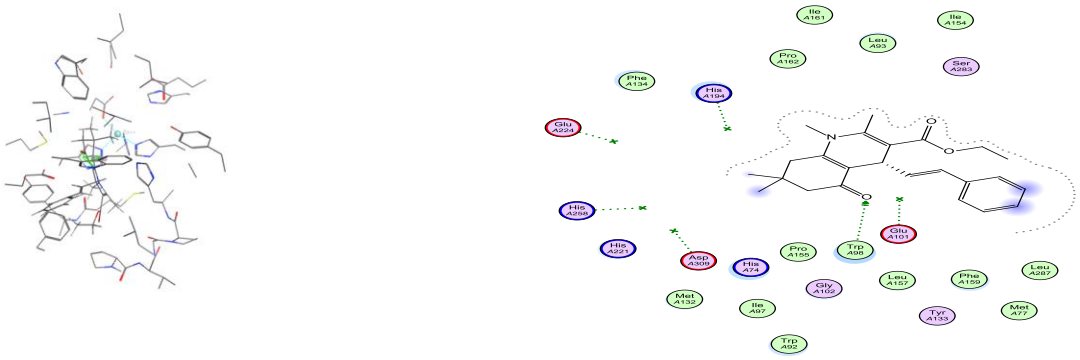

Q16. Ethyl (E)-1,2,7,7-tetramethyl-5-oxo-4-styryl-1,4,5,6,7,8-hexahydroquinoline-3-carboxylate

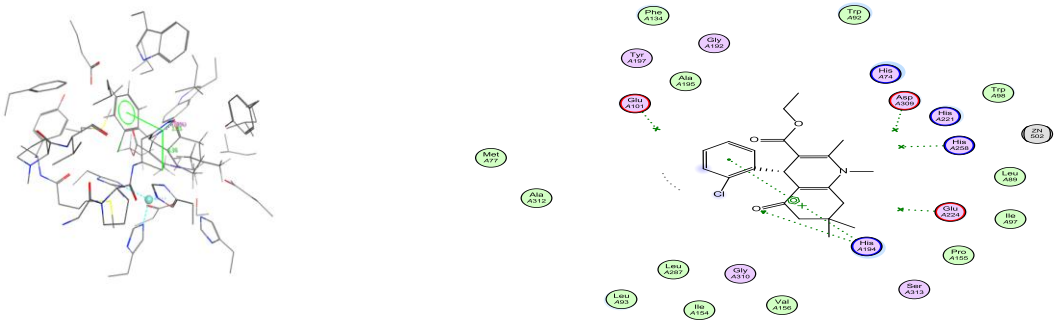

Q17 . Ethyl 4-(2-chlorophenyl)-1,2,7,7-tetramethyl-5-oxo-1,4,5,6,7,8-hexahydroquinoline-3-carboxylate

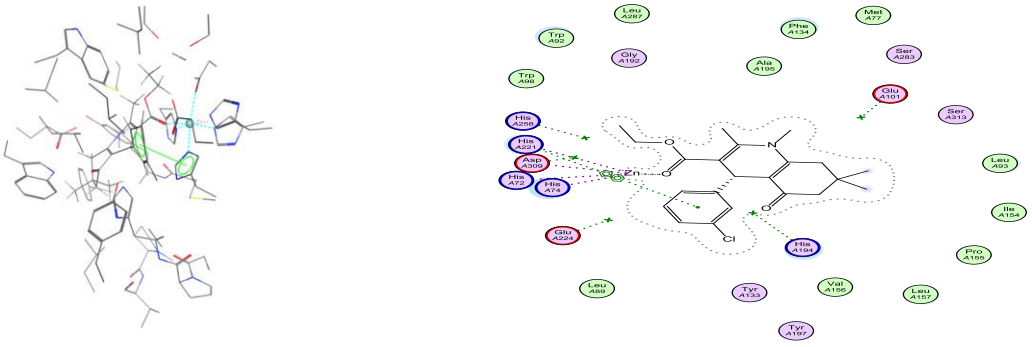

Q18. Ethyl 4-(3-chlorophenyl)-1,2,7,7-tetramethyl-5-oxo-1,4,5,6,7,8-hexahydroquinoline-3-carboxylate.

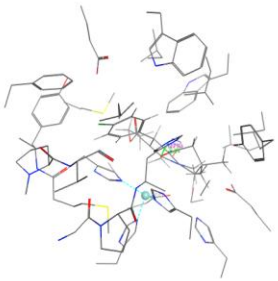

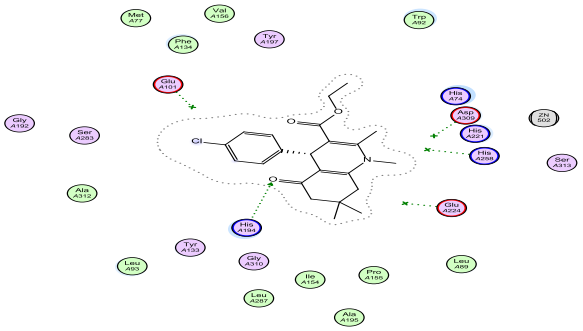

Q19. Ethyl 4-(4-chlorophenyl)-1,2,7,7-tetramethyl-5-oxo-1,4,5,6,7,8-hexahydroquinoline-3-carboxylate

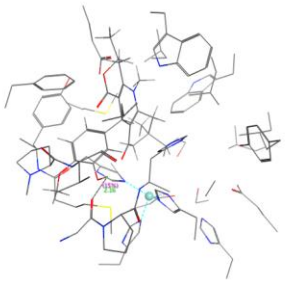

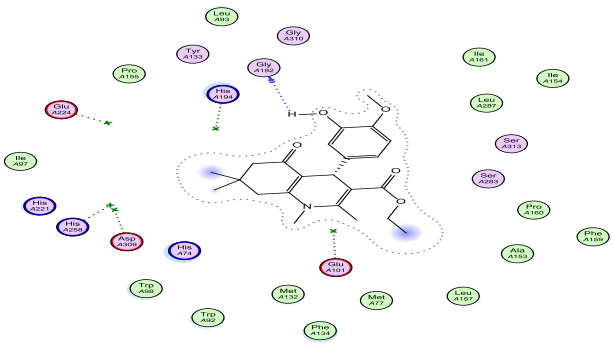

Q20. Ethyl 4-(3-hydroxy-4-methoxyphenyl)-1,2,7,7-tetramethyl-5-oxo-1,4,5,6,7,8-hexahydroquinoline-3-carboxylate.

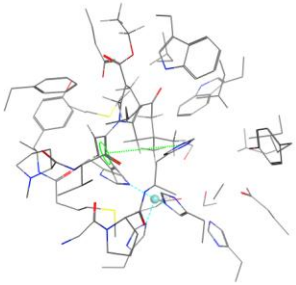

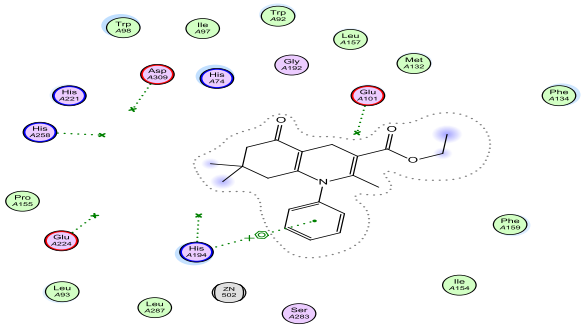

Q21. Ethyl 2,7,7-trimethyl-5-oxo-1-phenyl-1,4,5,6,7,8-hexahydroquinoline-3-carboxylate.

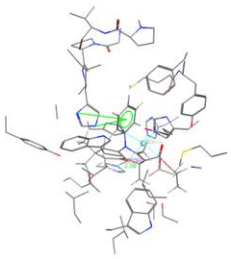

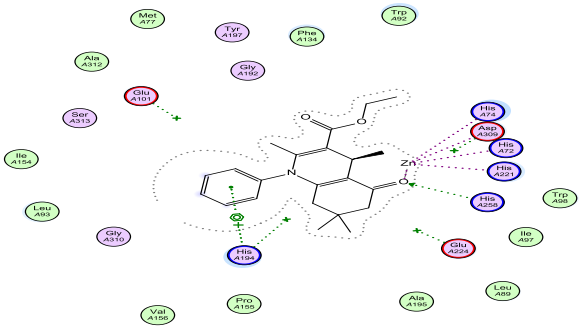

Q22. Ethyl 2,4,7,7-tetramethyl-5-oxo-1-phenyl-1,4,5,6,7,8-hexahydroquinoline-3-carboxylate

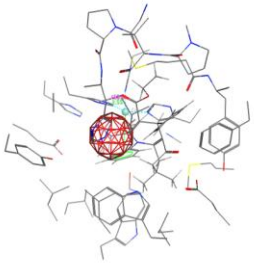

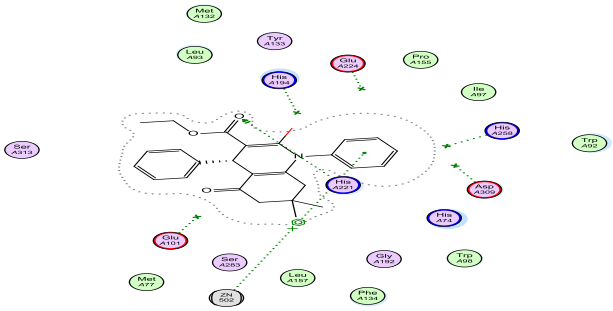

Q23. Ethyl 2,7,7-trimethyl-5-oxo-1,4-diphenyl-1,4,5,6,7,8-hexahydroquinoline-3-carboxylate

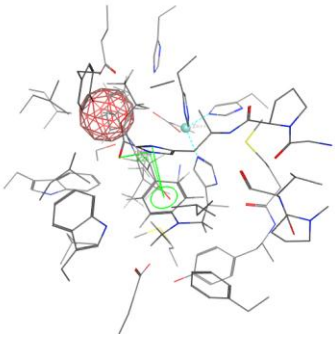

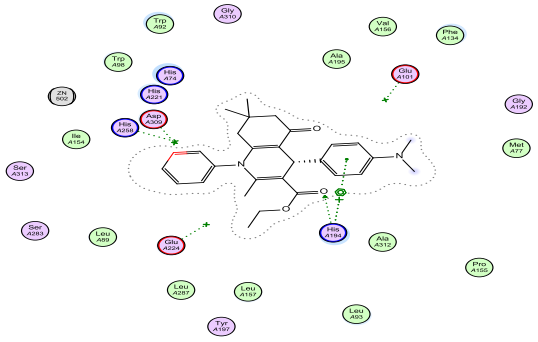

Q24. Ethyl 4-(4-(dimethylamino)phenyl)-2,7,7-trimethyl-5-oxo-1-phenyl-1,4,5,6,7,8-hexahydroquinoline-3-carboxylate.

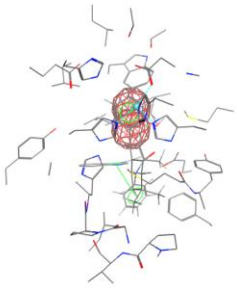

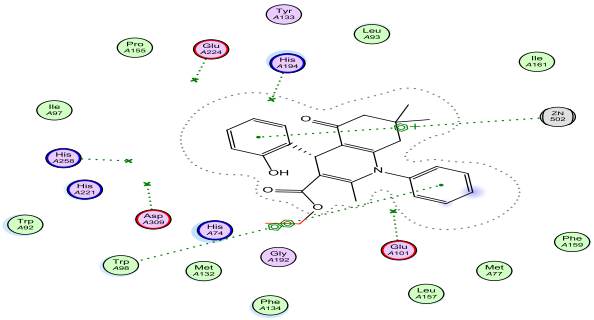

Q25. Ethyl 4-(2-hydroxyphenyl)-2,7,7-trimethyl-5-oxo-1-phenyl-1,4,5,6,7,8-hexahydroquinoline-3-carboxylate.

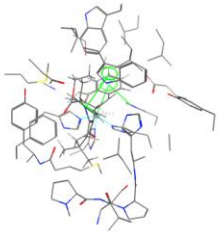

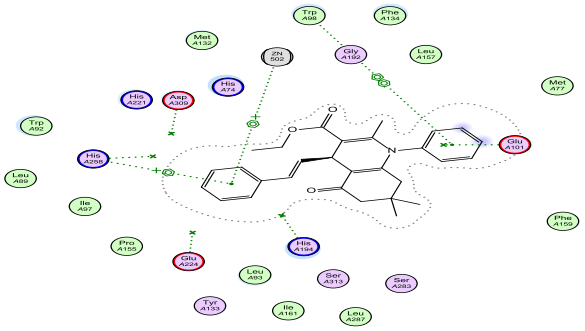

Q26. Ethyl (E)-2,7,7-trimethyl-5-oxo-1-phenyl-4-styryl-1,4,5,6,7,8-hexahydroquinoline-3-carboxylate.

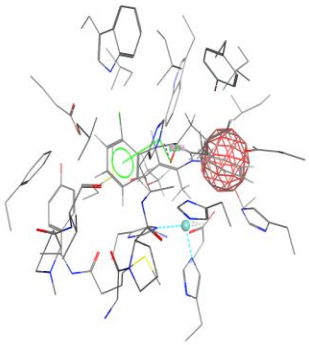

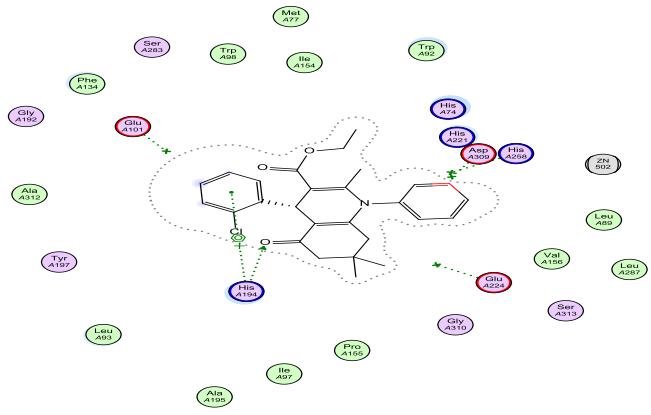

Q27. Ethyl 4-(2-chlorophenyl)-2,7,7-trimethyl-5-oxo-1-phenyl-1,4,5,6,7,8-hexahydroquinoline-3-carboxylate.

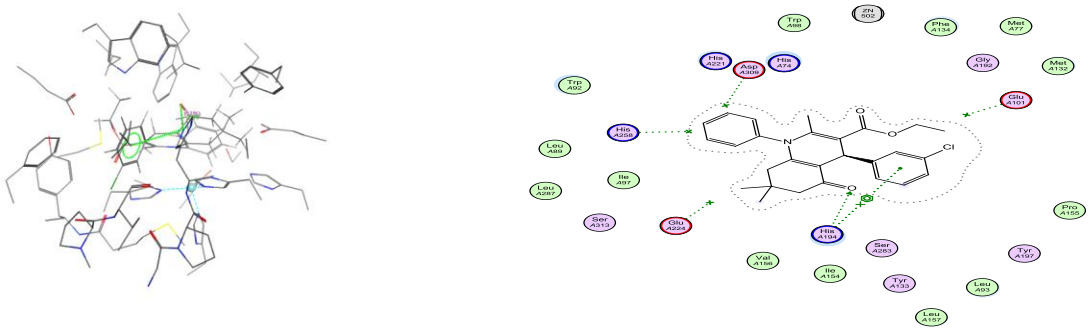

Q28. Ethyl 4-(3-chlorophenyl)-2,7,7-trimethyl-5-oxo-1-phenyl-1,4,5,6,7,8-hexahydroquinoline-3-carboxylate

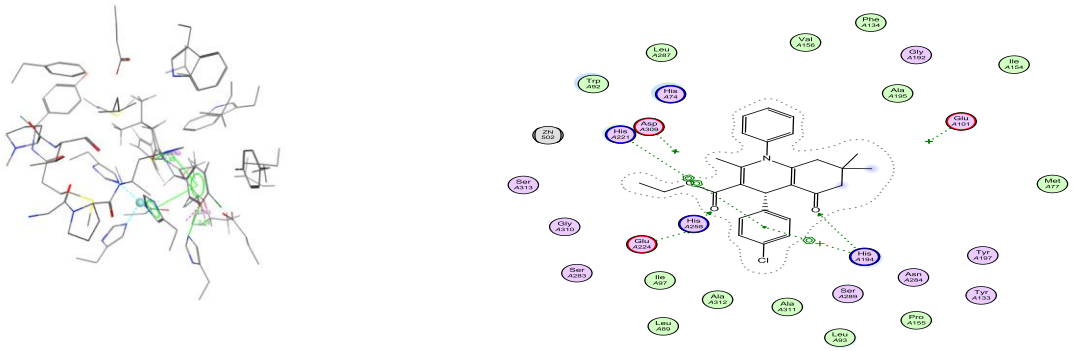

Q29. Ethyl 4-(4-chlorophenyl)-2,7,7-trimethyl-5-oxo-1-phenyl-1,4,5,6,7,8-hexahydroquinoline-3-carboxylate.

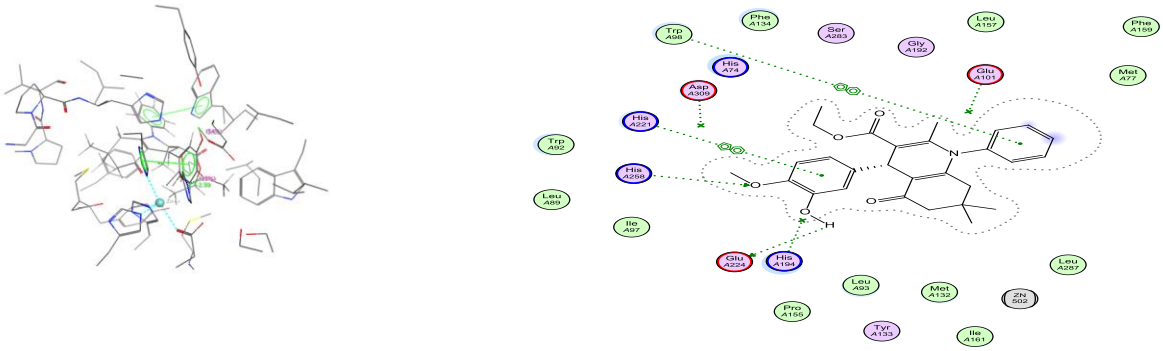

Q30. Ethyl 4-(3-hydroxy-4-methoxyphenyl)-2,7,7-trimethyl-5-oxo-1-phenyl-1,4,5,6,7,8-hexahydroquinoline-3-carboxylate.

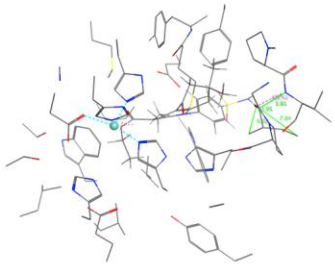

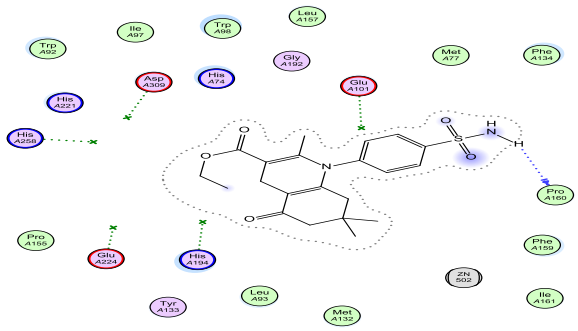

Q31. Ethyl 2,7,7-trimethyl-5-oxo-1-(4-sulfamoylphenyl)-1,4,5,6,7,8-hexahydroquinoline-3-carboxylate.

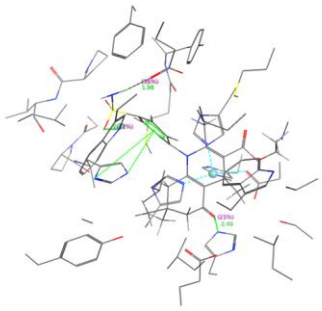

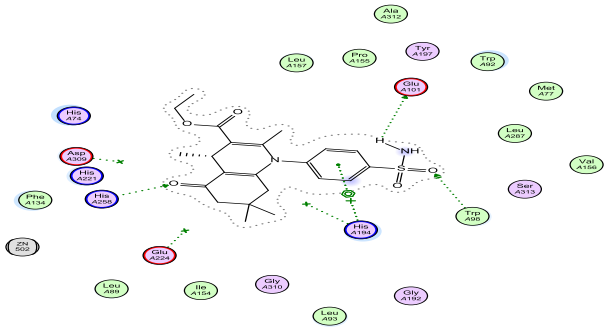

Q32. Ethyl 2,4,7,7-tetramethyl-5-oxo-1-(4-sulfamoylphenyl)-1,4,5,6,7,8-hexahydroquinoline-3-carboxylate.

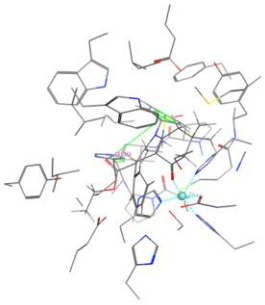

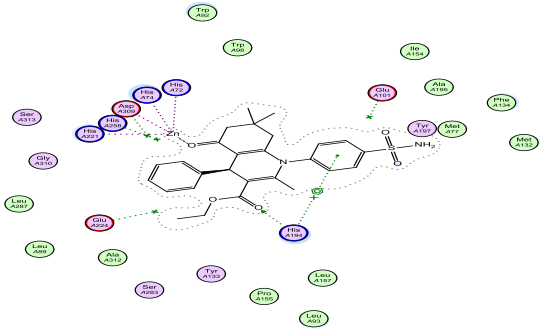

Q33. Ethyl 2,7,7-trimethyl-5-oxo-4-phenyl-1-(4-sulfamoylphenyl)-1,4,5,6,7,8-hexahydroquinoline-3-carboxylate.

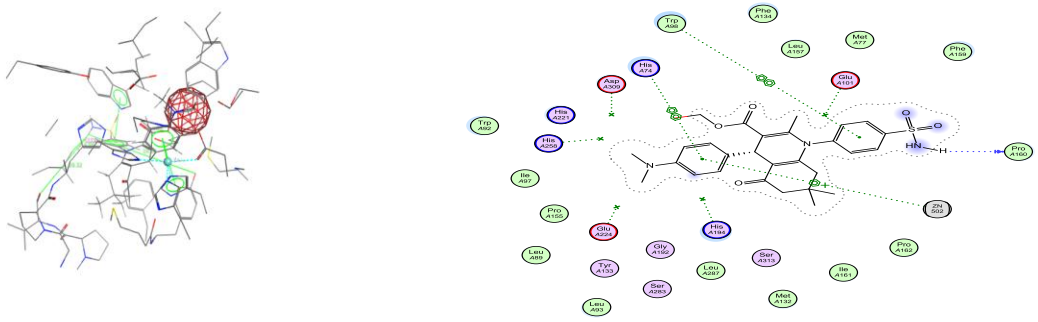

Q34. Ethyl 4-(4-(dimethylamino)phenyl)-2,7,7-trimethyl-5-oxo-1-(4-sulfamoylphenyl)-1,4,5,6,7,8-hexahydroquinoline-3-carboxylate.

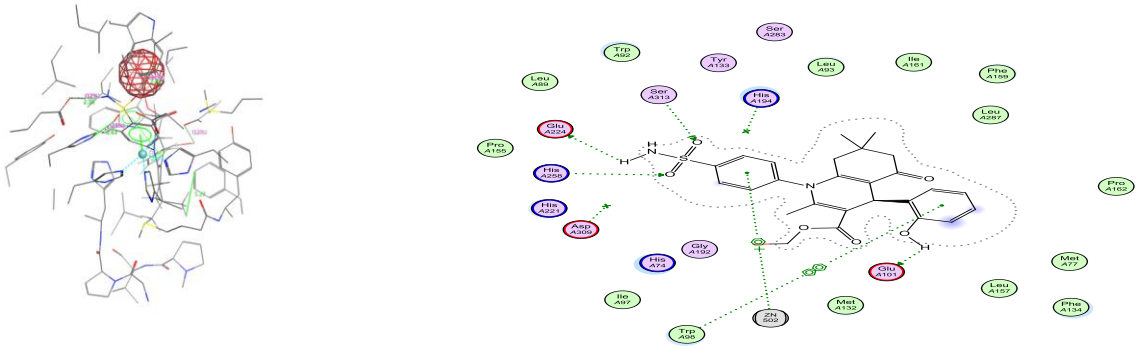

Q35. Ethyl 4-(2-hydroxyphenyl)-2,7,7-trimethyl-5-oxo-1-(4-sulfamoylphenyl)-1,4,5,6,7,8-hexahydroquinoline-3-carboxylate.

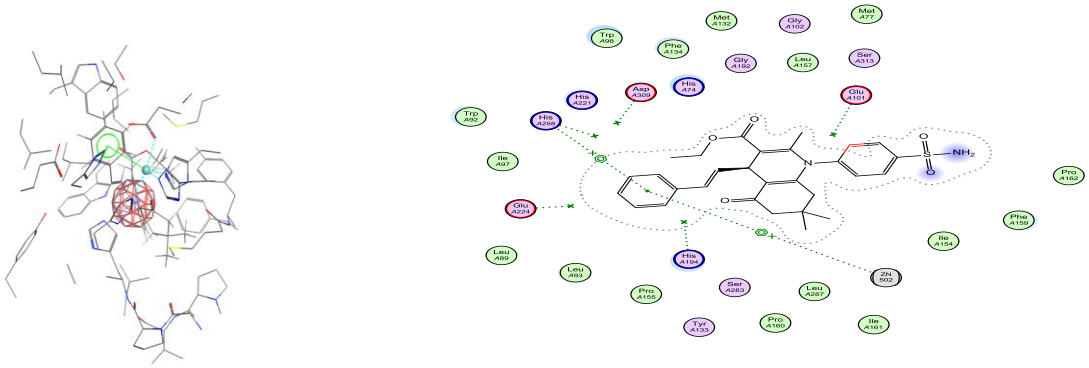

Q36. Ethyl (E)-2,7,7-trimethyl-5-oxo-4-styryl-1-(4-sulfamoylphenyl)-1,4,5,6,7,8-hexahydroquinoline-3-carboxylate.

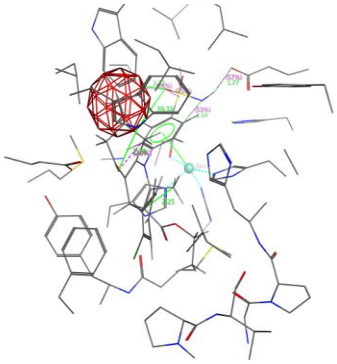

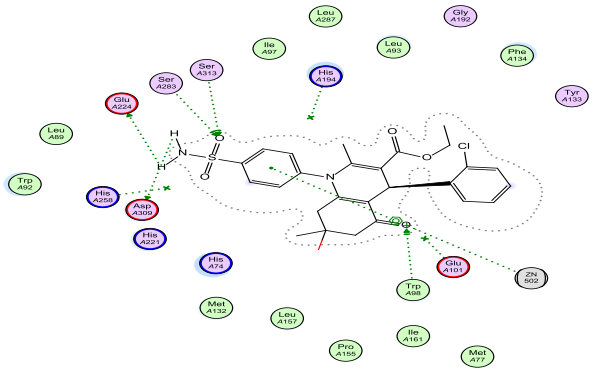

Q37. Eethyl 4-(2-chlorophenyl)-2,7,7-trimethyl-5-oxo-1-(4-sulfamoylphenyl)-1,4,5,6,7,8-hexahydroquinoline-3-carboxylate.

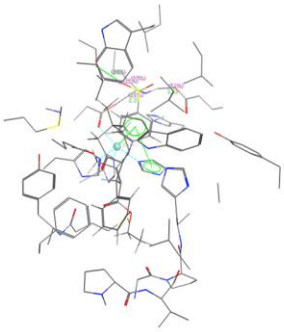

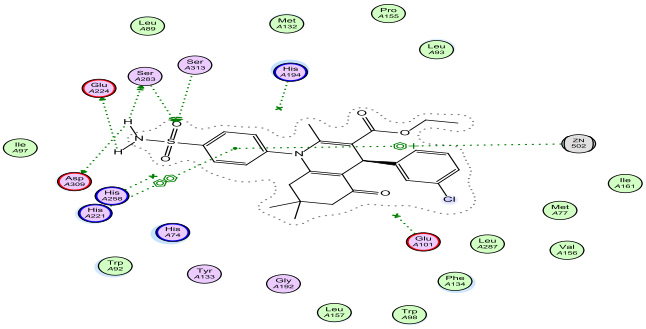

Q38. Ethyl 4-(3-chlorophenyl)-2,7,7-trimethyl-5-oxo-1-(4-sulfamoylphenyl)-1,4,5,6,7,8-hexahydroquinoline-3-carboxylate.

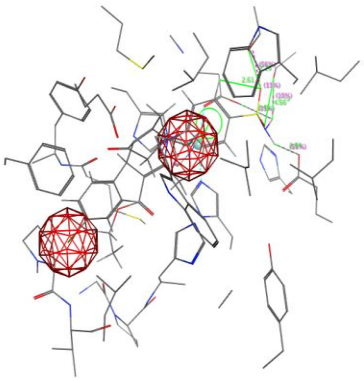

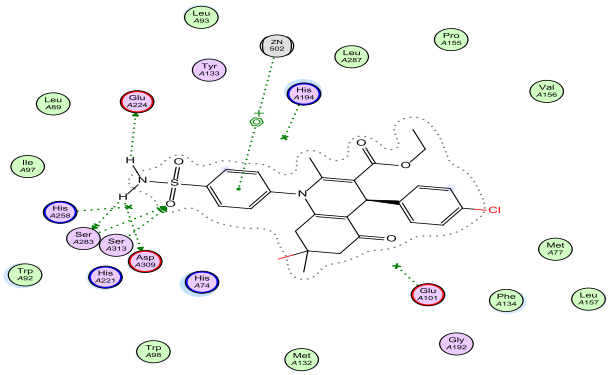

Q39. Ethyl 4-(4-chlorophenyl)-2,7,7-trimethyl-5-oxo-1-(4-sulfamoylphenyl)-1,4,5,6,7,8-hexahydroquinoline-3-carboxylate.

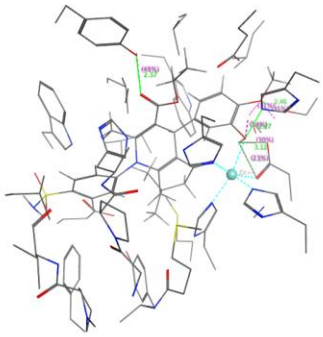

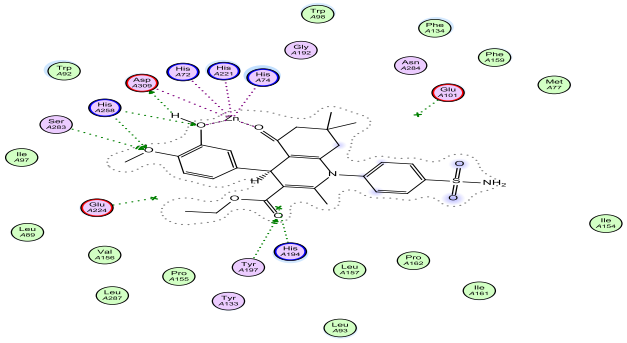

Q40. Ethyl 4-(3-hydroxy-4-methoxyphenyl)-2,7,7-trimethyl-5-oxo-1-(4-sulfamoylphenyl)-1,4,5,6,7,8-hexahydroquinoline-3-carboxylate.

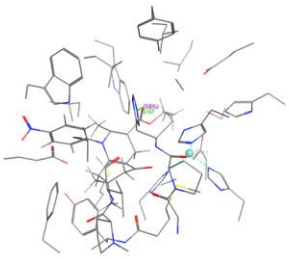

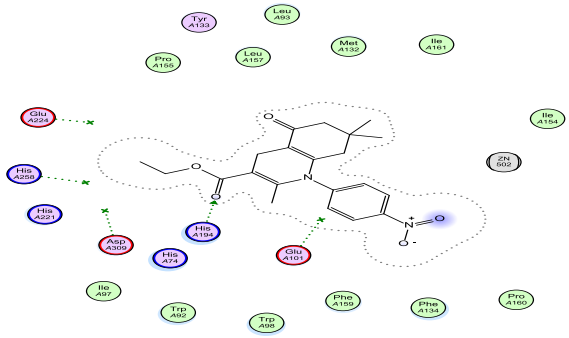

Q41. Ethyl 2,7,7-trimethyl-1-(4-nitrophenyl)-5-oxo-1,4,5,6,7,8-hexahydroquinoline-3-carboxylate

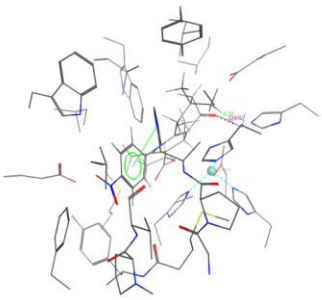

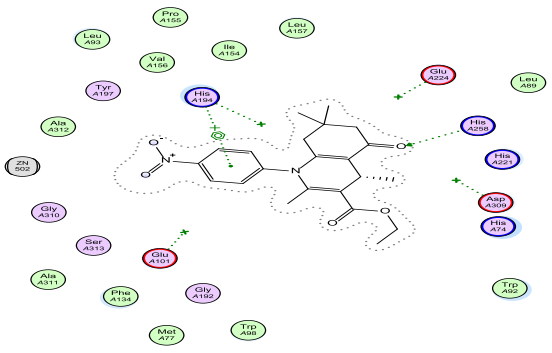

Q42. Ethyl 2,4,7,7-tetramethyl-1-(4-nitrophenyl)-5-oxo-1,4,5,6,7,8-hexahydroquinoline-3-carboxylate)

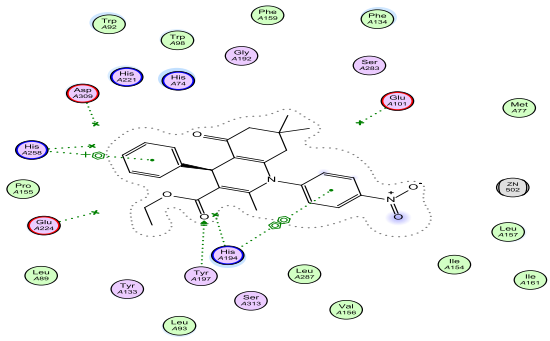

Q43. Ethyl 2,7,7-trimethyl-1-(4-nitrophenyl)-5-oxo-4-phenyl-1,4,5,6,7,8-hexahydroquinoline-3-carboxylate.

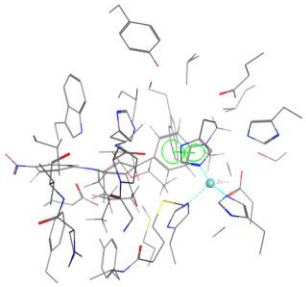

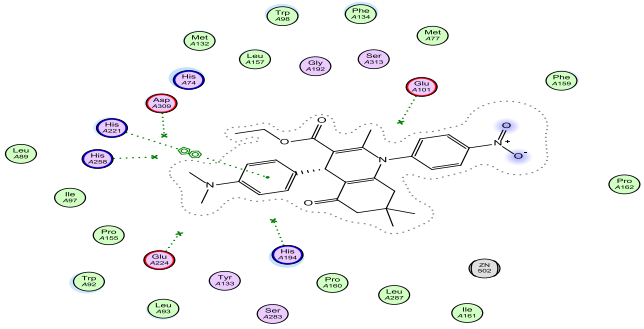

Q44. Ethyl 4-(4-(dimethylamino)phenyl)-2,7,7-trimethyl-1-(4-nitrophenyl)-5-oxo-1,4,5,6,7,8-hexahydroquinoline-3-carboxylate

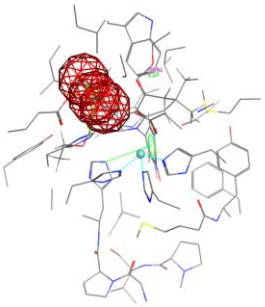

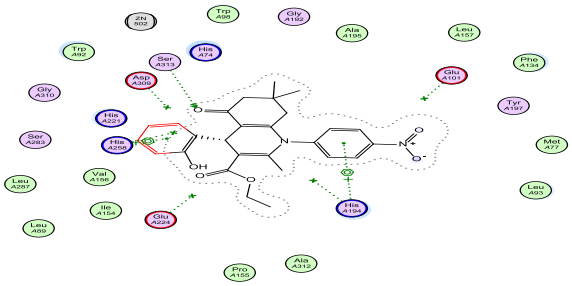

Q45. Ethyl 4-(2-hydroxyphenyl)-2,7,7-trimethyl-1-(4-nitrophenyl)-5-oxo-1,4,5,6,7,8-hexahydroquinoline-3-carboxylate.

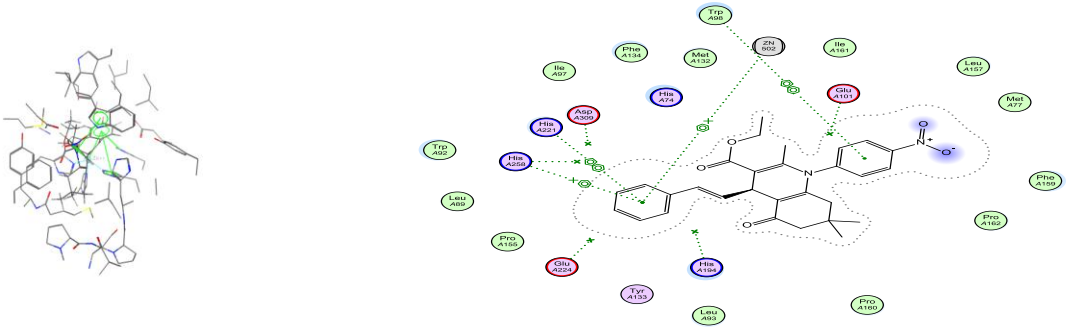

Q46. Ethyl (E)-2,7,7-trimethyl-1-(4-nitrophenyl)-5-oxo-4-styryl-1,4,5,6,7,8-hexahydroquinoline-3-carboxylate

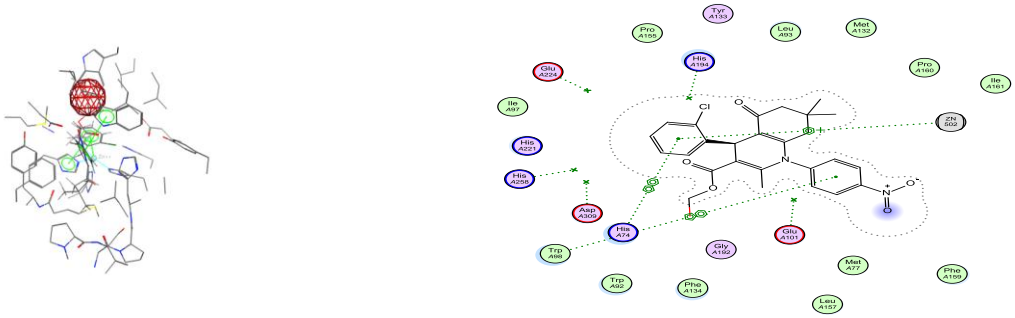

Q47. Ethyl 4-(2-chlorophenyl)-2,7,7-trimethyl-1-(4-nitrophenyl)-5-oxo-1,4,5,6,7,8-hexahydroquinoline-3-carboxylate

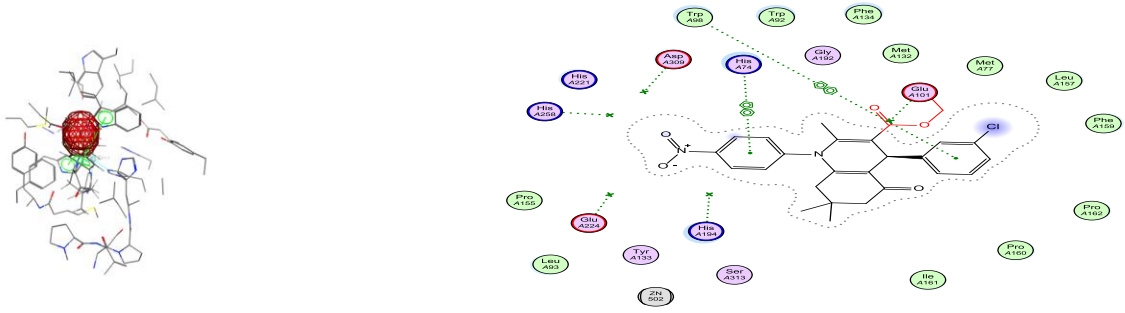

Q48. Ethyl 4-(3-chlorophenyl)-2,7,7-trimethyl-1-(4-nitrophenyl)-5-oxo-1,4,5,6,7,8-hexahydroquinoline-3-carboxylate

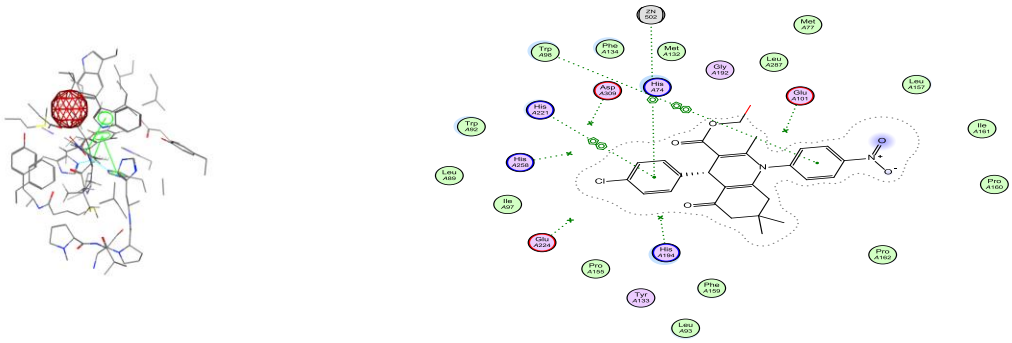

Q49. Ethyl 4-(4-chlorophenyl)-2,7,7-trimethyl-1-(4-nitrophenyl)-5-oxo-1,4,5,6,7,8-hexahydroquinoline-3-carboxylate

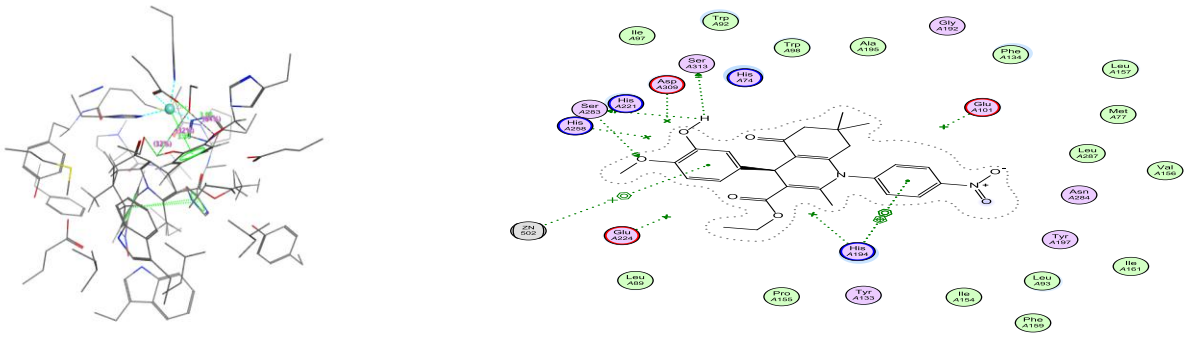

Q50. Ethyl 4-(3-hydroxy-4-methoxyphenyl)-2,7,7-trimethyl-1-(4-nitrophenyl)-5-oxo-1,4,5,6,7,8-hexahydroquinoline-3-carboxylate

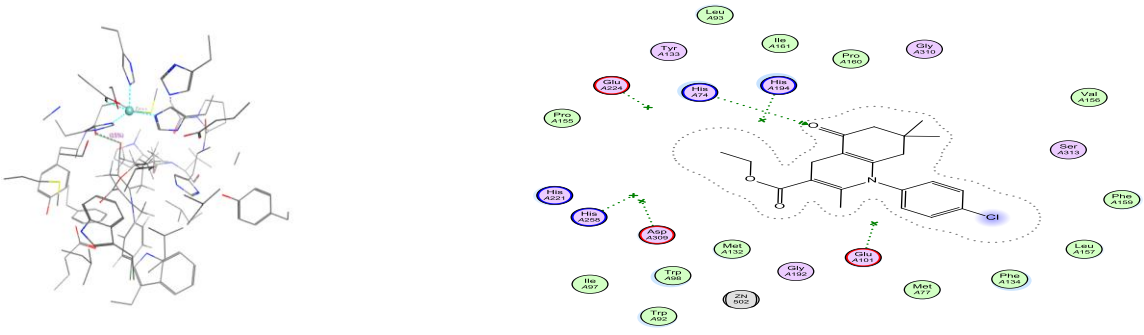

Q51. Ethyl 1-(4-chlorophenyl)-2,7,7-trimethyl-5-oxo-1,4,5,6,7,8-hexahydroquinoline-3-carboxylate

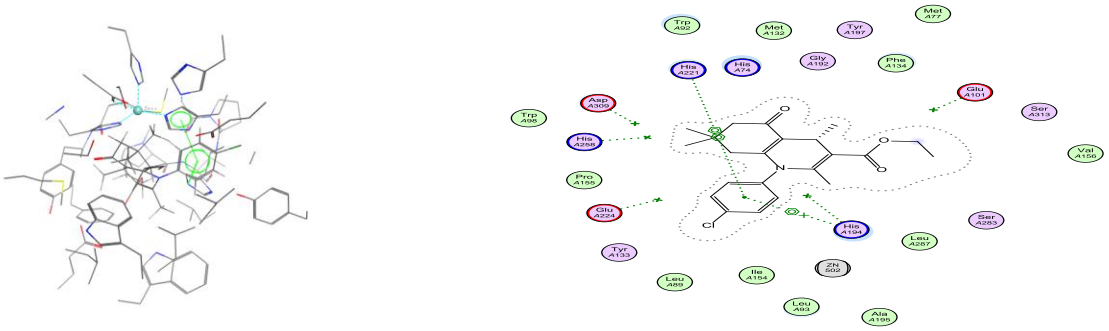

Q52. Ethyl 1-(4-chlorophenyl)-2,4,7,7-tetramethyl-5-oxo-1,4,5,6,7,8-hexahydroquinoline-3-carboxylate

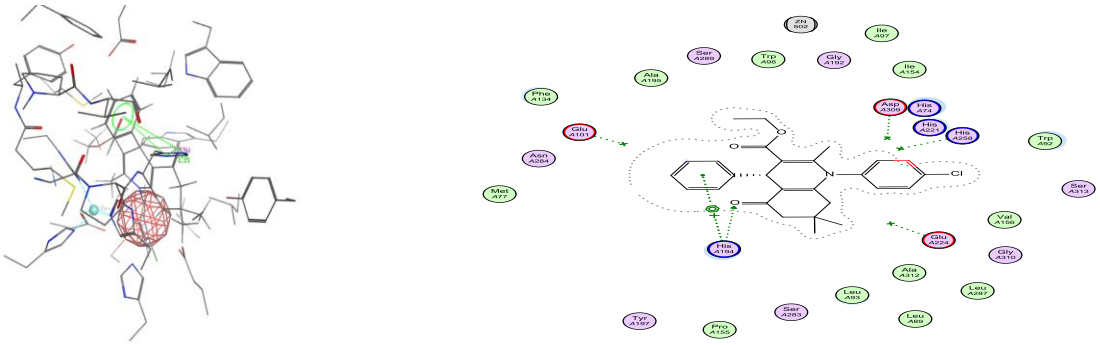

Q53. Ethyl 1-(4-chlorophenyl)-2,7,7-trimethyl-5-oxo-4-phenyl-1,4,5,6,7,8-hexahydroquinoline-3-carboxylate

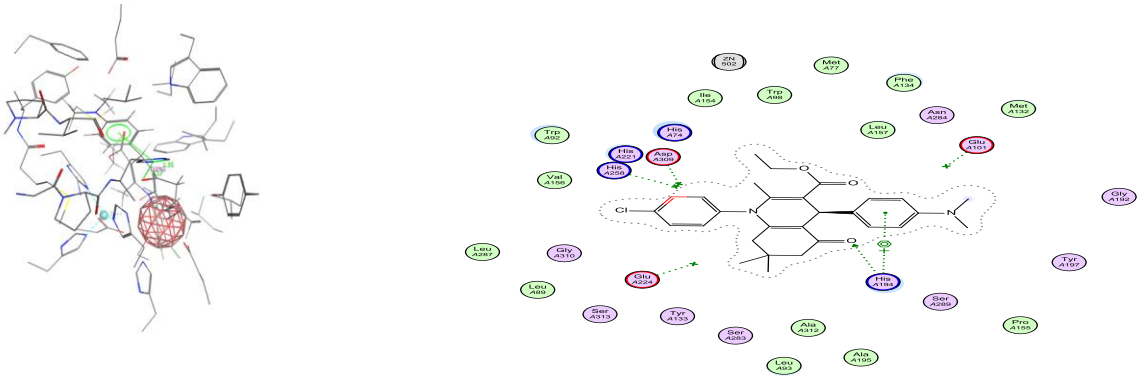

Q54. Ethyl 1-(4-chlorophenyl)-4-(4-(dimethylamino)phenyl)-2,7,7-trimethyl-5-oxo-1,4,5,6,7,8-hexahydroquinoline-3-carboxylate

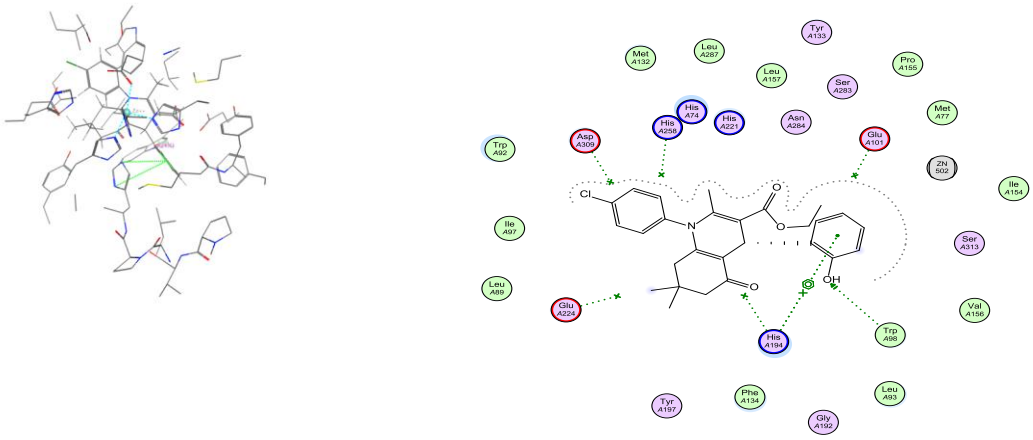

Q55. Ethyl 1-(4-chlorophenyl)-4-(2-hydroxyphenyl)-2,7,7-trimethyl-5-oxo-1,4,5,6,7,8-hexahydroquinoline-3-carboxylate

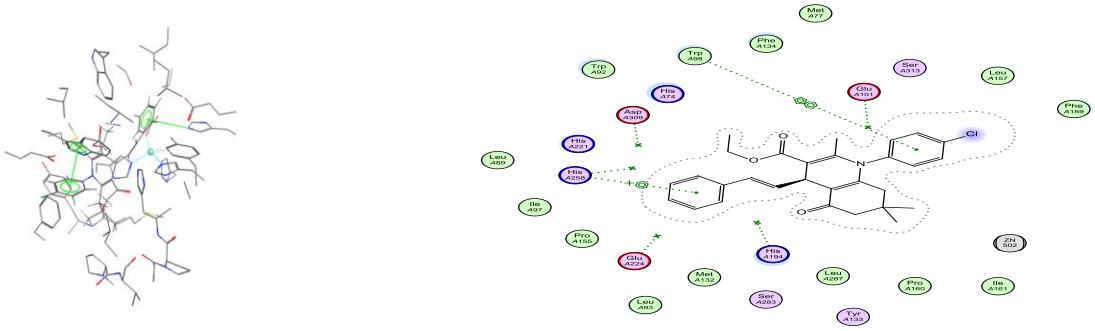

Q56. Ethyl (E)-1-(4-chlorophenyl)-2,7,7-trimethyl-5-oxo-4-styryl-1,4,5,6,7,8-hexahydroquinoline-3-carboxylate

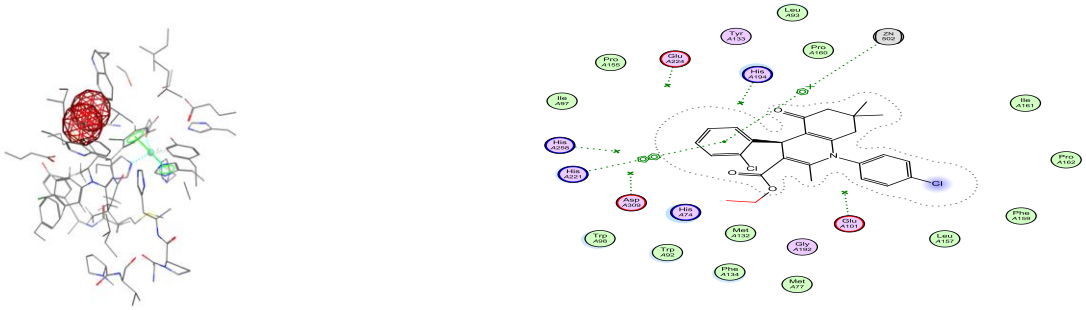

Q57. Ethyl 4-(2-chlorophenyl)-1-(4-chlorophenyl)-2,7,7-trimethyl-5-oxo-1,4,5,6,7,8-hexahydroquinoline-3-carboxylate

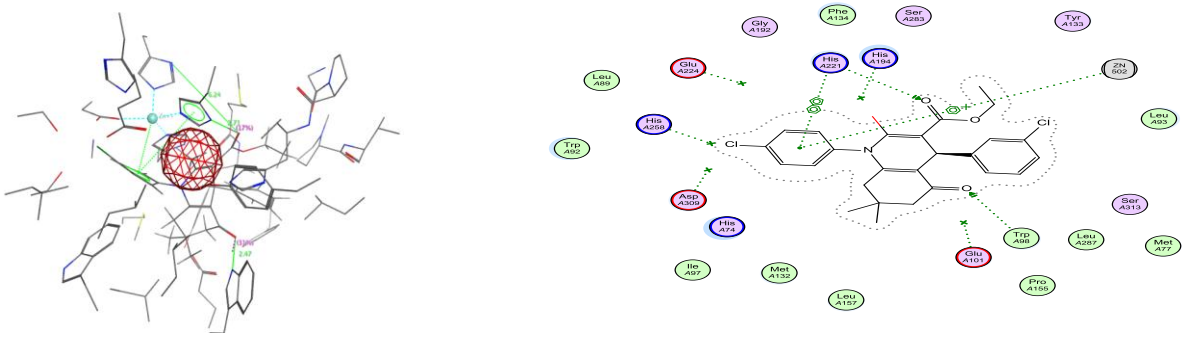

Q58. Ethyl 4-(3-chlorophenyl)-1-(4-chlorophenyl)-2,7,7-trimethyl-5-oxo-1,4,5,6,7,8-hexahydroquinoline-3-carboxylate

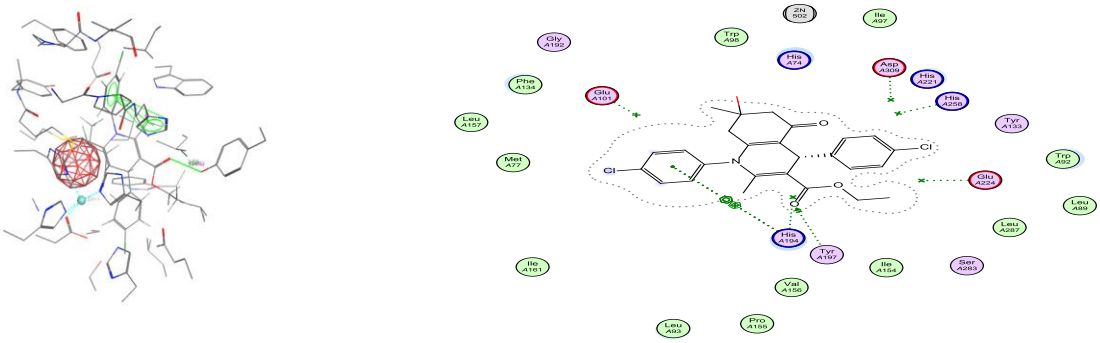

Q59. Ethyl 1,4-bis(4-chlorophenyl)-2,7,7-trimethyl-5-oxo-1,4,5,6,7,8-hexahydroquinoline-3-carboxylate

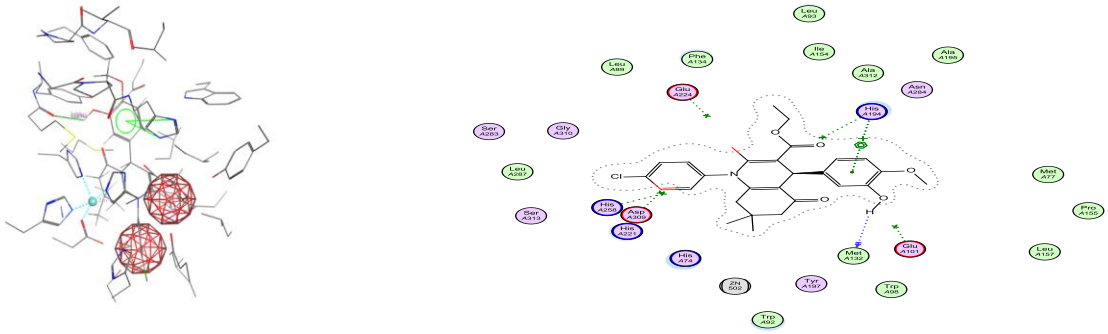

Q60. Ethyl 1-(4-chlorophenyl)-4-(3-hydroxy-4-methoxyphenyl)-2,7,7-trimethyl-5-oxo-1,4,5,6,7,8-hexahydroquinoline-3-carboxylate

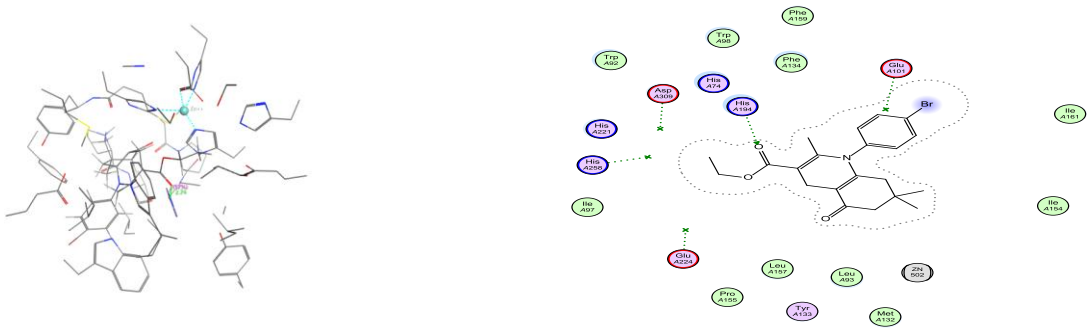

Q61. Ethyl 1-(4-bromophenyl)-2,7,7-trimethyl-5-oxo-1,4,5,6,7,8-hexahydroquinoline-3-carboxylate

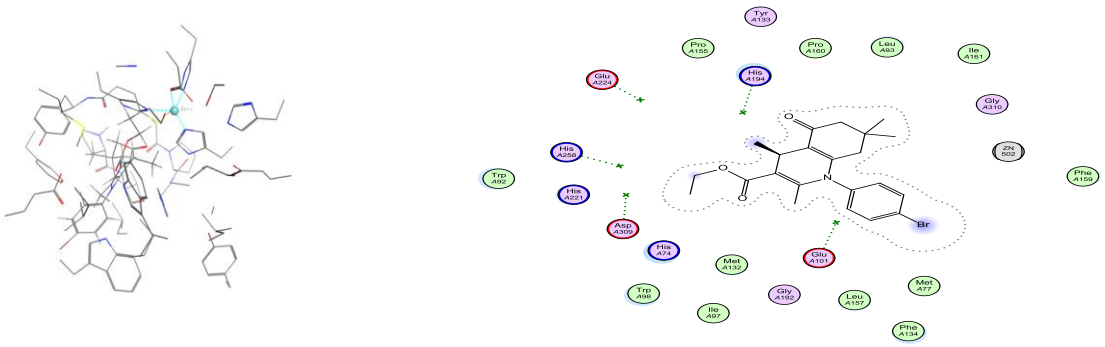

Q62. Ethyl 1-(4-bromophenyl)-2,4,7,7-tetramethyl-5-oxo-1,4,5,6,7,8-hexahydroquinoline-3-carboxylate

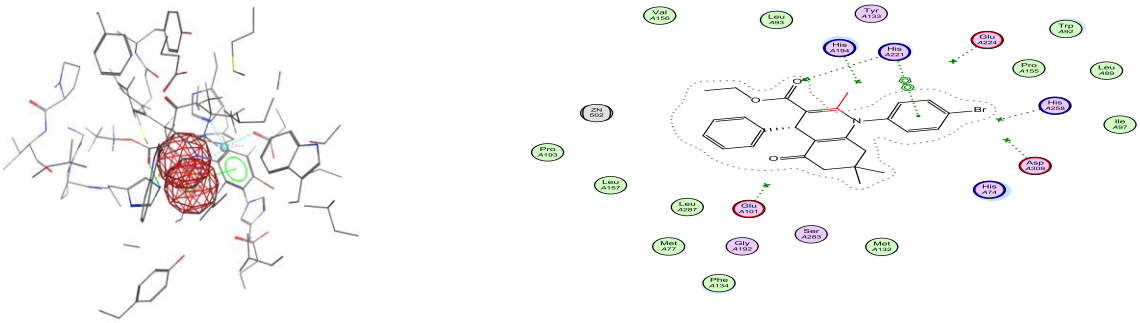

Q63. Ethyl 1-(4-bromophenyl)-2,7,7-trimethyl-5-oxo-4-phenyl-1,4,5,6,7,8-hexahydroquinoline-3-carboxylate

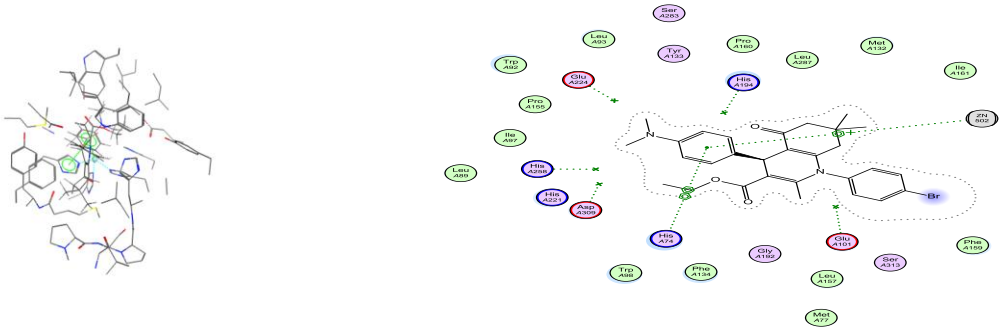

Q64. Ethyl 1-(4-bromophenyl)-4-(4-(dimethylamino)phenyl)-2,7,7-trimethyl-5-oxo-1,4,5,6,7,8-hexahydroquinoline-3-carboxylate

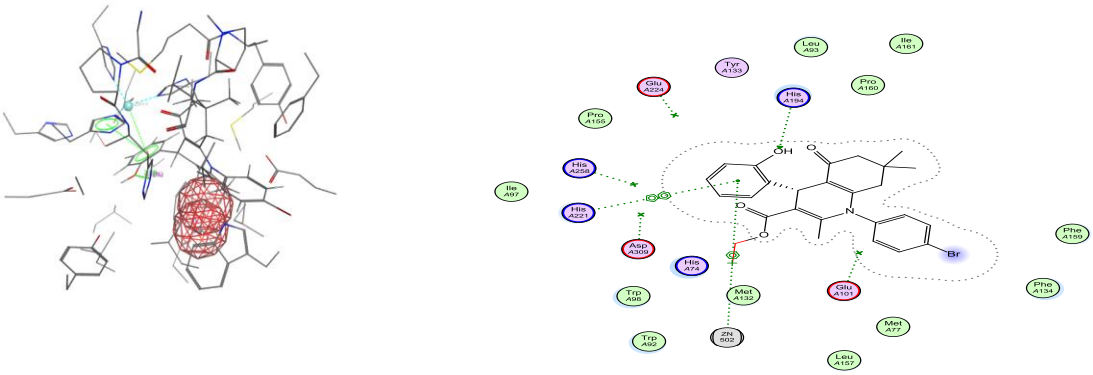

Q65. Ethyl 1-(4-bromophenyl)-4-(2-hydroxyphenyl)-2,7,7-trimethyl-5-oxo-1,4,5,6,7,8-hexahydroquinoline-3-carboxylate

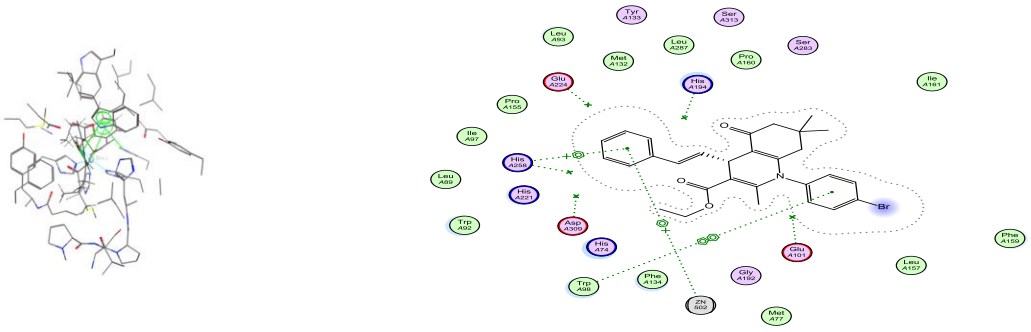

Q66. Ethyl (E)-1-(4-bromophenyl)-2,7,7-trimethyl-5-oxo-4-styryl-1,4,5,6,7,8-hexahydroquinoline-3-carboxylate

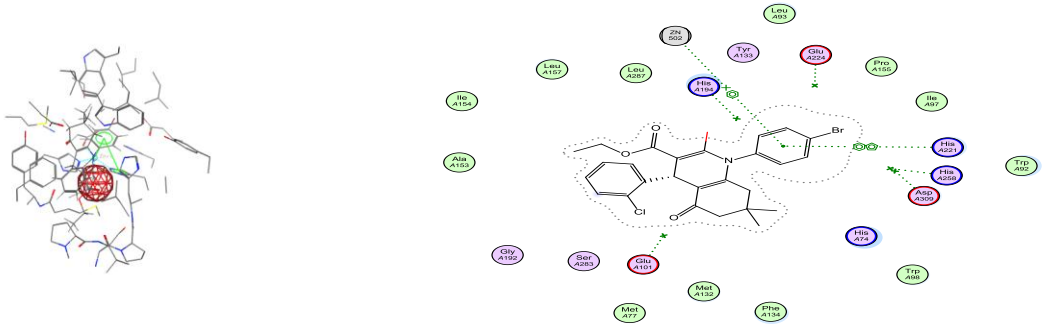

Q67. Ethyl 1-(4-bromophenyl)-4-(2-chlorophenyl)-2,7,7-trimethyl-5-oxo-1,4,5,6,7,8-hexahydroquinoline-3-carboxylate

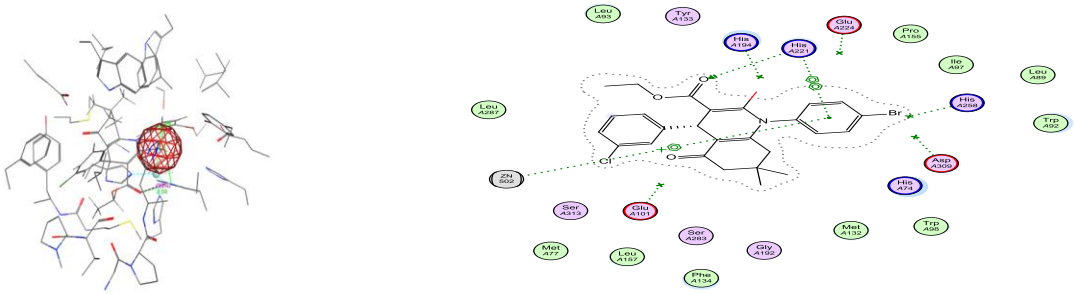

Q68. Ethyl 1-(4-bromophenyl)-4-(3-chlorophenyl)-2,7,7-trimethyl-5-oxo-1,4,5,6,7,8-hexahydroquinoline-3-carboxylate

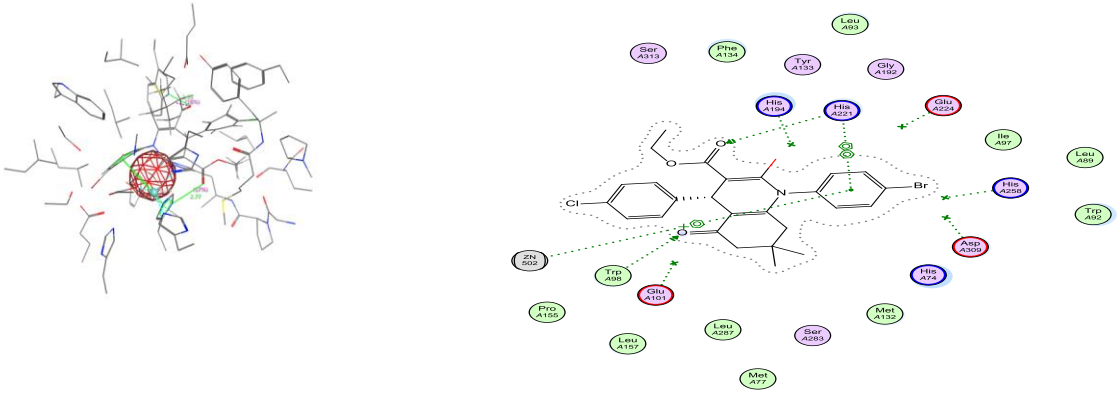

Q69. Ethyl 1-(4-bromophenyl)-4-(4-chlorophenyl)-2,7,7-trimethyl-5-oxo-1,4,5,6,7,8-hexahydroquinoline-3-carboxylate

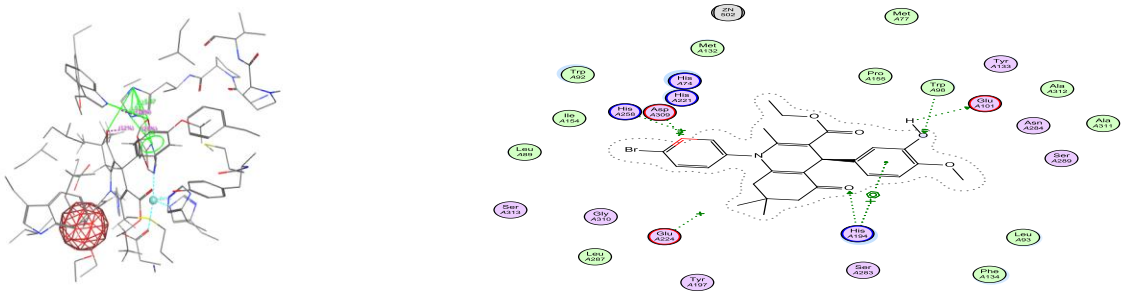

Q70. Ethyl 1-(4-bromophenyl)-4-(3-hydroxy-4-methoxyphenyl)-2,7,7-trimethyl-5-oxo-1,4,5,6,7,8-hexahydroquinoline-3-carboxylate

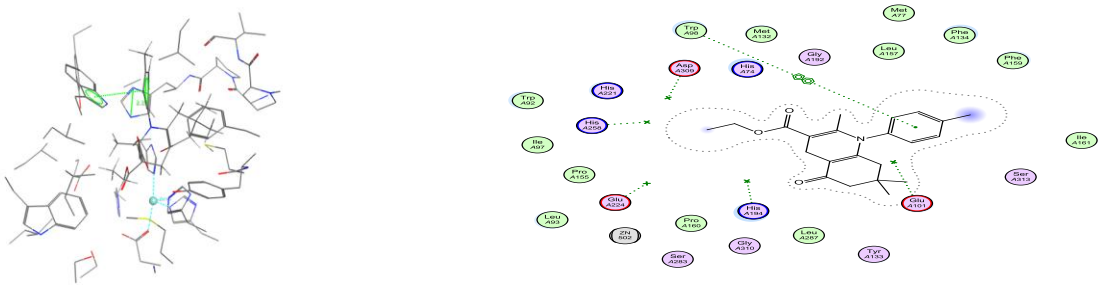

Q71. Ethyl 2,7,7-trimethyl-5-oxo-1-(p-tolyl)-1,4,5,6,7,8-hexahydroquinoline-3-carboxylate

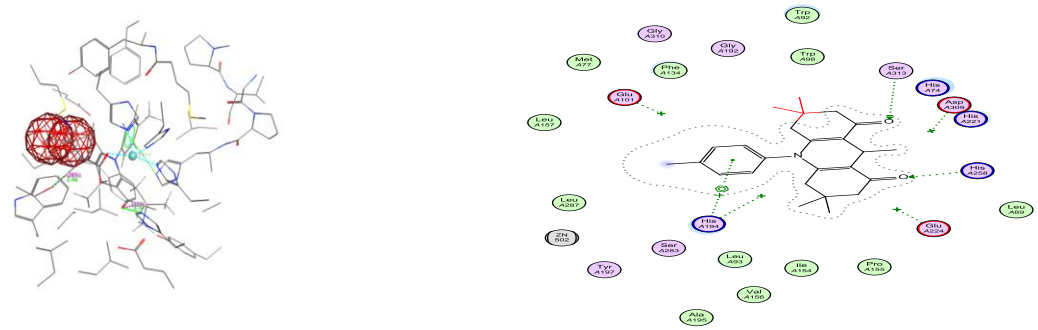

Q72. Ethyl 2,4,7,7-tetramethyl-5-oxo-1-(p-tolyl)-1,4,5,6,7,8-hexahydroquinoline-3-carboxylate

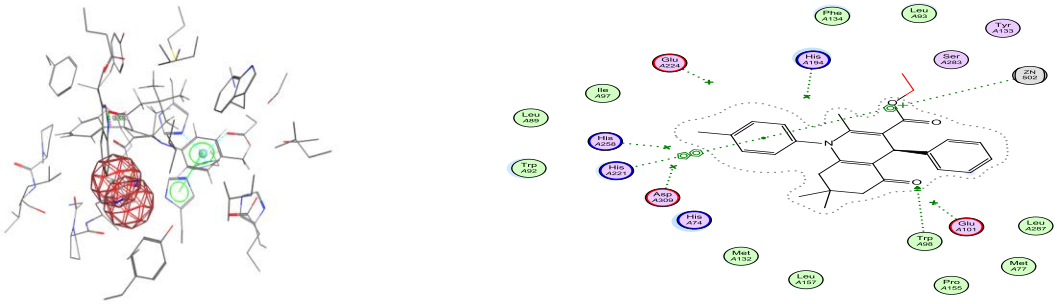

Q73. Ethyl 2,7,7-trimethyl-5-oxo-4-phenyl-1-(p-tolyl)-1,4,5,6,7,8-hexahydroquinoline-3-carboxylate

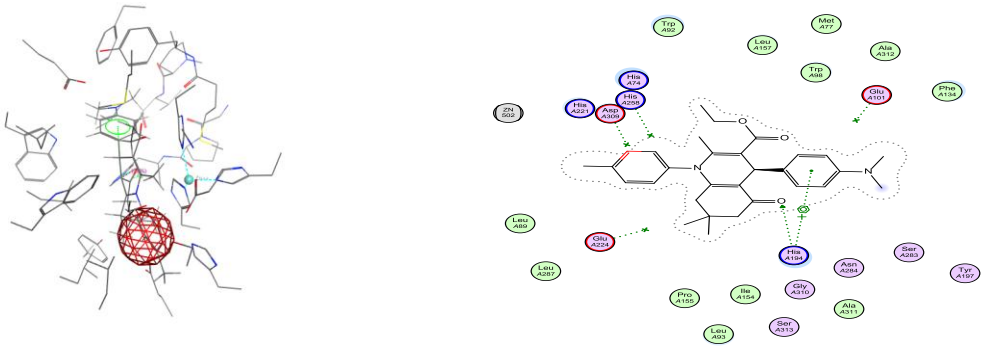

Q74. Ethyl 4-(4-(dimethylamino)phenyl)-2,7,7-trimethyl-5-oxo-1-(p-tolyl)-1,4,5,6,7,8-hexahydroquinoline-3-carboxylate

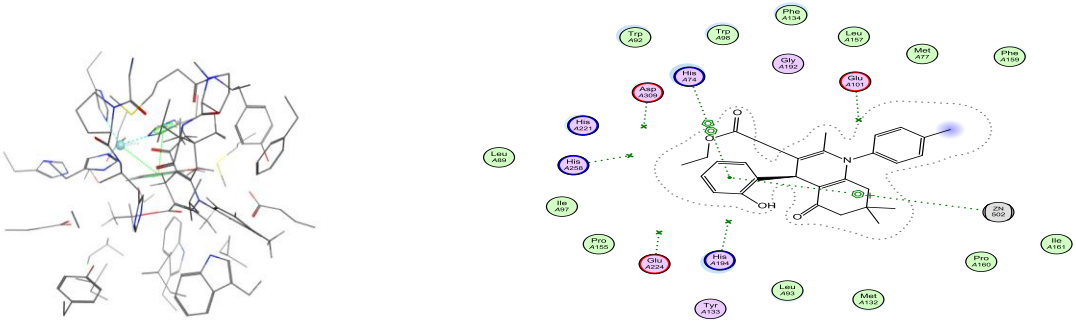

Q75. Ethyl 4-(2-hydroxyphenyl)-2,7,7-trimethyl-5-oxo-1-(p-tolyl)-1,4,5,6,7,8-hexahydroquinoline-3-carboxylate

A-IR,B-UV,C-1H-NMR, and D-MS spectra of 4-(9-(4-(dimethylamino)phenyl)-3,3,6,6-tetramethyl-1,8-dioxo-2,3,4,5,6,7,8,9-octahydroacridin-10(1H)-yl)benzenesulfonamide (I)

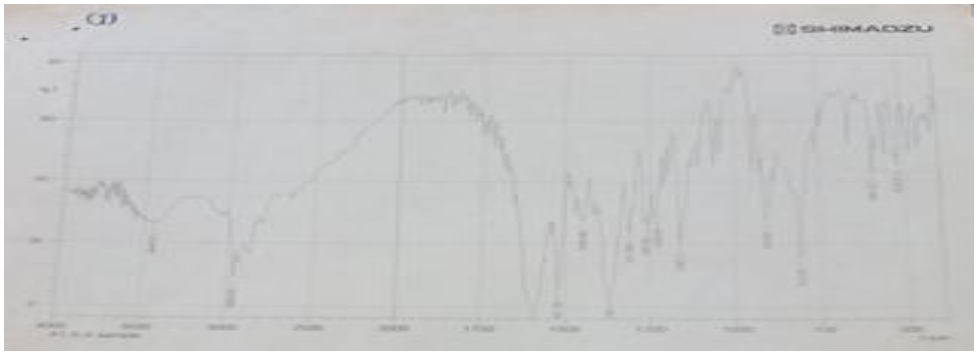

A

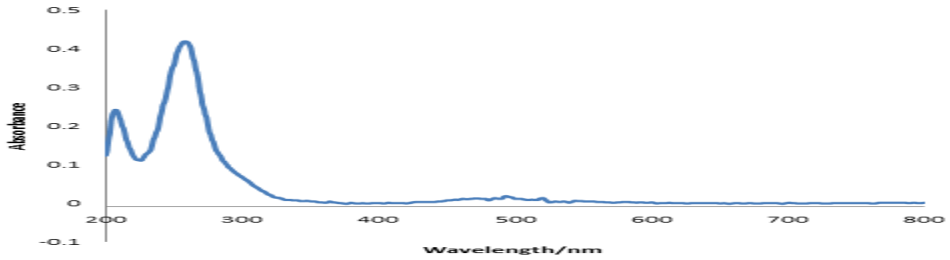

B

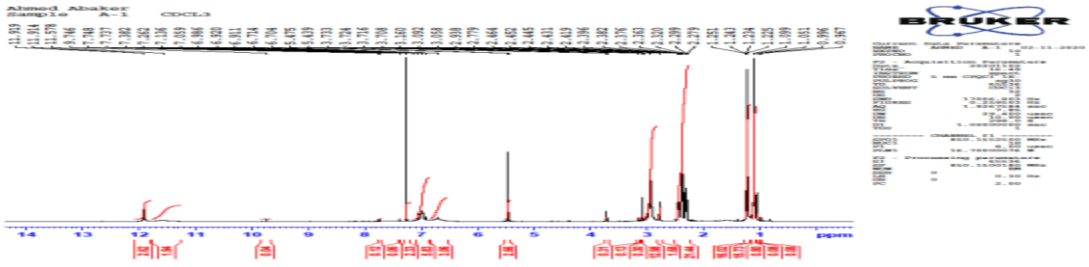

C

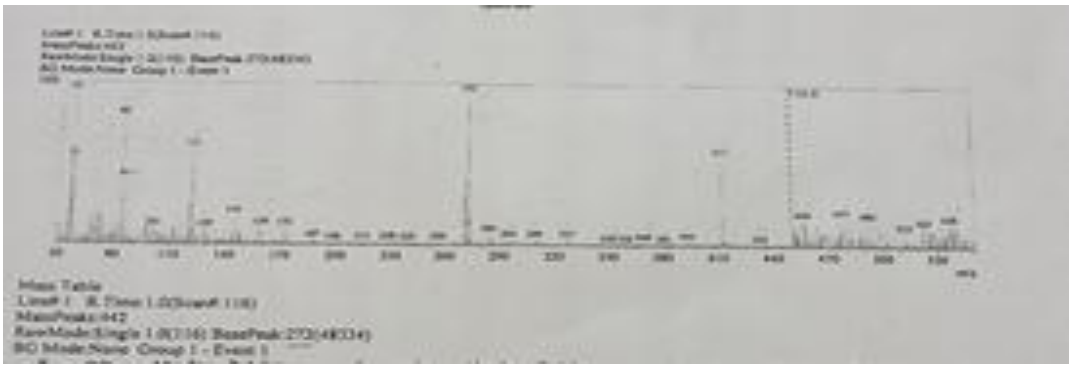

D

A-IR,B-UV,C-1H-NMR, and D-MS spectra of 9-(2-hydroxyphenyl)-3,3,6,6-tetramethyl-10-phenyl-3,4,6,7,9,10-hexahydroacridine-1,8(2H,5H)-dione (II)

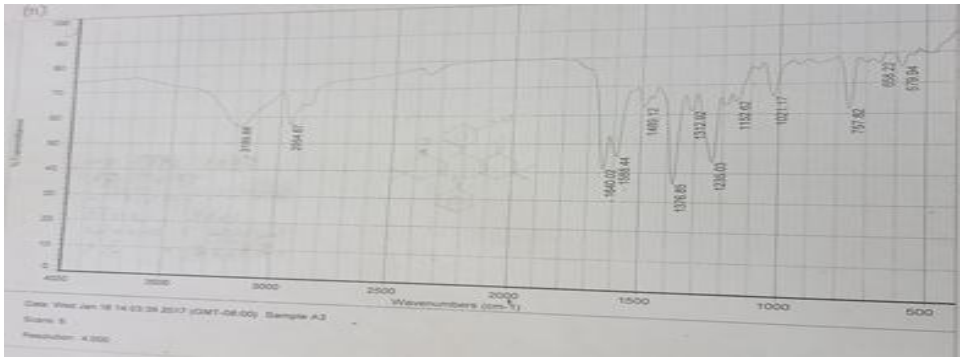

A

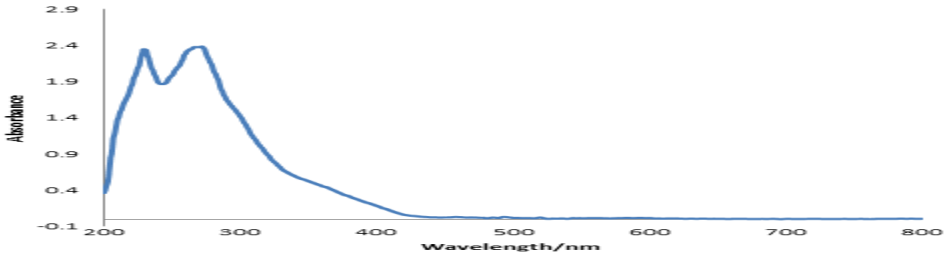

B

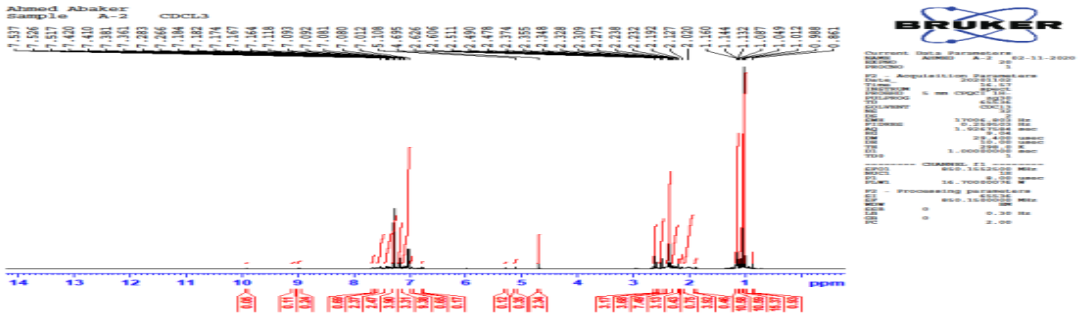

C

D

A-IR,B-UV,C-1H-NMR, and D-MS spectra of 4-(9-(2-hydroxyphenyl)-3,3,6,6-tetramethyl-1,8-dioxo-2,3,4,5,6,7,8,9-octahydroacridin-10(1H)-yl)benzenesulfonamide (III)

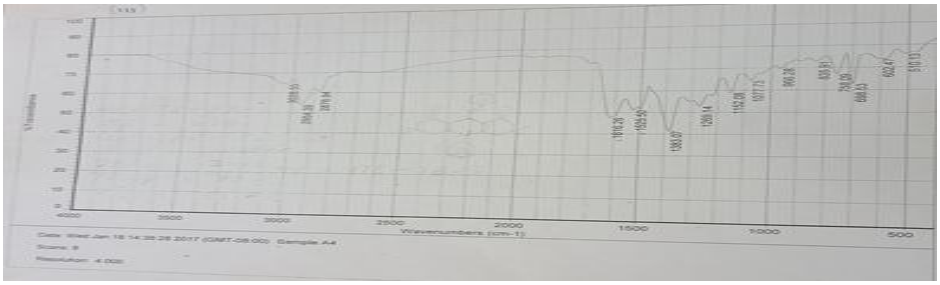

A

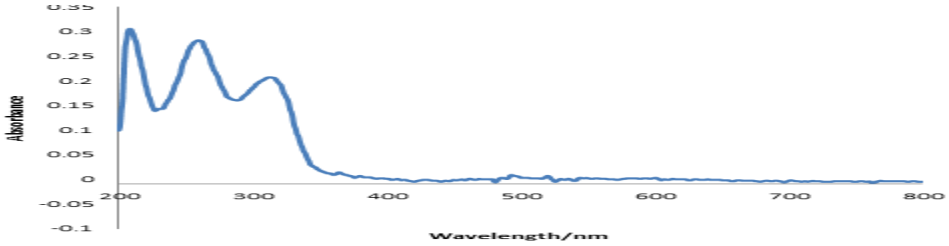

B

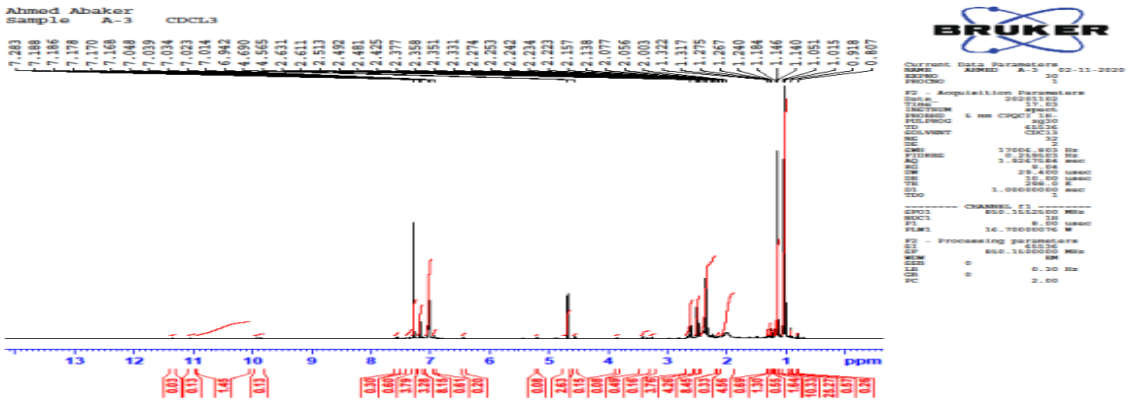

C

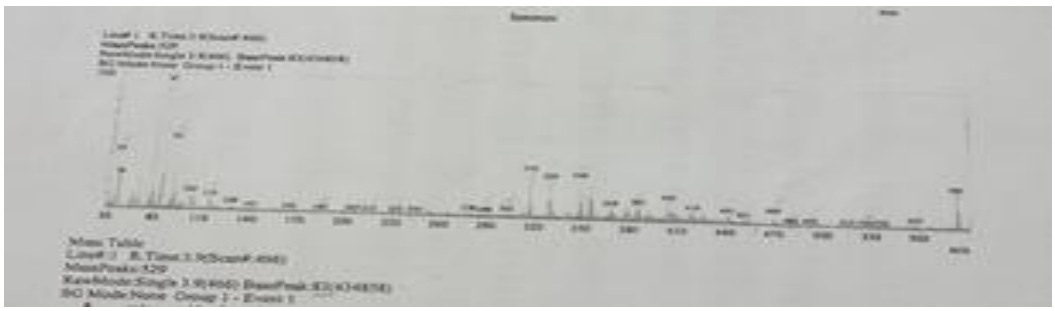

D

A-IR,B-UV,C-1H-NMR, and D-MS spectra of (E)-4-(3,3,6,6-tetramethyl-1,8-dioxo-9-styryl-2,3,4,5,6,7,8,9-octahydroacridin-10(1H)-yl)benzenesulfonamide (IV)

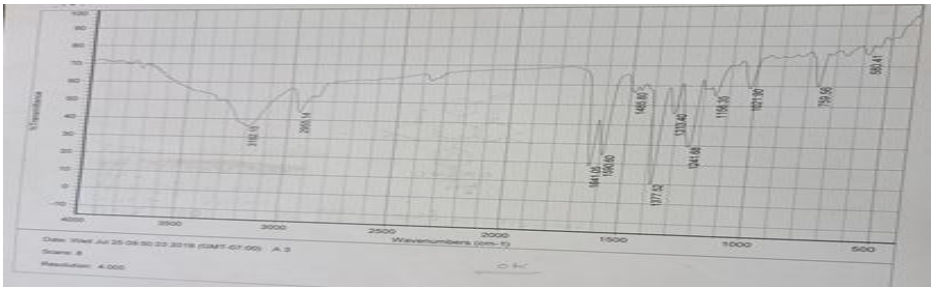

A

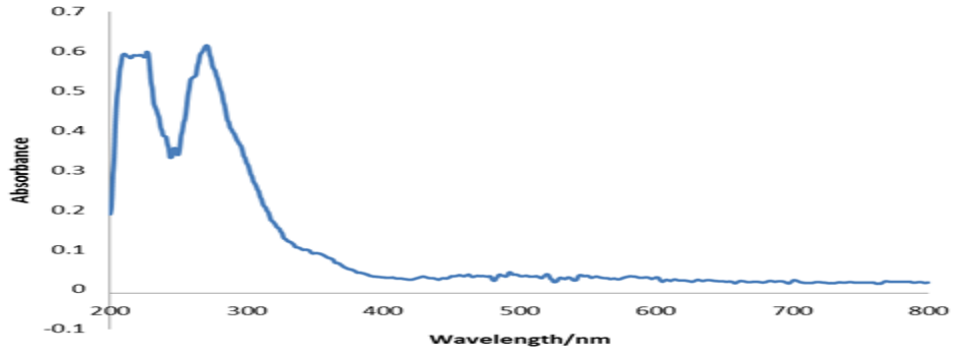

B

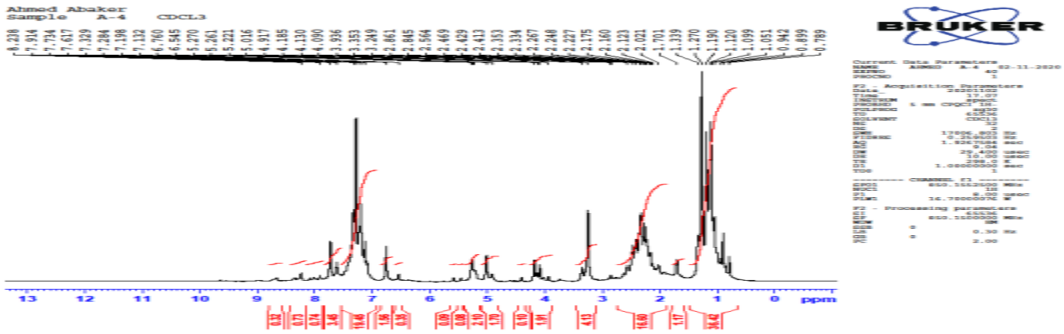

C

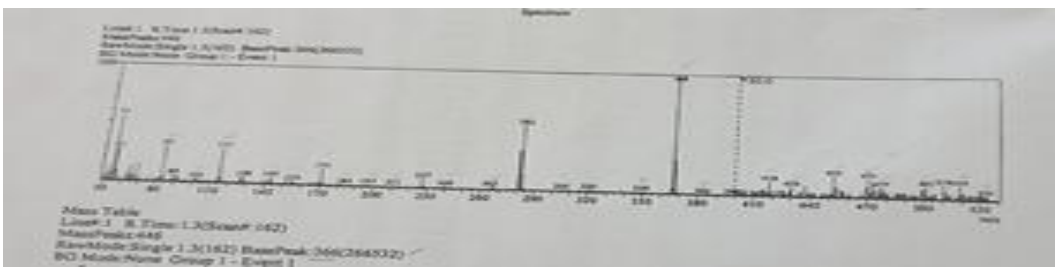

D

A-IR,B-UV,C-1H-NMR, and D-MS spectra of (E)-3,3,6,6-tetramethyl-10-phenyl-9-styryl-3,4,6,7,9,10-hexahydroacridine-1,8(2H,5H)-dione (V)

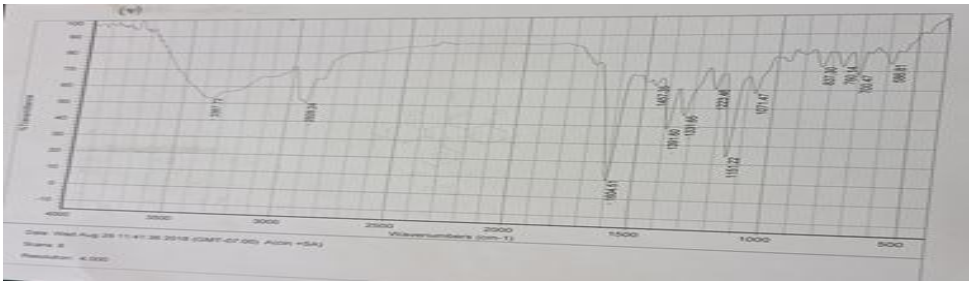

A

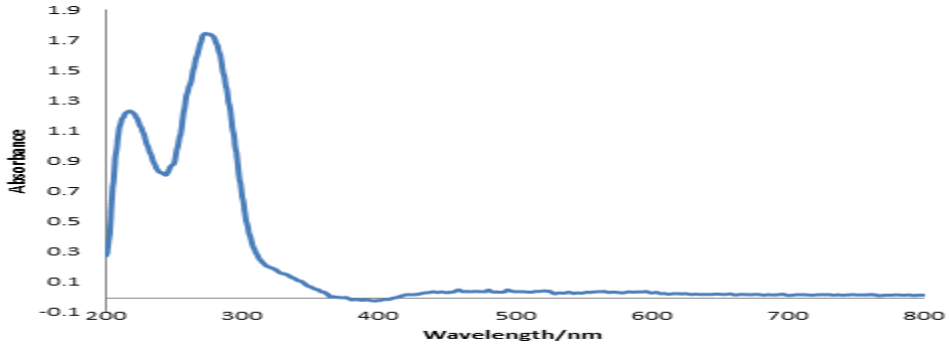

B

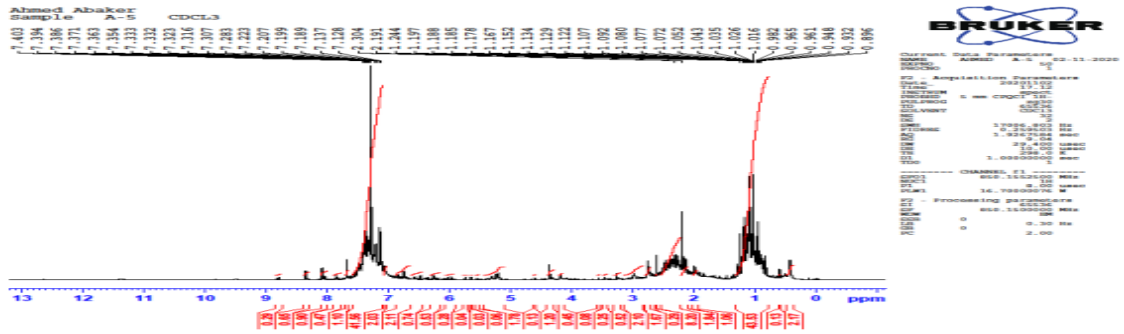

C

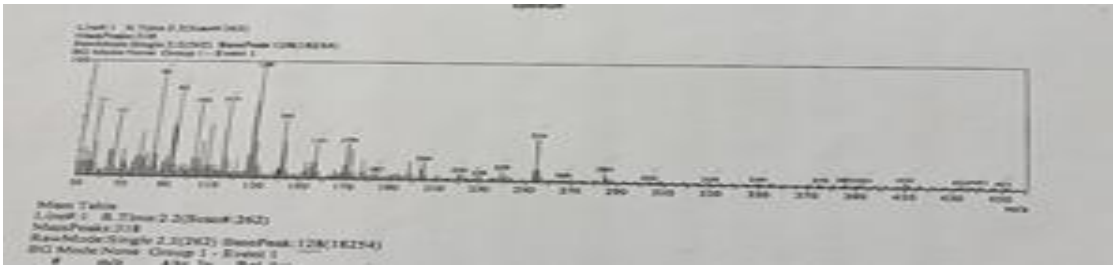

D

A-IR,B-UV,C-1H-NMR, and D-MS spectra of ethyl 2,7,7-trimethyl-5-oxo-1,4-diphenyl-1,4,5,6,7,8-hexahydroquinoline-3-carboxylate (VI)

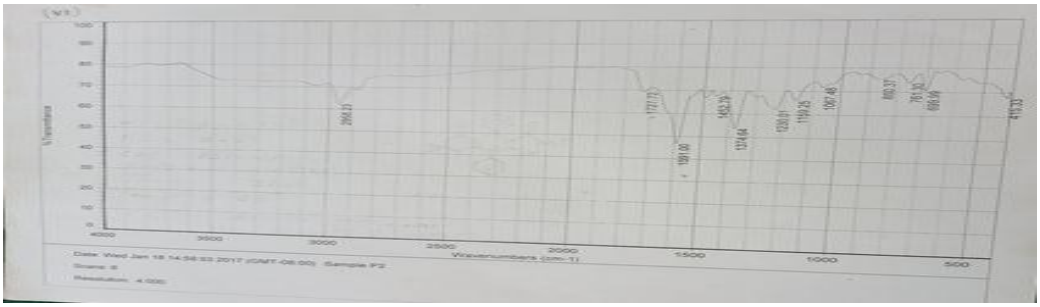

A

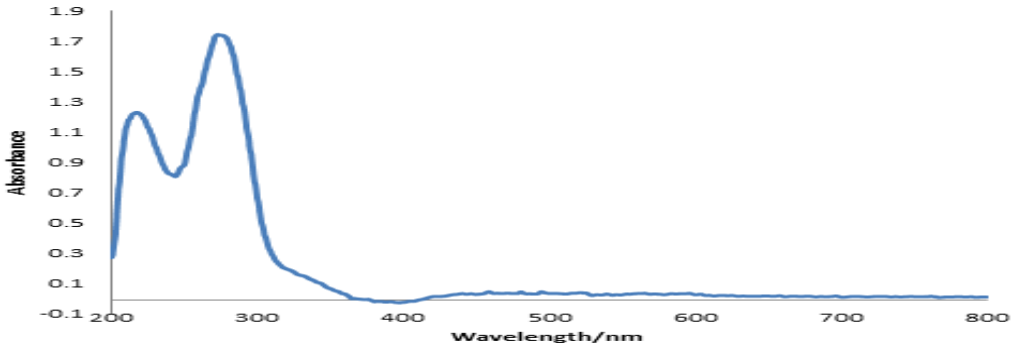

C

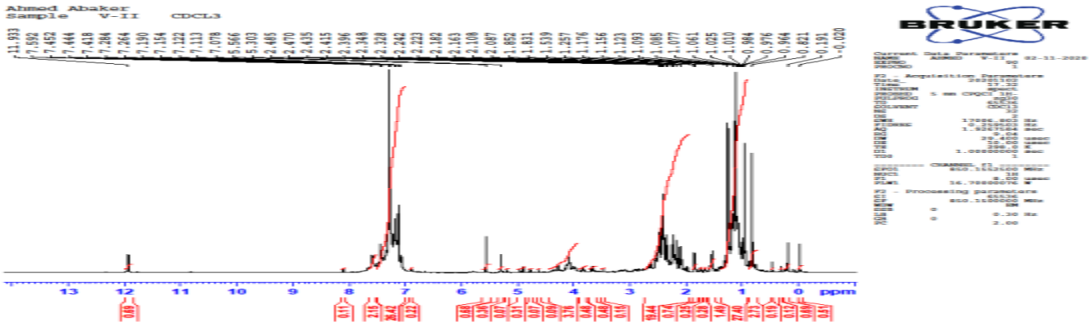

C

D

A-IR,B-UV,C-1H-NMR, and D-MS spectra of ethyl 4-(2-hydroxyphenyl)-2,7,7-trimethyl-5-oxo-1-phenyl-1,4,5,6,7,8-hexahydroquinoline-3-carboxylate (VII)

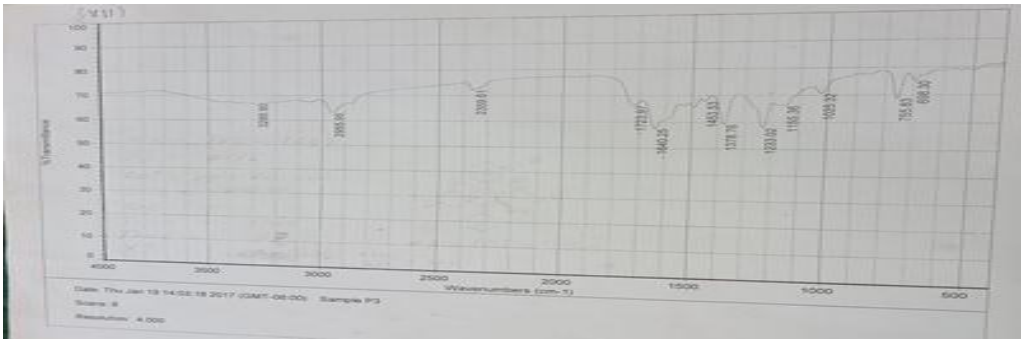

A

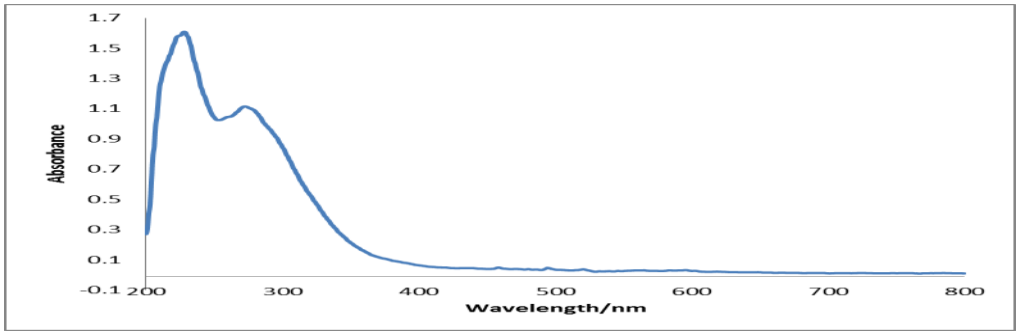

B

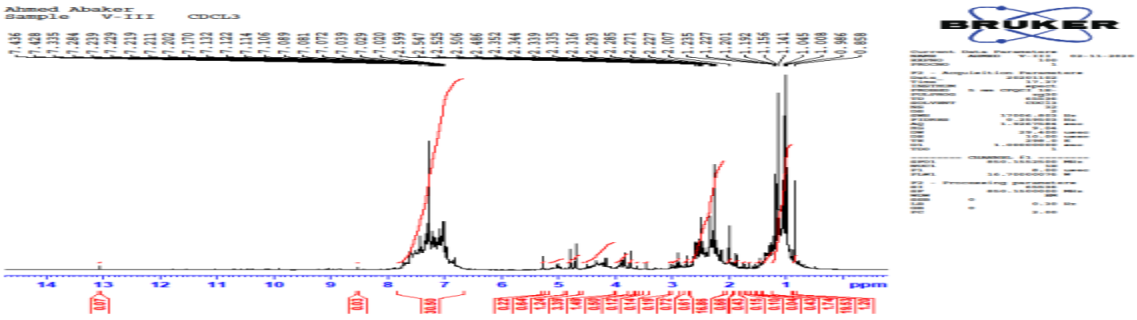

C

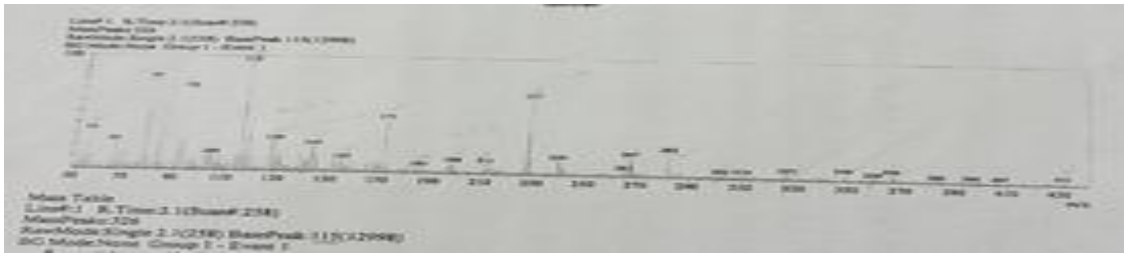

D

A-IR,B-UV,C-1H-NMR, and D-MS spectra of ethyl 4-(3-hydroxy-4-methoxyphenyl)-2,7,7-trimethyl-5-oxo-1-(4-sulfamoylphenyl)-1,4,5,6,7,8-hexahydroquinoline-3-carboxylate (VIII)

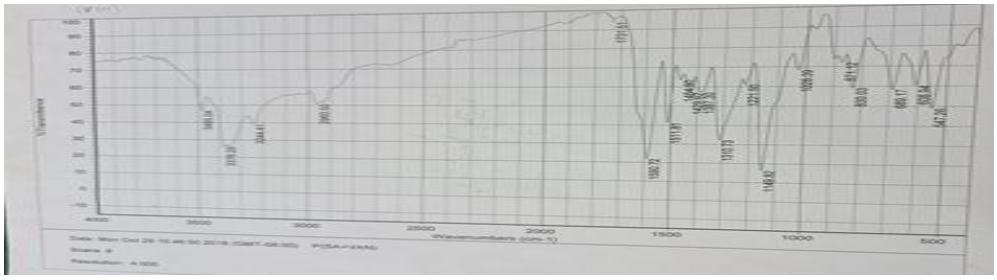

A

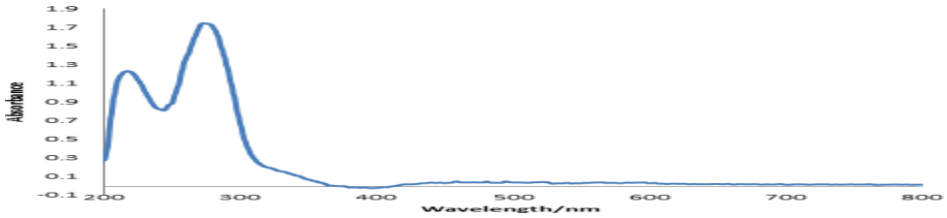

B

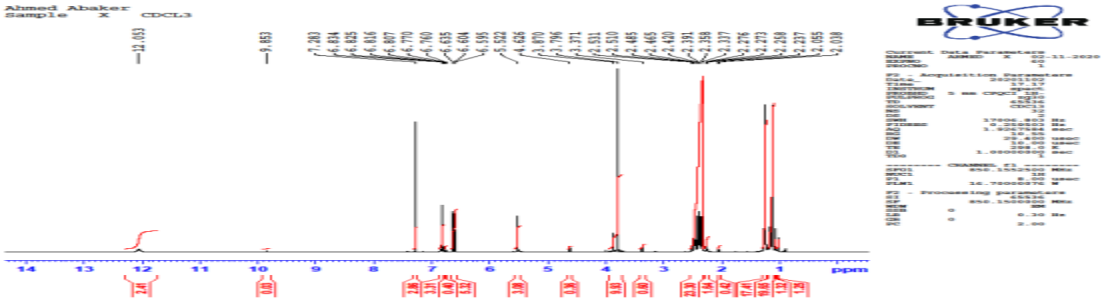

C

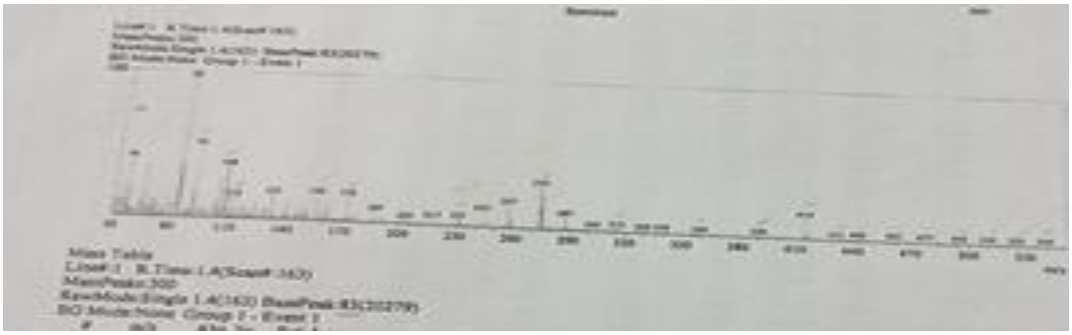

D

A-IR, B-UV, C-1H-NMR, and D-MS spectra of ethyl 4-(4-(dimethylamino) phenyl)-2,7,7-trimethyl-5-oxo-1-phenyl-1,4,5,6,7,8-hexahydroquinoline-3-carboxylate (IX)

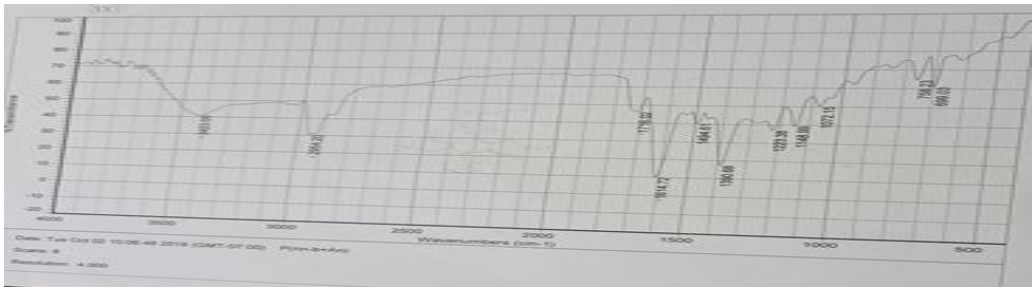

A

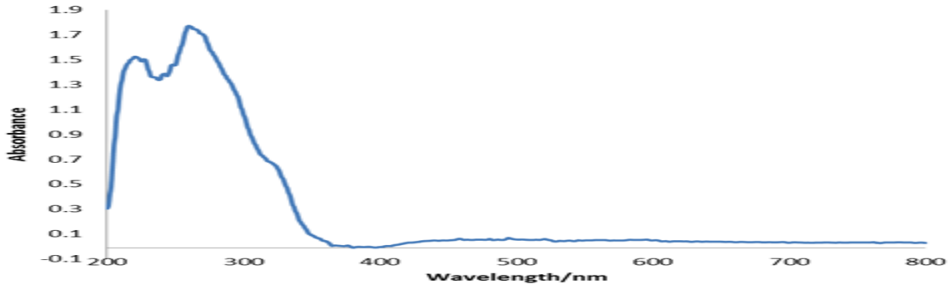

B

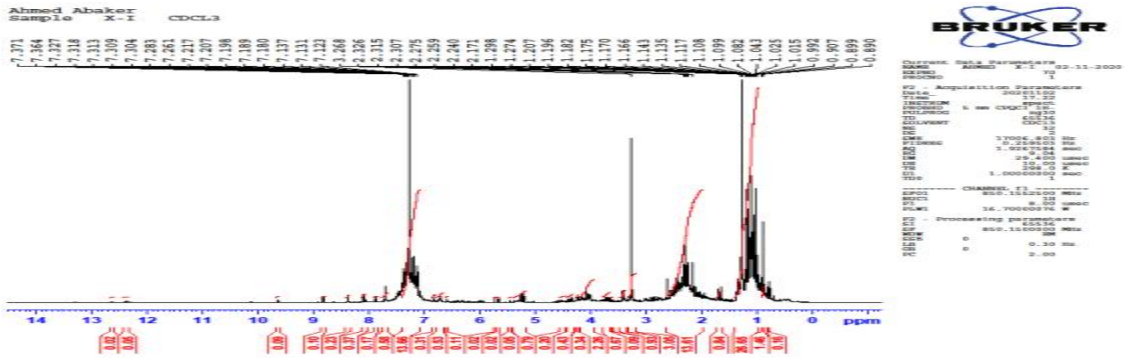

C

D

A-IR,B-UV,C-1H-NMR, and D-MS spectra of ethyl (E)-2,7,7-trimethyl-5-oxo-4-styryl-1-(4-sulfamoylphenyl)-1,4,5,6,7,8-hexahydroquinoline-3-carboxylate (X)

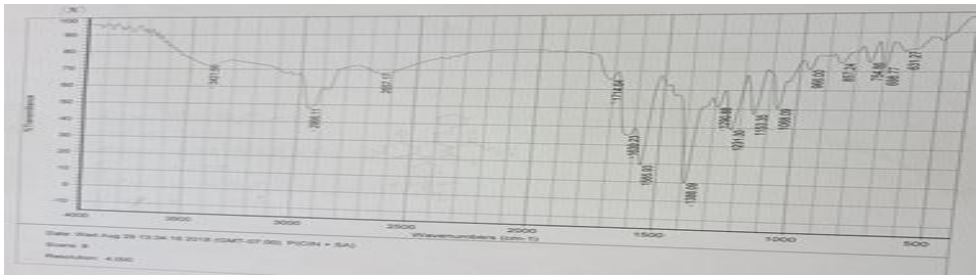

A

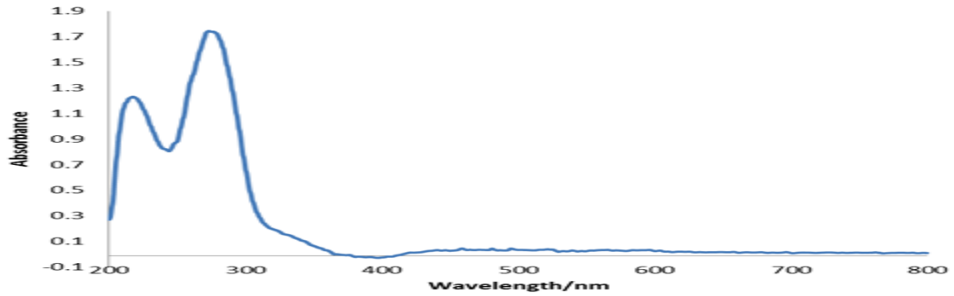

B

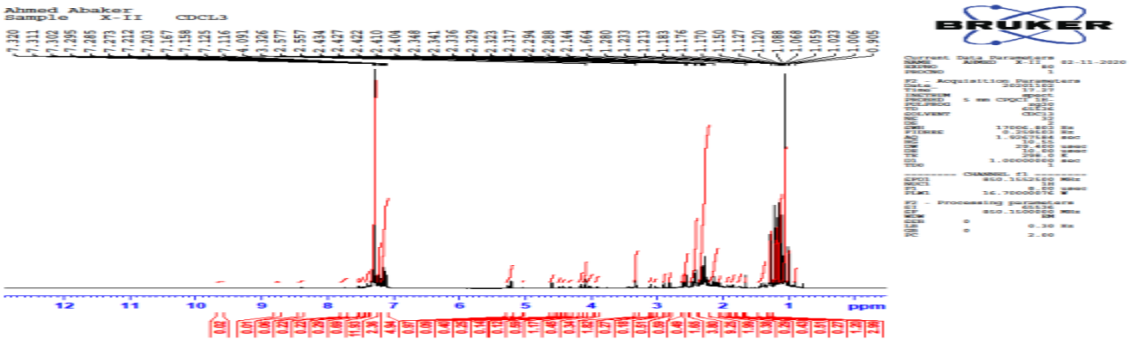

C

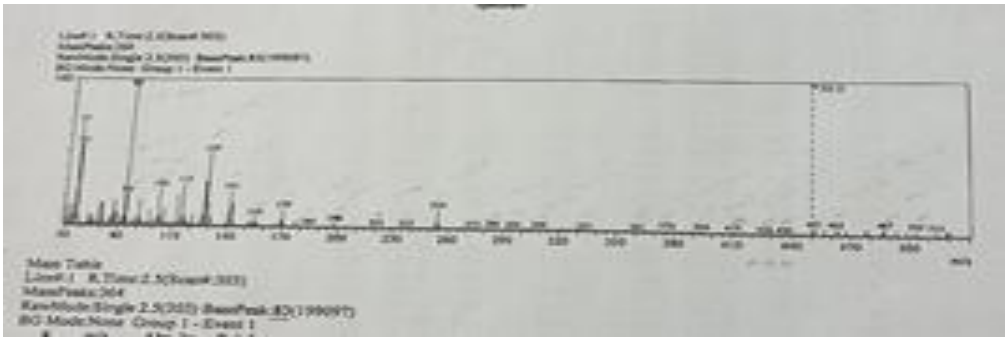

D